In vitro-Charakterisierung regulatorischer und sensorischer RNAs in Prokaryoten

Dissertation

zur Erlangung des akademischen Grades doctor rerum naturalium
(Dr. rer. nat.)

vorgelegt dem Rat der Biologisch-Pharmazeutischen Fakultät
der Friedrich-Schiller-Universität Jena

von Dipl.-Biologin

Nadja Heidrich
geboren am 19.04.1978
in Leipzig

Jena, im April 2007

Gutachter

1. HD Dr. Sabine Brantl

2. Prof. Frank Große

3. Prof. Udo Bläsi

Tag des Rigorosums: 31.05.2007

Tag der öffentlichen Verteidigung: 09.07.2007

Inhaltsverzeichnis

Abkürzungsverzeichnis **II**

1. Einleitung **1**

1.1. Regulatorische RNAs **1**

1.1.1. *Cis*-kodierte Antisense-RNAs **2**

1.1.2. *Trans*-kodierte Antisense-RNAs **5**

1.2. Das Hfq-Protein **9**

1.3. Sensorische RNAs **10**

1.3.1. RNA-Thermometer **10**

1.3.2. Riboswitches **11**

1.4. Zielsetzung **12**

2. Übersicht zu den Manuskripten **15**

3. Antisense RNA-mediated transcriptional attenuation in plasmid pIP501: the simultaneous interaction between two complementary loop pairs is required for efficient inhibition by the antisense RNA **18**

4. The small untranslated RNA SR1 from the *B. subtilis* genome is involved in the regulation of arginine catabolism **27**

5. *In vitro* analysis of the interaction between the small RNA SR1 and its primary target *ahrC*-RNA **45**

6. FourU – A novel type of RNA thermometer in *Salmonella* and other bacteria **82**

7. Gesamtdiskussion **112**

7.1. RNAIII: *cis*-kodierte Antisense-RNA vom Streptokokkenplasmid pIP501 **112**

7.1.1. Sequenz- und strukturspezifische Anforderungen an die inhibitorisch wirksame RNAIII des Plasmides pIP501 **112**

7.2. SR1: *trans*-kodierte Antisense-RNA aus dem *Bacillus subtilis*-Chromosom **116**

7.2.1. Biochemische Eigenschaften von SR1 **116**

7.2.2. *In vitro*-Charakterisierung der Interaktion von SR1 und *ahrC*-mRNA **118**

7.2.3. Wirkungsmechanismus von SR1 **120**

7.2.4. Die Rolle von Hfq **121**

7.3. FourU: neue RNA-Thermometerstruktur im *agsA*-Gen von *Salmonella enterica* **121**

7.3.1. Strukturelle und funktionelle Charakterisierung der *agsA*-Thermometerstruktur **122**

8. Zusammenfassung/Summary **123**

9. Literaturverzeichnis **129**

Abkürzungsverzeichnis

B. subtilis	*Bacillus subtilis*
bp	Basenpaar
DNA	Desoxyribonukleinsäure
E. coli	*Escherichia coli*
mRNA	messenger RNA (Boten-Ribonukleinsäure)
nt	Nukleotid
PCR	polymerase chain reaction (Polymerasekettenreaktion)
rRNA	ribosomale RNA
RBS	Ribosomenbindungsstelle
RNA	Ribonukleinsäure
RT	reverse Transkription (Umkehrtranskription)
SD	Shine-Dalgarno-Sequenz
t-RNA	transfer-RNA
5'-UTR	5'-untranslatierte Region

1. Einleitung

1.1. Regulatorische RNAs

Die RNA-Population einer Zelle wird in drei große Klassen mit unterschiedlichen biologischen Funktionen unterteilt: Messenger-RNAs (mRNAs), die als Überträger der genetischen Information zwischen DNA und Protein dienen, ribosomale-RNAs (rRNAs) und transfer-RNAs (t-RNAs), die wichtige Funktionsträger der Proteinbiosynthese sind. Seit über 30 Jahren sind regulatorische RNAs in Bakterien bekannt, die keiner der oben genannten Klassen angehören, aber diese aufgrund ihrer biologischen Bedeutung und ihrem großen regulatorischen Potential als faszinierende Minderheit ergänzen. Im Jahr 2001 führten systematische Genomanalysen prokaryotischer und eukaryotischer Modellorganismen zur Entdeckung eines ganzen „Universums regulatorischer RNAs“ und brachten einen Wendepunkt in der herkömmlichen Betrachtungsweise. RNA-Moleküle transportieren nicht nur die genetische Information von der DNA zu den Proteinmanufakturen der Zelle, sondern nehmen auch wichtige regulatorische Funktionen wahr. Regulatorische RNAs sind kleine, instabile, diffusionsfähige Moleküle, die in der Regel nicht translatiert werden. Die Mehrzahl der regulatorischen RNAs kann durch Basenpaarung regulierend auf Target-RNAs einwirken. Solche RNAs sind vollständig oder teilweise komplementär zu ihren Target-RNAs, den sogenannten Sense-RNAs, und werden als Antisense-RNAs bezeichnet. Bei den meisten Target-RNAs handelt es sich um mRNAs, die funktionell interessante Proteine kodieren. Klassische Antisense-RNAs wirken als negative Regulatoren, indem sie durch die Interaktion mit ihrem Target dessen Funktion inhibieren, jedoch sind auch aktivierend wirksame Antisense-RNAs bekannt. Natürlich vorkommende Antisense-RNAs wirken damit als Regulatoren der Genexpression auf post-transkriptionaler Ebene. Eine andere Gruppe regulatorischer RNAs wirkt durch die direkte Bindung an Proteine, indem sie die Struktur anderer RNA- oder DNA-Moleküle nachahmt.

Eine neue, erst kürzlich in vollem Umfang entdeckte Klasse nichttranslatierter RNAs in Eukaryoten ist durch ihre ungewöhnliche Länge von ≈22 nt gekennzeichnet. Diese *short interfering RNAs* (siRNAs) oder *microRNAs* (miRNAs) beeinflussen sowohl die Stabilität von mRNAs als auch deren Translation und sind daher wichtige zelluläre Regulatoren der Genexpression (Meister und Tuschl, 2004). siRNAs haben sich in kurzer Zeit zu bedeutenden Werkzeugen in der Grundlagenforschung entwickelt, mit deren Hilfe spezifisch Gene ausgeschaltet werden können. Des Weiteren stellen sie einen viel versprechenden und neuartigen Ansatz zur Therapie von unterschiedlichsten Krankheiten dar (Dykxhoorn und Lieberman, 2006). Bakterielle Antisense-RNAs sind mit einer Länge von ca. 50-250 Nukleotiden etwas größer und besitzen

charakteristische Stem-Loop-Strukturen, die ihnen eine erfolgreiche Interaktion mit ihren Target-RNA(s) ermöglichen.

1.1.1. *Cis*-kodierte Antisense-RNAs

Antisense-RNAs in Bakterien unterteilt man in zwei verschiedene Klassen: in *cis*-kodierte und *trans*-kodierte Antisense-RNAs. *Cis*-kodierte Antisense-RNAs werden vom selben DNA-Locus wie ihre Target-RNA, allerdings in unterschiedlicher Richtung, transkribiert. Sie sind deshalb über einen langen Sequenzabschnitt vollständig komplementär zu ihrer Target-RNA und können nur auf dieses eine Target regulierend einwirken. Im Gegensatz dazu sind die Gene *trans*-kodierter Antisense-RNAs an einer anderen Stelle im Genom als die ihrer Target-RNA(s) lokalisiert.

Die Mehrzahl der bakteriellen *cis*-kodierten Antisense-RNAs wurde in prokaryotischen Begleitelementen wie Plasmiden, Phagen und Transposons sowie in Einzelfällen bei chromosomalen Bakteriengenen entdeckt und studiert (Wagner und Simons, 1994; Wagner *et al.,* 2002; Brantl, 2002). *Cis*-kodierte Antisense-RNAs regulieren eine Vielzahl biologischer Prozesse wie Replikation, Segregationsstabilität und Konjugation in Plasmiden, Transposition von Transposons und den Wechsel zwischen lytischer und lysogener Entwicklung in Phagen (Wagner *et. al.,* 2002), (s. Tabelle 1). In der Mehrzahl aller Fälle inhibieren sie die Genexpression auf post-transkriptionaler Ebene mit Hilfe unterschiedlicher Mechanismen. Regulationsmechanismen sind Inhibierung der Primerreifung, Verhinderung der 'leader'-Peptid-Translation, Inhibierung der Bildung eines RNA-Pseudoknotens, Blockierung des Ribosomenbindungsortes und Transkriptionsattenuierung. Ein Großteil dieser Mechanismen wird von zahlreichen Plasmiden zur Kontrolle ihrer Kopiezahl verwendet (s. Abb.1).

Im Folgenden soll speziell auf die Antisense-RNA-vermittelte Regulation der Replikation von Streptokokkenplasmid pIP501 eingegangen werden. Das Kontrollsystem der Replikation von pIP501 ist das am besten untersuchte System bei grampositiven Bakterien überhaupt. Die Replikation von pIP501 wird von den Produkten zweier nichtessentieller Gene*, copR* und *rnaIII,* kontrolliert (Brantl und Behnke, 1992a). Diese regulieren die Syntheserate des geschwindigkeitslimitierenden Replikationsinitiatorproteins RepR (Brantl und Behnke, 1992b). Das *rnaIII*-Gen codiert eine 136 nt lange Antisense-RNA (RNAIII), die komplementär zu einem Teil der nichttranslatierten 'leader'-Region der *repR*-mRNA (RNAII) ist. Diese 'leader'-Region kann zwei alternative Konformationen annehmen. Die eine Konformation, die die im Entstehen begriffene (naszente) *repR*-mRNA in Abwesenheit der Antisense-RNA ausbildet, erlaubt die Transkription einer vollständigen *repR*-mRNA. In Anwesenheit der Antisense-RNA kommt es durch Wechselwirkung zwischen Sense- und Antisense-

RNA in der 'leader'-Region zur Ausbildung eines Transkriptionsterminators. Das führt zu einem vorzeitigen Transkriptionsabbruch (Attenuierung) der *repR*-mRNA (Brantl *et al.*, 1993; Brantl und Wagner 1994, 1996). Auf diese Weise reguliert die Antisense-RNA RNAIII über Transkriptionsattenuierung der essentiellen *repR*-mRNA die Replikation des Streptokokkenplasmides pIP501.

RNA-RNA-Interaktionen basieren neben den sequenzspezifischen auf strukturellen Eigenschaften der Interaktionspartner. Diese wurden durch eine extensive Mutationsanalyse am Beispiel der plasmidkodierten Antisense-RNA CopA von R1 ermittelt (Hjalt und Wagner, 1992, 1995). Die Loops der Stem-Loop-Strukturen sind entscheidende Faktoren für die Interaktion zwischen Antisense- und Sense-RNA. Sie sind im Optimalfall 5-8 Nukleotide groß und GC-reich. Die Stems sind wichtig für die metabolische Stabilität der Antisense-RNA und verfügen über mehrere perfekt gepaarte Nukleotide. Wenn sie länger als 10 bp sind, werden sie durch imperfekte Stellen (Bulges) unterbrochen. Diese schützen die Antisense-RNAs vor Angriffen durch die doppelstrangspezifische RNase III und ermöglichen eine effiziente Paarung mit den entsprechenden Sense-RNAs. Häufig findet man in den 'recognition'-Loops der Stem-Loop-Strukturen von Antisense-RNAs oder ihrer Target-RNA(s) ein 5'-YUNR-Sequenzmotiv, das einen U-turn ausbilden kann. Durch diese Biegung im RNA-Zucker-Phosphat-Rückgrat wird ein Gerüst geschaffen, das eine schnelle Interaktion zwischen komplementären RNAs ermöglicht (Franch *et al.*, 1999; Heidrich und Brantl 2003).

Im Verlauf der letzten 25 Jahre wurden viele Antisense/Sense-RNA-Systeme sehr detailliert *in vivo* und *in vitro* untersucht. Dabei zeigte sich, dass die Paarung zwischen Sense- und Antisense-RNA im Allgemeinen mit einer Konstante von $\approx 10^6\ M^{-1}s^{-1}$ verläuft. Der initiale Kontakt zwischen Antisense-RNA und ihrer Target-RNA erfolgt zwischen einzelsträngigen Regionen und führt zur Ausbildung eines 'kissing'-Komplexes, der anschließend in eine vollständige Duplex umgewandelt wird (Wagner *et al.,* 2002). Bisher konnten für die Interaktion zwischen Sense- und Antisense-RNA zwei Paarungsmechanismen aufgeklärt werden ('Two-step pathway': CopA/CopT, Eguchi und Tomizawa 1991; 'One-step pathway': hok/Sok, Gerdes *et al.,* 1997). Bei beiden Paarungsmechanismen wurde gezeigt, dass für die inhibitorische Wirkung der Antisense-RNA die Ausbildung einer vollständigen Duplex mit der Target-RNA nicht erforderlich ist, sondern ein Bindungsintermediat für eine effiziente Kontrolle ausreicht (zusammengefasst in: Wagner und Brantl, 1998; Wagner *et al.,* 2002). Im Fall von RNAII/RNAIII wurde der Bindungsweg noch nicht aufgeklärt, doch auch hier konnte im Rahmen dieser Arbeit gezeigt werden, dass Bindungsintermediate die biologisch aktiven Strukturen sind (Heidrich und Brantl, 2007).

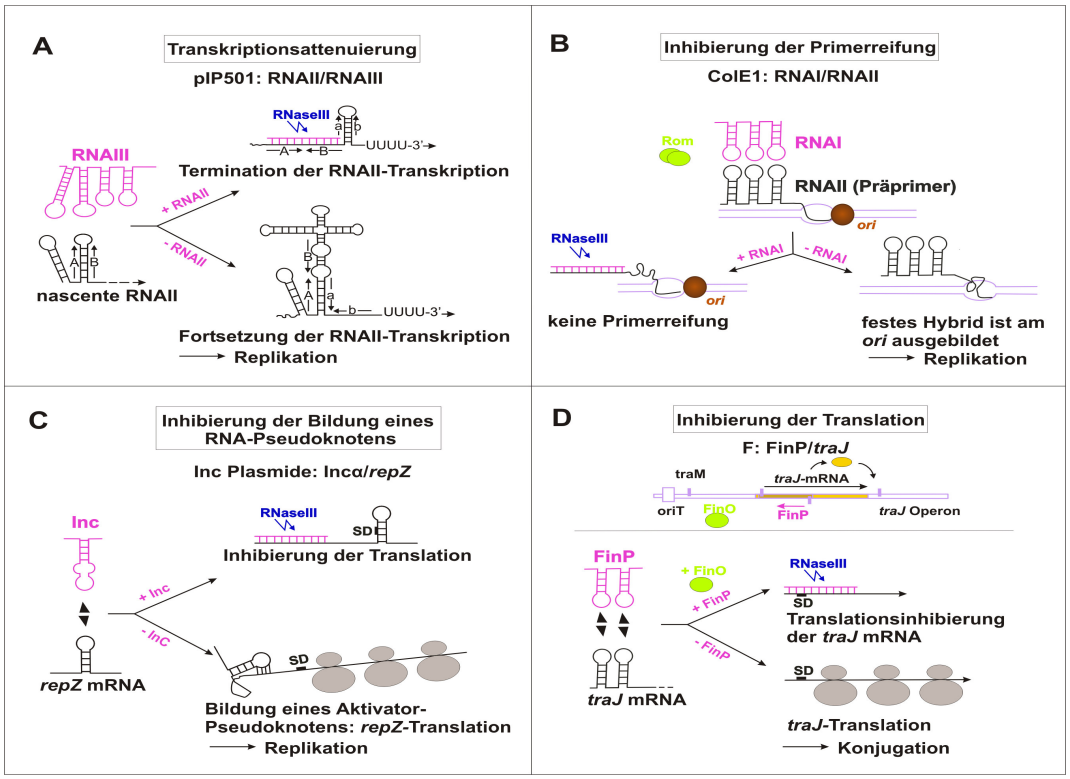

Abb. 1: Wirkungsmechanismen *cis*-kodierter Antisense-RNAs. rosa: Antisense-RNA; schwarz: Sense-RNA; (A) die komplementären Sequenzelemente möglicher Basenpaarung sind mit A, B, a und b bezeichnet; (B) ori: Replikationsursprung; brauner Kreis: RNA-Polymerase; (C) und (D) graue Ovale: Untereinheiten des Ribosoms (nach Brantl, 2007)

Tabelle 1. Beispiele *cis*-kodierter Antisense/Target-RNAs

Biologisches System	Antisense-RNA/ Target	Biologische Funktionen	Mechanismus	Referenz
Plasmide				
ColE1	RNAI/RNAII primer	Replikationskontrolle	Inhibierung der Primerreifung	Eguchi und Tomizawa, 1991
R1(IncFII-ähnliche)	CopA/CopT	Replikationskontrolle	Translationsinhibierung	Malmgren *et al.*, 1996
R1	Sok/*hok* mRNA	Segregationsstabilität	Translationsinhibierung	Gerdes *et al.*, 1997
pAD1	RNAII/RNAI	Segregationsstabilität	Translationsinhibierung	Greenfield *et al.*, 2000
R1/F	FinP/*traJ* mRNA	Konjugationskontrolle	Translationsinhibierung	Frost *et al.*, 1989; Koraimann *et al.*, 1991
pIP501	RNAIII/RNAII	Replikationskontrolle	Transkriptionsattenuierung	Brantl *et al.*, 1993
pT181	RNAI,II/*repC* mRNA	Replikationskontrolle	Transkriptionsattenuierung	Novick *et al.*, 1989
CollB-P9 (IncIα/ IncB)	Inc/*repZ* mRNA	Replikationskontrolle	Inhibierung der 'pseudoknot'- Bildung	Asano *et al.*,1991 Wilson *et al.*,1993
Transposons				
IS10/Tn10	RNA-OUT/RNA-IN	Transposition	Translationsinhibierung	Ma & Simons, 1990
IS30	RNA-C/*tnp* mRNA	Transposition	Inhibierung der Translationselongation	Arini *et al.*, 1997
Bacteriophagen				
λ	OOP/*cII* mRNA	Lysis/Lysogenie-Wechsel	mRNA-Stabilität	Krinke und Wulff, 1990
P22	SAR/*arc-ant* mRNA	Lysis/Lysogenie-Wechsel	Translationsinhibierung	Liao *et al.*, 1987
Chromosomal kodierte Antisense-RNAs				
Bacillus subtilis	RatA/*txpA* mRNA	Toxin/Antitoxin	mRNA-Abbau (?)	Silvaggi *et al.*, 2005
Escherichia coli	GadY/*gadX*	Säure-Stress	mRNA-Stabilisierung (?)	Opdyke *et al.*, 2004

(?) vorgeschlagener, aber noch nicht experimentell bestätigter Mechanismus

1.1.2. *Trans*-kodierte Antisense-RNAs

Im Unterschied zu den *cis*-kodierten Antisense-RNAs sind die *trans*-kodierten Antisense-RNAs in intergenischen Regionen im Chromosom von Bakterien zu finden und an einer anderen Stelle als ihre Target-RNA(s) kodiert. Deshalb sind sie nur teilweise komplementär zu ihren Target-RNA(s) und können durch unvollständige Basenpaarung auf eine Vielzahl von Target-RNA(s) regulierend einwirken. Bis vor einigen Jahren waren nur einige wenige *trans*-kodierte Antisense-RNAs in Bakterien bekannt, die meisten davon im Chromosom von *E. coli* (DicF, MicF, OxyS, DsrA; Wassarman *et al.,* 1999). Im Jahr 2001 konnten mit Hilfe bioinformatischer und experimenteller Strategien ungefähr 45 weitere *trans*-kodierte Antisense-RNAs im Genom von *E. coli* identifiziert werden (Argaman *et al.,* 2001; Rivas *et al.,* 2001; Wassarman *et al.,* 2001; Chen *et al.,* 2002). Mittlerweile sind über 70 solcher RNAs gefunden wurden. Während die Suche nach neuen kleinen RNAs in anderen Bakterien weitergeht, konnte in *E. coli* ungefähr 20 dieser neuen RNAs eine Funktion zugeschrieben, und einige wenige davon konnten biochemisch charakterisiert werden (zusammengefasst in: Storz *et al.,* 2005; Majdalani *et al.,* 2005). Die Mehrzahl der bisher funktionell charakterisierten *trans*-kodierten Antisense-RNAs sind wichtige Regulatoren der Stressantwort. Sie werden durch unterschiedliche Stressbedingungen in ihrer Umwelt induziert und sind an der Regulation einer Vielzahl von biologischen Prozessen beteiligt: Eisen-Metabolismus (RyhB, Massé und Gottesman, 2002; PrrF1 und PrrF2, Wilderman *et al.,* 2004), Galactoseverwertung (Spot42, Møller *et al.,* 2002b), Phosphozuckerstress (SgrS, Vanderpool und Gottesman, 2004, Kawamoto *et al.,* 2005), SOS-Antwort (IstR, Vogel *et al.,* 2004), Stationärphase-Regulation (DsrA, OxyS, RprA, zusammengefasst in: Repoila *et al.,* 2003), Membran-Zusammensetzung (MicA, Rasmussen *et al.,* 2005, Udekwu *et al*., 2005; MicF, Delihas und Forst, 2001; MicC, Chen *et al.,* 2004; OmrA-OmrB, Guillier und Gottesman, 2006), Biolumineszenz und Virulenz (Qrr1-Qrr4, Lenz *et al.,* 2004).

Die Mehrzahl der bisher charakterisierten regulatorischen RNAs ist im Genom von gramnegativen Bakterien kodiert. Nur eine sehr geringe Anzahl *trans*-kodierter Antisense-RNAs ist in grampositiven Bakterien bekannt. Dazu zählen RNAIII (Morfeldt *et al.,* 1995; Huntzinger *et al.,* 2005) und SprA-SprG (Pichon und Felden, 2005) aus *Staphylococcus aureus*, FasX (Kreikemeyer *et. al.,* 2001) und Pel (Mangold *et. al.,* 2004) aus *Streptococcus pyogenes* sowie VR RNA (Shimizu *et al.,* 2002) und VirX (Ohtani *et. al.,* 2002) aus *Clostridium perfringens*. Diese RNAs sind direkt oder indirekt an der Regulation der Expression von Virulenzgenen beteiligt (zusammengefasst in: Romby *et al.,* 2006). Mit Ausnahme von RNAIII ist für keine der anderen RNAs ein Wirkungsmechanismus aufgeklärt worden. Das trifft auch für die erst vor kurzem im

Genom von *Listeria monocytogenes* entdeckten regulatorischen RNAs zu, von denen auch angenommen wird, dass sie für die Ausbildung pathogener Eigenschaften eine Rolle spielen (Christiansen *et al.,* 2006; Mandin *et al.,* 2007). Auch im Chromosom von *Bacillus subtilis*, dem Untersuchungsorganismus dieser Arbeit, wurden einige regulatorische RNAs zum einen mit Hilfe von RNA-Expressionsanalysen unter Verwendung eines „Antisense *Bacillus subtilis* Genom-Array" (Lee *et al*., 2001) und zum anderen mit Hilfe von Computerprogrammen als nicht-kodierende Transkripte in intergenischen Regionen vorhergesagt (Licht *et al.,* 2005). Allerdings konnten nur 4 dieser RNAs experimentell detektiert und funktionell charakterisiert werden: BS203 (Ando *et al*., 2002), BS190 (Suzuma *et al*., 2002), bei denen es sich um die zwei 6S RNAs von *B. subtilis* handelt (siehe unten), RatA, die als Antitoxin den Abbau der Toxin-kodierenden *txpA* RNA fördert (Silvaggi *et al*., 2005), und SR1 (small RNA1), die im Rahmen dieser Arbeit biochemisch und funktionell charakterisiert wurde. Für 12 weitere regulatorische RNAs, die von Lee vorhergesagt wurden, konnte jetzt gezeigt werden, dass sie nur unter Bedingungen der Sporulation in *Bacillus subtilis* exprimiert werden (Silvaggi *et al.,* 2006). Ihre Targets, Funktionen und Wirkungsweisen müssen jedoch noch aufgeklärt werden. Es ist anzunehmen, dass sowohl in *B. subtilis* als auch in *E. coli* eine große Anzahl kleiner regulatorischer RNAs existieren, die neben den bisher bekannten Prozessen der Stressantwort eine Vielzahl anderer Prozesse wie Sporulation, Kompetenz oder Sekretion kontrollieren könnten.

Als Regulatoren der Genexpression auf post-transkriptionaler Ebene können *trans*-kodierte Antisense-RNAs die Translation und Stabilität ihrer Target-mRNAs sowohl negativ als auch positiv beeinflussen (s. Abb. 2A). Die Mehrzahl der bisher untersuchten RNAs inhibiert die Translationsinitiation durch Blockierung der Ribosomenbindungsstelle (RBS) und fördert gleichzeitig den Abbau der Target-mRNA durch Ribonukleasen (z. B. OxyS bei *fhlA* RNA, Altuvia *et al*., 1998; Spot42 bei *galK* RNA, Møller *et al*., 2002b; SgrS bei *ptsG* RNA, Vanderpool und Gottesman, 2004, Kawamoto *et al.,* 2005; RyhB bei *sodB* RNA, Massé und Gottesman, 2002, Massé *et al.,* 2003, Geissmann und Touati, 2004, Afonyushkin *et al*., 2005 und MicA bei *ompA* RNA, Rasmussen *et al*., 2005, Udekwu *et al*., 2005). In einigen Fällen bewirkt die Interaktion zwischen Antisense-RNA und Target-mRNA eine Konformationsänderung in der mRNA. Dadurch wird eine Anlagerung der Ribosomen an die RBS der mRNA und damit die Translation überhaupt erst ermöglicht (z. B. RNAIII bei *hla* RNA, Morfeldt *et al.,* 1995; DsrA bei *rpoS* RNA, Majdalani *et al.,* 1998, Lease und Belfort, 2000, Lease *et al.,* 1998; RprA bei *rpoS* RNA, Majdalani *et al.,* 2002).

Im Gegensatz dazu nutzen einige der bisher entdeckten regulatorischen RNAs nicht das Prinzip der RNA-RNA Interaktion, sondern interagieren mit einem Protein und

wirken auf diese Weise regulierend. Dazu gehört die 6S RNA (184 nt) aus *E. coli*, deren Funktion lange Zeit unbekannt war. Mittlerweile konnte aufgeklärt werden, dass sie spezifisch und fest an die RNA-Polymerase in Anwesenheit des Sigmafaktors 70 (σ^{70}) bindet, weil sie aufgrund ihrer Struktur der offenen DNA-Konformation von σ^{70}-Promotoren sehr ähnlich ist (Wassarman und Storz, 2000; Trotochaud und Wassarman, 2004). Dadurch wird die Bindung der σ^{70}-Form der RNA-Polymerase an Promotoren verhindert und der anderen alternativen Sigmafaktor S (σ^{S})-gebundenen Form der RNA-Polymerase eine Bindung in der Stationärphase erleichtert. Die 6S RNA wurde sowohl in gramnegativen als auch in grampositiven Bakterien gefunden. Interessanterweise wurde in *Bacillus subtilis* neben zwei 6S-ähnlichen RNAs noch eine dritte RNA identifiziert, die eine alternative Form der RNA-Polymerase bindet, mit der insgesamt 17 verschiedene Sigma-Faktoren wechselwirken (Trotochaud und Wassarman, 2005; Barrick *et al.,* 2005). Diese Tatsache lässt vermuten, dass weitere kleine regulatorische RNAs existieren, die verschiedene Formen der RNA-Polymerase binden und modulieren.

Darüber hinaus wurde eine Familie kleiner regulatorischer RNAs identifiziert, die mit Translationsregulatoren interagieren und diese damit ihrer Funktion an ihren Target-mRNAs entziehen. Dazu zählen CsrB und CsrC in *E. coli* (Weilbacher *et al.,* 2003) sowie RsmY und RsmZ in *Pseudomonas fluorescens* (Valverde *et al.,* 2004), die die biologischen Funktionen (z. B. Glykogen-Biosynthese, Biofilm-Produktion) der Regulatorproteine CsrA und RsmA inhibieren (zusammengefasst in: Romeo, 1998). Abbildung 2B zeigt schematisch den Wirkungsmechanismus dieser Art von regulatorischen RNAs am Beispiel der CsrB-RNA.

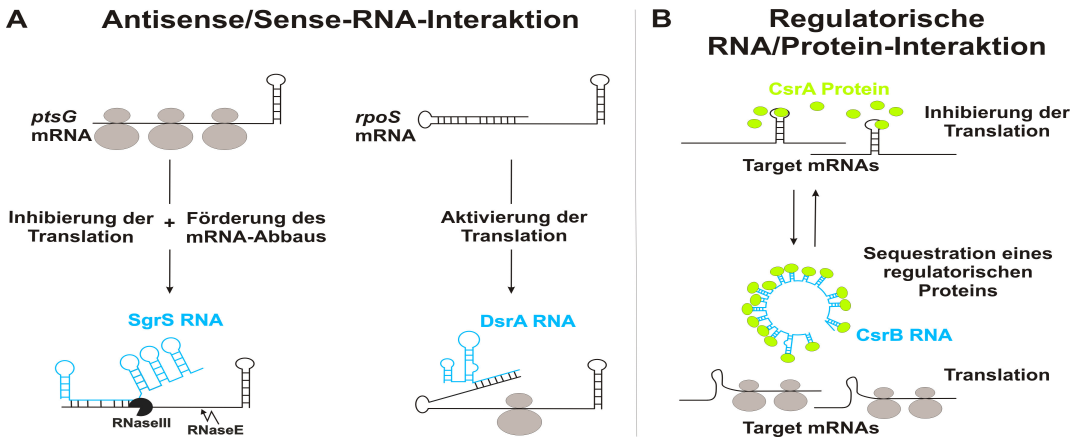

Abb. 2: Wirkungsmechanismen regulatorischer RNAs. (A) blau: Antisense-RNAs; schwarz: Sense-RNAs; graue Ovale: Untereinheiten des Ribosoms; (B) blau: Antisense-RNA; grüner Kreis: Translationsregulator; schwarz: Target-mRNAs; graue Ovale: Untereinheiten des Ribosoms; Erläuterungen s. Text (nach The RNA World, 2006, S. 575 und 584)

Tabelle 2. Beispiele *trans*-kodierter regulatorischer RNAs

RNA	bekannte Target(s)	Biologische Funktion	Mechanismus	Referenz
Antisense/Sense-RNA-Interaktion				
Escherichia coli				
MicA	*ompA**	Membran-Zusammensetzung	Translationsinhibierung und mRNA-Abbau	Rasmussen *et al.,* 2005 Udekwu *et al.,* 2005
MicC	*ompC**			Chen *et al.,* 2004
MicF	*ompF**			Andersen *et al.,* 1989
OmrA/OmrB	*ompT, cirA, fecA, fepA*			Guillier und Gottesman, 2006
RseX	*ompA*, ompC*		*?*	Douchin *et al.,* 2006
RyhB	*sodB*, acnA sdhD, fumA, bfr, ftn*	Eisen-Metabolismus	Translationsinhibierung und mRNA-Abbau	Masse *et al.,* 2005 Geissmann und Touati, 2004
Spot42	*galK**	Galactoseverwertung	Translationsinhibierung	Møller *et al.,* 2002b
SgrS	*ptsG**	Glucose-Transport	Translationsinhibierung und mRNA-Abbau	Vanderpool und Gottesman, 2004, Kawamoto *et al.,* 2005
OxyS	*rpoS**	Stationärphaseregulation	Sequestration von Hfq	Zhang *et al.,* 1998
	fhlA,*	Format-Metabolismus	Translationsinhibierung und mRNA-Abbau	Altuvia *et al.,* 1998
DsrA	*rpoS**	Stationärphaseregulation	Translationsaktivierung	Sledjeski *et al.,* 1996
	*hnS**	Nucleoid-Struktur/ Genrepression	Translationsinhibierung und mRNA-Abbau	Sledjeski und Gottesman, 1995
RprA	*rpoS**	Stationärphasereguletion	Translationsaktivierung	Majdalani *et al.,* 2002
IstR	*tisAB**	Antitoxin/Toxin	Translationsinhibierung und mRNA-Abbau	Vogel *et al.,* 2004
Vibrio cholerae				
Qrr1-Qrr4	*hapR*	Virulenz	Translationsinhibierung und mRNA-Abbau	Lenz *et al.,* 2004
Salmonella typhimurium				
MicA	*ompA,*	Membran-Zusammensetzung	?	Papenfort *et al.,* 2006
RybB	*ompC*,*			
	ompD, ompN**		?	Papenfort *et al.,* 2006
Pseudomonas aeruginosa				
PrrF1/PrrF2	*sodB, sdhD, bfr*	Eisen-Metabolismus	Translationsinhibierung und mRNA-Abbau	Wilderman *et al.,* 2004
Bacillus subtilis				
SR1	*ahrC**	Arginin-Katabolismus	Translationsinhibierung	Heidrich *et al.,* 2006
Staphylococcus aureus				
RNAIII	*hla*	Hämolysin-Synthese	Translationsaktivierung	Morfeldt *et al.,* 1995
	*spa**	Wirt-Pathogen-Interaktion	Translationsinhibierung und mRNA-Abbau	Huntzinger *et al.,* 2005
SprA-SprG	?	?	?	Pichon und Felden, 2005
Streptococcus pyogenes				
FasX	?	Virulenz	?	Kreikemeyer *et al.,* 2001
Pel	?	Virulenz	?	Mangold *et al.,* 2004
Clostridium perfringens				
VR RNA	?	Virulenz	?	Shimizu *et al.,* 2002
VirX	?	Virulenz	?	Ohtani *et al.,* 2002
Chlamydia trachomatis				
LhtA	*Hc1*	Nucleoid-Struktur	?	Grieshaber *et al.,* 2006
RNA/Protein-Interaktion				
Escherichia coli				
CsrB/CsrC	CsrA-Protein	Glykogen-Biosynthese, Biofilm-Produktion	Protein-Sequestration	Weilbacher *et al.,* 2003,
6S	σ^{70}-Form der RNA-Polymerase	Stationärphaseregulation	Protein-Sequestration	Wassarman und Storz, 2000
Vibrio cholerae				
CsrB/CsrC/ CsrD	CsrA-Protein	Virulenz	Protein-Sequestration	Lenz *et al.,* 2005
Pseudomonas fluorescens				
RsmZ/RsmY RsmX	RsmA-Protein	Sekundär-Metabolismus	Protein-Sequestration	Kay *et al.,* 2005 Valverde *et al.,* 2004
Pseudomonas aeruginosa				
RsmZ/RsmB	RsmA-Protein	Sekundär-Metabolismus	Protein-Sequestration	Burrowes *et al.,* 2005, Heurlier *et al.,* 2004

*Die Interaktion zwischen Antisense-RNA und Target-mRNA wurde experimentell bestätigt. (?), Target(s), Mechanismus und Funktion sind noch nicht bekannt.

1.2. Das Hfq-Protein

Für viele *trans*-kodierte Antisense-RNAs konnte gezeigt werden, dass sie das Protein Hfq als Co-Faktor benötigen, um regulatorisch wirken zu können. Das RNA-Chaperon Hfq wurde in *E. coli* als ein Wirtsfaktor (host factor) identifiziert, der für die Replikation des Bakteriophagen Qβ essentiell ist (Franze de Fernandez *et al.,* 1968). Hfq ist in einer Vielzahl von Bakterienspezies konserviert und variiert in seiner Länge zwischen 70 und 100 Aminosäuren. Als abundantes Protein (60.000 Moleküle pro Zelle) kommt es im Cytoplasma in Assoziation mit den Ribosomen vor. Es konnte gezeigt werden, dass es direkt über die 30S Untereinheit mit den 70S Ribosomen interagiert (DuBow *et al.,* 1977). Die Inaktivierung des *hfq*-Gens in *E. coli* verursacht pleiotrope Effekte (Abnahme der Wachstumsrate, UV-Licht-Empfindlichkeit und Zunahme der Zellänge; Tsui *et al.,* 1994; Muffler *et al.,* 1997) und zeigt die biologische Relevanz dieses Proteins für die Genexpression. Für Hfq wurde nachgewiesen, dass es an der mRNA-Stabilität, mRNA-Polyadenylierung und Translation beteiligt ist. In mehreren Fällen gelang der Nachweis, dass Hfq an einzelsträngige RNA-Bereiche mit einer Präferenz für A/U-reiche Sequenzen bindet: Qβ-RNA (Senear und Steitz, 1976), *ompA*-mRNA (Vytvytska *et al.,* 2000; Moll *et al.,* 2003), DsrA (Brescia *et al.,* 2003), OxyS (Zhang *et al.,* 2002) und Spot42 (Møller *et al.,* 2002a). Die Bindungsstellen für Hfq werden generell von 1-2 Stem-Loops flankiert. Damit zeigt Hfq große Übereinstimmungen mit der Sm- und Sm-ähnlichen (Lsm) Proteinfamilie, die eine Schlüsselrolle im RNA-Metabolismus von Eukaryoten spielt. Mit Hilfe von Kristallstrukturanalysen konnte gezeigt werden, dass Hfq nur ein Sm1-Motiv enthält und eine Homohexamer-Ringstruktur ausbildet (Schuhmacher *et. al.,* 2002; Sauter *et al.,* 2003). Als einzelstrangbindendes Protein hat Hfq in *E. coli* zum einen auf die Struktur vieler *trans*-kodierter Antisense-RNAs einen stabilisierenden Effekt (DsrA, Sledjeski *et al.,* 2001; Spot42, Møller *et al.,* 2002a; RyhB, Massé *et al.,* 2003; Moll *et al.,* 2003), und/oder fördert zum anderen die Interaktion mit ihren Target-RNA(s) (OxyS/*fhlA*,*rpoS,* Zhang *et al.,* 2002; Spot42*/galK,* Møller *et al.,* 2002a; RyhB/*sodB*, Geissmann und Touati, 2004; Afonyushkin *et al.,* 2005; MicA/*ompA*, Rasmussen *et al.,* 2005).

Eine Bedeutung von Hfq für den Regulationsprozess von Antisense-RNAs in grampositiven Bakterien war bisher nicht nachweisbar. Einige der bisher identifizierten RNAs binden zwar Hfq (RNAIII aus *Staphylococcus aureus*, Huntzinger *et al.,* 2005, und LhrA-LhrC aus *Listeria monocytogenes*, Christiansen *et al.,* 2006), jedoch hatte Hfq im Fall von RNAIII weder einen Effekt auf die Stabilität dieser RNA noch förderte es die Interaktion mit ihren Target-RNAs (Bohn *et al.,* 2007). Es kann jedoch nicht ausgeschlossen werden, dass Hfq für andere, bislang noch nicht wahrgenommene

Aufgaben benötigt wird. Alternativ ist auch vorstellbar, dass in grampositiven Bakterien andere RNA-Chaperone die Funktionen von Hfq übernehmen. Ein geeigneter Kandidat dafür ist das Hbsu-Protein, für das gezeigt werden konnte, dass es RNA bindet (Nakamura *et al.*, 1999).

1.3. Sensorische RNAs

Erst seit einiger Zeit ist bekannt, dass RNAs auch als Sensoren von Umweltbedingungen eine zentrale Rolle für die genetische Kontrolle metabolischer Prozesse in Prokaryoten spielen (Winkler und Breaker, 2005). In den meisten Fällen sind sensorische RNAs in der 5'-untranslatierten Region (5'-UTR) von mRNAs lokalisiert. Hier bilden sie komplexe RNA-Strukturen aus, die über Signal-induzierte Konformationsänderungen die Expression stromabwärts gelegener Gene kontrollieren. Diese Signale können physikalischen (RNA-Thermometer) oder chemischen (Riboswitches) Ursprungs sein (Naberhaus *et. al.,* 2006).

1.3.1. RNA-Thermometer

RNA-Sensoren, die die Temperatur direkt messen, werden als RNA-Thermometer bezeichnet. Sie sind an der Kontrolle einer Vielzahl von zellulären Prozessen in Prokaryoten wie Hitze- und Kälteschockantworten sowie der Expression von Virulenzgenen in pathogenen Bakterien beteiligt (zusammengefasst in: Gualerzi *et. al.,* 2003; Naberhaus *et al.,* 2006). RNA-Thermometer bilden komplexe RNA-Strukturen aus einem oder mehreren Stem-Loops aus, die ihre Konformation in Abhängigkeit von der Temperatur verändern und damit die Expression von Genen regulieren (Johansson *et al.,* 2002; Waldminghaus *et al.,* 2005). Alle bisher bekannten RNA-Thermometer kontrollieren die Translationsinitiation. Als *cis*-aktive regulatorische Elemente sind sie auf der m-RNA lokalisiert. Dort blockieren sie bei niedrigen Temperaturen den Zugang zur RBS und verhindern die Translation bestimmter Hitzeschock- und Virulenzgene. Ein Temperaturanstieg führt zum Aufschmelzen der RNA-Struktur, wodurch die Anlagerung des Ribosoms an die Shine-Dalgarno(SD)-Sequenz der mRNA gefolgt von der Proteinbiosynthese ermöglicht wird. Zusätzlich schützen die translatierenden Ribosomen die mRNA vor einem Abbau durch Ribonukleasen (s. Abb. 3A), (zusammengefasst in: Naberhaus *et. al.,* 2006).

Eines der am besten charakterisierten RNA-Thermometer ist an der Kontrolle der Expression von Hitzeschockproteinen (Hsps) in *E. coli* beteiligt. Die Mehrzahl der Hitzeschockproteine in *E. coli* wird auf der Ebene der Transkription durch den Hitzeschock-Sigmafaktor σ^{32} (RpoH) positiv reguliert (Yura *et. al.,* 2000). Die

Translationskontrolle des Sigmafaktors erfolgt über ein RNA-Thermometer, das aus zwei Segmenten besteht, die bis in die kodierende Region des *rpoH*-Transkripts hineinreichen (Morita *et. al.,* 1999a; Morita *et. al.,* 1999b). Die Ausbildung einer Sekundärstruktur innerhalb dieser Segmente blockiert die Translation bei optimalen Wachstumstemperaturen. Bei Hitzeschock-Temperaturen konnte gezeigt werden, dass es zum Aufschmelzen der *rpoH*-Thermometerstruktur kommt.

Eines der am weitesten verbreiteten RNA-Thermometer ist das ROSE-Element (Repression Of heat Shock gene Expression), das in *Bradyrhizobium japonicum* entdeckt wurde (Naberhaus *et. al.,* 1998). Mittlerweile wurden mehr als 40 weitere ROSE-ähnliche Thermometer in diversen anderen α- und γ-Proteobakterien vorhergesagt, die alle stomaufwärts von Genen für kleine Hitzeschockproteine lokalisiert sind (Nocker *et al*. 2001; Balsiger *et al*., 2004; Waldminghaus *et. al.,* 2005). Wie beim *rpoH*-Thermometer gewährleisten auch beim ROSE-Element imperfekte Basenpaarungen ein Aufschmelzen der Sekundärstruktur bei erhöhten Temperaturen und ermöglichen eine anschließende Translation der ROSE-kontrollierten Gene unter Hitze-Schock-Bedingungen.

Für die Expression von Kälteschockgenen als Antwort auf das Absinken der Temperatur wird ebenfalls vermutet, dass sie auf einer temperaturabhängigen Kontrolle ihrer eigenen RNA-Strukturen basiert (zusammengefasst in: Thieringer *et al.,* 1998; Gualerzi *et. al.,* 2003). Nicht zuletzt gibt es Beweise, dass RNA-thermosensitive Strukturen an der Regulation und Produktion von Virulenzfaktoren in humanpathogenen Bakterien beteiligt sind (Hoe & Goguen, 1993; Johansson *et. al.,* 2002).

1.3.2. Riboswitches

Ein ähnliches Prinzip wie bei RNA-Thermometern wird von den ebenfalls erst vor einigen Jahren entdeckten Riboswitches (Riboschaltern) in Prokaryoten verwendet. Diese *cis*-aktiven Regulationselemente binden unterschiedliche zelluläre Metabolite wie z. B. Coenzyme, Aminosäuren, Nukleotide, Zucker-Moleküle oder Ionen (Mg^{2+}) und sind in der 5'-UTR einer großen Zahl von Genen lokalisiert. Durch die spezifische Bindung dieser Moleküle an die RNA wird eine strukturelle Veränderung induziert, durch die die Expression der nachfolgenden Gene entweder an- oder abgeschaltet wird. Dabei kann die Kontrolle der Genexpression auf der Ebene von Translationsinitiation, Transkriptionstermination oder durch RNA-Abbau erfolgen (Winkler and Breaker, 2005). Das erste publizierte Beispiel ist der Riboflavin-Riboswitch in *Bacillus subtilis*, der über den Mechanismus der Transkriptionsattenuierung wirkt (Mironov *et al.,* 2002). Die Wirkungsweise des

Riboflavin-Riboswitches ist in Abbildung 3B schematisch dargestellt. Die Entdeckung sensorischer RNA-Sequenzen wie RNA-Thermometer und Riboswitches unterstützt nach der Entdeckung der Ribozyme als katalytisch aktiver RNAs die Theorie einer RNA-Welt vor dem Auftreten von Proteinen.

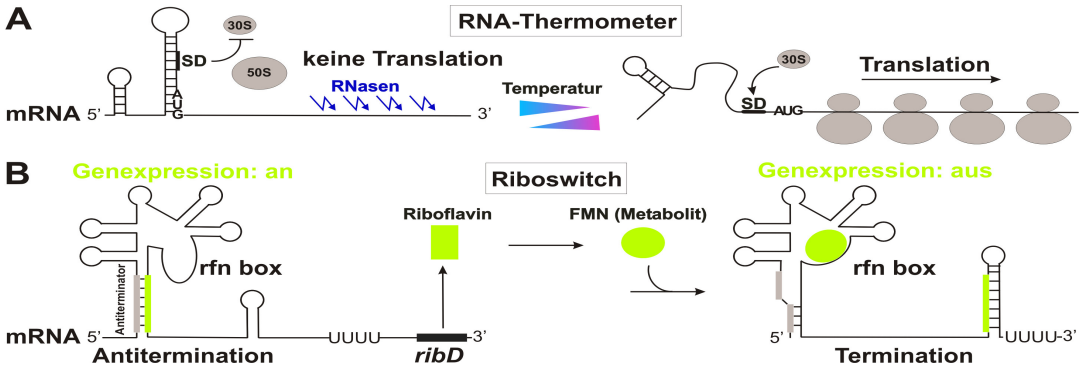

Abb. 3: Wirkungsmechanismen sensorischer RNAs. (A) RNA-Thermometer; schwarz: mRNA; graue Ovale: 30S und 50S Untereinheit des Ribosoms; Temperaturänderungen sind durch blau (kälter) und rot (wärmer) dargestellt; Erläuterungen s. Text (nach Naberhaus *et al.*, 2006); (B) Riboflavin-Riboswitch. In Abwesenheit von FMN faltet sich die 'leader'-Region der *ribD*-mRNA in eine Antiterminator-Struktur (graues Rechteck). In Anwesenheit von FMN (Flavin-Mononukleotid: grüner Kreis) wird durch die Bindung des Metaboliten an die rfn (Rifampin)-Box die Ausbildung einer Terminator-Struktur gefördert, wodurch die Transkription frühzeitig abgebrochen und die Riboflavin-Biosynthese verhindert wird (nach Brantl, 2004).

1.4. Zielsetzung

Regulatorische und sensorische RNAs bei Pro- und Eukaryoten rückten in den letzten 5 Jahren in den Blickpunkt der Aufmerksamkeit und widerlegten eindrucksvoll die Annahme der Nutzlosigkeit vieler Transkripte. Für die geringe Anzahl der bisher charakterisierten regulatorischen und sensorischen RNAs in Prokaryoten hat man vielfältige funktionelle Aktivitäten festgestellt. Es ist daher anzunehmen, dass die detaillierte Charakterisierung weiterer RNA-Moleküle und ihrer Targets noch viele Überraschungen parat halten wird und neue biologische Funktionen und Wirkungsmechanismen aufgeklärt werden können. Im Rahmen dieser Arbeit sollen eine *cis*-kodierte und eine *trans*-kodierte Antisense-RNA aus *Bacillus subtilis* sowie eine RNA-Thermometerstruktur aus *Salmonella enterica in vitro* strukturell und funktionell charakterisiert und damit die bisherigen Forschungsergebnisse wirkungsvoll ergänzt werden.

Die *cis*-kodierte Antisense-RNA RNAIII (136 nt) reguliert über Transkriptions-attenuierung der essentiellen *repR*-mRNA (RNAII) die Replikation des Streptokokkenplasmides pIP501. Ziel dieser Arbeit war es, die minimalen Sequenz-

und Struktur-Anforderungen an eine inhibitorische RNAIII zu ermitteln und zu untersuchen, ob die Loops L3 und L4 von RNAIII von gleicher Bedeutung für den initialen Kontakt mit der Target-RNA (RNAII) sind. Dazu sollte zunächst eine detaillierte Sekundärstruktur von RNAIII (136 nt full-length-Spezies) ermittelt und der Komplex aus RNAII und RNAIII kartiert werden. Um die Frage zu beantworten, ob nur ein Loop-Loop-Kontakt zwischen RNAIII-L3/RNAII-L2 und/oder RNAIII-L4/RNAII-L1 als inhibitorischer Komplex notwendig ist und sich kein Komplex mit in die Helices hineinreichenden Dupleces ausbildet (’extended-kissing’-Komplex), wurden Mutationen im unteren Stem-Bereich von RNAIII-L3 und/oder -L4 und im Spacer zwischen den Stem-Loops L3 und L4 erzeugt und deren Einfluss auf die Effizienz der Transkriptionstermination mittels Bestimmung der Inhibitionskonstanten der entsprechenden Mutanten in einem 'single-round’-Transkriptionstest untersucht **(Manuskript I)**.

SR1 (small RNA1), die in der *phd-speA*-intergenischen Region im Chromosom von *B. subtilis* kodiert ist, wird beim Übergang in die stationäre Wachstumsphase exprimiert und ist nicht essentiell für *B. subtilis* sowie bei Überexpression nicht toxisch. Mittels 2D-Gelanalysen von Proteinrohextrakten aus Wildtyp- und SR1-knockout-Stämmen wurden 3 mögliche Targets identifiziert, RocA, D und F. Sie unterliegen alle einer positiven Kontrolle durch die Transkriptionsaktivatoren AhrC und RocR. Eine Computer-Analyse der RNA-Sequenzen der identifizierten Targets sowie der *ahrC*-mRNA und *rocR*-mRNA ergab jedoch nur zwischen SR1 und der *ahrC*-mRNA einen Bereich partieller Komplementarität.
Ziel dieser Arbeit war die Analyse der Interaktion mit *ahrC*-mRNA, dem ersten potentiellen primären Target von SR1, und die Untersuchung der Wirkungsweise von SR1. Zunächst sollten Gelshiftassays zum direkten Nachweis der spezifischen Komplexbildung zwischen *ahrC*-RNA und SR1 durchgeführt und die entsprechende Paarungskonstante bestimmt werden, um AhrC als erstes primäres Target zu bestätigen. Zur Untersuchung der Frage, ob die Komplementarität zwischen *ahrC*-RNA und SR1 für den Abbau oder für die Translationsinhibierung der *ahrC*-RNA eine Rolle spielt, sollte zunächst mit Hilfe einer RT-PCR die Menge an *ahrC*-RNA im Wildtyp- und SR1-knockout-Stamm sowie im Hfq-knockout- und RNase III-defizienten-Stamm bestimmt werden. Bei unveränderter Menge an *ahrC*-RNA sollte anschließend der Einfluss von SR1 auf die Proteinmenge an AhrC in einem *in vitro*-Translationsassay analysiert werden **(Manuskript II)**.

Aufbauend auf den Daten von Manuskript II war eine detaillierte *in vitro*-Analyse sowohl zur SR1/*ahrC*-Komplexbildung als auch zum Mechanismus der SR1-Wirkung das Ziel dieser Arbeit. Dazu wurden sowohl die Sekundärstruktur von SR1 als auch die Sekundärstruktur des SR1/*ahrC*-Komplexes bestimmt. Um festzustellen, welche Segmente am initialen Schritt der SR1/*ahrC*-Interaktion beteiligt sind, sollten Komplexbildungsstudien mit sukzessive verkürzten SR1- oder *ahrC*-RNA-Spezies durchgeführt und dann durch Analysen von Punkmutationen in den entsprechenden Segmenten unterlegt werden. Um auszuschließen, dass die Effekte auf veränderten Sekundärstrukturen und nicht auf veränderten SR1-Größen beruhen, war es außerdem erforderlich, die Sekundärstrukturen der verkürzten SR1-Spezies zu kartieren. Um die Frage zu beantworten, ob Hfq zur Stabilisierung der Interaktion zwischen beiden RNAs benötigt wird, sollte die Komplexbildung parallel in An- und Abwesenheit von Hfq untersucht und der Bindungsort von Hfq an SR1 und/oder AhrC eingegrenzt werden. Toeprint-Analysen in Gegenwart von SR1 sollten die Untersuchungen zum Mechanismus der SR1-vermittelten Translationsinhibierung aus Manuskript II im Hinblick auf die Blockierung der RBS der *ahrC*-mRNA ergänzen. Darüber hinaus wurde die SR1-Konzentration in der log-Phase und in der Stationär-Phase (zum Zeitpunkt ihrer maximalen Expression) bestimmt, um abzuschätzen, in welchem Überschuss SR1 gegenüber ihrem Target vorliegt **(Manuskript III)**.

In *Salmonella enterica* konnte mit Hilfe von Computerprogrammen eine potentielle RNA-Thermometerstuktur stromaufwärts des Hitzeschockgens *agsA* vorhergesagt werden, die keinem der bisher identifizierten RNA-Thermometer-Typen entspricht. Ziel dieser Arbeit war es, die tatsächliche RNA-Struktur des gesamten *agsA*-Thermometers *in vitro* aufzuklären, um einen Einblick in den temperaturabhängigen Wirkungsmechanismus dieser RNA-Struktur zu gewinnen. Dazu wurden die Sekundärstrukturen des RNA-Thermometers bei 30° C und bei 42° C bestimmt. Darüber hinaus sollten Toeprint-Analysen bei entsprechenden Temperaturen nachweisen, dass tatsächlich nur bei erhöhten Temperaturen die Bindung von Ribosomen an die mRNA erfolgen kann **(Manuskript IV)**.

2. Übersicht zu den Manuskripten

Manuskript I

Nadja Heidrich and Sabine Brantl (2007):

Antisense RNA-mediated transcriptional attenuation in plasmid pIP501: the simultaneous interaction between two complementary loop pairs is required for efficient inhibition by the antisense RNA

Microbiology, 153, 420-427

In dieser Publikation werden die seuqenz- und strukturspezifischen Eigenschaften der inhibitorisch wirksamen *cis*-kodierten Antisense-RNA RNAIII des Streptokokken-plasmides pIP501 untersucht. Detaillierte *in vitro*-Analysen des inhibitorischen Komplexes zwischen RNAIII und ihrer Target-RNA (RNAII) geben Aufschluss über die minimalen Sequenz- und Struktur-Anforderungen an eine effiziente Interaktion zwischen Antisense- und Sense-RNA in einem plasmidkodierten Kontrollsystem grampositiver Bakterien.

Alle Experimente in dieser Publikation wurden von Nadja Heidrich erdacht, durchgeführt und ausgewertet. Der erste Entwurf zum Manuskript wurde von Sabine Brant erstellt. Nadja Heidrich und Sabine Brantl haben gemeinsam das Manuskript korrigiert und verbessert.

Manuskript II

Nadja Heidrich, Alberto Chinali, Ulf Gerth and Sabine Brantl (2006):

The small untranslated RNA SR1 from the *B. subtilis* genome is involved in the regulation of arginine catabolism

Molecular Microbiology, 62, 520-36

Diese Publikation beschreibt die strukturelle und funktionelle *in vitro*-Charakterisierung der chromosomal kodierten RNA SR1 aus *Bacillus subtilis* sowie die Identifizierung ihres ersten primären Targets und untersucht den Einfluss von Hfq auf die Stabilität von SR1 *in vivo*. Eine Kombinaton aus 2D-Gelanalysen, Northernblots, *in vitro*-Komplexbildungsstudien und *in vitro*-Translationsassays sowie *in vivo*-Reportergen-fusionstests und RT-PCR zeigt erstmals, dass es sich bei SR1 um eine regulatorische Antisense-RNA handelt, die an der Regulation des Arginin-Katabolismus in *B. subtilis* beteiligt ist.

Die 2D-Gelanalysen zur Identifizierung der sekundären Targets RocA, D aund F (Enzyme des Arginin-Katabolismus, die einer positiven Kontrolle von AhrC unterliegen) von SR1 wurden im Labor von Dr. Ulf Gerth an der Ernst-Moritz-Arndt-Universität Greifswald durchgeführt. Northernblot-Analysen zur Verifizierung dieser Daten und eine Computeranalyse zur Vorhersage komplementärer Bereiche zwischen SR1 und *ahrC*-mRNA wurden von Alberto Chinali durchgeführt. Alberto Chinali untersuchte auch den Einfluss von Hfq auf die Stabilität von SR1 *in vivo.* Sowohl die *in vitro*-Analyse der Interaktion mit *ahrC*-mRNA, dem ersten potentiellen primären Target von SR1, mittels Komplexbildungsstudien und Kompetitionsexperimenten als auch die Untersuchung der Wirkungsweise von SR1 mit Hilfe von RT-PCR und *in vitro*-Translationsassays wurden von Nadja Heidrich geplant und durchgeführt. Sabine Brantl bestätigte mit Hilfe von *in vivo*-Reportergenfusionstests die Ergebnisse der *in vitro*-Experimente von Nadja Heidrich. Nadja Heidrich und Sabine Brantl haben das Konzept zum Manuskript verfasst. Alle anderen Autoren haben das Manuskript korrigiert und ergänzt.

Manuskript III

Nadja Heidrich, Isabella Moll and Sabine Brantl:

***In vitro* analysis of the interaction between the small RNA SR1 and its primary target *ahrC*-RNA**

Manuskript für *Nucleic Acids Research*, eingereicht am 20.04.2007

Diese Publikation stellt die Ergebnisse einer detaillierten *in vitro*-Analyse zur SR1/*ahrC*-Komplexbildung und zum Mechanismus der SR1-vermittelten Translationsinhibierung der *ahrC*-mRNA dar und untersucht die Bedeutung des Hfq-Chaperons für die SR1/*ahrC*-Interaktion sowohl *in vitro* als auch *in vivo*. Darüber hinaus wurde neben der Sekundärstruktur von SR1 und des SR1/*ahrC*-Komplexes die intrazelluläre Konzentration von SR1 unter unterschiedlichen Wachstumsbedingungen bestimmt.

Bis auf die von Sabine Brantl durchgeführte Analyse zur Bedeutung von Hfq für die SR1/*ahrC*-Interaktion *in vivo* wurden alle Experimente in dieser Arbeit von Nadja Heidrich konzipiert, durchgeführt und ausgewertet. Die ausgewerteten Daten wurden mit Isabella Moll und Sabine Brantl diskutiert. Das Manuskript wurde von Sabine Brantl verfasst. Nadja Heidrich und Isabella Moll haben das Manuskript korrigiert, vervollständigt und verbessert.

Manuskript IV

Torsten Waldminghaus, Nadja Heidrich, Sabine Brantl and Franz Naberhaus:

FourU – A novel type of RNA thermometer in *Salmonella* and other bacteria

Manuskript für *Molecular Microbiology*, eingereicht am 31.03.2007

In dieser Publikation wird die Existenz einer potentiellen RNA-Thermometerstruktur im Hitzeschockgen *agsA* von *Salmonella enterica* nachgewiesen und damit das erste Mitglied einer ganz neuen Klasse an RNA-Thermometern strukturell und biochemisch charakterisiert.

Die potentielle RNA-Thermometerstruktur wurde mit Hlife einer computergestützten Genomanalyse von Torsten Waldminghaus in der 5'-UTR des *agsA*-Gens vorhergesagt. Die strukturelle Analyse der thermosensitiven RNA-Struktur in der 5'-UTR von *agsA* wurde zu gleichen Teilen von Nadja Heidrich und Torsten Waldminghaus geplant und durchgeführt. Toeprint-Analysen zum direkten Nachweis der temperaturabhängigen Ribosomenbindung an die *agsA*-mRNA wurden von Nadja Heidrich geplant, durchgeführt und ausgewertet. Reportergenfusionstests zum funktionellen Nachweis des RNA-Thermometers *in vivo* und Mutagenesestudien wurden von Torsten Waldminghaus konzipiert, durchgeführt und ausgewertet. Torsten Waldminghaus hat den Hauptteil des Manuskriptes verfasst. Nadja Heidrich, Sabine Brantl und Franz Naberhaus haben das Manuskript korrigiert, ergänzt und verbessert.

3. Antisense RNA-mediated transcriptional attenuation in plasmid pIP501: the simultaneous interaction between two complementary loop pairs is required for efficient inhibition by the antisense RNA

[Manuskript I]

Nadja Heidrich[1] and Sabine Brantl[1]

[1]AG Bakteriengenetik, Friedrich-Schiller-Universität Jena, Philosophenweg 12, D-07743 Jena, Germany

publiziert in *Microbiology*, **153**: 420-427

Microbiology (2007), **153**, 420–427 DOI 10.1099/mic.0.2006/002329-0

Antisense RNA-mediated transcriptional attenuation in plasmid pIP501: the simultaneous interaction between two complementary loop pairs is required for efficient inhibition by the antisense RNA

Nadja Heidrich and Sabine Brantl

Friedrich-Schiller-Universität Jena, AG Bakteriengenetik, Philosophenweg 12, D-07743 Jena, Germany

Correspondence
Sabine Brantl
Sabine.Brantl@uni-jena.de

Received 12 September 2006
Revised 2 November 2006
Accepted 14 November 2006

Streptococcal plasmid pIP501 uses antisense RNA-mediated transcriptional attenuation to regulate its replication. Previous *in vitro* assays suggested that binding intermediates between RNAII (sense RNA) and RNAIII (antisense RNA) are sufficient for inhibition, and a U-turn structure on RNAII loop L1 was found to be crucial for the interaction with RNAIII. Here, sequence and structural requirements for an efficient RNAII–RNAIII interaction were investigated. A detailed probing of RNA secondary structure combined with *in vitro* single-round transcription assays indicated that complex formation between the two molecules progresses into the lower stems of both loop pairs of the sense and antisense RNAs, but that the complex between RNAII and RNAIII is not a full duplex. Stem–loops L3 and L4 were required to be linked to one other for efficient contact with the complementary loops L2 and L1 of the sense RNA, indicating a simultaneous interaction between these two loop pairs. Thereby, the sequence and length of the spacer connecting L3 and L4 were shown not to be important for inhibition.

INTRODUCTION

Antisense RNA-mediated gene regulation has been found and studied in prokaryotic accessory DNA elements such as plasmids, phages and transposons, and a broad variety of regulatory mechanisms has been observed (reviewed by Brantl, 2004). During the past 5 years, a growing number of recently identified chromosomally encoded small RNAs have been included in such studies (e.g. Zhang *et al.*, 2002; Rasmussen *et al.*, 2005; Udekwu *et al.*, 2005). Independently of whether binding initiates by loop–loop contacts (plasmid copy number control systems) or linear region–loop contacts (e.g. hok/sok of plasmid R1; Thisted *et al.*, 1994), a rapid interaction between antisense and target RNA has been shown to be crucial for regulation (reviewed by Wagner *et al.*, 2002). Structural requirements for efficient antisense RNAs have been defined (Hjalt & Wagner, 1992, 1995) and pairing rate constants for sense/antisense RNA pairs calculated to be mainly in the range of 10^6 M^{-1} s^{-1}. Only for a few plasmid-encoded antisense RNA systems has a detailed biochemical analysis been performed to investigate the structural and sequence requirements for inhibition (e.g. Asano & Mizobuchi, 2000; Greenfield *et al.*, 2001). For CopA (antisense RNA) of plasmid R1, the multistep pathway of interaction with its sense RNA (CopT) has been elucidated in detail, and a four-helix junction has been identified as the inhibitory intermediate (Kolb *et al.*, 2000a, b). A subsequent study on Inc RNA/*repZ* mRNA of Col1b-P9 suggests that similar pathways are used to form inhibitory antisense–target RNA complexes (Kolb *et al.*, 2001). Apparently, in many cases, kissing is sufficient for inhibition, and inhibitory intermediates as in R1 are only slowly converted into full duplexes (Wagner & Brantl, 1998; Malmgren *et al.*, 1997).

Streptococcal plasmid pIP501 exerts its replication control by the concerted action of a small antisense RNA (RNAIII, 136 nt) and a transcriptional repressor, CopR (Brantl & Behnke, 1992). The deletion of either control component causes a 10- to 20-fold increase in plasmid copy number; a simultaneous deletion has, however, no additive effect. RNAIII functions by transcriptional attenuation of the *repR* mRNA (RNAII) that encodes the rate-limiting replication initiator protein (Brantl *et al.*, 1993). CopR acts as a transcriptional repressor at the essential *repR* promoter (Brantl, 1994). Additionally, it has a second function: since RNAIII, with an half-life of ~30 min, is unusually stable (Brantl & Wagner, 1996), it would not be able to correct downward fluctuations in copy number. Therefore, CopR is

Abbreviations: CMCT, 1-cyclohexyl-3(2-morpholinoethyl) carbodiimide metho-*p*-toluenesulfonate; RT, reverse transcription.

required to prevent convergent transcription from the sense promoter pII and the antisense promoter pIII, thereby indirectly increasing the amount of RNAIII (Brantl, 1994; Brantl & Wagner, 1997). When copy number decreases, decreased CopR synthesis will derepress pII. This results in increased transcription of RNAII and convergent transcription, which decreases transcription of RNAIII. Both effects increase RepR synthesis and, consequently, the replication frequency. Fig. 4(A) presents a model of replication control of pIP501.

In vitro assays show that RNAIII-mediated inhibition occurs faster than complete duplex formation, suggesting that binding intermediates between RNAII and RNAIII are sufficient for inhibition (Brantl & Wagner, 1994). Furthermore, the deletion of stem–loops L1 and L2 at the 5′ end of RNAIII has no effect on the inhibitory function of RNAIII *in vivo* (Brantl *et al.*, 1993), whereas mutations in loop L3 of RNAIII lead to new incompatibility groups (Brantl & Wagner, 1996), indicating that L3 is the recognition loop. However, since a U-turn structure on loop L1 of RNAII complementary to L4 of RNAIII proves to be important for an efficient interaction with RNAIII, we have suggested that L3 and L4 are of equal importance for the initial contact (Heidrich & Brantl, 2003).

Here, we investigate the sequence and structural requirements for an efficient RNAII–RNAIII interaction of plasmid pIP501 by a combination of secondary-structure probing and attenuation assays with wild-type and mutated RNAIII species, as well as single stem–loops. Our results demonstrate that helix formation progresses into the lower parts of stems L3 and L4, whereas the 6 nt spacer separating them remains unpaired. The sequence and length of this spacer are not important for efficient inhibition, and the exclusive function of the spacer is to present both stem–loops simultaneously for interaction with the complementary loop pair L1/L2 of RNAII.

METHODS

Enzymes and chemicals. Chemicals used were of the highest purity available. T7 RNA polymerase and T4 polynucleotide kinase were purchased from NEB, Firepol Taq polymerase from Solis Biodyne, and Thermoscript reverse transcriptase from Invitrogen. *Bacillus subtilis* RNA polymerase was prepared by J. M. Sogo, Universidad Autónoma de Madrid. 1-Cyclohexyl-3(2-morpholinoethyl) carbodiimide metho-*p*-toluenesulfonate (CMCT) and lead acetate from Merck, and DMSO from Fluka, were used for the chemical probing.

In vitro transcription. *In vitro* transcription experiments were performed as described previously (Brantl & Wagner, 1996; Heidrich & Brantl, 2003). Templates for *in vitro* transcription of mutated RNAIII species were generated by PCR on plasmid pPR1 as template (Brantl & Behnke, 1992), with oligonucleotide SB1 (Brantl & Wagner, 1994) and one of the following mutagenic oligodeoxyribonucleotides:

SB547: 5′ TTA ATT GAT TGG TGG TAA TCA ATT AAC CGA TAC AGT TAA AGT TTC TCA GGC TTT AAC TGG TCG TGG CTC TT 3′

SB548: 5′ TTA ATT GAT TGG TGG TAA TCA ATT AAG CGC AGT TAA AGT TTC TCA GGC TTT AAC TGG TCG TGG CTC TT 3′

SB 570: 5′ TTA ATT GAT TGG TGG TAA TCA ATT AAC AGT TAA AGT TTC TCA GGC TTT AAC TGG TCG TGG CTC TT 3′

SB571: 5′ TTA ATT GAT TGG TGG TAA TCA ATT AAG GCT CGA CAC GGC AGT TAA AGT TTC TCA GGC TTT AAC TGG TCG TGG CTC TT 3′

SB619: 5′ AAT ATT GAT TGG TGG TAA TCA ATA TTG GCT CGG TCT TAA AGT TTC TCA GGC TTT AAG ACG TCG TGG CTC TT 3′

SB620: 5′ AAT TTT GAT TGG TGG TAA TCA AAA TTG GCT CGG TCA TAA AGT TTC TCA GGC TTT ATG ACG TCG TGG CTC TT 3′

SB645: 5′ AAT TTT GAT TGG TGG TAA TCA AAA TTG GCT CGC AGT TAA AGT TTC TCA GGC TTT AAC TGG TCG TGG CTC TT 3′

The template for $RNAIII_{72}$ was generated as described previously (Brantl & Wagner, 1994).

The template fragment for RNAII complementary to SB645 was generated by a two-step PCR on pPR1 as template, with outer primers SB6 and SB7 (Brantl & Wagner, 1994) and the following mutagenic oligonucleotides as inner primers:

SB646: 5′ TTT AAC TGC GAG CCA ATT TTG ATT ACC ACC AAT CAA AAT TAG AAG TCG AGA CCC 3′

SB647: 5′ GGG TCT CGA CTT CTA ATT TTG ATT GGT GGT AAT CAA AAT TGG CTC GCA GTT AAA 3′

Loops L3 and L4 of RNAIII were synthesized *in vitro* and consisted of the following sequences:

L3: 5′ AAU UGA UUG GUG GUA AUC AAU U 3′

L4: 5′ GUU AAA GUU UCU CAG GCU UUA AC 3′

Secondary structure analysis. Secondary-structure probing with chemical probes (Pb^{2+}, CMCT and DMSO) using 2 pmol of unlabelled RNAIII in a total volume of 20 µl was carried out according to Brunel & Romby, 2000, as follows. Reaction buffers of the following final concentrations were used: for CMCT, 25 mM borate-NaOH, pH 8.0, 5 mM magnesium acetate, 75 mM potassium acetate, 5 mM β-mercaptoethanol; for DMSO, 25 mM Tris/HCl, pH 7.5, 5 mM $MgCl_2$, 75 mM KCl, 5 mM β-mercaptoethanol; for Pb^{2+}, 25 mM Tris-acetate, pH 7.5, 5 mM magnesium acetate, 25 mM sodium acetate. Denaturing buffers were: for CMCT, 25 mM borate-NaOH, 1 mM EDTA; for DMSO, 25 mM Tris/HCl, pH 7.5, 1 mM EDTA. RNA-removal buffers for the CMCT and DMSO reactions contained 10 mM Tris/HCl, pH 7.5, 1.5 mM EDTA and 0.1 % SDS. A subsequent reverse-transcription (RT) reaction was used to visualize the products. Primer hybridization was done in a total volume of 12 µl containing 9 µl of the modified RNA, 1 µl with 100 000 c.p.m. of 5′ [^{32}P]-labelled oligonucleotide SB2 (Hartmann Analytic) (Brantl & Wagner, 1994) and 2 µl 10 mM dNTPs for 5 min at 65 °C, followed by RT with ThermoScript reverse transcriptase (2 U, Invitrogen) in 20 µl for 45 min at 55 °C. Partial digestions of *in vitro*-synthesized, unlabelled RNAIII and RNAII species with ribonucleases T1, T2 and V were performed in the same way as those described previously for 5′ end-labelled species (Heidrich & Brantl, 2003), except that digestions were followed by an RT reaction with 5′ end-labelled primer SB2 (see above). All reaction products were subjected to electrophoresis in 8 % denaturing polyacrylamide gels.

Single-round transcription assays and calculation of inhibition rate constant k_{inhib}. Single-round transcription assays were performed as described previously (Brantl & Wagner, 1994), using PCR-generated 500 bp DNA fragments of pPR1 (comprising promoters p_{II} and p_{III}, the attenuator and 100 bp downstream) as templates and *B. subtilis* RNA polymerase prepared by J. M. Sogo. The protocol of the attenuation experiments was as described previously (Brantl & Wagner, 1994), with one alteration: the concentration of the unlabelled RNAIII species included was determined by UV spectrophotometry. The inhibition rate constants were calculated as described previously (Brantl & Wagner, 1994).

RESULTS AND DISCUSSION

Pairing between RNAII and RNAIII does not yield a full duplex

Previously, the secondary structures of RNAIII and RNAII were probed with RNases T1 (single-stranded Gs), T2 (single-stranded region with a slight preference for As) and V (double-stranded and stacked regions) (Brantl & Wagner, 1994). To obtain more detailed information about the 3′

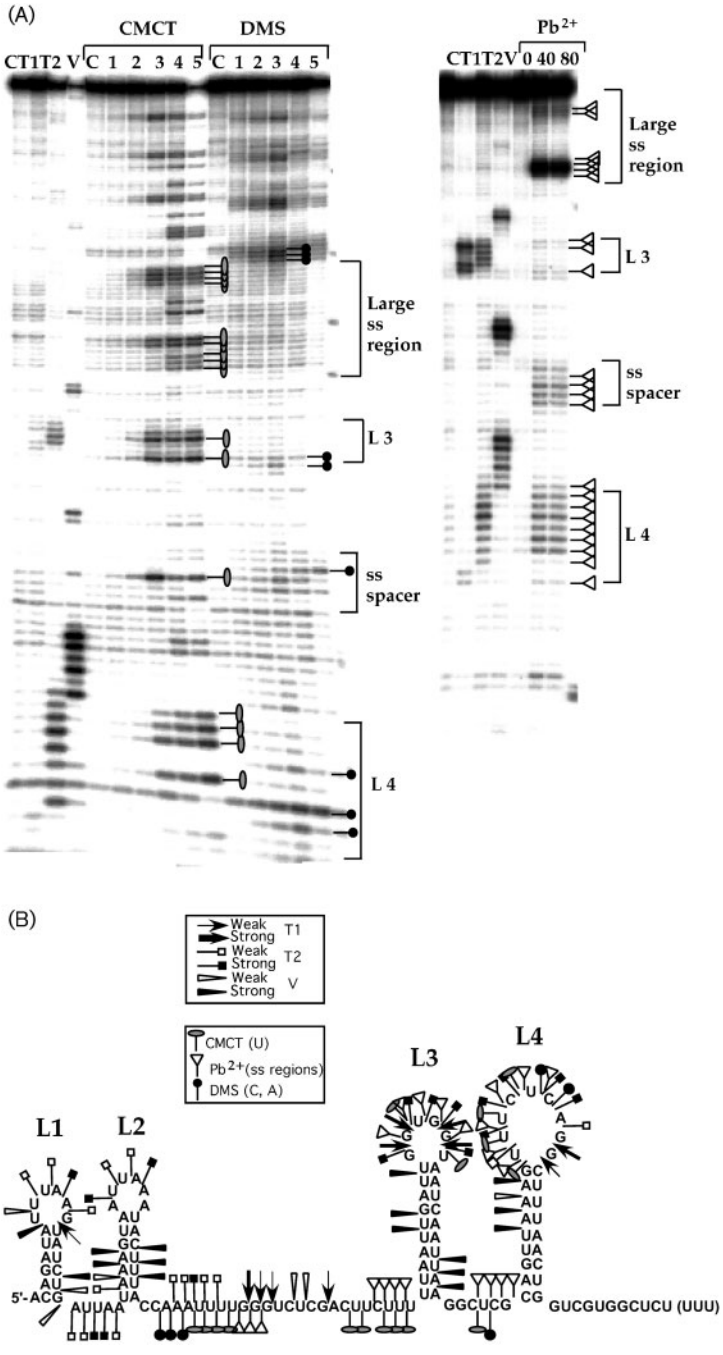

Fig. 1. Fine mapping of the secondary structure of RNAIII by a combination of enzymic and chemical probes. A secondary-structure probing of wild-type $RNAIII_{136}$ with three different RNases and chemical probes is shown. Purified, unlabelled RNA species were subjected to limited cleavage with RNases T1, T2 or V, or alternatively treated with CMCT, DMSO or Pb^{2+}, as indicated, and afterwards subjected to an RT reaction with 5′ end-labelled primer SB2, as described in Methods. The reaction products were separated on 8% denaturing gels. (A) PhosphorImager prints. The RNase concentrations used were: T1, 10^{-2} U μl^{-1}; T2, 10^{-1} U μl^{-1}; V, 10^{-1} U ml^{-1}. C, control without RNases. Concentrations used for CMCT were: 5 mM (lane 1), 10 mM (lanes 2 and 4) and 25 mM (lanes 3 and 5); for DMSO, 50 mM (lane 1), 100 mM (lanes 2 and 4) and 200 mM (lanes 3 and 5). For both CMCT and DMSO, lanes 4 and 5 show treatment under denaturing conditions. For Pb^{2+} treatment, concentrations of 40 and 80 mM were used. Signals obtained with the chemical probes are indicated in the autoradiograms of the corresponding gels and explained in the key in (B). Brackets denote loops L3 and L4, the single-stranded (ss) spacer between these loops and the large single-stranded region 5′ of L3. (B) Secondary structure of $RNAIII_{136}$ based on the cleavage data and additional experiments (not shown). The keys show the symbols used to designate contacts obtained by enzymic or chemical probing.

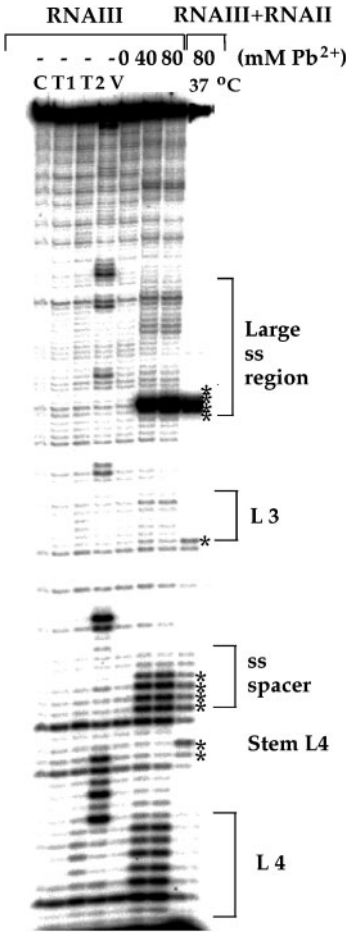

Fig. 2. Pb^{2+} probing of RNAIII and the RNAIII–RNAII complex. Purified, unlabelled RNAIII (0.5 pmol) was incubated with unlabelled RNAII (5 pmol), and the complex was allowed to form for 5 min at 37 °C and subjected to cleavage with Pb^{2+} followed by an RT reaction with 5′ end-labelled primer SB2, as described in Methods. In parallel, unlabelled RNAIII alone was subjected to cleavage with the RNases T1, T2 and V, or with 40 and 80 mM Pb^{2+}, and the products subjected to an RT reaction with labelled primer SB2. The reaction products were separated on 8% denaturing gels. An autoradiogram is shown. RNase concentrations used were as in Fig. 1. C, control without RNase treatment. Asterisks denote the alteration of the Pb^{2+} cleavage pattern upon pairing. Brackets indicate loops L3 and L4, the single-stranded (ss) spacer between these loops and the large single-stranded region 5′ of L3.

stem–loops L3 and L4 and the spacer in between them, additional structure-probing experiments were performed with CMCT (Us), Pb^{2+} (single-stranded regions) and DMSO (Cs and As), as described in Methods. The results are shown in Fig. 1. Four cuts for Pb^{2+} and one cut each for DMSO and CMCT within the spacer region, as well as three cuts for V in the lower stem of L3, confirmed that the spacer between L3 and L4 is indeed 6 nt long. Furthermore, the sizes of L3 with 6 nt and of L4 with 9 nt as well as that of the large single-stranded region 5′ of stem–loop L3 were corroborated by a combination of enzymic and chemical probing.

Since Pb^{2+} is a sensitive probe for single-stranded sequences, it was used to probe the structure of a complex between the 5′ 184 nt of RNAII (containing the target for RNAIII) and 5′-labelled full-length $RNAIII_{136}$. For comparison, unpaired RNAIII was probed with T1, T2, V and Pb^{2+}. As shown in Fig. 2, cleavage positions indicated that the RNAII–RNAIII complex is not fully base-paired in the single-stranded region between L3 and L4 of RNAIII. Four significant Pb^{2+} cuts within the large single-stranded region 5′ of L3 that were not reduced upon pairing with RNAII suggested that at least part of this region also remained single stranded. By contrast, the loops were found to be almost completely paired, with the exception of the 3′ outermost U of L3. Interestingly, 2 nt of the 5′ half of stem L4 became single stranded (asterisks in Fig. 2). Lead cleavage cannot be used to assess whether the stems of L3/L2 and L4/L1 are engaged in intramolecular or intermolecular helices.

To answer this question and to evaluate the role of the spacer region between L3 and L4, single-round transcription experiments were performed to determine the inhibition rate constants of mutated antisense RNAs with either wild-type or complementary sense RNAs. In all these experiments, $RNAIII_{72}$, consisting only of stem–loops L3 and L4 with their 6 bp spacer region, was used as a 'wild-type' species, since previous experiments had shown that inhibition does not require stem–loops L1 and L2 and the large single-stranded region (Brantl & Wagner, 1994).

The stems are involved in the formation of intermolecular helices

In RNAIII of pIP501, the stems of L3 and L4 consist of only 10 and 9 bp, respectively, and are not interrupted by bulges that, in longer helices, protect the antisense RNAs against degradation by RNase III and are required for efficient strand opening (Hjalt & Wagner, 1995). To find out whether pairing is restricted to the 6 and 9 nt loops L3 and L4, respectively, mutated RNAIII species with 3 or 4 bp heterologous stem bases of L3 and L4 were assayed in single-round transcription experiments (Fig. 3A). Whereas a heterologous 3 bp stem base in L3 and L4 yielded twofold lower inhibition rate constants ($RNAIII_{619}$), an extension to 4 heterologous bp in L3 and L4 reduced k_{inhib} fourfold ($RNAIII_{620}$). The reduced inhibition rate constants with wild-type RNAII could, at least partially, be compensated when a complementary mutated RNAII was used. This was shown with $RNAIII_{645}$, which contained a heterologous 4 bp stem base in L3 alone. These data (summarized in Table 1) demonstrate that in the inhibitory complex, pairing progresses into the lower part of stems L3 and L4 of RNAIII, and that the stems are involved in the formation of intermolecular helices with the sense RNA (RNAII). A recent analysis of the FinP/*traJ* system of the F plasmid that acts by inhibition of *traJ* translation has also revealed that base pairing proceeds from an initial loop–loop interaction

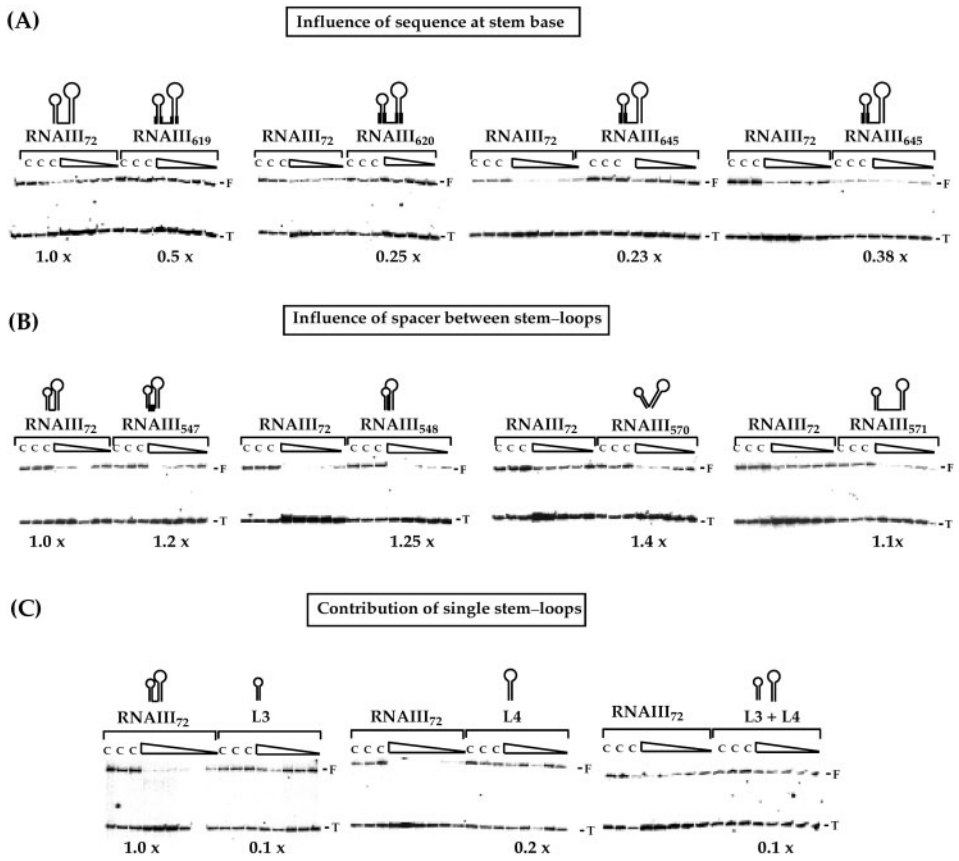

Fig. 3. Single-round transcription assays with wild-type and mutated RNAIII species. *In vitro* attenuation assays were performed with wild-type $RNAIII_{72}$ containing stem–loops L3 and L4 and a series of truncated and mutated RNAIII species. RNAIII species were incorporated at different concentrations (1.0, 0.6, 0.4, 0.2, 0.1 and 0.05×10^{-7} M for $RNAIII_{72}$, and 1.0, 0.6, 0.4, 0.2 and 0.1×10^{-7} M for the mutated species), denoted by a triangle, and their effects on induced transcription termination were determined at a 10 min time point. The figure shows PhosphorImager prints with the positions of full-length run-off *repR*-RNA (~365 nt, F) and terminated *repR*-RNA (~260 nt, T). Calculation of band intensity, background substraction and calculation of the inhibition rate constant k_{inhib} were performed as described previously (Brantl & Wagner, 1994; Heidrich & Brantl, 2003). Three buffer controls (C) show the value in the absence of antisense RNA. The mean intensity of the F band in the buffer controls was set to 100 % (regulatable F). Below the gels, the relative inhibition rate constants k_{inhib} are shown. The calculated k_{inhib} values and the mutations present in the different RNAIII species are summarized in Table 1. (A) Influence of the sequence at the stem base; (B) influence of the spacer between the stem–loops; (C) contribution of single stem–loops.

through the top portion of the stems to a stable duplex (Gubbins *et al.*, 2003). By contrast, in the inhibitory intermediate of CopA and CopT of plasmid R1, only the upper parts of the stems of the decisive 3′ CopA stem–loop pair containing a bulge region are involved in intermolecular helices, whereas the lower parts remain paired intramolecularly (Kolb *et al.*, 2000a).

The sequence and length of the spacer between L4 and L3 do not affect the inhibitory function of RNAIII

In sense–antisense systems containing two complementary loop pairs, the length of the spacer between the two stem–loops is found to be different (for examples, see Brantl, 2004). To analyse the influence of the length and sequence of the spacer between L3 and L4, mutated RNAIII species with varying spacer lengths and with a heterologous spacer were investigated in the attenuation assay. As shown in Fig. 3(B), $RNAIII_{547}$, which contains a heterologous spacer, was slightly more inhibitory than the wild-type, indicating that the sequence of the spacer is not important. This corresponds well with the results of the Pb^{++}-based secondary-structure probing of the RNAII–RNAIII complex, in which this spacer was still lead sensitive, i.e. single stranded, although the loops were almost completely paired (Fig. 2). Both $RNAIII_{548}$ with a 3 nt spacer and $RNAIII_{571}$ with a 12 nt spacer were as efficient in inhibition

Table 1. Inhibition rate constants of wild-type and mutated RNAIII species

Values represent the means of at least three independent determinations. The inhibition rate constant for RNA_{72} is the mean of 33 independent determinations.

RNA species	Characteristics	Inhibition rate constant k_{inhib} (M^{-1} s^{-1})	Relative k_{inhib}
RNA_{619}	Heterologous 3 bp stem base in L3/L4	0.75×10^6	0.5
RNA_{620}	Heterologous 4 bp stem base in L3/L4	0.4×10^6	0.25
RNA_{645}	Heterologous 4 bp stem base in L3 wild-type template	0.37×10^6	0.23
RNA_{645}	Heterologous 4 bp stem base in L3 complementary template	0.6×10^6	0.38
RNA_{547}	Heterologous 6 nt spacer	1.9×10^6	1.2
RNA_{548}	3 nt spacer	2.0×10^6	1.25
RNA_{570}	No spacer between L3 and L4	2.2×10^6	1.4
RNA_{571}	12 nt spacer	1.8×10^6	1.1
$RNAIII_{72}$	Wild-type L3 and L4, 6 bp spacer	1.6×10^6	1
Stem–loop L3	Synthetic RNA oligonucleotide	1.4×10^5	0.1
Stem–loop L4	Synthetic RNA oligonucleotide	3.0×10^5	0.2
Stem–loops L3+L4	Mixed 1:1	1.25×10^5	0.1

as the wild-type with a 6 nt spacer, suggesting that the spacer length can be varied. Interestingly, $RNAIII_{570}$, which does not contain a spacer between L3 and L4, exhibited an increase of 1.4-fold in k_{inhib} compared with the wild-type. These results prove unequivocally that neither the sequence nor the length of the spacer between L3 and L4 influences the inhibitory function of RNAIII.

A simultaneous interaction between both loop pairs of RNAII and RNAIII is required for inhibition

Based on the results with the spacer mutants, we asked whether a mixture of the unlinked stem–loops L3 and L4 is efficient in inhibition. For this purpose, synthetic RNA

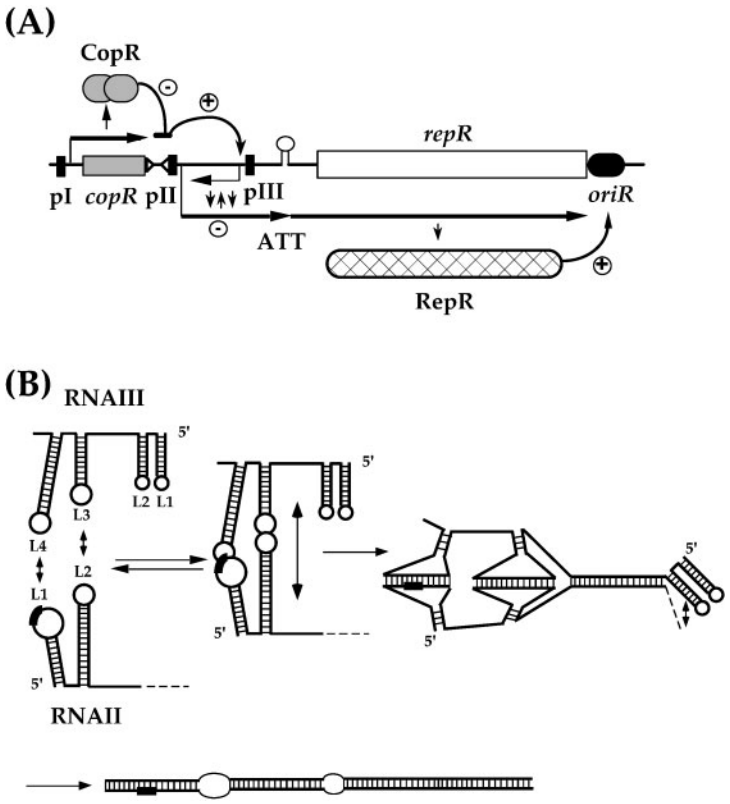

Fig. 4. Model for the interaction between RNAIII and RNAII in the context of replication control of plasmid pIP501. (A) Working model of copy number control of plasmid pIP501 in *B. subtilis*. Black boxes, promoters; rectangles, ORFs; thick arrows, RNAs; grey/stippled, proteins; *oriR*, replication origin; stem–loop/ATT, transcriptional attenuator (rho-independent terminator); +, activation; −, repression/inhibition. (B) Putative binding pathway of RNAII and RNAIII of pIP501. A putative RNAIII–RNAII binding pathway was derived from the experimental data presented in Figs 1–3. First, loop pairs L1 (U-turn motif highlighted in black)/L4 and L2/L3 interact simultaneously. Subsequently, basepairing is extended into the lower stem regions, and the large spacer region of RNAIII comes into contact with the complementary region in RNAII. Finally, only the spacer separating L3 and L4 in RNAIII and L1 and L2 in RNAII, as well as the 5′ 4 nt of the large single-stranded region 5′ of L3, remain single-stranded.

oligonucleotides containing either L3 or L4 were used. First, each stem–loop was investigated separately in the attenuation assay (Fig. 3C). As expected, L3 and L4 alone were 10-fold and fivefold less efficient, respectively, than $RNAIII_{72}$. This is in good correlation with the previous result, whereby a less than 0.1-fold inhibitory activity was found for $RNAIII_{47}$ containing only the large single-stranded region and L3 (Brantl & Wagner, 1994). Surprisingly, a 1 : 1 mixture of L3 and L4 was as inefficient in inhibition as L3 alone. Therefore, we can conclude that L3 and L4 have to be attached to one other to ensure efficient inhibition. Apparently, this function is provided by the 6 nt spacer in wild-type RNAIII, which acts as a scaffold for both stem–loops. Consequently, a simultaneous interaction between the two loop pairs of RNAIII and RNAII is required for transcriptional attenuation to occur. This finding is in accordance with our previous result that L4, which is complementary to U-turn loop L1 of RNAII, is important for an efficient contact with the sense RNA (Heidrich & Brantl, 2003). Fig. 4(B) relates the results of this study to the working model of copy-number control. A requirement for both stem–loops of the antisense RNA (RNAI) for efficient complex formation with the sense RNA, *repC* mRNA, was also found in an *in vitro* study of the transcription attenuation system of staphylococcal plasmid pT181. Here, two antisense RNAs, $RNAI_{84}$ (stem loops L1 and L2 connected by an 8 nt spacer) and $RNAI_{146}$ (stem–loops L1 to L 4) are expressed *in vivo* that bound equally well to *repC* mRNA. However, upon deletion of either L1 or L2 or the 3′ part of L2, pairing was reduced 10- to 100-fold (Brantl & Wagner, 2000). By contrast, in plasmid R1, the initial contact with the target RNA is made by the 3′ stem–loop of the antisense RNA CopA, and the 5′ stem–loop is only involved in later pairing intermediates (see Kolb *et al.*, 2000a).

The recently found chromosomally encoded bona fide antisense regulators belong mainly to the trans-encoded RNAs that are only partially complementary to their targets. However, searches for cis-encoded antisense RNAs from different bacterial genomes are under way, and it remains to be seen how new results for such RNAs will expand our knowledge of RNA–RNA interactions involved in prokaryotic gene regulation.

ACKNOWLEDGEMENTS

We acknowledge E. Birch-Hirschfeld (Institute for Virology, Jena) for synthesizing various oligodeoxyribonucleotides, and Margarita Salas and J. M. Sogo, Universidad Autónoma de Madrid, for providing us with purified *B. subtilis* RNA polymerase. This work was supported by grant BR 1552/4-4 from the Deutsche Forschungsgemeinschaft (to S. B.).

REFERENCES

Asano, K. & Mizobuchi, K. (2000). Structural analysis of late intermediate complex formed between plasmid ColIb-P9 Inc RNA and its target RNA. How does a single antisense RNA repress translation of two genes at different rates? *J Biol Chem* **275**, 1269–1274.

Brantl, S. (1994). The *copR* gene product of plasmid pIP501 acts as a transcriptional repressor at the essential *repR* promoter. *Mol Microbiol* **14**, 473–483.

Brantl, S. (2004). Plasmid replication controlled by antisense RNAs. In *The Biology of Plasmids*, chapter 3, pp. 47–62. Edited by B. Funnell & G. Phillips. Washington, DC: AMS Press.

Brantl, S. & Behnke, D. (1992). Copy number control of the streptococcal plasmid pIP501 occurs at three levels. *Nucleic Acids Res* **20**, 395–400.

Brantl, S. & Wagner, E. G. H. (1994). Antisense RNA-mediated transcriptional attenuation occurs faster than stable antisense/target RNA pairing: an *in vitro* study of plasmid pIP501. *EMBO J* **13**, 3599–3607.

Brantl, S. & Wagner, E. G. H. (1996). An unusually long-lived antisense RNA in plasmid copy number control: *in vivo* RNAs encoded by the streptococcal plasmid pIP501. *J Mol Biol* **255**, 275–288.

Brantl, S. & Wagner, E. G. H. (1997). Dual function of the *copR* gene product of plasmid pIP501. *J Bacteriol* **179**, 7016–7024.

Brantl, S. & Wagner, E. G. H. (2000). Antisense RNA-mediated transcriptional attenuation: an *in vitro* study of plasmid pT181. *Mol Microbiol* **35**, 1469–1482.

Brantl, S., Birch-Hirschfeld, E. & Behnke, D. (1993). RepR protein expression on plasmid pIP501 is controlled by an antisense RNA-mediated transcription attenuation mechanism. *J Bacteriol* **175**, 4052–4061.

Brunel, C. & Romby, P. (2000). Probing RNA structure in solution. *Methods Enzymol* **318**, 3–21.

Greenfield, T. J., Franch, T., Gerdes, K. & Weaver, K. E. (2001). Antisense RNA regulation of the *par* post-segregational killing system: structural analysis and mechanism of binding of the antisense RNA, RNAII and its target, RNAI. *Mol Microbiol* **42**, 527–537.

Gubbins, M. J., Arthur, D. C., Ghetu, A. F., Glover, J. N. M. & Frost, L. S. (2003). Characterizing the structural features of RNA/RNA interactions of the F-plasmid FinOP fertility inhibition system. *J Biol Chem* **278**, 27663–27671.

Heidrich, N. & Brantl, S. (2003). Antisense-RNA mediated transcriptional attenuation: importance of a U-turn loop structure in the target RNA of plasmid pIP501 for efficient inhibition by the antisense RNA. *J Mol Biol* **333**, 917–929.

Hjalt, T. & Wagner, E. G. H. (1992). The effect of loop size in antisense and target RNAs on the efficiency of antisense RNA control. *Nucleic Acids Res* **20**, 6723–6732.

Hjalt, T. & Wagner, E. G. H. (1995). Bulged-out nucleotides in an antisense RNA are required for rapid target RNA binding *in vitro* and inhibition *in vivo*. *Nucleic Acids Res* **23**, 580–587.

Kolb, F. A., Engdahl, H. M., Slagter-Jäger, J. G., Ehresmann, B., Ehresmann, C., Westhof, E., Wagner, E. G. H. & Romby, P. (2000a). Progression of a loop-loop complex to a four-way junction is crucial for the activity of a regulatory antisense RNA. *EMBO J* **19**, 5905–5915.

Kolb, F. A., Malmgren, C., Westhof, E., Ehresmann, C., Ehresmann, B., Wagner, E. G. H. & Romby, P. (2000b). An unusual structure formed by antisense-target RNA binding involves an extended kissing complex with a four-way junction and a side-by-side helical alignment. *RNA* **6**, 311–324.

Kolb, F. A., Westhof, E., Ehresmann, B., Ehresmann, C., Wagner, E. G. H. & Romby, P. (2001). Four-way junctions in antisense RNA-mRNA complexes involved in plasmid replication control: a common theme? *J Mol Biol* **309**, 605–614.

Malmgren, C., Wagner, E. G. H., Ehresmann, C., Ehresmann, B. & Romby, P. (1997). Antisense RNA control of plasmid R1 replication: the dominant product of the antisense RNA-mRNA binding is not a full RNA duplex. *J Biol Chem* **272**, 12508–12512.

Rasmussen, A. A., Eriksen, M., Gilany, K., Udesen, C., Franch, T., Petersen, C. & Valentin-Hansen, P. (2005). Regulation of *ompA* mRNA stability: the role of a small regulatory RNA in growth phase-dependent control. *Mol Microbiol* **58**, 1421–1429.

Thisted, T., Sørensen, N., Wagner, E. G. H. & Gerdes, K. (1994). Mechanism of postsegregational killing: Sok antisense RNA interacts with Hok mRNA via its 5′-end single-stranded leader and competes with the 3′-end of Hok mRNA for binding to the *mok* translational initiation region. *EMBO J* **13**, 1960–1968.

Udekwu, K. I., Darfeuille, F., Vogel, J., Reimegard, J., Holmqvist, E. & Wagner, E. G. H. (2005). Hfq-dependent regulation of OmpA synthesis is mediated by an antisense RNA. *Genes Dev* **19**, 2355–2366.

Wagner, E. G. H. & Brantl, S. (1998). Kissing and RNA stability in antisense control of plasmid replication. *Trends Biochem Sci* **23**, 451–454.

Wagner, E. G. H., Altuvia, S. & Romby, P. (2002). Antisense RNAs in bacteria and their genetic elements. In *Adv in Genetics*, pp. 361–398. Edited by J. C. Dunlap & C. Wu. London: Academic Press.

Zhang, A., Wassarman, K. M., Ortega, J., Steven, A. C. & Storz, G. (2002). The Sm-like Hfq protein increases OxyS RNA interaction with target mRNAs. *Mol Cell* **9**, 11–22.

Edited by: L. S. Frost

4. The small untranslated RNA SR1 from the *B. subtilis* genome is involved in the regulation of arginine catabolism

[Manuskript II]

Nadja Heidrich[1], Alberto Chinali[1], Ulf Gerth[2] and Sabine Brantl[1]

[1]AG Bakteriengenetik, Friedrich-Schiller-Universität Jena, Philosophenweg 12, D-07743 Jena, Germany
[2]Institut für Mikrobiologie, Ernst-Moritz-Arndt-Universität Greifswald, F.-L.-Jahn-Str. 15, D-17487 Greifswald, Germany

publiziert in *Molecular Microbiology*, **62**: 520-36

Molecular Microbiology (2006) **62**(2), 520–536
doi:10.1111/j.1365-2958.2006.05384.x
First published online 20 September 2006

The small untranslated RNA SR1 from the *Bacillus subtilis* genome is involved in the regulation of arginine catabolism

Nadja Heidrich,[1] Alberto Chinali,[1] Ulf Gerth[2] and Sabine Brantl[1]*
[1]*AG Bakteriengenetik, Friedrich-Schiller-Universität Jena, Philosophenweg 12, Jena D-07743, Germany.*
[2]*Institut für Mikrobiologie, Ernst-Moritz-Arndt-Universität Greifswald, F.-L.-Jahn-Straße 15, D-17487 Greifswald, Germany.*

Summary

Whereas about 70 small non-coding RNAs have been found in the *Escherichia coli* genome, relatively little is known about regulatory RNAs from Gram-positive bacteria. Here, we demonstrate that the recently identified small untranslated RNA SR1 from the *Bacillus subtilis* genome is a regulatory RNA involved in fine-tuning of arginine catabolism. 2D protein gel electrophoresis indicated three possible SR1 targets that are regulated by the transcriptional activator AhrC, which was shown to be the primary target of SR1. *In vitro* pairing studies and an *in vivo* reporter gene test demonstrated a specific interaction between SR1 and *ahrC* mRNA. This interaction did not lead to degradation of *ahrC* mRNA, but inhibited translation at a post-initiation stage. Our data show that the Hfq chaperone was not required for the stabilization of SR1 *in vivo*. The amount of SR1 was increased upon addition of L-arginine and L-ornithine, but not L-citrulline or L-proline.

Introduction

Small non-coding RNAs have been the focus of many articles during the past 4 years. In the *Escherichia coli* genome, approximately 100 such RNAs have been predicted and about 70 have been confirmed (Argaman *et al*., 2001; Rivas *et al*., 2001; Wassarman *et al*., 2001; Chen *et al*., 2002; Zhang *et al*., 2002; Vogel *et al*., 2003). However, the biological function and the inhibitory or activating mechanism of only a minority of these RNAs have been elucidated. Examples include MicF (for a review see Delihas and Forst, 2001), OxyS (Altuvia *et al*., 1997; 1998), DsrA (Majdalani *et al*., 1998; Lease and Belfort, 2000), GcvB (Urbanowski *et al*., 2000), Spot42 RNA (Møller *et al*., 2002a), RprA (Majdalani *et al*., 2001), RyhB-RNA (Massé and Gottesman, 2002) and, more recently, GadY (Opdyke *et al*., 2004), MicC (Chen *et al*., 2004), MicA (Rasmussen *et al*., 2005; Udekwu *et al*., 2005), SgrS (Vanderpool and Gottesman, 2004), IstR1 (Vogel *et al*., 2004) and multiple small RNAs involved in quorum sensing in *Vibrio cholerae* (Lenz *et al*. 2004). Common to all examples studied in detail seems to be an inducible expression of these RNAs and the frequent lack of phenotypes upon inactivation or overexpression, which supports the assumption that these chromosomally encoded RNAs are mainly involved in fine-tuning of gene expression or metabolic processes.

At least 10 of the newly identified chromosomally encoded small RNAs bind the Sm-like abundant RNA binding protein Hfq (Wassarman *et al*., 2001). Hfq binding was also demonstrated for OxyS (Zhang *et al*., 1998; 2002), DsrA (Sledjeski *et al*., 2001), RprA (Majdalani *et al*., 2001) and Spot42 RNA (Møller *et al*., 2002b), among these OxyS and DsrA were shown to require Hfq for regulation. The reason for the Hfq requirement seems to be the need to stabilize the partial duplexes formed between *trans*-encoded antisense RNAs and their target RNAs.

In contrast to the situation in Gram-negative bacteria, little is known about regulatory RNAs encoded in the genomes of Gram-positive bacteria. Examples include a small RNA that is involved in nitrogen metabolism in *Clostridium acetobutylicum* (Fierro-Monti *et al*., 1992), the multifunctional RNAIII from the *agr* locus of *Staphylococcus aureus* (Morfeldt *et al*., 1995; Huntzinger *et al*., 2005), which has been studied in detail for over a decade and the recently detected Pel RNA in group A streptococci (Mangold *et al*., 2004). In the *Bacillus subtilis* genome, only four small RNAs have been detected so far: BS203 encoded in the *yocI–yocJ* intergenic region (Ando *et al*., 2002), BS190 in the *asp–yrvM* intergenic region (Suzuma *et al*., 2002), SR1 encoded in the *pdhD–yktA* intergenic region (Licht *et al*., 2005) and RatA overlapping the *txpA* gene (Silvaggi *et al*., 2005). Recently, it became clear that BS203 and BS190 are the two 6S RNAs of *B. subtilis* (Barrick *et al*. 2005; Trotochaud and Wassarman, 2005).

Accepted 15 August, 2006. *For correspondence. E-mail Sabine.Brantl@rz.uni-jena.de; Tel. (+49) 3641 949 570/571.

RatA (222 nt) was found to act as an antitoxin most probably triggering the degradation of *txpA*-mRNA encoding the toxic peptide TxpA by base pairing to the 3′ terminal 75 nt of this RNA (Silvaggi *et al*., 2005). The detection of RatA was based on a previous RNA expression analysis using an antisense *B. subtilis* genome array that revealed a few non-coding transcripts in intergenic regions (Lee *et al*., 2001).

SR1 was found in our group by a computational approach and subsequent verification by Northern blotting. It is 205 nt long and contains an open reading frame (ORF) for 39 amino acids preceded by a weak Shine–Dalgarno (SD) sequence. We could show that this ORF is not translated in *B. subtilis* under conditions where *sr1* was transcribed. Homologous RNAs containing this ORF have been found in *Bacillus licheniformis*, where an RNA similar in length and sequence to SR1 was predicted, but also in *Bacillus anthracis*, *Bacillus cereus* and *Geobacillus kaustophilus* (Licht *et al*., 2005). Neither overexpression nor knockout of the *sr1* gene proved to be detrimental for the growth of *B. subtilis*. SR1 was found to be maximally expressed under gluconeogenic conditions and repressed under glycolytic conditions. We identified two proteins, CcpN and CcpA, responsible for sugar-mediated repression of SR1 transcription and narrowed down their binding regions (Licht *et al*., 2005). However, the target(s) and the biological function of this novel untranslated RNA remained to be elucidated.

Arginine degradation in *B. subtilis* is regulated by at least two proteins: RocR and AhrC (Calogero *et al*., 1994; Gardan *et al*., 1997). RocR is a transcriptional activator of the catabolic *rocABC* and *rocDEF* operons that are transcribed by a sigL-dependent RNA polymerase. The *rocA* gene encodes a pyrroline-5-carboxylate dehydrogenase, *rocB* encodes a protein of unknown function, *rocC* and *rocE* may encode amino acid permeases, *rocD* encodes ornithine aminotransferase (OAT) and *rocF* encodes arginase. RocR exerts its activating function by binding to two UAS sequences (UAS1 and UAS2) upstream of the *rocABC* and the *rocDEF* promoter, respectively, whereas it negatively regulates its own synthesis (Calogero *et al*., 1994; Gardan *et al*., 1997). AhrC is similar to *E. coli* ArgR repressor and binds *in vitro* to the promoter of the *argCJBD-carAB-argF* (arginine biosynthetic) operon. On the other hand, it is also a positive regulator of the catabolic *rocABC* and *rocDEF* operons, and footprinting experiments indicated that it binds *in vitro* in the presence of arginine upstream of *rocA* in the –22/+1 promoter region (Klingel *et al*., 1995), but its role at molecular level remained unclear. Subsequently, a detailed biochemical analysis of AhrC binding at ARG boxes upstream of *rocA* and *rocD* led to the derivation of an improved *B. subtilis* ARG box consensus sequence and to the suggestion of a novel model for the assembly of a higher affinity form of AhrC at operator sites (Miller *et al*., 1997). Later, it was suggested that AhrC might directly interact with RocR bound to UAS thereby enhancing the RocR activity and that the positive role of AhrC involves this protein–protein interaction with RocR (Gardan *et al*., 1997). Recently, elaborate modification interference and footprinting analyses with purified ArgR from *E. coli* and from *Bacillus stearothermophilus* demonstrated that either a hexamer or two trimers of ArgR bound by arginine bind to ARG boxes immediately upstream of promoters for genes involved in arginine metabolism and that binding was increased in the presence of arginine (Song *et al*., 2002). Furthermore, the authors showed that in *E. coli* and *Thermotoga neapolitana* two consecutive arginine boxes were present, whereas in *B. subtilis* genes either one (*roc* genes) or two (*arg* genes) arginine boxes were found.

Here, we demonstrate that the small untranslated RNA SR1 that we discovered recently in the *B. subtilis* genome is a regulatory RNA involved in arginine catabolism. Our data show that the primary target of SR1 is *ahrC* mRNA, encoding the common positive regulator of the arginine catabolic operons *rocABC* and *rocDEF*. Using 2D gel electrophoresis with protein extracts from wild-type and *sr1* knockout strains we found alterations in the expression patterns of RocA, D and F. A combination of Northern blot analyses, *in vitro* RNA pairing and translation studies, an *in vivo* reporter gene test as well as reverse transcription polymerase chain reaction (RT-PCR) indicated that SR1 is an antisense RNA acting by base pairing with *ahrC* mRNA, thereby inhibiting translation of *ahrC* mRNA. Furthermore, the Hfq chaperone did not stabilize SR1. Northern blots demonstrated that SR1 transcription is upregulated by L-arginine and L-ornithine.

Results

SR1 affects the expression of the rocABC *and the* rocDEF *operons*

Bacillus subtilis wild-type and SR1 knockout strains [described in the study by Licht *et al*. (2005)] were grown in TY medium at 37°C, samples were taken at $OD_{560} = 5.0$ (maximal expression of *sr1*) and protein extracts prepared. These extracts were subjected to two-dimensional protein gel electrophoresis as described in *Experimental procedures*. The results (Fig. 1) show a difference in the expression levels of three proteins, RocA, RocD and RocF, between wild-type and *sr1* knockout strain: The amount of all three proteins was found to be increased in the Δ*sr1* strain. The identity of the three proteins was confirmed by extraction of the corresponding gel slices from Coomassie-stained gels and subsequent MALDI-TOF-MS analysis.

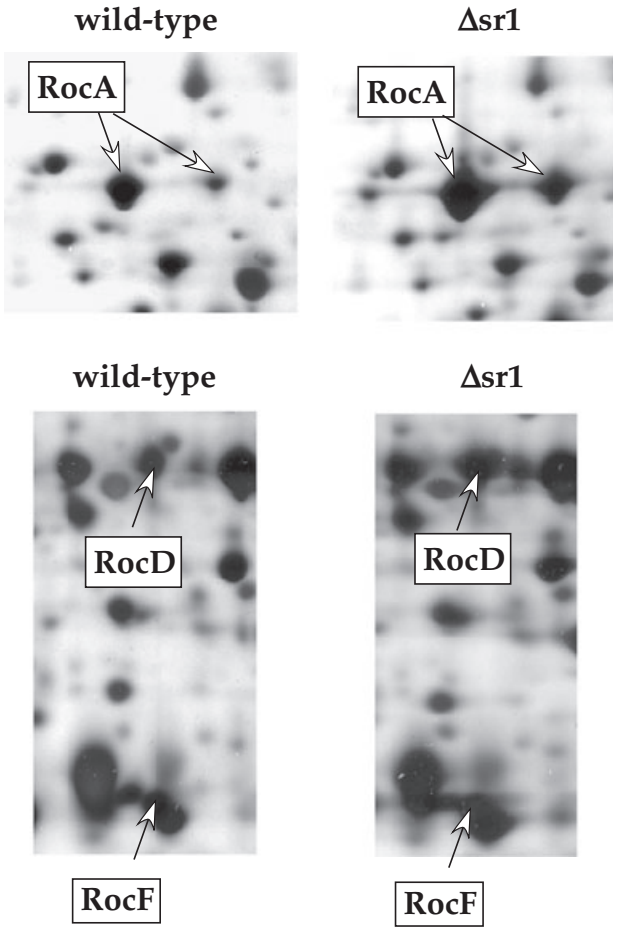

Fig. 1. Two-dimensional protein gel electrophoresis. Cuttings of silver-stained 2D protein gels from wild-type and *sr1* mutant cells are shown. The labelled protein spots were identified from corresponding Coomassie-stained 2D gels by MALDI-TOF-MS as described in *Experimental procedures*. Arrows indicate protein spots that were altered between *B. subtilis* wild-type and *sr1* mutant cells.

To find out, whether the increase in the protein levels was due to an increase in the amount of the corresponding mRNAs, wild-type and *sr1* knockout strains were grown as above, time samples were taken at $OD_{560} = 5.0$, total RNA was prepared, purified by CsCl gradient centrifugation and analysed by Northern blotting. Appropriate double-stranded DNA probes for all putative target RNAs were generated by PCR using chromosomal DNA of *B. subtilis* 168 and the corresponding oligonucleotides (see Table S1 in *Supplementary materials*). As shown in Fig. 2 and Table 1, the expression level of the *rocDEF* and the *rocABC* operons was about sevenfold and fourfold, respectively, higher in the Δ*sr1* strain compared with the wild-type strain. These results were substantiated by the analysis of wild-type and *sr1*-knockout strain grown in CSE minimal medium with L-arginine. Again, the expression level of the *rocDEF* operon was higher in the knockout strain compared with the wild-type strain (data not shown). In the absence of L-arginine, the *roc* operons are not expressed. Therefore, no signals were visible in the Northern blots independent of the expression of *sr1*. Computer searches did not reveal any complementarity between SR1 and different regions within these two operons, indicating that these genes might be secondary or downstream targets of SR1.

Recently, we have shown that the ORF encoded by *sr1* is not expressed in *B. subtilis* (Licht *et al.*, 2005). However, to rule out a possible role of this ORF for the effect of SR1 on the *roc* operons, plasmid pUCBS12 was constructed containing a TAG stop codon instead of an ATG start codon of the *sr1* ORF and comprising 100 bp upstream of p_{SR1}. DB104 (*Δsr1::cat*) was transformed with pUCBS12, transformants grown in TY with kanamycin, RNA prepared and analysed by Northern blotting. Plasmid pUCBS12 could fully complement the lack of the chromosomal *sr1* copy demonstrating that the SR1 effect on the *roc* operons was not due to a protein encoded by the *sr1* ORF (gel not shown).

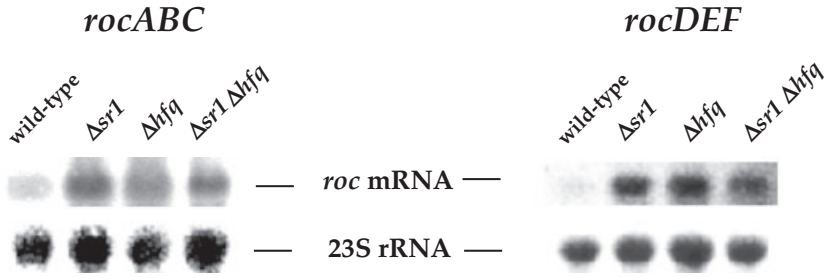

Fig. 2. Effects of SR1 and Hfq on the amounts of *rocABC* and *rocDEF* mRNA. Cells were grown in TY medium at 37°C, samples taken at $OD_{560} = 5.0$ and used for the preparation of total RNA by CsCl purification. RNA was treated with glyoxal, separated on an 1.2% agarose gel, blotted onto a nylon membrane and hybridized with [α^{32}-P]-dATP-labelled DNA probes specific for *rocABC* and *rocDEF* respectively. To allow for the correction of loading errors, filters were reprobed with a [γ^{32}-P]-ATP-labelled oligonucleotide specific for 23S rRNA. A quantification of the gel is shown in Table 1. Autoradiographs of the Northern blots are shown.

Table 1. Quantification of the amount of *rocABC* and *rocDEF*-mRNA in the presence and absence of SR1, Hfq and SR1/Hfq.

Strain	Relative amount of *rocABC*-RNA	Relative amount of *rocDEF*-RNA
DB104	×	×
DB104 (*Δsr1::cat*)	4.10 ± 0.6×	7.29 ± 0.6×
DB104 (*Δhfq::cat*)	3.08 ± 0.7×	6.42 ± 0.6×
DB104 (*Δsr1::phleo*, *Δhfq::cat*)	2.87 ± 0.3×	4.85 ± 0.2×

Values represent the averages of at least three independent determinations.

AhrC might be a primary target of SR1

Both *roc* operons are known to be regulated by two transcriptional activators, AhrC and RocR (Calogero *et al*., 1994; Gardan *et al*., 1997). Complementarity searches between SR1 and *ahrC* mRNA showed several consecutive stretches of complementarity in the 3′ portions of both RNAs, whereas no significant complementarity was observed between SR1 and *rocR* mRNA. Figure 3 represents one of several folding alternatives between SR1 and *ahrC* mRNA that all have a similar free energy and were predicted as described in *Experimental procedures*. Several attempts to detect *ahrC* mRNA in Northern blots failed, most probably due to its very low expression level. Therefore, RT-PCR of CsCl-purified total RNA from wild-type, *sr1* and *hfq* knockout strains as well as *rnc* strain BG218 (C-terminally truncated RNase III) was performed as described in *Experimental procedures* using oligo-

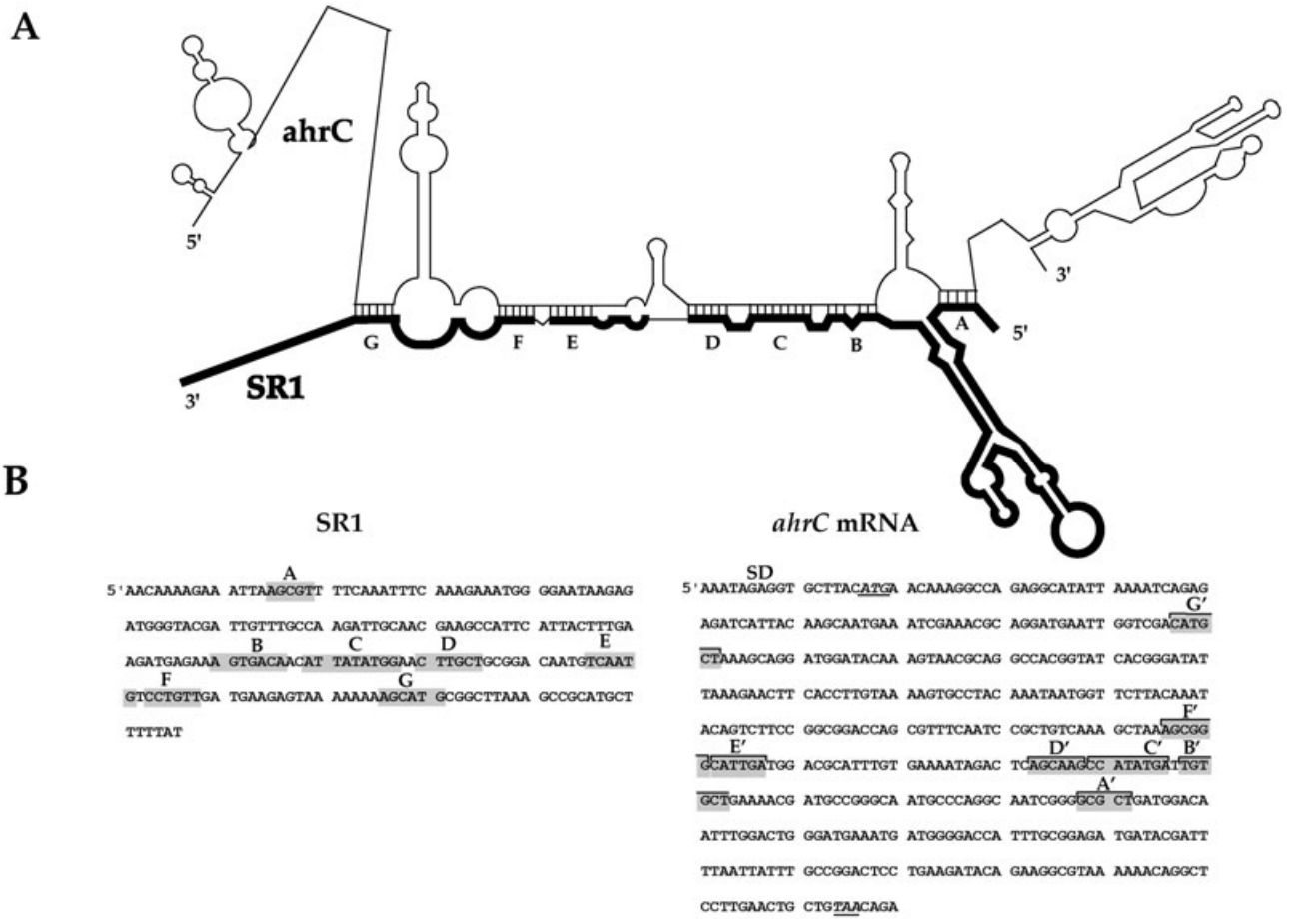

Fig. 3. Computer prediction for complementary pairing between SR1 and *ahrC* mRNA.
A. Schematic drawing of the interaction between SR1 (thick line) and *ahrC* mRNA (thin line) based on prediction with the program RNAfold as described in *Experimental procedures*. Predicted duplexes between both molecules are shown as paired regions and designated A, B, C, D, E, F and G. Each predicted base pair between SR1 and *ahrC* mRNA within A–G is indicated by one thin vertical line.
B. Sequences of SR1 and *ahrC* mRNA used for the prediction shown in A. Sequences in SR1 involved in base pairing with *ahrC* mRNA are shown as grey boxes and designated A–G, whereas the corresponding sequences in *ahrC* mRNA are designated A′–G′.

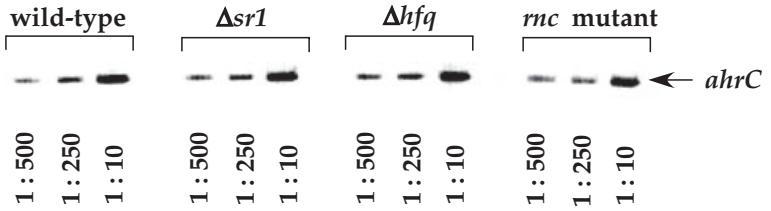

Fig. 4. Amount of *ahrC* mRNA in the presence and absence of SR1 *in vivo*. Total RNA was prepared from *B. subtilis* DB104, DB104 (*Δsr1::cat*), DB104 (*Δhfq::cat*) and BG218 (C-terminally truncated RNase III) strains, reverse-transcribed, diluted as indicated and amplified by PCR as described in *Experimental procedures*. As internal control for quantification of the amounts of RNA, *pnp* mRNA was used. Ethidium bromide-stained 3% agarose gels with the RT-PCR products are shown.

nucleotides complementary to the 5′ and 3′ region of *ahrC* mRNA and oligos complementary to the 5′ and 3′ end of *pnp* mRNA as an internal control (Table S1, *Supplementary material*). However, as shown in Fig. 4, no differences in the amount of the *ahrC* mRNA could be detected between these strains indicating that a possible interaction between SR1 and *ahrC* mRNA does not lead to degradation of the latter one by RNase III or another RNase.

In vitro *pairing experiments demonstrate a direct interaction between SR1 and* ahrC *mRNA*

To find out, whether SR1 and *ahrC* mRNA can interact directly with each other, complex formation between *in vitro* synthesized [γ^{32}-P]-ATP-labelled SR1 and different amounts of the 3′ part of *in vitro* synthesized unlabelled *ahrC* mRNA comprising nt 109–nt 483 was studied as described in *Experimental procedures*. Complexes were separated on native polyacrylamide gels at 4°C followed by PhosphorImaging. As can be seen in Fig. 5A, complexes between SR1 and the 3′ portion of *ahrC* mRNA form, similar to the case of Spot42/*galK*-RNA, at rather high concentrations (starting with 10–40 nM) of *ahrC* mRNA. Using the gel in Fig. 5A, an equilibrium dissociation constant of the SR1/*ahrC* mRNA complex of 3.21×10^{-7} M was calculated. This is rather high compared with other systems and suggests that an additional factor – like the RNA chaperone Hfq – might be required for efficient complex formation *in vivo*. To determine the apparent pairing constant for the SR1/*ahrC* complex, a constant amount of *ahrC* mRNA was incubated with SR1, time samples were taken and immediately loaded onto a running gel. Figure 5A (right half) shows such a gel. The k_{app} was calculated to be 1.25×10^{3} M^{-1} s^{-1}, about two to three orders of magnitude lower compared with other RNA/RNA interaction systems (for RNAII/RNAIII of pIP501 we measured $\approx 1 \times 10^{5}$ M^{-1} s^{-1}, Brantl and Wagner, 1994). Again, it is conceivable that a factor promoting complex formation is needed *in vivo*.

To prove that the interaction between SR1 and *ahrC* mRNA is specific, complex formation between *ahrC* mRNA and a heterologous antisense RNA, RNAIII of plasmid pIP501, was investigated. As shown in Fig. 5B, no interaction between these two RNAs could be detected, although RNAIII concentrations in the same range as for SR1 were used. Furthermore, competition experiments with unlabelled SR1 were performed to displace labelled SR1 from the complex. Indeed, a 250-fold excess of unlabelled SR1 was able to displace labelled SR1 almost completely from the complex with *ahrC* mRNA. In contrast, the same amount of unlabelled RNAIII was not able to remove labelled SR1 from the complex with its target (Fig. 5C). These data demonstrate that the interaction between SR1 and *ahrC* mRNA is specific.

SR1 inhibits translation of ahrC *mRNA*

As the RT-PCR data excluded that SR1 promotes *ahrC* mRNA degradation, a possible inhibition of *ahrC* mRNA translation by SR1 was investigated by *in vitro* translation experiments with *in vitro* synthesized, gel-purified *ahrC* mRNA. As an internal control, equimolar amounts of *sodB* mRNA were used, whose translation should not be affected by SR1. As shown in Fig. 6A, translation of *ahrC* mRNA *in vitro* yielded the 16.7 kDa AhrC protein and translation of *sodB* mRNA the 21.3 kDa SodB protein. The amount of both products increased with increasing amounts of mRNA (not shown). Upon addition of an excess of SR1 compared with *ahrC* and *sodB* mRNAs, the amount of AhrC decreased, whereas the amount of SodB remained unaffected. As expected, an excess of the cognate antisense RNA RyhB complementary to the 5′ region of *sodB* mRNA (Massé and Gottesman, 2002) decreased the synthesis of SodB, but not AhrC (Fig. 6A). These results are in accordance with the SR1/*ahrC* RNA binding experiments (Fig. 5) and demonstrate that SR1 exerts its effect by inhibiting translation of *ahrC* mRNA. As translation of AhrC was influenced by SR1, and complementary regions between SR1 and *ahrC* mRNA were found starting about 90 nt downstream

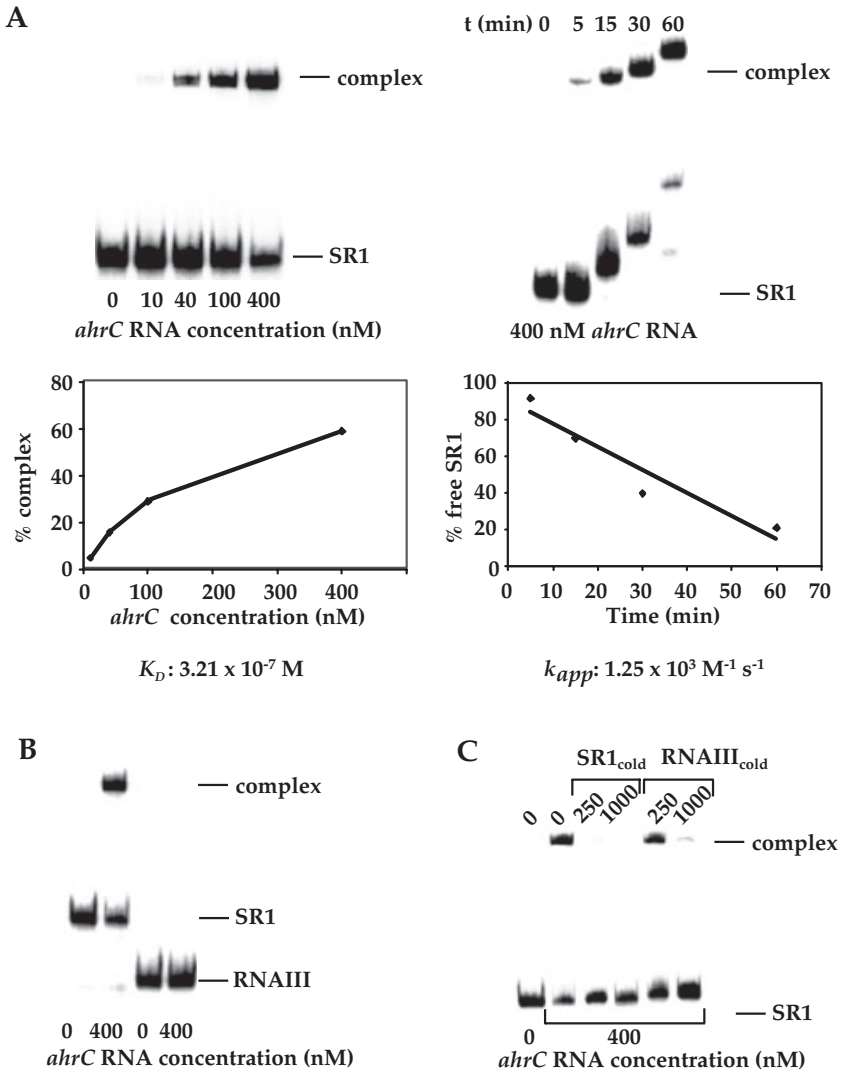

Fig. 5. Complex formation between SR1 and ahrC RNA *in vitro*. The binding assay was performed as described in *Experimental procedures*. The autoradiographs of the gel shift assays are shown. SR1 was labelled with [γ^{32}-P]-ATP and included at a final concentration of 5 nM. The concentrations of unlabelled *ahrC* mRNA are indicated.
A. Complex formation between labelled SR1 and unlabelled *ahrC* mRNA. Left: Different concentrations of unlabelled *ahrC* mRNA were used and a constant incubation time of 15 min at 37°C was applied. Below: The apparent equilibrium dissociation constant K_D (M) of the SR1–*ahrC* complex was determined. Right: *ahrC* RNA was used at a concentration of 400 nM, and complex formation was assayed at different time points as indicated. Below: The apparent pairing constant of the kissing complex k_{app} (M^{-1} s^{-1}) of the SR1-*ahrC* pair was determined.
B. Complex formation between labelled SR1 or labelled RNAIII and *ahrC* RNA. The assay was performed as in A, and 5 nM SR1 or 5 nM labelled RNAIII, respectively, were used.
C. Competition experiment. Unlabelled SR1 or unlabelled RNAIII at the indicated excess was mixed with labelled SR1 and, subsequently, unlabelled *ahrC* RNA was added to a final concentration of 400 nM, and complex was allowed to form for 15 min at 37°C.

from the natural SD sequence (see Fig. 3), experiments were designed to exclude that translation initiation was affected by SR1. To this end, three chimeric RNA species were synthesized composed of either the 5′ part of *sodB* fused in frame to the 3′ part of *ahrC* or, comprising two different 5′ parts of *ahrC* – containing or lacking complementary sequences to SR1 – fused in frame to the 3′ part of *sodB* lacking the RyhB target region. As internal control that is neither affected by SR1 nor by RyhB, the *E. coli ppiB* mRNA was included. As shown in Fig. 6B, the translation of the chimeric mRNA *F1* containing the 5′ 148 nt of *sodB* fused to the 3′ part of *ahrC* lacking the SD sequence and the 5′ 100 nt, was inhibited nearly completely by RyhB, and, to a lesser extend, by SR1, but not by RNAIII, suggesting that RyhB inhibited translation initiation and SR1 might obstruct ribosome movement along the chimeric mRNA. By contrast, the translation of the chimeric *ahrC-sodB* mRNA *F2* comprising the 5′ 100 nt of *ahrC* including SD sequence but lacking all SR1 target regions fused to the 3′ part of *sodB* lacking the RyhB target sequence was not inhibited by SR1, indicating that SR1 does not exert its function by inhibiting translation initiation from the *ahrC* SD sequence. These results were further substantiated by translation of a third chimeric RNA *F3* encompassing the 5′ 280 nt of *ahrC* including SD sequence and regions G, F and E complementary to SR1 fused to the 3′ part of *sodB*: Here, SR1 inhibited the synthesis of the AhrC-SodB fusion protein, confirming again that repression occurs after translation initiation. In all three cases, RNAIII as heterologous antisense RNA did not influence the translation of any fusion protein.

In vivo *reporter gene tests confirm the* in vitro *translation data*

To confirm *in vivo* that the interaction between SR1 and *ahrC* RNA inhibits translation, three translational fusions

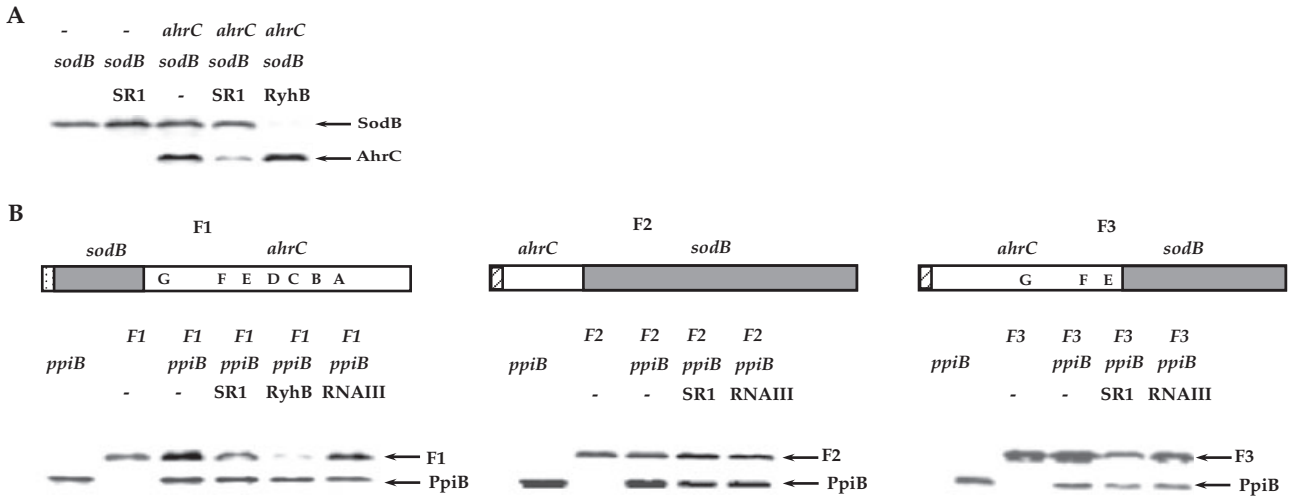

Fig. 6. *In vitro* translation of *ahrC* mRNA and chimeric RNAs in the presence and absence of SR1.
A. Inhibition of *ahrC* mRNA translation by SR1. *In vitro* translation was performed as described in *Experimental procedures* using 4 pmol of *in vitro* transcribed full-length *ahrC* mRNA and, as an internal control, full-length *sodB* mRNA as templates. Translation reactions were carried out in the absence or presence of an at least 10-fold molar excess of SR1 or RyhB. PhosphorImages of the dried gels are shown. The positions of [^{35}S]-labelled SodB (21.3 kDa) and AhrC (16.7 kDa) proteins are indicated by arrows.
B. Inhibition of translation of chimeric *sodB–ahrC* and *ahrC–sodB* mRNAs *F1*, *F2* and *F3* by SR1. *In vitro* translation was performed as above in the presence or absence of SR1 or RyhB or – as control, heterologous RNAIII – but instead of full-length *ahrC* mRNA, three different chimeric RNAs were used, *F1* containing 5′ 148 nt of *sodB* with the RyhB target region fused in frame to the 3′ 384 nt of *ahrC* containing all regions (G–A) complementary to SR1, but lacking the SD sequence and the 5′ 100 nt, *F2* containing the 5′ 100 nt of *ahrC* fused in frame to the 3′ *sodB* lacking both the SR1 and the RyhB complementary sequences and *F3* composed of the 5′ 280 nt of *ahrC* containing regions G, F and E complementary to SR1 fused to the 3′ part of *sodB* lacking the RyhB target sequences. As internal control that is neither affected by SR1 or RyhB, the *E. coli ppiB* mRNA was included yielding an 18 kDa protein. In all cases, 4 pmol of *in vitro* transcribed RNA was used as templates for translation, and an at least 10-fold molar excess of SR1, RyhB or RNAIII was added. The positions of the [^{35}S]-labelled fusion proteins F1 (22 kDa), F2 (21.5 kDa) and F3 (21.5 kDa) are indicated by arrows. Above the gels a schematic representation of the corresponding chimeric RNA is shown. Thereby, *ahrC* sequences are shown in white, *sodB* sequences in grey, the *ahrC* SD is shown as a stippled box, the *sodB* SD as hatched box. A–G denote the presence of the regions complementary to SR1 (see Fig. 3).

of *ahrC* with the promoterless reporter gene encoding the heat-stable β-galactosidase from *B. stearothermophilus* were constructed: the first comprises the 5′ 100 transcribed bp including SD sequence but lacking any region complementary to SR1 (plasmid pGGA1), the second contains the 5′ 280 transcribed bp of *ahrC* including the three regions G, F and E (see Fig. 3) complementary to SR1 (pGGA3) and the third encompasses the 5′ 350 transcribed bp of the *ahrC* gene with all seven complementary regions A–G (pGGA5). All three fusions were integrated into the *amyE* locus of the chromosome of *B. subtilis* strains DB104 and DB104(*Δsr1::phleo*). Strains were grown in TY medium till onset of stationary phase, when SR1 is expressed, samples withdrawn and β-galactosidase activities determined. Table 2 presents the results. In the presence of SR1, the β-galactosidase activity was highest in the case of pGGA1 lacking any region complementary to SR1. By contrast, β-galactosidase activities decreased ≈30-fold when three regions complementary to SR1 were present (pGGA3) and ≈70-fold – to almost the level of the empty vector pGFgaB –, when all seven regions complementary to SR1 were present (pGGA5). In the absence of SR1, no differences in the β-galactosidase activities were observed between the three constructs.

Three transcriptional fusions comprising the same sequences as the translational fusions but lacking SD sequence and start codon of *ahrC* were integrated into the *amyE* locus of *B. subtilis* strains DB104 and DB104(*Δsr1::phleo*). The results of the β-galactosidase measurements confirmed that the observed effects were due to inhibition of translation and not due to degradation of *ahrC* RNA in the presence of SR1: in all three cases – pACD1, pACD2 and pACD3 – no differences in the β-galactosidase activities were observed between the corresponding wild-type strain DB104 and the *sr1* knockout strains (Table 2). Interestingly, the β-galactosidase values differed between transcriptional fusions with shorter and longer *ahrC* sequences significantly, suggesting the presence of SR1 independent target sites for RNases within the 5′ 100 nt and within the 3′ 200 nt of *ahrC* RNA, which might be masked in the presence of translation.

These results strengthen the conclusion that SR1 acts by the inhibition of translation of *ahrC* RNA and not by RNA degradation, and that the inhibition of translation occurs at a post-initiation stage.

Table 2. β-Galactosidase activities of transcriptional *ahrC–lacZ* fusions and translational *ahrC*–BgaB fusions in the presence and absence of SR1.

Strain	*ahrC* sequence	β-Galactosidase activity (Miller units)
DB104::pACD1	100 nt (no)	2.85 ± 0.4
DB104::pACD1 (*Δsr1::phleo*)	100 nt (no)	3.02 ± 0.3
DB104::pACD3	280 nt (G, F, E)	202 ± 18
DB104::pACD3 (*Δsr1::phleo*)	280 nt (G, F, E)	244 ± 22
DB104::pACD2	479 nt (G, F, E, D, B, C, A)	49.4 ± 6
DB104::pACD2 (*Δsr1::phleo*)	479 nt (G, F, E, D, B, C, A)	59.2 ± 8
DB104::pAC6	No	1.29 ± 0.04
DB104::pAC6 (*Δsr1::phleo*)	No	1.35 ± 0.2
DB104::pGGA1	100 nt (no)	251 ± 28
DB104::pGGA3	280 nt (G, F, E)	7.6 ± 2
DB104:: pGGA5	479 nt (G, F, E, D, B, C and A)	3.5 ± 1.4
DB104::pGF-BgaB	No	2.9 ± 0.5
DB104::pGGA1 (*Δsr1::phleo*)	100 nt (no)	263 ± 30
DB104::pGGA3 (*Δsr1::phleo*)	280 nt (G, F, E)	198 ± 15
DB104:: pGGA5 (*Δsr1::phleo*)	479 nt (G, F, E, D, B, C and A)	230 ± 40
DB104::pGF-BgaB (*Δsr1::phleo*)	No	3.0 ± 0.4

All values represent averages of at least three independent determinations.
pACD1, pACD2 and pACD 3 containing *ahrC* sequences without SD and with an CTG instead of ATG codon fused to the promoterless *lacZ* gene were inserted into the *amyE* locus. Plasmid pAC6 is the empty vector (Table 3). pGGA1, pGGA3 and pGGA5 containing *ahrC* sequences fused in frame to the promoterless, SD less *gaB* gene encoding the heat-stable β-galactosidase of *B. stearothermophilus* were inserted into the *amyE* locus. pGF-BgaB is the empty vector (Table 3). β-Galactosidase activities for the *lacZ* and the BgaB fusions were measured at 28°C and 55°C, respectively, and, as the reporter genes are different, absolute enzyme activities are not comparable between transcriptional and translational fusions. In brackets, the presence of regions complementary to SR1 according to Fig. 3 is indicated.

SR1 has a half-life of ≈3.4 min in TY medium

To determine the half-life of SR1, *B. subtilis* strain DB104 was grown in TY medium at 37°C till beginning of the stationary growth phase (optical density of 5.0), where expression of SR1 was found to be maximal (see earlier). Rifampicin was added to a final concentration of 100 μg ml^{-1}, time samples were taken and used for the preparation of total RNA with subsequent Northern blotting as described in *Experimental procedures.* Quantification of the corresponding gels (Fig. 7) yielded a half-life of SR1 of approximately 3.4 min. Determinations of SR1 half-lives in TY medium at other temperatures gave the same results. This half-life was not significantly altered in the absence of its primary target, *ahrC* RNA (Fig. 7) as determined with DB104 (*ΔahrC::cat*) grown under the same conditions.

Hfq does not stabilize SR1

Many small RNAs from *E. coli* need Hfq for either stability or their interaction with their targets (see *Introduction*). As

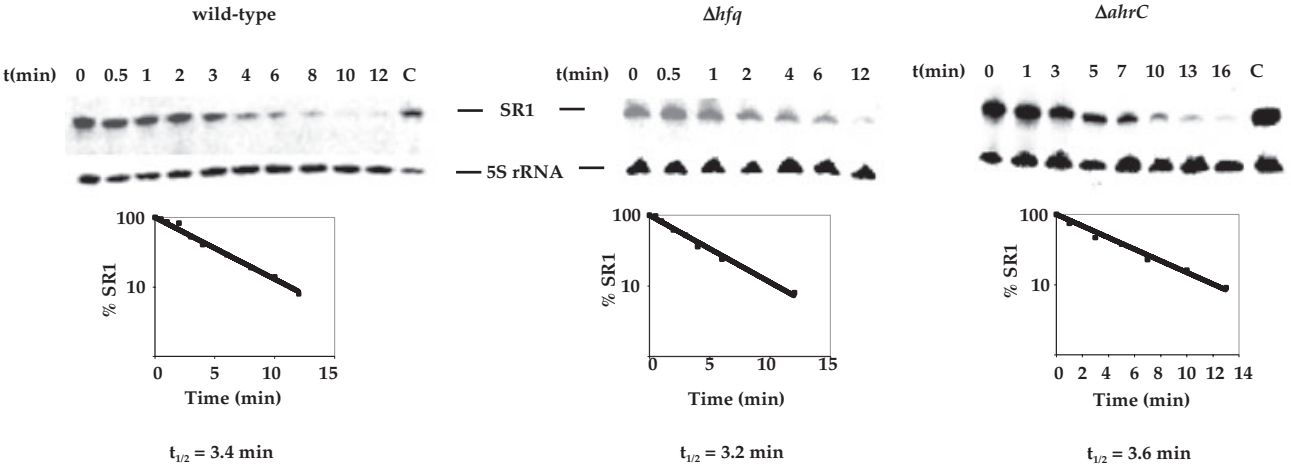

Fig. 7. Role of Hfq *in vivo*. Half-life of SR1 in the presence and absence of Hfq. *B. subtilis* strain DB104, DB104 (*Δhfq::cat*) or DB104 (*Δahr::cat*) was grown in TY medium at 37°C. At OD_{560} = 5.0, rifampicin was added to a final concentration of 100 μg ml^{-1} and samples were taken at the times indicated. To correct for loading errors, filters were reprobed with 5′ labelled oligonucleotide C-767 complementary to 5S rRNA. C, control without rifampicin. The autoradiographs of the Northern blots and below a graphical representation of the half-life determination are shown.

the equilibrium dissociation constant K_D of the SR1/*ahrC* complex was with 3.7×10^{-7} M very high, whereas the pairing rate constant was unusually low compared with other systems, we wanted to investigate, whether Hfq is required for stabilization of SR1 or promotion of complex formation with *ahrC* RNA. To this end, a *B. subtilis hfq* knockout strain was constructed by replacing the chromosomal *hfq* gene *ymaH* by a chloramphenicol resistance cassette using plasmid pINT2 as described in *Experimental procedures*. This strain proved to be viable and showed only a slight growth retardation compared with the isogenic wild-type strain. To find out, whether Hfq had an influence on the stability of SR1, both SR1 levels and SR1 half-life (Fig. 7) were determined in the *Δhfq* strain in comparison with the wild-type strain. As both half-life (3.4 versus 3.2 min) and amount of SR1 were comparable in both strains, we could conclude that Hfq does not stabilize SR1. The same result was obtained in the absence of *ahrC* mRNA (Fig. 7) and upon SR1 expression from the tetracycline-inducible promoter on plasmid pWSR1 in the presence or absence of *hfq* indicating that the presence of the target *ahrC* RNA did not play a role (Fig. S1, *Supplementary materials*). Preliminary *in vitro* interaction studies between *ahrC* RNA and SR1 in the presence of purified *B. subtilis* Hfq protein indicate that Hfq does not promote complex formation between both RNAs *in vitro* (data not shown).

However, Northern blots with RNA prepared from wild-type and *Δhfq* strains at $OD_{560} = 5.0$ showed an approximately 2.5-fold (*rocABC*) or sixfold (*rocDEF*) increase in the amount of the *roc* operon mRNAs (Fig. 2, Table 1), and this increase was almost as significant as that observed with the SR1 knockout strain. Three alternative explanations for this result were conceivable: First, Hfq might promote the interaction between SR1 and *ahrC* mRNA encoding the positive regulator of the *roc* operons. Alternatively, Hfq might have a direct influence on the folding or stability of the *roc* mRNAs or *ahrC* mRNA. Third, Hfq could influence a second, still unidentified factor involved in *roc* operon expression. To distinguish between these possibilities, an *sr1*/*hfq* double knockout strain was constructed as described in *Experimental procedures* and the amount of *rocABC* and *rocDEF* mRNAs was compared between wild-type strain, *hfq* knockout strain and *sr1*/*hfq* double knockout strains. As shown in Fig. 2 and Table 1, approximately the same increase in the amount of both *roc* mRNAs was found in the single and the double knockout strains, suggesting that SR1 and Hfq act in the same pathway.

In summary, these data prove that the RNA chaperone Hfq is not required for the stabilization of SR1 and suggest that it most likely does not promote the interaction between SR1 and its target *ahrC* mRNA. A direct effect of Hfq on folding or stability of the *roc* mRNAs or the *ahrC* mRNA cannot be excluded.

The amount of SR1 is increased in the presence of L-arginine and L-ornithine

Recently, we reported that SR1 expression is maximal under conditions of gluconeogenesis, but repressed under glycolytic conditions (Licht *et al*., 2005). Two proteins are responsible for sugar-mediated repression of SR1 transcription: CcpN as a major regulator mediating a repression effect by glucose and other sugars like sucrose, arabinose, fructose, or even glycerol, and, as a minor regulator, CcpA, the catabolite control protein. Whereas the *ccpN* operator is located 23 bp upstream of the –35 box of p_{SR1}, the unusually distant *cre* site (binding site for CcpA/Hpr) was found 239 bp upstream of the –35 box of p_{SR1} (Licht *et al*., 2005).

As we found that the primary target of SR1 is a transcriptional regulator of arginine catabolism, we analysed the influence of arginine and its degradation products ornithine and citrulline on growth of *B. subtilis* and the expression of *sr1*. First, to investigate, whether SR1 affects the growth of *B. subtilis* in minimal medium in the presence and absence of L-arginine, DB104 and DB104*(Δsr1::cat)* were grown in CSE minimal medium with glucose, without glucose and L-arginine and without glucose, but with L-arginine. No significant differences were observed between wild-type and *sr1* knockout strain (Fig. S2, *Supplementary material*).

Second, *B. subtilis* strain DB104 was grown in CSE medium without glucose and at $OD_{560} = 0.7–1.0$ (onset of stationary phase), L-arginine, L-ornithine, L-citrulline or L-proline were added to a final concentration of 20 mM, time samples taken and used for the preparation of total RNA and Northern blotting. As shown in Fig. 8A and B, the addition of L-arginine and L-ornithine led to an approximately two- to threefold increase in the amount of SR1, whereas L-citrulline and L-proline had no effect.

To test whether the effect of L-arginine and L-ornithine on the SR1 level was due to decreased degradation of SR1, rifampicin was added to DB104 cultures growing in CSE without glucose and, 15 min later, L-arginine was added. However, no effect on the SR1 level was found, indicating that L-arginine did not stabilize SR1 directly (data not shown). Furthermore, the L-arginine effect was not observed when DB104 (*Δsr1::cat*, pGKSR50) expressing *sr1* from p_{SR1} with a 50 bp upstream region was analysed. Apparently, in the presence of L-arginine, a regulatory factor seems to increase transcription from the *sr1* promoter, most probably by binding to a region more than 50 bp upstream of p_{SR1}. Analysis of DB104 (*Δsr1*::*phleo*) containing plasmids pACS12 and pACS14 that comprise the entire *sr1* gene with 87 bp and 250 bp, respectively, upstream of p_{SR1} revealed that the putative binding region must be located between 87 and 250 bp upstream of the –35 box of p_{SR1} (Fig. 8C, left).

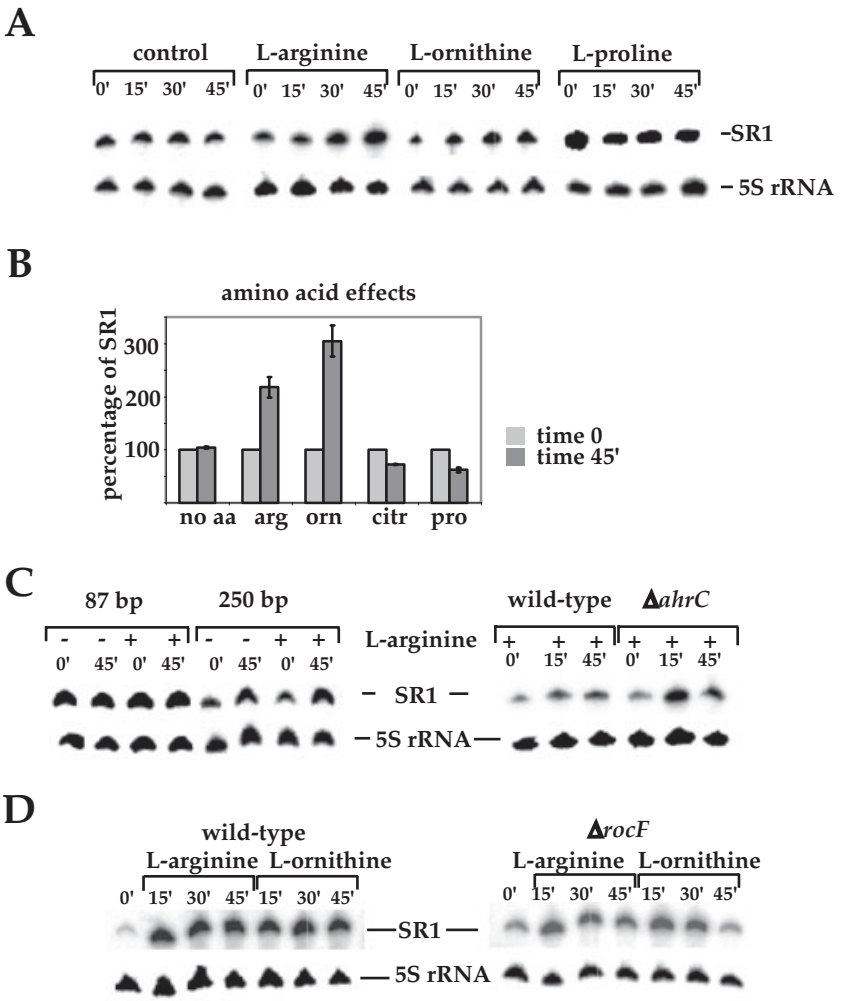

Fig. 8. Effect of L-arginine on the expression of SR1. Autoradiographs of Northern blots are shown. In all cases, *B. subtilis* strains were grown in CSE medium without glucose till OD_{560} = 1.0, L-arginine or other amino acids were added to a final concentration of 20 mM, time samples taken, total RNA prepared and a Northern blot performed as described in *Experimental procedures.* Reprobing was performed as in Fig. 7.
A. Effect of L-arginine, L-ornithine and L-proline on the expression of *sr1*. *B. subtilis* DB104 was used, L-arginine, L-ornithine or L-proline were added and samples taken at the times indicated.
B. Graphic representation of the amino acid effects. The amounts of SR1 found in the absence or presence of L-arginine, L-ornithine, L-citrulline and L-proline at time points 0 and 45 min are shown by columns.
C. Effect of the *sr1* upstream region and of AhrC on the L-arginine-dependent expression of *sr1*. *B. subtilis* DB104 (*Δsr1::phleo*) containing a copy of the *sr1* gene with different lengths' upstream regions integrated into the *amyE* locus was grown till OD_{560} = 1.0, L-arginine was added and samples were taken at the indicated times. pACS12 comprises 87 bp and pACS14 comprises 250 bp, respectively, upstream of the −35 box of p_{SR1}. *B. subtilis* strains DB104 and DB104(*ΔahrC::cat*) were grown till OD_{560} = 1.0, L-arginine was added to 20 mM and time samples taken. +, addition of L-arginine; –, no L-arginine added.
D. Influence of the *rocF* gene. *B. subtilis* 168 and 168 (Δ*rocF*) were grown till OD_{560} = 1.0, L-arginine or L-ornithine were added to 20 mM and samples taken at the indicated times.

To find out whether AhrC itself was responsible for the arginine effect on SR1, an *ahrC* knockout strain where *ahrC* in the chromosome was replaced by a chloramphenicol cassette using vector pINT6 was analysed. However, the same increase in the amount of SR1 was observed in this strain after addition of L-arginine (Fig. 8C, right) suggesting that it is not AhrC binding upstream of p_{SR1} that caused the effect on the SR1 level observed under wild-type conditions.

To analyse whether L-arginine is the responsible substance for the increase of the amount of SR1, the experiments were repeated with a *B. subtilis rocF* strain lacking arginase that converts L-arginine into L-ornithine. Figure 8D shows the results: Both in *B. subtilis* 168 and in the isogenic *rocF* strain, L-arginine and L-ornithine led to an increase of the amount of SR1. The increase obtained with L-arginine in the *rocF* strain excludes L-ornithine as the only player of the effect, because it cannot be produced in high amounts due to the lack of arginase.

Discussion

Here, we show that SR1 is a regulatory RNA involved in arginine catabolism that inhibits translation of *ahrC* mRNA by complementary base pairing. *In vitro* and *in vivo* assays (Fig. 5) demonstrated a direct interaction between both RNAs. Competition studies and interaction studies with a heterologous antisense RNA, RNAIII of plasmid pIP501, clearly showed that the SR1/*ahrC* interaction is specific (Fig. 5B and C). Furthermore, *in vitro* RNA/RNA interaction studies and *in vivo* reporter gene fusions indicated that the interaction does not require the 5′ 100 nt of *ahrC* mRNA. Currently, experiments are underway to narrow down the regions of SR1 and *ahrC* RNA required for the first contact between both molecules and to map the complex between SR1 and *ahrC* RNA with different RNases.

A variety of mechanisms have been found for the action of small regulatory RNAs encoded by either plasmids (for a review see Brantl, 2002) or the chromosome.

The majority of chromosomally encoded inhibitory regulators from *E. coli* analysed to date act either by direct blocking of the ribosome binding site by binding to the 5′ untranslated region or the 5′ part of the translated region of the target RNA (e.g. OxyS on *fhlA*-RNA, Altuvia *et al*., 1998; Spot42 RNA on *galK*-RNA, Møller *et al*., 2002a; or MicA on *ompA*-mRNA, Udekwu *et al*., 2005), or support degradation of the target RNA by RNase III or RNase E (e.g. RyhB RNA on *sod*B RNA, Massé and Gottesman, 2002; Afonyushkin *et al*., 2005). However, it is also conceivable that a regulatory RNA could decrease the processivity of translation elongation by binding downstream from the 5′ end and within the 3′ region of a target RNA. This seems to be the case for SR1: The SR1/*ahrC* RNA interaction did not lead to degradation of *ahrC* mRNA by RNaseIII or another RNase, as both RT-PCR on *ahrC* mRNA in wild-type, *sr1* knockout and *rnc* mutant strains and the transcriptional *ahrC–lacZ* fusions in the presence and absence of SR1 excluded this mechanism (Fig. 4, Table 2). As the region of complementarity between SR1 and *ahrC* mRNA does not comprise the SD sequence or the first 100 nt of *ahrC* mRNA, and SR1 binding was observed in the absence of these sequences (Fig. 5), an inhibition of translation initiation by SR1/*ahrC* pairing seemed unlikely. However, *in vitro* translation experiments showed that the amount of synthesized AhrC was decreased in the presence of an excess of SR1, but not of a heterologous RNA (Fig. 6A). Furthermore, *in vitro* translation experiments with three chimeric mRNA species supported the hypothesis that inhibition occurs after translation initiation (Fig. 6B). It is tempting to speculate that SR1 binding to the complementary regions in *ahrC* mRNA causes elongating ribosomes to stall and, subsequently, be rescued by the action of tmRNA. The *in vitro* translation data were confirmed *in vivo* by translational *ahrC*-reporter gene fusions: In the absence of sequences complementary to SR1, β-galactosidase activity was high, whereas in the presence of regions G, F and E or all regions A–G, β-galactosidase activity decreased significantly. It remains to be investigated whether other small regulatory RNAs exist that use the same inhibitory mechanism. Furthermore, it will be interesting to find out whether SR1 acts by the same mechanism on other target RNAs in *B. subtilis*.

The intracellular concentration of an RNA depends on both transcription and degradation rates. Interestingly, the determination of half-lives of recently discovered small regulatory RNAs from *E. coli* (see Vogel *et al*., 2003) showed a broad variation: both short-living RNAs like GcvB or SraJ (half-life < 4 min) as well as long-living RNAs like SroB or SraH (half-life ≥ 30 min) and RNAs with intermediate half-lives (8–15 min) like CsrC were found. The half-life of SR1 at 37°C was determined to be ≈3.5 min. Obviously, SR1 belongs to the group of short-living ncRNAs like GcvB, an RNA involved in the expression regulation of peptide transport systems. A short half-life – which has also been found for antisense RNAs regulating plasmid copy numbers some time ago (see Brantl, 2002) – is not unexpected for an RNA involved in fine-tuning of gene regulation.

The same half-life of 3.2–3.6 min was calculated in the presence or absence of its primary target *ahrC* mRNA (Fig. 7) indicating that – due to the high excess of SR1 over *ahrC* mRNA – degradation of SR1 is not influenced significantly by the pairing with this target. This observation further substantiates that the complex between SR1 and *ahrC* is not the target for an RNase.

Furthermore, both in the wild-type strain (single *sr1* copy in the chromosome) as well as in an overexpression strain DB104 (pWSR1) allowing rapid induction of high amounts of SR1 from the inducible *tet* promoter, the half-life of SR1 was not affected by the presence and absence of Hfq (Fig. 7 and Fig. S1 *Supplementary materials*). This is in contrast to several *E. coli* sense/antisense RNA systems investigated recently, where Hfq was found to be required for the stability of the small regulatory RNA (e.g. Wassarman *et al*., 2001). Preliminary *in vitro* data (not shown) indicate that *B. subtilis* Hfq does not promote complex formation with *ahrC* mRNA. Furthermore, the RT-PCR data on *ahrC* RNA in the *hfq* knockout strain (Fig. 4) showed that Hfq does not affect the amount of this primary target of SR1. Together with these results, our data on the downstream targets of SR1, *rocABC* and *rocDEF*-mRNA in the *hfq* knockout strain suggest that Hfq acts on the *roc*-operon mRNAs in the same pathway as SR1 (Fig. 2), at the same or at different steps. It is not excluded that Hfq binds directly to the *roc* mRNAs and influences their folding or stability, whereas SR1 binds to *ahrC* mRNA.

Interestingly, the amount of SR1 is upregulated by L-arginine and its degradation product L-ornithine (Fig. 8A) about two- to threefold, and our data show that a region between 87 and 250 bp upstream of the –35 region of p_{SR1} might be responsible for this effect (Fig. 8C, left). Because Northern blots with RNA from an *ahrC* knockout strain showed the same increase as those from the wild-type strain (Fig. 8C, right), AhrC can be excluded as the responsible factor. The lack of induction observed with addition of L-citrulline and L-proline was surprising. It is known that the expression of the *rocABC* and *rocDEF* operons can be induced, albeit to a varying degree of intensity, by all four of the above-mentioned amino acids, with L-ornithine or L-citrulline being the real inducer molecule, while L-arginine and L-proline effects are dependent on the presence of arginase (*rocF* gene product) and ornithine aminotransferase (*rocD* gene product) respectively (Gardan *et al*., 1997). A similar behaviour would have been expected for SR1 induction. The above results,

together with the lack of direct *ahrC* involvement, seem to exclude the involvement of an intracellular sensor-protein and might instead point to a membrane protein as sensor, which would be responsible for the first step of a cascade leading to the observed SR1 induction. It is fascinating to speculate that either RocC or RocE, both putative amino acid permeases, could be involved in the process. Experiments are underway to isolate and identify a protein mediating the L-arginine-dependent increase in SR1 expression.

Our results show that SR1 interacts with *ahrC* mRNA resulting in a decreased translation of this transcriptional activator and, consequently, a decreased expression of the *rocABC* and *rocDEF* operons. To date, SR1 is the first factor known to regulate the *ahrC* gene in *B. subtilis*. Because SR1 did not affect the growth of *B. subtilis* under conditions of glycolysis or gluconeogenesis in the presence or absence of L-arginine (Fig. S2 *Supplementary materials*), SR1 seems to fulfil a minor, fine-tuning role in the regulation of arginine catabolism. This is in agreement with other small regulatory RNAs, the absence or overexpression of which did not cause detrimental growth effects (e.g. Argaman *et al*., 2001).

Other bacterial species contain ArgR repressor instead of AhrC, which is only 27% identical but shows the same 3D structure, and *E. coli* argR mutants can be functionally complemented by AhrC. In *E. coli*, argR is regulated by two promoters, one of which is negatively autoregulated. By contrast, *B. subtilis ahrC* transcription starts from one promoter and is not autoregulated. SR1-mediated regulation of *ahrC* might provide a regulatory level similar to that of the autoregulated promoter in *E. coli*. Moreover, it cannot be excluded that SR1 is not the only small RNA involved in fine-tuning of the arginine metabolism and that the picture is more complicated as assumed so far. As has been shown for the *E. coli rpoS* gene, at least four different small RNAs are required to regulate translation (DsrA, RprA, OxyS) or transcription (6S RNA) of this gene encoding the stationary-phase sigma factor.

Among the Gram-negative bacteria, almost all small RNAs detected in *E. coli* are at least present in one or two other species, as this was one criterion for the verification of initial computer predictions (Argaman *et al*., 2001; Vogel *et al*., 2003). Previously, we reported that in four other *Bacillus/Geobacillus* genomes, the SR1 ORF is present, which – under normal growth conditions in complex and minimal media – is not translated in *B. subtilis* (Licht *et al*., 2005). Among these four species, in *B. licheniformis*, *B. cereus* and *B. anthracis*, a RNA similar to SR1 could be predicted, but only that of *B. licheniformis* had a similar length. In *G. kaustophilus*, no rho-independent terminator of a putative RNA could be identified. Like several low G + C Gram-positive bacteria, which harbour multiple *argR*-like genes, *B. licheniformis* has both an *argR* gene and an *ahrC* gene. The *argR* gene, under anaerobic conditions, participates in the activation of the *arcABCD* operon enzymes of the arginine deiminase pathway. Complementarity searches (see *Experimental procedures*) between the *B. licheniformis* SR1 and its arginine-regulating genes (Rey *et al*., 2004) revealed that in this species, the *argR* gene is likely the target of SR1: At least eight complementary stretches of 5–16 nt have been found. Future studies will be aimed at the elucidation of the SR1 function in this host.

As known from small RNAs in *E. coli*, many of them have multiple targets, e.g. DsrA binds *rpoS* and *hns* mRNA (Majdalani *et al*., 1998) and RyhB regulates *sodB*, *sdhCDAB*, *bfr*, *acn* and *fumA* (Massé and Gottesman, 2002). At present, it is not clear whether *ahrC* is the only target of SR1. Although the results of the 2D gel electrophoresis did not show significant alterations in the amounts of proteins other than RocF, RocD and RocA, only 25% of all *B. subtilis* proteins can be separated using this method, either due to an aberrant pI value, the inability to be solubilized or very low abundance. Therefore, alternative analyses are underway to search for other targets of SR1 and to analyse the possible mechanism by which SR1 might exert its inhibitory or activating role on them.

Experimental procedures

Enzymes and chemicals

Chemicals used were of the highest purity available. *Taq* DNA polymerase was purchased from Roche or SphaeroQ, Netherlands, respectively, RNA ligase from New England Biolabs and Thermoscript reverse transcriptase from Invitrogene. Firepol polymerase was purchased from Solis Biodyne, Estonia. An *in vitro* translation kit from Promega was used. Sequencing reactions were performed according to Sanger *et al*. (1977) using a Sequenase Kit from Amersham Bioscience.

Strains, media and growth conditions

Escherichia coli strains TG1 and DH5α were used for cloning. *B. subtilis* strains DB104 (*his*, *nprR2*, Δ*aprA3*, *nprE18*; Kawamura and Doi, 1984), wild-type *B. subtilis* 168, *B. subtilis* 168 *rocF* and *B. subtilis rnc* strain *BG218* (C-terminally truncated RNase III; Oguro *et al*., 1998) were used for the isolation of total RNA under different conditions. *E. coli* strains were grown in complex TY medium (16 g Bacto-Tryptone, 10 g Yeast extract, 5 g NaCl per 1 l). *B. subtilis* strains were grown either in TY medium or – under conditions of gluconeogenesis – in CSE-minimal medium (see Faires *et al*., 1999). The carbon sources in CSE in the absence of glucose are glutamate and succinate.

Construction of plasmids to supply SR1 in trans

Plasmid pUCBS1 (see Table 3 for all plasmids used in this study) expressing wild-type *sr1* under its own promoter was

Table 3. Plasmids used in this study.

Plasmid	Description	Reference
pUC19	*E. coli* cloning vector, Ap^R, MCS	Sambrook *et al.* (1989)
pUCB2	*E. coli*/*B. subtilis* shuttle vector, high copy number Ap^R, Km^R derived from pUC19/pUB110	Brantl and Wagner (1996)
pAC6	Integration vector for *amyE* gene, Ap^R, Cat^R, *lacZ* without promoter, with SD, for transcriptional fusions	Stülke *et al.* (1997)
pGF-BgaB	Integration vector for *amyE* gene, heat-stable β-galactosidase from *B. stearothermophilus* without SD for translational fusions, Km^R, Ap^R	Stoß *et al.* (1997)
pCAT	pUC19 with CAT gene as EcoRI/SalI fragment	Licht *et al.* (2005)
pUCSR1/2	pUC19 with *sr1* gene as BamHI/HindIII fragment	Licht *et al.* (2005)
pCBACK1	pBACK1 with CAT gene from pCAT	Licht *et al.* (2005)
pINT1	pUC19 with pFRONT1 BamHI/EcoRI fragment and pCBACK1 EcoRI/PstI fragment	Licht *et al.* (2005)
pINT1P	As pINT1, but with $Phleo^R$ instead of CAT gene	Licht *et al.* (2005)
pACR1	pAC6 with *rnaIII* gene under control of p_{SR1}	Licht *et al.* (2005)
pFRONT2	pUC19 with 800 bp upstream of *hfq* as BamHI/EcoRI fragment	This study
pCBACK2	puC19 with CAT gene from pCAT and 800 bp downstream from *hfq* as SalI/PstI fragment	This study
pINT2	pUC19 with pFRONT2 BamHI/EcoRI fragment and pCBACK2 EcoRI/PstI fragment, EcoRI/SalI cat gene fragment	This study
pFRONT6	pUC19 with 800 bp upstream of *ahrC* as BamHI/EcoRI fragment	This study
pCBACK6	As pCBACK2, but fragment downstream from *ahrC*	This study
pINT6	pUC19 with *ahrC* FRONT and *ahrC* BACK fragment separated by the EcoRI/SalI cat gene fragment	This study
pUCAhrC	pUC19 with entire *ahrC* gene as EcoRI/BamHI fragment	This study
pUCBS1	pUCB2 with wild-type sr1 gene under own promoter	This study
pUCBS12	As pUCBS1, but *sr1* gene with ATG-TAG exchange	This study
pUCSR1/12	pUC19 with *sr1* gene with 87 bp upstream of p_{SR1} as EcoRI/BamHI fragment	This study
pACS12	pAC6 with EcoRI/BamHI fragment of pUCSR1/12	This study
pUCSR1/14	As pUCSR1/12, but with 250 bp upstream of p_{SR1}	This study
pACS14	pAC6 with EcoRI/BamHI fragment of pUCSR1/14	This study
pGGA1	pGF-BgaB with 97 bp 5′-*ahrC*	This study
pGGA3	pGF-BgaB with 280 bp 5′-*ahrC*	This study
pGGA5	pGF-BgaB with 355 bp 5′-*ahrC*	This study
pACD1	pAC6 vector with 97 bp 5′-*ahrC*	This study
pACD3	pAC6 vector with 280 bp 5′-*ahrC*	This study
pACD2	pAC6 vector with 355 bp 5′-*ahrC*	This study

constructed by cloning a BamHI/HindIII fragment obtained by PCR with primers SB423 and SB317 into the BamHI/HindIII-digested pUCB2 vector. Plasmid pUCBS12 comprising the *sr1* gene with a TAG stop codon instead of the ATG start codon of the *sr1* ORF was constructed in a two-step PCR using inner primers SB838 and SB839 and outer primers SB423 and SB317 on chromosomal DNA of *B. subtilis* as template. Plasmid pUCBS12 comprises 100 bp upstream of p_{SR1}. All mutations were confirmed by sequencing.

Construction of plasmids for the translational and transcriptional reporter gene fusions

For the construction of the three translational fusions, chromosomal DNA from *B. subtilis* DB104 was used as template in three PCRs with upstream primer SB979 and the corresponding downstream primers SB967 (pGGA1), SB976 (pGGA3) and SB982 (pGGA5). All fragments were digested with BamHI and EcoRI and inserted into the BamHI/EcoRI vector pGF-BgaB (Stoß *et al.*, 1997) encoding the promoterless heat-stable β-galactosidase from *B. stearothermophilus*.

Corresponding transcriptional fusions that did not allow translation (deleted SD sequence, start codon ATG replaced by CTG) were constructed by three PCRs on chromosomal DNA with upstream primer SB1004 and downstream primers SB922 (pACD1), SB983 (pACD3) and SB923 (pACD2). The three fragments were cleaved with EcoRI and BamHI and inserted into the EcoRI/BamHI vector pAC6 encoding the promoterless β-galactosidase from *E. coli* (Stülke *et al.*, 1997).

Construction of an hfq *knockout, an* hfq/sr1 *double knockout strain as well as an* ahrC *knockout strain*

To obtain an *hfq* knockout strain, plasmid pINT2 was constructed in the following way:

First, plasmid pFRONT2 containing 800 bp upstream of the *hfq* gene, was obtained by cloning a BamHI/EcoRI-digested PCR fragment obtained on chromosomal DNA with primers SB402 and SB403 into the pUC19 BamHI/EcoRI vector. Plasmid pCBACK2 was constructed by cloning a SalI/PstI fragment comprising the 800 bp downstream from the *B. subtilis hfq* gene obtained with primer pair SB404 and SB405 into the SalI/PstI vector of pCBACK1 (Licht *et al.*, 2005). Subsequently, the BamHI/EcoRI fragment of plasmid pFRONT2 and the EcoRI/PstI fragment of plasmid pCBACK2 were jointly inserted into the pUC19 BamHI/PstI vector resulting in pINT2.

Subsequently, plasmid pINT2 was linearized with ScaI and used to replace the *hfq* gene of *B. subtilis* resulting in strain DB104 (*Δhfq*::*cat*). For the construction of the *hfq*/*sr1* double knockout strain, DB104 (*Δsr1*::*phleo*) was transformed with

the ScaI-linearized pINT2 vector and transformants were selected for phleomycin and chloramphenicol resistance. The successful double crossing-over was in both cases confirmed by PCR with *hfq* or *sr1* specific primers on chromosomal DNA prepared from the transformants.

To construct an *ahrC* knockout strain of DB104, the same approach was used as for the *hfq* knockout strain: First, plasmid pINT6 was constructed using a BamHI/EcoRI-digested PCR fragment for the *ahrC* upstream region obtained with primers SB879 and SB880, the EcoRI/SalI fragment for the *cat* cassette and a PstI/SalI-digested PCR fragment comprising the *ahrC* downstream region obtained with primers SB881 and SB882 on chromosomal DNA. This plasmid was integrated into the *B. subtilis* DB104 chromosome as described above resulting in DB104(Δ*ahrC::cat*).

Construction of plasmids for the analysis of the L*-arginine effect*

Plasmid pUCSR1/12 was constructed by inserting an EcoRI/BamHI fragment generated with primers SB827 and SB845 on plasmid pUCBS12 into the EcoRI/BamHI pUC19 vector. Plasmid pACS12 was obtained by cloning the pUCSR1/12 EcoRI/BamHI fragment into the pAC6 vector cleaved with the same pair of enzymes. Plasmid pACS14 was constructed in the following way: A PCR fragment generated by a two-step PCR on plasmid pUCBS12 with primer pair SB838/SB845 and *B. subtilis* chromosomal DNA with primer pair SB421/SB839, respectively, amplified in a second PCR with outer primers SB421 and SB845, subsequently digested with EcoRI and BamHI and inserted into the EcoRI/BamHI vector of pUC19 yielding pUCSR1/14. Afterwards, the EcoRI/BamHI fragment of pUCSR1/14 was cloned into the EcoRI/BamHI vector of pAC6 resulting in pACS14.

Isolation of chromosomal DNA from B. subtilis

Chromosomal DNA from *B. subtilis* was isolated as described recently (Licht *et al*., 2005).

In vitro *transcription*

In vitro transcription experiments were performed as described previously (Brantl and Wagner, 1996; Heidrich and Brantl, 2003).

In vitro *translation*

Commercial S30 extracts (Promega) were used to translate *in vitro* transcribed and gel-purified RNAs according to the manufacturer's instructions. The translation reactions were incubated for 60 min at 37°C in the presence of [^{35}S]methionine and terminated by addition of four volumes of cold 100% acetone, followed by 15 min on ice and subsequent centrifugation at 10 000 *g* at 4°C for 10 min. The pellets were dried, resuspended in protein loading buffer, boiled for 5 min and aliquots were separated on 15% Tris-glycine polyacrylamide gels. Dried gels were analysed by PhosphorImaging.

Isolation of total RNA for Northern blot analyses

Overnight cultures of *B. subtilis* strains were diluted 100-fold and grown on complex or minimal medium. At different optical densities between 0.5 (OD_{560} = 5–12) and 2 ml (OD_{560} = 0.2) of each culture was immediately frozen in liquid nitrogen. In cases where RNA half-lives were analysed, rifampicin was added (final concentration: 200 μg ml^{-1}) when the desired OD_{560} was reached. Samples were taken at the indicated time points and immediately frozen in liquid nitrogen. Frozen samples were stored at −20°C for later preparation of total RNA as described previously (Licht *et al*., 2005).

DNA-free RNA used for the analysis in agarose gels and for RT experiments was prepared as follows: Cells, frozen in liquid nitrogen, were harvested at 6000 r.p.m. and the pellet from 20 ml logarithmic or 12 ml stationary-phase cultures was suspended in 1 ml of lysis buffer. Cells were broken in 2 ml vials filled halfway with glass beads five times for 30 s each using a bead beater, the supernatant was collected and mixed 1:1 with CsCl solution 1 (1 g ml^{-1} CsCl, 25 mM EDTA, 50 mM Tris/HCl pH 8.0, 0.5% Sarcosyl). A gradient composed of 1.5 ml of CsCl solution 2 (5.7 M CsCl, 0.1 M EDTA), 1 ml of CsCl solution 1 and the supernatant was prepared, and centrifuged at 20°C at 35.000 r.p.m. overnight. The pellet containing the RNA was collected, precipitated, dissolved in 500 μl of DEPC water and precipitated with ethanol. The final pellet was dissolved in 50 μl of DEPC water and treated with 1 μl of DNase (Roche) for 15 min at 37°C. DNase was removed by phenol/chloroform extractions and ethanol precipitation. The resulting RNA was quantified by spectrophotometry.

To visualize larger RNA species, 1% or 1.5% gels (without ethidium bromide) in BPTE buffer (10 mM PIPES, 30 mM Bis-Tris, 1 mM EDTA pH 8, final pH 6.5) were used. The RNA samples were treated for 1 h at 50°C with glyoxal (2 μl of RNA, 10 μl of 4 M or 60% glyoxal) prior to electrophoresis.

Northern blot analysis

For the analysis of small RNA species, 6% denaturing polyacrylamide gels were used and electrotransfer was performed as described (Licht *et al*., 2005).

For the analysis of larger target RNA species, 1% or 1.5% agarose gels without ethidium bromide were run and blotted by downward capillary transfer on Biodyne A transfer membranes. Before blotting the gels were treated on a rotary shaker for 20 min in 0.05 M NaOH, then equilibrated with 20× SSC. The transfer was performed for 3 h in 20× SSC.

Subsequently, the RNA was bound to the membrane by UV-crosslinking. Prehybridization was carried out for 2–4 h at 62°C in 10 ml of prehybridization buffer (6× SSC, 3× Denhardt, and 0.5% SDS, 0.3 mg ml^{-1} salmon sperm DNA). Hybridization was performed overnight at 62°C in the same buffer lacking salmon sperm DNA but containing 1–2 × 10^6 cpm ml^{-1} of labelled probe ([α-^{32}-P]-dATP-labelled double-stranded DNA-fragment generated by PCR or [γ-^{32}-P]-ATP-labelled oligonucleotides). Membranes were washed once for 30 min at 62°C in 2× SSC, 0.5% SDS and once for 30 min in 0.5× SSC, 0.5% SDS. Signals were quantified in a Fuji PhosphorImager. Wet membranes were stored at

–20°C to allow reprobing. Removal of labelled probe was performed by boiling (10 min in 1% SDS) followed by prehybridization. To correct for loading errors, reprobing was carried out with either [γ-^{32}P]-ATP-labelled oligonucleotide C767-27 (5′GGG TGT GAC CTC TTC GCT ATC GCC ACC) that is complementary to *B. subtilis* 5S rRNA or – for agarose gels – with oligo SB746 (5′-ACC CGA CAA GGA ATT TCG C) complementary to 23S rRNA; both prehybridization and hybridization were performed at 62°C in 6× SSC, 3× Denhardt and 0.5% SDS (probe: 3×10^5 cpm ml^{-1}). Filters were washed and quantified as described above. All Northern blot analyses and subsequent calculations were performed in triplicate on total RNA isolated independently from different cultures.

RT-PCR

In this study 50 ng of total RNA isolated by CsCl gradient centrifugation from DB104 wild-type, DB104 (*Δsr1::cat*) and DB104 (*Δhfq::cat*) was used for reverse transcription in a total volume of 20 μl in three steps for 20 min each at 55°C, 60°C and 65°C with the Thermoscript RT system (*Invitrogene*) and oligonucleotides SB684 (complementary to *ahrC* RNA) and SB792 (complementary to *pnp*-RNA) followed by 5 min at 85°C. One microlitre of the total reaction was used for 30 rounds of PCR amplification (30 s each at 94°C, 37°C and 72°C) with Firepol *Taq* polymerase and oligonucleotides SB791 and SB792 complementary to *pnp*-mRNA as internal control. The resulting DNA fragments were separated in 3% agarose gels, the band intensities quantified and used for corresponding dilutions of the RT mixes. In this study 1:10, 1:250 and 1:500 dilutions of the RT mixes were used in a touch-down PCR with *ahrC*-specific primers SB683 and SB684 (eight cycles 94°C, 30 s; 55°C, 30 s; 72°C, 45 s, followed by 20 cycles 94°C, 30 s; 52°C, 30 s; 72°C, 45 s). The PCR mixes were ethanol-precipitated and separated in a 3% agarose gel. Negative controls were obtained by PCR amplification without previous RT and with water instead of total RNA.

Analysis of RNA–RNA complex formation

Both target RNA (3′ 376 nt of *ahrC* mRNA) and SR1 were synthesized *in vitro* from PCR-generated template fragments with primer pairs as indicated in Table S1 (*Supplementary materials*) using T7 RNA polymerase (NEB) and purified from 6% denaturing polyacrylamide gels as described (Heidrich and Brantl, 2003). The concentration of the unlabelled RNAs was determined by UV spectrophotometry, and the concentration of SR1, end-labelled with [γ^{32}-P]-ATP after treatment with alkaline phosphatase, was measured using a scintillation counter. Both RNAs were resolved in TMN buffer (20 mM Tris-acetate pH 7.5, 2 mM $MgCl_2$, 100 mM NaCl) and incubated for 2 min at 95°C, 2 min on ice followed by 30 min at 37°C to allow for proper folding. Various concentrations of unlabelled target RNA (10^{-8}–10^{-6} M) were incubated with 15 000 cpm of labelled SR1 in TMN buffer with 0.1 μg μl^{-1} tRNA for 15 min at 37°C, one volume of stop solution (1× TMN, 50% glycerol, 0.5% bromphenol blue and xylene cyanol) was added, the mixtures rapidly cooled on ice and immediately loaded onto a 6% native polyacrylamide gel (acrylamide:bisacrylamide = 37.5:1) containing 1× TBE and separated in running buffer (0.5-fold TBE) for 4 h at 20 mA at 4°C. Dried gels were analysed by PhosphorImaging.

Preparation of protein extracts and 2D gel electrophoresis

In this study 50 ml of *B. subtilis* wild-type 168 or knockout strain was grown in TY medium until $OD_{650} = 5.0$. Cells were harvested by centrifugation, the pellets were suspended in TE buffer pH 8.0 containing 0.1% PMSF and sonicated in a total volume of 500 μl three times for 30 s each. Lysates were centrifuged at 4°C for 30 min, the supernatant used for the determination of the protein concentration with BRADFORD agent and subsequently stored at –20°C.

For 2D protein gel electrophoresis and silver staining, 80 μg of each protein lysate was used. 2D protein electrophoresis and identification of Coomassie-stained protein spots by MALDI-TOF-MS were performed as described before (Eymann *et al*., 2004).

RNA bimolecular folding and structure prediction

RNA sequences used for secondary structure prediction were derived from the corresponding DNA sequences contained in the *B. subtilis* genome available from the NCBI database (http://www.ncbi.nlm.nih.gov/ Sequence ref. no. NC_000964). Bimolecular RNA structures were predicted using RNAStructure (http://128.151.176.70/RNAstructure.html Mathews *et al*., 2004). The structure with highest pairing between the two RNAs under investigation was chosen among the various predicted structures with lowest free energy levels.

Acknowledgements

The authors thank Eckhard Birch-Hirschfeld, Jena, for synthesis of the oligodeoxyribonucleotides. Furthermore, we acknowledge Dörte Becher for the identification of Roc proteins by MALDI-TOFF-MS and Annette Tschirner for excellent 2D protein separation (both from Greifswald). We thank Michel Débarbouillé, Paris, for the *rocF* strain and David Bechhofer, New York, for the BG218 strain. This work was supported by Grant BR1552/6-1 from the Deutsche Forschungsgemeinschaft to S. Brantl. A. Chinali is financed by Grant 0312704 A from the BMBF.

References

Afonyushkin, T., Vecerek, B., Moll, I., Blasi, U., and Kaberdin, V.R. (2005) Both RNase E and RNAse III control the stability of *sodB* mRNA upon translational inhibition by the small regulatory RNA RyhB. *Nucleic Acids Res* **33:** 1678–1689.

Altuvia, S., Weinstein-Fischer, D., Zhang, A., Postow, L., and Storz, G. (1997) A small, stable RNA induced by oxidative stress: role as a pleiotropic regulator and antimutator. *Cell* **90:** 443–453.

Altuvia, S., Zhang, A., Argaman, L., Tiwari, A., and Storz, G. (1998) The *Escherichia coli* OxyS regulatory RNA represses *fhlA* translation by blocking ribosome binding. *EMBO J* **20:** 6069–6075.

Ando, Y., Asari, S., Suzuma, S., Yamane, K., and Nakamura, K. (2002) Expression of a small RNA, BS203 RNA, from the *yocI–yocJ* intergenic region of *Bacillus subtilis* genome. *FEMS Microbiol Lett* **207:** 29–33.

Argaman, L., Herschberg, R., Vogel, J., Bejerano, G., Wagner, E.G.H., Margalit, H., and Altuvia, S. (2001) Novel small RNA-encoding genes in the intergenic regions of *Escherichia coli*. *Curr Biol* **11:** 941–950.

Barrick, J.E., Sudarsan, N., Weinberg, Z., Ruzzo, W.L., and Breaker, R.R. (2005) 6S RNA is a widespread regulator of eubacterial RNA polymerase that resembles an open promoter. *RNA* **11:** 774–784.

Brantl, S. (2002) Antisense-RNA regulation and RNA interference. *Biochim Biophys Acta* **1575:** 15–25.

Brantl, S., and Wagner, E.G.H. (1994) Antisense RNA-mediated transcriptional attenuation occurs faster than stable antisense/target RNA pairing: an *in vitro* study of plasmid pIP501. *EMBO J* **13:** 3599–3607.

Brantl, S., and Wagner, E.G.H. (1996) An unusually long-lived antisense RNA in plasmid copy number control: *in vivo* RNAs encoded by the streptococcal plasmid pIP501. *J Mol Biol* **255:** 275–288.

Calogero, S., Gardan, R., Glaser, P., Schweizer, J., Rapoport, G., and Débarbouillé, M. (1994) RocR, a novel regulatory protein controlling arginine utilization in *Bacillus subtilis*, belongs to the *NtrC/NifA* family of transcriptional activators. *J Bacteriol* **176:** 1234–1241.

Chen, S., Lesnik, E.A., Hall, T.A., Sampath, R., Griffey, R.H., Ecker, D.J., and Blyn, L.B. (2002) A bioinformatics based approach to discover small RNA genes in the *Escherichia coli* genome. *Biosystems* **65:** 157–177.

Chen, S., Zhang, A., Blyn, L.G., and Storz, G. (2004) MicC, a second small-RNA regulator of omp protein expression in *Escherichia coli*. *J Bacteriol* **186:** 6689–6697.

Delihas, N., and Forst, S. (2001) MicF: an antisense RNA gene involved in response of *Escherichia coli* to global stress factors. *J Mol Biol* **313:** 1–12.

Eymann, C., Dreisbach, A., Albrecht, D., Bernhardt, J., Becher, D., Gentner, S., *et al.* (2004) A comprehensive proteome map of growing *Bacillus subtilis* cells. *Proteomics* **10:** 2849–2876.

Faires, N., Tobisch, S., Bachem, S., Martin-Verstraete, I., Hecker, M., and Stülke, J. (1999) The catabolite control protein CcpA controls ammonium assimilation in *Bacillus subtilis*. *J Mol Microbiol Biotechnol* **1:** 141–148.

Fierro-Monti, I.P., Reid, S.J., and Woods, D.R. (1992) Differential expression of a *Clostridium acetobutylicum* antisense RNA: implications for regulation of glutamine synthetase. *J Bacteriol* **174:** 7642–7647.

Gardan, R., Rapoport, G., and Débarbouillé, M. (1997) Role of the transcriptional activator RocR in the arginine-degradation pathway of *Bacillus subtilis*. *Mol Microbiol* **24:** 825–837.

Heidrich, N., and Brantl, S. (2003) Antisense-RNA mediated transcriptional attenuation: importance of a U-turn loop structure in the target RNA of plasmid pIP501 for efficient inhibition by the antisense RNA. *J Mol Biol* **333:** 917–929.

Huntzinger, E., Boisset, S., Saveanu, C., Benito, Y., Geissmann, T., Namane, A., *et al.* (2005) *Staphylococcus aureus* RNAIII and the endoribonuclease III coordinately regulate *spa* gene expression. *EMBO J* **24:** 824–835.

Kawamura, F., and Doi, R.H. (1984) Construction of a *Bacillus subtilis* double mutant deficient in extracellular alkaline and neutral proteases. *J Bacteriol* **160:** 442–444.

Klingel, U., Miller, C.M., North, A.K., Stockley, P.G., and Baumberg, S. (1995) A binding site for activation by the *Bacillus subtilis* AhrC protein, a repressor/activator of arginine metabolism. *Mol Gen Genet* **248:** 329–340.

Lease, A.L., and Belfort, M. (2000) A *trans*-acting RNA as a control switch in *Escherichia coli*: DsrA modulates function by forming alternative structures. *Proc Natl Acad Sci USA* **97:** 9919–9924.

Lee, J.M., Zhang, S., Saha, S., Santa Anna, S., Jiang, C., and Perkins, J. (2001) RNA expression analysis using an antisense *Bacillus subtilis* genome array. *J Bacteriol* **183:** 7371–7380.

Lenz, D.H., Mok, K.C., Lilley, B.N., Kulkarni, R.V., Wingreen, N.S., and Bassler, B.L. (2004) The small RNA chaperone Hfq and multiple small RNAs control quorum sensing in *Vibrio harveyi* and *Vibrio cholerae*. *Cell* **118:** 69–82.

Licht, A., Preis, S., and Brantl, S. (2005) Implication of CcpN in the regulation of a novel untranslated RNA (SR1) in *B. subtilis*. *Mol Microbiol* **58:** 189–206.

Majdalani, N., Cunning, C., Sledjeski, D., Eliott, T., and Gotttesman, S. (1998) DsrA RNA regulates translation of RpoS message by an anti-antisense mechanism, independent of its action as an antisilencer of transcription. *Proc Natl Acad Sci USA* **95:** 12462–12467.

Majdalani, N., Chen, S., St. Murrow, J., John, K., and Gotttesman, S. (2001) Regulation of RpoS by a novel small RNA: the characterization of RprA. *Mol Microbiol* **39:** 1382–1394.

Mangold, M., Siller, M., Roppenser, B., Vlaminckx, B.J., Penfound, T.A., Klein, R., *et al.* (2004) Synthesis of group A streptococcal virulence factors is controlled by a regulatory RNA molecule. *Mol Microbiol* **53:** 1515–1527.

Massé, E., and Gottesman, S. (2002) A small RNA regulates the expression of genes involved in iron metabolism in *Escherichia coli*. *Proc Natl Acad Sci USA* **99:** 4620–4625.

Mathews, D.H., Disney, M.D., Childs, J.L., Schroeder, S.J., Zuker, M., and Turner, D.H. (2004) Incorporating chemical mocification constraints into a dynamic programming algorithm for prediction of RNA secondary structure. *Proc Natl Acad Sci USA* **101:** 7287–7292.

Miller, C.M., Baumberg, S., and Stockley, P.G. (1997) Operator interactions by the *Bacillus subtilis* arginine repressor/activator, AhrC: novel positioning and DNA-mediated assembly of a transcriptional activator at catabolic sites. *Mol Microbiol* **26:** 37–48.

Møller, T., Franch, T., Udesen, C., Gerdes, K., and Valentin-Hansen, P. (2002a) Spot 42 RNA mediates discoordinate expression of the *E. coli* galactose operon. *Genes Dev* **16:** 1696–1706.

Møller, T., Franch, T., Hojrup, P., Keene, D.R., Bächinger, H.P., Brennan, R.G., and Valentin-Hansen, P. (2002b) Hfq: a bacterial Sm-like protein that mediates RNA–RNA interaction. *Mol Cell* **9:** 23–30.

Morfeldt, E., Taylor, D., von Gabain, A., and Arvidson, S. (1995) Activation of alpha-toxin translation in *Staphylococcus areus* by the *trans*-encoded antisense RNA, RNAIII. *EMBO J* **14:** 4569–4577.

Oguro, A., Kakeshita, H., Nakamura, K., Yamane, K., Wang, W., and Bechhofer, D. (1998) *Bacillus subtilis* RNase III cleaves both 5′- and 3′-sites of the small cytoplasmic RNA precursor. *J Biol Chem* **273:** 19542–19547.

Opdyke, J.A., Kang, J.-G., and Storz, G. (2004) GadY, a small RNA regulator of acid response genes in *Escherichia coli*. *J Bacteriol* **186:** 6698–6705.

Rasmussen, A.A., Eriksen, M., Gilany, K., Udesen, C., Franch, T., Petersen, C., and Valentin-Hansen, P. (2005) Regulation of *ompA* mRNA stability: the role of a small regulatory RNA in growth phase-dependent control. *Mol Microbiol* **58:** 1421–1429.

Rey, M.W., Ramaiya, P., Nelson, B.A., Brody-Karpin, S.D., Zaretsky, E.J., Tang, M., *et al.* (2004) Complete genome sequence of the industrial bacterium *Bacillus licheniformis* and comparisons with closely related *Bacillus* species. *Genome Biol* **5:** R77.

Rivas, E., Klein, R.J., Jones, T.A., and Eddy, S.R. (2001) Computational identification of noncoding RNAs in *E. coli* by comparative genomics. *Curr Biol* **11:** 1369–1373.

Sambrook, J., Fritsch, E.F., and Maniatis, T. (1989) *Molecular Cloning. A Laboratory Manual*. New York: Cold Spring Harbor Laboratory Press.

Sanger, F., Nicklen, S., and Coulson, A.R. (1977) DNA sequencing with chain terminating inhibitors. *Proc Natl Acad Sci USA* **74:** 5463–5467.

Silvaggi, J.M., Perkins, J.B., and Losick, R. (2005) Small untranslated RNA antitoxin in *Bacillus subtilis*. *J Bacteriol* **187:** 6641–6650.

Sledjeski, D.D., Whitman, C., and Zhang, A. (2001) Hfq is necessary for regulation by the untranslated RNA DsrA. *J Bacteriol* **183:** 1997–2005.

Song, H., Wang, H., Gigot, D., Dimova, D., Sakanyan, V., Glansdorff, N., and Charlier, D. (2002) Transcription regulation in thermophilic bacteria: high resolution contact probing of *Bacillus stearothermophilus* and *Thermotoga neapolitana* arginine repressor–operator interactions. *J Mol Biol* **315:** 255–274.

Stoß, O., Mogk, A., and Schumann, W. (1997) Integrative vector for contsructing single-copy translational fusions between regulatory regions of *Bacillus subtilis* and the *bgaB* reporter gene encoding a heat-stable β galactosidase. *FEMS Microbiol Lett* **150:** 49–54.

Stülke, J., Martin-Verstraete, I., Zagorec, M., Rose, M., Klier, A., and Rapoport, G. (1997) Induction of the *Bacillus subtilis ptsGHI* operon by glucose is controlled by a novel antiterminator, GlcT. *Mol Microbiol* **25:** 65–78.

Suzuma, S., Asari, S., Bunai, K., Yoshino, K., Ando, Y., Kakeshita, H., *et al.* (2002) Identification and characterization of novel small RNAs in the *aspS–yrvM* intergenic region of the *Bacillus subtilis* genome. *Microbiology* **148:** 2591–2598.

Trotochaud, A.E., and Wassarman, K.M. (2005) A highly conserved 6S RNA structure is required for regulation of transcription. *Nat Struct Mol Biol* **12:** 313–319.

Udekwu, K.I., Darfeuille, F., Vogel, J., Reimegard, J., Holmqvist, E., and Wagner, E.G.H. (2005) Hfq-dependent regulation of OmpA synthesis is mediated by an antisense RNA. *Genes Dev* **19:** 2355–2366.

Urbanowski, M.L., Stauffer, L.T., and Stauffer, G.V. (2000) The *gcvB* gene encodes a small untranslated RNA involved in expression of the dipeptide and oligopeptide transport systems in *Escherichia coli*. *Mol Microbiol* **37:** 856–868.

Vanderpool, C.K., and Gottesman, S. (2004) Involvement of a novel transcriptional activator and small RNA in post-transcriptional regulation of the glucose phosphoenolpyruvate phosphotransferase system. *Mol Microbiol* **54:** 1076–1089.

Vogel, J., Bartels, V., Tang, T.H., Churakov, G., Slagter-Jäger, J.G., Hüttenhofer, A., and Wagner, E.G.H. (2003) RNomics in *Escherichia coli* detects new sRNA species and indicates parallel transcriptional output in bacteria. *Nucleic Acids Res* **31:** 6435–6443.

Vogel, J., Argaman, L., Wagner, E.G.H., and Altuvia, S. (2004) The small RNA IstR inhibits synthesis of an SOS-induced toxic peptide. *Curr Biol* **14:** 2271–2276.

Wassarman, K.M., Repoila, F., Rosenow, C., Storz, G., and Gottesman, S. (2001) Identification of novel small RNAs using comparative genomics and microarrays. *Genes Dev* **15:** 1637–1651.

Zhang, A., Altuvia, S., Tiwari, A., Argaman, L., Hengge-Aronis, R., and Storz, G. (1998) The *oxyS* regulatory RNA represses *rpoS* translation by binding Hfq (HF-1) protein. *EMBO J* **17:** 6061–6068.

Zhang, A., Wassarman, K.M., Ortega, J., Steven, A.C., and Storz, G. (2002) The Sm-like Hfq protein increases OxyS RNA interaction with target mRNAs. *Mol Cell* **9:** 11–22.

Supplementary material

The following supplementary material is available for this article online:

Fig. S1. Role of Hfq *in vivo*.

Fig. S2. Influence of SR1 on the growth of *B. subtilis* in the presence and absence of glucose or L-arginine.

Table S1. Oligodeoxyribonucleotides used for the construction of plasmids, for *in vitro* transcription and as probes for Northern blotting.

This material is available as part of the online article from http://www.blackwell-synergy.com

5. *In vitro* analysis of the interaction between the small RNA SR1 and its primary target *ahrC*-RNA

[Manuskript III]

Nadja Heidrich[1], Isabella Moll[2] and Sabine Brantl[1]

[1]AG Bakteriengenetik, Friedrich-Schiller-Universität Jena, Philosophenweg 12, D-07743 Jena, Germany
[2]Institut für Genetik u. Mikrobiologie, Max F. Perutz Laboratories, Dr. Bohrgasse 9/3, A-1030 Wien, Austria

eingereicht bei *Nucleic Acids Research*

In vitro analysis of the interaction between the small RNA SR1 and its primary target *ahrC* mRNA

Nadja Heidrich[1], Isabella Moll[2] and Sabine Brantl[1*]

Address:

[1]AG Bakteriengenetik, Friedrich-Schiller-Universität Jena, Philosophenweg 12, Jena D-07743, Germany
Tel: +49-3641-949570/571
Fax: +49-3641-949572
email: Sabine.Brantl@rz.uni-jena.de

[2] Max F. Perutz Laboratories, Department of Microbiology and Immunobiology, University Departments at the Vienna Biocenter, Dr. Bohrgasse 9/4, 1030 Vienna, Austria.

Running title: *In vitro* analysis of the small RNA SR1 from *B. subtilis*
Key words: small regulatory RNA/riboregulator/SR1/antisense RNA /target RNA interaction/Hfq

* Corresponding author

Abstract

Small regulatory RNAs (sRNAs) from bacterial chromosomes became the focus of research over the past five years. However, relatively little is known in terms of structural requirements, kinetics of interaction with their targets and degradation in contrast to well-studied plasmid-encoded antisense RNAs. Here, we present a detailed *in vitro* analysis of SR1, a sRNA of *B. subtilis* that is involved in regulation of arginine catabolism by basepairing with its target, *ahrC* mRNA. The secondary structures of SR1 species of different lengths and of the SR1/*ahrC* RNA complex were determined and functional segments required for complex formation narrowed down. The initial contact between SR1 and its target was shown to involve the 5' part of the SR1 terminator stem and a region 100 bp downstream from the *ahrC* transcriptional start site. Toeprinting studies and secondary structure probing of the *ahrC*/SR1 complex indicated that SR1 inhibits translation initiation by inducing structural changes downstream from the *ahrC* RBS. Furthermore, it was demonstrated that Hfq, which binds both SR1 and *ahrC* RNA was not required to promote *ahrC*/SR1 complex formation but to enable the translation of *ahrC* mRNA. The intracellular concentrations of SR1 were calculated under different growth conditions.

Introduction

Small regulatory RNAs (sRNAs) are expressed in both prokaryotes and eukaryotes, primarily as posttranscriptional regulators. Over the past 6 years, about 70 sRNAs have been discovered in *E. coli*, and about 20 of them have been assigned a function. Many of these trans-encoded RNAs are involved in metabolic processes (e.g. Spot42, DsrA, RprA, RyhB, SgrS, GadY, rev. in 1) and at least 8 sRNAs regulate the expression of membrane proteins (reviewed in 2). To date, relatively few systematic searches have been performed in Gram-positive bacteria. Among the recently discovered sRNAs in Gram-positive hosts are RatA from the *B. subtilis* chromsome (3) which came up in a systematic search (4) together with 12 other sRNAs that proved to be sporulation-controlled, but still await the identification of their targets (5). Furthermore, in addition to the well-studied RNAIII from *Staphylococcus aureus* (e.g. 6), 12 novel sRNAs from *Staphylococcus aureus* pathogenicity islands have been detected (7) as well as three Hfq-binding sRNAs of *Listeria monocytogenes* with still unknown function (8), and 9 novel sRNAs from *Listeria monocytogenes* within intergenic regions found by in silico-based approaches (9). Additionally, more than 100 potential 6S RNA species have been identified by bioinformatics approaches, and many of them were verified experimentally, among them two 6S RNA species in *B. subtilis* (10, 11). Still, the identification of mRNA targets of the recently discovered sRNAs is a challenging issue, and has been successful only in less than one third of all cases.

One important hallmark of many trans-encoded regulatory RNAs from *E. coli* is their ability to bind the Sm-like abundant RNA chaperone Hfq (12). While several sRNAs have been found to require Hfq for their stability, some were shown to need Hfq for efficient complex formation with their target RNA (e.g. 13, 14). For DsrA/*rpoS*/Hfq, the pathway of complex formation has been investigated by biophysical techniques (15). However, for sRNAs from Gram-positive bacteria, the putative function of Hfq is still elusive. At least in one case, staphylococcal RNAIII/*spa* interaction, no influence of Hfq has been found (16).

In contrast to the cis-encoded sRNAs from accessory genetic elements like plasmids, phages, transposons that have been studied in detail over the past 25 years (rev. in 17), relatively little is known about structural requirements, binding kinetics and mechanisms or degradation pathways of these new trans-encoded regulatory sRNAs. Although complexes between sRNA and mRNA have been detected *in vitro* in some instances, only in five cases secondary structures of such complexes predicted by Mfold have been confirmed by experimental secondary structure probing. These include MicF/*ompF* (18), Spot42/*galK* (19), RyhB/*sodB* (20), MicA/*ompA* (14, 21) from

E. coli and RNAIII/*spa* from *S. aureus* (22). So far, the region of initial contact between a trans-encoded sRNA and a target RNA sharing more than one complementary region has not been narrowed down. The mechanism of action has been proposed in some cases, but not always corroborated by a combination of *in vivo* and *in vitro* experiments.

The 205 nt untranslated RNA SR1 from the *B. subtilis* genome was found in our group by a combination of computer predictions and Northern blotting (23). Recently, we have shown that SR1 is a *bona fide* antisense RNA that acts by basepairing with its primary target, *ahrC* mRNA, the transcriptional activator of the *rocABC* and *rocDEF* arginine catabolic operons (24). *In vitro* translation data and translational reporter gene fusions suggested that SR1 might inhibit *ahrC* translation at a postinitiation stage. Hfq was shown to be dispensable for the stability of SR1.

Here, we provide a detailed *in vitro* characterization of SR1 and the SR1/*ahrC* complex with and without Hfq. We determined the region of initial contact between SR1 and *ahrC*. Furthermore, a combination of toeprinting and SR1/*ahrC* complex probing studies demonstrated that SR1 inhibits translation initiation of *ahrC* mRNA by inducing structural changes between the *ahrC* SD sequence and the first complementary region G. In contrast to many *E. coli* sense/antisense systems, Hfq was shown to be exclusively required for translation of *ahrC* RNA, but not for promoting the SR1/*ahrC* interaction. The intracellular concentration of SR1 in *B. subtilis* was calculated to be 30 nM in log phase and 315 nM in stationary phase in complex TY medium.

Materials and Methods

Enzymes and chemicals

Chemicals used were of the highest purity available. Taq DNA polymerase was purchased from Roche or SphaeroQ, Netherlands, respectively, RNA ligase from New England Biolabs and Thermoscript reverse transcriptase and M-MuLV reverse transcriptase from Invitrogene and Fermentas, respectively. Firepol polymerase was purchased from Solis Biodyne, Estonia.

Strains, media and growth conditions

E. coli strains DH10Band ER2566*(Δhfq::kan*) were used for cloning and for expression of the *B. subtilis hfq* gen, respectively. *B. subtilis* strains DB104 (25) and *E. coli* strains were grown in complex TY medium (see 24).

In vitro transcription and secondary structure analysis of SR1, ahrC and SR1/ahrC complexes

In vitro transcription and partial digestions of *in vitro* synthesized, 5'-end-labelled SR1 and *ahrC* RNA species with ribonucleases T1, T2 and V were carried out as described (26). For the analysis of SR1/*ahrC* complexes with T1, T2 and V, either SR1 or *ahrC* were 5' end-labelled and a 6- to 60-fold excess of the cold complementary RNA was added prior to RNase digestion.

Analysis of RNA-RNA complex formation

Both *ahrC* RNA and SR1 were synthesized *in vitro* from PCR-generated template fragments with primer pairs indicated in Table 1 *Suppl. Mat.* SR1/*ahrC* complex formation studies were performed as described previously (24). Complex formation in the presence of Hfq was assayed in TMN buffer (24) using purified Hfq from *B. subtilis*.

Purification of B. subtilis Hfq

For the purification of *B. subtilis* Hfq, the IMPACT^{TM}-CN system from New England Biolabs was used. To prevent the purification of *E. coli/B. subtilis* Hfq-heterohexamers, *E. coli* strain ER2566(*hfq::kan*) was transformed with plasmid pTYB11-Bs-Hfq. The resulting strain was grown at 37^{o} C till OD_{560} = 0.7, induced with 0.25 mM IPTG, and grown at 18^{o} C for further 18 hr. The fusion protein was purified by affinity chromatography on a chitin column as described by the manufacturer. On-column cleavage was performed with 20 mM Tris-HCl pH 8.0, 500 mM NaCl and 50 mM DTT

for 20 hr at room temperature. Millipore microcon columns were used to concentrate the eluted Hfq protein and to exchange the buffer for 50 mM Tris-HCl pH 8.0. The purified protein was stored at 4° C.

Construction of plasmids for the in vivo reporter gene test system

For the construction of the three translational fusions, chromosomal DNA from *B. subtilis* DB104 was used as template in three PCR reactions with upstream primer SB979 and the corresponding downstream primers SB980 (pGGA4), SB987 (pGGA6) and SB1065 (pGGA8). All fragments were digested with BamHI and EcoRI and inserted into the BamHI/EcoRI vector pGF-BgaB (27) encoding the promoterless heat-stable β-galactosidase from *B. stearothermophilus*. For the construction of plasmid pGGA7 carrying an internal deletion of 11 bp (nt 102 to nt 112) of *ahrC*, a two step PCR with outer primers SB979 and SB976 and internal primers SB989 and SB988 was performed on chromosomal DNA as template, the third PCR product obtained with SB979 and SB976 cleaved with BamHI and EcoRI and inserted into the BamHI/EcoRI vector pGF-BgaB.

Toeprinting analysis

The toeprinting assays were carried out using 30S ribosomal subunits, *ahrC* mRNA and $tRNA^{fMet}$ basically according to (28). 30S ribosomal subunits devoid of initiation factors were prepared from *E. coli* strain MRE600 essentially as described by Spedding (29). The 5'-[^{32}P]labelled *ahrC*-specific oligonucleotide SB1068 (5' TAC CGT GGC CTG CGT TAC) complementary to *ahrC* mRNA was used as a primer for cDNA synthesis in the toeprinting reactions. An aliquot of 0.04 pmol of *ahrC* mRNA annealed to primer SB1068 was incubated at 37°C without or with 0.4 pmol of 30S subunits and 8 pmol of uncharged $tRNA^{fMet}$ (Sigma) before supplementing with 1µl M-MuLV-RT (80 units). cDNA synthesis was performed at 37°C. Reactions were stopped after 10 minutes by adding formamide loading dye. The samples were separated on a denaturing 8 % polyacrylamide gel. Toeprint efficiency was determined by PhosphorImaging using the Image-quant software package (PC-BAS 2.0).

Preparation of total RNA and Northern blotting

Preparation of total RNA and Northern blotting were carried out as described previously (23).

Results

Secondary structures of SR1 and truncated SR1 species

So far, only for a few chromosomally encoded regulatory sRNAs, secondary structures have been determined experimentally. Examples include MicF (18), OxyS (30), RNAIII of *S. aureus* (31), DsrA (32), Spot42 (19), RyhB (20) and MicA (14, 21). Since computer predicted RNA structures often deviate from experimentally determined ones (e.g. RNAIII of pIP501, 33, or RNAI/RNAII of pT181, 34), we performed limited digestions with structure-specific ribonucleases *in vitro* to determine the secondary structure of SR1. The wild-type SR1 (205 nt) as well as the 3' truncated species $SR1_{132}$, the 5' truncated species $SR1_{98}$ and the 5' and 3' truncated species $SR1_{78}$ were 5'-end labelled, gel-purified and treated with RNases T1 (cleaves 3' of unpaired G residues), T2 (unpaired nucleotides with a slight preference for A residues) and V1 (double-stranded or stacked regions). Fig. 1A shows an analysis of $SR1_{205}$ and the truncated species $SR1_{132}$ and $SR1_{78}$, whereas Fig. 2B contains the schematic representation of the structure of $SR1_{205}$ derived from the cleavage data. The experimentally determined structure for wild-type SR1 comprises three main stem-loops: SL1 (nt 1 to 112), SL2 (nt 138 to 154) and the terminator stem-loop SL3 (nt 173 to 203) interrupted by two single stranded regions SSR1 (nt 113 to 137) and SSR2 (nt 155 to 172). It deviates from the structure predicted with Mfold in the 5' as well as in the 3' portion: The 5' part was found to be single-stranded between nt 38 and 51, and the double-stranded stem proved to be much longer than predicted and comprises 20 paired nucleotides (nt) interrupted by 3 internal loops or bulged-out bases, respectively, compared to only 10 paired nt in the predicted structure. For the 3' part, 2 stem-loops and the terminator stem-loop were predicted by Mfold, whereas the structure probing data support in addition to the terminator stem-loop only the second stem-loop SL2 in the centre of a long single-stranded region.

Structure probing of the 5' 132 nt of SR1 (Fig. 1A, central part) showed that this portion of the molecule folded independently and exactly as in the full-length sRNA. The secondary structure for the 3' 98 nt of SR1 contained exactly the terminator stem-loop as in wild-type SR1 (not shown) and the secondary structure for $SR1_{78}$ comprising nt 109 to nt 186 revealed the single stem-loop SL2 surrounded by single-stranded regions as expected (Fig. 1A, right).

The information on the secondary structures of the truncated derivatives was necessary to asses the data on complex formation between different SR1 species and its target, *ahrC* mRNA.

Binding kinetics of truncated SR1/ahrC mRNA pairs

Previously, we have shown that SR1 binds to the 376 3' nt of *ahrC* mRNA (*ahrC*$_{376}$, Fig. 2C) with an equilibrium dissociation rate constant K_D of 3.21 x 10^{-7} M (24). Since 7 regions of complementarity have been predicted between SR1 and *ahrC* mRNA (24 and Figure 2C), we intended to narrow down the segment of SR1 that is required for the initial contact with its target. To this end, SR1 species of different lengths were generated by *in vitro* transcription with T7 RNA polymerase, 5' end-labelled, gel-purified and used for binding assays with the *ahrC*$_{376}$ RNA. The results are shown in Fig. 2A: 3' truncated SR1 derivatives SR1$_{132}$ and SR1$_{104}$ comprising only stem-loop SL1 and lacking SL2 and the terminator stem-loop, were not able to form complexes with *ahrC* mRNA even at 400 nM. In contrast, 5' truncated species SR1$_{78}$ comprising only the single stranded region, SL2 and the 5' half of the terminator stem-loop, was as efficient in complex formation as SR1$_{186}$, a species that only lacked the 3' half of the terminator stem-loop, but otherwise contained the complete wild-type sequences and structures. In accordance with these data, both SR1$_{169}$ lacking SL3 completely and SR1$_{61}$, lacking SL1 and SL3, were significantly impaired in the interaction with their target and only at 400 nM *ahrC* mRNA, a weak complex was observed.

From these results we can conclude that for efficient complex formation between SR1 and *ahrC* mRNA, SL1 and the the 3' half of SL3 are not required. Furthermore, the opening of the terminator-stem-loop SL3 seems to be essential for an efficient interaction and a sequence located in the 5' half of SL3 proved to be important for the contact between antisense-RNA and target.

To analyse the regions of *ahrC* required for efficient pairing with SR1, five 5' labelled *ahrC* RNA species (shown schematically in Fig. 2C) were used in complex formation experiments with SR1$_{186}$ (Fig. 2B). As expected, labelled *ahrC*$_{376}$ comprising nt 108 to nt 483 of *ahrC* RNA, but lacking the 5' part and the SD sequence of *ahrC* formed a complex with unlabelled SR1$_{186}$ with the same K_D as determined previously for the labelled SR1/unlabelled *ahrC*$_{376}$ pair. The same efficiency for complex formation was observed for *ahrC*$_{88}$ containing region G' but lacking the SD sequence. By contrast, labelled *ahrC*$_{136}$ and *ahrC*$_{196}$ comprising the 5' 136 and 196 nt of *ahrC* mRNA, respectively, including SD sequence and region G', were significantly impaired in complex formation with unlabelled SR1$_{186}$. The complete *ahrC*$_{483}$ mRNA including 5' end, SD and all complementary regions to SR1 formed a weak complex with SR1 only at 400 nM concentration. These results suggest that the SD sequence of *ahrC* mRNA might be sequestered by intramolecular basepairing and that a factor might be needed to facilitate ribosome binding.

Secondary structure of the SR1/ahrC complex

The results from the binding assays indicate that $SR1_{78}$ is sufficient for efficient complex formation with *ahrC* mRNA and that without opening of the 5' half of the terminator stem loop no efficient complex can form. To investigate the alterations in the secondary structures of SR1 and *ahrC* upon pairing, the secondary structure of the $SR1_{186}$/$ahrC_{376}$ complex was determined. To ascertain alterations in the SR1 structure, labelled $SR1_{186}$ was incubated with a 6- to 60-fold excess of unlabelled *ahrC* RNA, the complex was allowed to form for 5 min at 37° C, and, subsequently, partially digested with RNases T1, T2 and V1. In parallel, free $SR1_{186}$ was treated in the same way. Fig. 3A shows the result. As expected, no significant alterations were observed within the 5' 112 nt of SR1 that contain only region A (nt 15 to 19) complementary to *ahrC*. By contrast, significant alterations in the T1, T2 and V cleavage pattern were observed within the other 6 complementary regions B, C, D, E, F and G (Fig 3A, right half). The data are summarized in Fig. 3C: Whereas in region B, only one reduced T1 cut was detected at G_{113}, drastic alterations were observed in both regions C and G: In C, all 9 nt complementary to *ahrC* showed reduced T2 cleavages, G_{126} and G_{127} exhibited reduced T1 cleavage and at U_{123} and U_{125}, an induction of V1 cleavage was detected indicating that this region became double-stranded upon pairing with *ahrC*. The same was true for region G, where the clevage pattern at all positions was altered compared to free SR1: nt 175 to 181 showed a decreased T2 cleavage, among them G_{176} and G_{181} a reduced T1 cleavage, whereas at U_{180} and G_{181} new V cuts appeared. Fewer changes were found in regions D, E and F, where G_{133} (region D), U_{146} and A_{147} (region E) and G_{156}, U_{157} and U_{158} (region F) were not single-stranded anymore and, instead, U_{132} and U_{133} (region D), A_{148} and A_{149} (region E) as well as U_{155} and G_{156} (region F) showed induced V cleavages, i.e. became double-stranded.

To further substantiate these results, secondary structure probing was performed with a complex formed between labelled *ahrC* and a 6- to 60-fold excess of unlabelled SR1. To corroborate our previous hypothesis that SR1 does not inhibit the translation initiation at the *ahrC* SD sequence, both the complex between $ahrC_{136}$ (5' 136 nt of *ahrC* including SD sequence and region G') and the complex between $ahrC_{376}$ (lacking the 5' 112 nt of *ahrC* including SD, but comprising all regions complementary to SR1) were probed with RNases T1, T2 and V. The results are shown in Fig. 3B: In the case of $ahrC_{376}$, induced V cuts were visible in regions E and G. Furthermore, between region E and D and in region C, T2 cuts were induced which is expected when one strand of a double-stranded region interacts with SR1, and the other half becomes, consequently, single-stranded. The same holds true for the induced T1 cuts in region B and the induced T2 cut in the region upstream of B.

The lower part of Fig. 3B presenting the results of SR1/*ahrC*$_{136}$ interaction clearly shows that the *ahrC* SD sequence itself was not affected upon addition of increasing amounts of unlabelled SR1. Surprisingly, a number of alterations could be observed further downstream from it and upstream of complementary region G'. In particular, prominent V cuts were induced at nt 41, nt 46/47, nt 53, nt 70 and 90/91, accompanied by induced T2 cuts around nt 55 and 74, 76 and 77 (Figure 3B left). These data suggest that binding of SR1 causes structural changes in the 5' part of *ahrC* mRNA between the SD sequence and region G'.

The initial contact between SR1 and ahrC RNA requires complementary region G

As published previously (24), one out of seven regions of complementarity between SR1 and *ahrC* RNA comprises nt 176 to 181 within the 5' half of the SR1 terminator stem-loop SL3 (designated G) and nt 113 to 118 of *ahrC* mRNA (designated G'). If these two regions were involved in a first contact between SR1 and *ahrC* RNA, nucleotide exchanges in either SR1 or *ahrC* RNA should impair or abolish complex formation, and compensatory mutations should, at least partially, restore binding. To test this hypothesis, three mutated SR1$_{186}$ species with either a 10 nt exchange (5'AGCAUGCGGC to 5' UCGUACGCCG) between nt 176 and nt 185 denoted SR1$_{186_G10}$, a 6 nt exchange (5'AGCAUG to 5'UCGUAC), denoted SR1$_{186_G6}$ or a 2 nt exchange ($G_{177}C_{178}$ to $T_{177}T_{178}$) denoted SR1$_{186_G2}$, were assayed in complex formation with wild-type *ahrC*$_{88}$ comprising nt 109 to 196 of *ahrC* mRNA (region G'). The 6 and 10 nt exchanges were designed such that the GC/AU content of the region was not altered compared with the wild-type. As shown in Fig. 4A, no interaction between these three mutated SR1 species and wild-type *ahrC* RNA was observed. By contrast, the exchange of only C_{178} to G (SR1$_{186_G1}$) did not impede complex formation, suggesting that either G_{176} is most important for the initial contact or that substitution of one nucleotide is not sufficient to cause an effect. Interestingly, when *ahrC* RNA$_{88_G'2}$, a derivative of the same length carrying the compensatory mutations to SR1$_{186_G2}$ was used, binding could be restored (Figure 4A and B) confirming a specific basepairing interaction between SR1 and *ahrC* mRNA. When a longer *ahrC*$_{376}$ RNA comprising all 7 complementary regions G' to A' was analysed, binding was abolished by the above mentioned mutations too, and partially restored with the compensatory mutation *ahrC*$_{376\_G'2}$ mRNA (not shown). These data indicate that the complementary region G of SR1 (nt 176 to nt 181) plays an important role for the recognition of *ahrC* mRNA.

To investigate the contribution of the other regions of SR1 complementary to *ahrC* RNA to efficient binding with its target, two SR1$_{186}$ species carrying 9 nt

exchanges each in either region C (nt 119 to nt 127) – $SR1_{S5}$ – or region E and the first 2 nt of region F (comprising nt 146 to 154) – $SR1_{S6}$ – were analysed for complex formation with *ahrC* RNA carrying the wild-type or mutated regions (Fig. 4C). Complex formation was significantly impaired in both cases: $SR1_{S5}$ exhibited an about 10-fold and $SR1_{S6}$ an about 30-fold decreased efficiency to pair with *ahrC* RNA. A combined substitution of regions C, E and 5' F ($SR1_{S7}$) or a combined exchange of regions C, D, E and 5' F ($SR1S_9$) resulted in a complete loss of pairing. Fig. 4D shows a schematic representation of the 4 mutated $SR1_{186}$ species.
These data indicate that, although region G is crucial, regions C, D, E and F contribute to efficient pairing.

An in vivo reporter gene test system confirmed the importance of region G for the interaction between SR1 and ahrC mRNA

To test the importance of region G' (nt 113 to 118 of *ahrC*-mRNA complementary to nt 176-181 of SR1) for the interaction with SR1 *in vivo* in *B. subtilis*, the following three translational *ahrC-BgaB* fusions were constructed: pGGA6 containing nt 1 to 113 but lacking all but one nt of region G, pGGA4 comprising nt 1 to 119, i.e. the entire region G + 1 additional nt, and, hence, no other complementary region, and pGGA7 identical to pGGA3 (comprising G, F and E, ref. 24) but lacking nt 102 to 112 upstream of G. All fusions were integrated into the *amyE* locus of the *B. subtilis* DB104 chromosome, grown till $OD_{560} \approx 5$ (maximal expression of SR1) and β-galactosidase activities measured. As shown in Table 2, β-galactosidase activities measured with pGGA4 and pGGA7 were, in both cases, about 30-fold lower than that of the pGGA6-integration strain lacking any complementary region to SR1. Since pGGA4 yielded the same decrease in β-galactosidase activity compared to a construct lacking any complementarity with SR1 as our previous construct pGGA3 that encompassed regions G, E and F, it can be concluded that region G alone is sufficient to inhibit *ahrC* translation almost completely. The results obtained with pGGA7 and pGGA4 exclude the possibility that the sequences immediately adjacent to region G are involved in the observed decrease of β-galactosidase activity, e.g. by providing a cleavage site for an RNase.

To test whether point mutations in region G' abolish the effect of SR1 on *ahrC* translation, pGGA8 was constructed carrying the same 2 nt exchange as $SR1_{186\_G\text{-}2}$ analysed in the binding assay (Fig. 4A), but lacking any sequences downstream from nt 118 (3' end of region G') and integrated into the *amyE* locus of *B. subtilis*. The β-galactosidase activity measured with pGGA8 was nearly the same as with pGGA6

(Table 2), confirming the *in vitro* result that the 2 nt exchange in region G prevented the interaction between SR1 and *ahrC*.

Hfq does not promote the interaction between SR1 and ahrC mRNA, but is required for the translation of ahrC mRNA

Many small RNAs from *E. coli* need Hfq for either stability or their interaction with their targets (see *Introduction*). Previously, we have shown that Hfq is neither required for the stabilisation of SR1 nor that of *ahrC* (24). However, in the absence of Hfq, but presence of SR1, the expression of the downstream SR1 targets, *rocABC* mRNA and *rocDEF* mRNA, was about 3-fold and 6-fold, respectively, increased. Therefore, we wanted to investigate, whether Hfq is required for the promotion of complex formation with *ahrC* RNA.

To investigate whether Hfq binds SR1, different concentrations of purified *B. subtilis* Hfq were added to labelled wild-type SR1 and two 3' truncated species $SR1_{186}$ and $SR1_{104}$, and a gel-shift assay was performed. As shown in Figure 5A, all three SR1 species bound Hfq at concentrations of 3 to 10 µM. To analyse binding of Hfq to *ahrC* RNA, full-length and truncated *ahrC* species were assayed for Hfq binding: As shown in Fig. 5B, $ahrC_{136}$, $ahrC_{196}$ and $ahrC_{483}$ (full-length) that contain the SD sequence, bound Hfq very efficiently. By contrast, $ahrC_{376}$ lacking the SD sequence bound Hfq less efficiently than $ahrC_{483}$.

Since both SR1 and *ahrC* RNA bound Hfq, we analysed whether Hfq is able to promote the complex formation between both RNAs *in vitro*. For this purpose, purified *B. subtilis* Hfq was added to a final concentration of 10 µM (amount required to bind 50 % SR1), to the mixture of 1.0 nM labelled SR1 and different amounts of unlabelled *ahrC* mRNA, incubated for 15 min at 37° C and complexes were separated on 6% native PAA gels. Although a ternary SR1/*ahrC*/Hfq complex formed, this complex was not observed at lower *ahrC* concentrations compared to the binary SR1/*ahrC* complex, and the amount of this complex did not increase with increasing concentrations of unlabelled *ahrC* RNA (Fig. 5C). In contrast, upon higher concentrations of unlabelled *ahrC* RNA (≥100 nM), this RNA, apparently, successfully competed with SR1 for Hfq binding, so that the amount of unbound labelled SR1 increased again (Fig. 5C). In summary, all these data clearly prove that the RNA chaperone Hfq does not facilitate the interaction between SR1 and its target *ahrC* mRNA.

To reconcile these observations as well as the lacking effect of Hfq on SR1 stability with the increase of the *rocABC* and *rocDEF* mRNA levels in the *hfq* knockout strain, we tested whether the translation of *ahrC* is affected by Hfq. For this purpose, the *ahrC-Bgab* translational fusion pGGA6 was integrated into the *amyE* locus of

DB104 (*Δhfq::cat*), and β-galactosidase activity was measured and compared to that determined in the presence of Hfq in DB104. A 250-fold lower β-galactosidase activity was detected in the absence of Hfq, indicating that this RNA chaperone is required for efficient translation of *ahrC* mRNA *in vivo* (Table 2).

To substantiate the role of Hfq in promoting translation of *ahrC* mRNA, the secondary structures of *ahrC* mRNA and SR1 were probed probed with RNases T1 and T2 in the presence and absence of Hfq. As shown in Fig. 5D, one binding site of Hfq on *ahrC* mRNA (5' AAAUA) is located immediately upstream of the SD sequence. The same assay was used to determine the binding site(s) of Hfq on SR1. Here, one binding site around nt 9-13 in the 5' part of SR1 and a second in the bulge of stem-loop SL1 (nt 43 to 47) were found (gel not shown). The facts that Hfq gel-shifts with wild-type SR1 and $SR1_{104}$ comprising only the 5' stem-loop were identical (Fig. 5A), support the absence of Hfq binding sites on SR1 downstream from nt 104.

SR1 blocks ribosome binding to the ahrC mRNA translation initiation region

Although the first complementary region between *ahrC* and SR1 is located 87 nt downstream from the *ahrC* SD sequence, we performed a toeprinting analysis (28) to examine the effect of SR1 on formation of the translation initiation complex at *ahrC* mRNA. Fig. 6A shows that in the presence of initiator $tRNA^{fMet}$, 30S ribosomal subunits bind to the *ahrC* translation initiation region and block reverse transcription of a labelled primer, annealed downstream, at the characteristic position +15 (start codon A is +1). This signal provides a measure for the formation of the ternary complex, since it is dependent on both 30S subunits and initiator $tRNA^{fMet}$. Addition of increasing amounts of $SR1_{WT}$ or $SR1_{186}$ prior to addition of 30S subunits and $tRNA^{fMet}$ interfered with ternary complex formation, resulting in a weaker toeprint signal (Fig. 6A and C). By contrast, both the addition of a noncognate small RNA, SR2 from *B. subtilis* or RyhB from *E. coli,* failed to decrease the toeprint signal on *ahrC* mRNA (summarized in Fig. 6C) indicating that SR1-dependent inhibition of ribosome binding was specific. To support the specificity of the SR1 inhibitory action on ternary complex formation on *ahrC* mRNA, a control toeprint was performed with SR1 and *sodB* mRNA (target of RyhB). Since SR1 did not affect ternary complex formation on *sodB* mRNA (Fig. 6B), whereas RyhB did as expected, it can be excluded that the effect of SR1 on *ahrC* mRNA is simply due to binding to the ribosome. In summary, these data demonstrate that binding of SR1 to *ahrC* mRNA prevents the formation of translation initiation complexes.

The intracellular concentration of SR1 increases about 10-fold in stationary phase

To determine the intracellular concentration of SR1 in *B. subtilis* in logarithmic and stationary growth phase, strain DB104 was grown in complex medium, and samples were withdrawn at OD 2 (log phase) and OD 4.5 (onset of stationary phase). Cell numbers were determined upon plating of appropriate dilutions of the harvested cultures on agar plates. Total RNA was prepared, separated on a denaturing polyacrylamide gel alongside defined amounts of *in vitro* synthesized SR1 and subsequently, subjected to Northern blotting (Fig. 7). Losses during RNA preparation were calculated using *in vitro* synthesized SR1 mixed with the same amount of DB104::*Δsr1* cells at the beginning of the RNA preparation. A comparison with the same amounts of untreated RNA yielded about 80 % loss. Loading errors were corrected by reprobing with labelled oligonucleotide C767 complementary to 5S rRNA. Using this quantification procedure, the amount of SR1 within one *B. subtilis* cell was calculated to be ≈20 molecules in log phase and 200-250 molecules in stationary phase, corresponding to an approximate intracellular concentration of 30 and 315 nM, respectively.

Discussion

For all recently discovered trans-encoded sRNAs the targets of which have been identified, only one or two complementary regions were found. In the majority of cases, these regions covered the 5' part of the target RNA, mostly including the SD sequence, and the mechanism of action was found to be inhibition or activation of translation initiation. Rather unusually, SR1 and *ahrC* mRNA contain 7 regions of complementarity that comprise the 3' half of SR1 and the central and 3' portion of *ahrC* mRNA (24). This prompted us to determine the secondary structures of SR1 and the *ahrC*/SR1 complex and to investigate the structural requirements for efficient *ahrC*/SR1 pairing.

Figure 1B shows that SR1 is composed of one large 5' stem-loop (SL 1) structure with a prominent bulge, a central small stem-loop SL2 and the terminator stem-loop SL3 separated by two single-stranded regions. 6 out of 7 regions of complementarity to *ahrC* RNA (B to G) are located in the 3' 100 nt of SR1. Secondary structure probing of labelled SR1 in complex with increasing concentrations of unlabelled *ahrC* and *vice versa* (Figure 3A and B) revealed structural alterations in 6 of the 7 complementary regions. In SR1, all positions in region C and G as well as a few positions in B, D, E and F were affected (summarized in Figure 3C). In *ahrC*, alterations in regions C, E, F and G as well as additional alterations between regions D and E were found. Interestingly, structural changes over a stretch of ≈50 nt were also observed upstream of region G (Fig. 3B left), although the *ahrC* SD sequence (nt 21 to 25) and the start codon remained unaffected indicating that binding of SR1 causes structural changes in the 5' part of *ahrC*-mRNA, too.

Whereas for cis-encoded antisense RNAs from plasmids, phages and transposons, a number of studies have been performed to elucidate binding pathways and to determine structural requirements for the two contacting RNA molecules (17), little is known, so far, about the formation of initial contacts between trans-encoded sRNAs and their targets. Here, we show that a solely 78 nt long SR1 species spanning nt 109 to nt 186 is sufficient for efficient complex formation with *ahrC* mRNA, i.e. the 5' portion of SR1 is not needed (Figure 2A). Generally, all SR1 species lacking the 5' half of SL3 with region G or comprising a complete SL3 were significantly impaired in pairing with *ahrC* RNA. This might indicate that *in vivo* some factor – most likely a protein or an RNase cutting within the loop of SL3 – opens the terminator stem-loop to promote complex formation. Since *in vivo* only full length $SR1_{205}$ can be observed (Northern blots and 3' RACE, 23), the involvement of an endoribonuclease is highly unlikely. The possibility that the RNA chaperone Hfq that binds upstream of the terminator stem-loop of SR1 is responsible for opening up this structure, can be

eliminated, too (see below). Most probably, another, yet unknown RNA binding protein is needed to open SL3.

Two lines of evidence show that the initial contact between SR1 and *ahrC* RNA occurs at complementary region G of SR1: Complex formation assays of truncated SR1/*ahrC* pairs containing mutations and compensatory mutations in region G (Fig. 4) and translational *ahrC-lacZ* reporter gene fusions with the same point mutations (Table 2). Furthermore, complex formation assays with SR1 mutants affected in regions C, D, E/F or a combination thereof and a *lacZ* fusion with regions E', F' and G' revealed a contribution of the other complementary regions to SR1/*ahrC* pairing. In summary, since, i) in the absence of region G, no efficient complex could form, ii) in the presence of wild-type regions A to E, a 2 nt-exchange within G inhibits pairing and iii) in the presence of G, significant simultaneous alterations in regions C, E and F did affect complex formation, we can conclude, that region G is responsible for the initial contact between SR1 and *ahrC* RNA, but the other complementary regions add to efficient antisense/target RNA pairing.

Region G' in unpaired *ahrC* mRNA is single-stranded (Fig. 3B left) and, as proposed above, some factor is needed to melt or open up region G in SR1, so that the two single-stranded regions can interact. Our data suggest that pairing initiates at G, but for subsequent steps and stable complex formation, a contribution of the other complementary regions B to F is needed. This is reminiscent of the binding pathway of the antisense/sense RNA pair CopA/CopT involved in regulation of plasmid R1 replication (reviewed in 35). Here, binding starts with the interaction of two single-stranded kissing loops and, afterwards, a second region is needed to overcome the torsional stress and to propagate the helix. By contrast, for the antisense/sense RNA pair RNAIII/RNAII of plasmid pIP501, the simultaneous interaction of two complementary loop pairs was found to be required (36). In other cases, a single stranded region and a loop form the first complex (e.g. Sok/hok of plasmid R1 or RNA-OUT/RNA-IN of transposon IS10, reviewed in 17).

For many trans-encoded sRNAs in *E. coli*, the RNA chaperone Hfq has been shown to be required for either stabilization of the sRNA or/and efficient duplex formation with the target RNA (see Introduction). Previous experiments have demonstrated that Hfq does not stabilize SR1 (24). This report shows that although *B. subtilis* Hfq binds both SR1 and *ahrC* RNA, it is not able to promote complex formation between SR1 and *ahrC* (Figure 5). This is in agreement with data obtained for the RNAIII/*spa* interaction in *S. aureus*, for which Hfq was found to be dispensable for RNAIII/*spa* complex formation (22, 16). The fact that no requirement for Hfq was observed in the RatA/*txpA* system of *B. subtilis* (3), too, suggests that in Gram-positive

bacteria Hfq might not be needed for sRNA/target RNA interaction or, alternatively, that another RNA chaperone may fulfil the function of Hfq. One candidate might be HBsu, for which RNA binding activity was demonstrated (37).

However, our previous observation that the levels of the secondary targets of SR1, *rocABC* and *rocDEF* mRNA, were increased 3- to 6-fold in an *hfq* knockout strain (24) raised the question on the role of this chaperone in the SR1/*ahrC* system. Suprisingly, *ahrC* mRNA proved to be not translated in a *B. subtilis hfq* knockout strain (Table 2). This indicates that Hfq is required for efficient translation of *ahrC,* possibly by opening up some secondary structures that otherwise inhibit binding of the 30S initiation complex. This is supported by the finding of one Hfq binding site (5' AAAUA) immediately upstream of the *ahrC* ribosome binding site (RBS). Interestingly, for *E. coli rpoS* mRNA it has been also shown that Hfq is essential for efficient translation (38). In contrast to *ahrC*, the binding of Hfq to SR1 does not seem to play a role in this context. The fact that Hfq binds upstream of 6 out of 7 SR1 regions complementary to *ahrC* mRNA supports the failure of Hfq to promote complex SR1/*ahrC* formation. However, we cannot exclude that Hfq binding might be important for the interaction of SR1 with other, still unidentified target mRNAs.

Based on a series of translational *ahrC-lacZ* fusions, the dispensability of the *ahrC* SD sequence for pairing with SR1 and *in vitro* translation data with chimeric *ahrC/sodB* RNAs, we suggested previously that SR1 might affect *ahrC* translation at a postinitiation stage (24). However, the structural alterations found in the *ahrC* mRNA downstream from the SD sequence in the presence of increasing amounts of SR1 prompted us to re-evaluate our previous data using a toeprinting analysis (Figure 6). Both $SR1_{WT}$ and $SR1_{186}$, but not two heterologous RNAs, were able to inhibit binding of the 30S ribosomal subunit and formation of a ternary complex with 30S and $tRNA_f^{Met}$ on full-length *ahrC* mRNA. These results – together with the structure probing data – demonstrate that binding of SR1 induces structural changes in a ≈65 nt long stretch of *ahrC* RNA between SD sequence and complementary region G that eventually inhibit formation of the 30S initiation complex. Since the 30S ribosomal subunit covers 54 nt, i.e. 35 (+/-2) nt upstream and 19 nt downstream from the start codon (39), the 5' part of the SR1-induced structural alterations of *ahrC* mRNA coincides exactly with this region. The toeprinting results are not opposed to the previously observed translation inhibition of *ahrC-lacZ* fusions (24), as this inhibition can be explained by SR1-induced structural changes in the 5' part of *ahrC* RNA, too. Therefore, we can conclude that the mechanism of action employed by SR1 is inhibition of translation initiation. This is the first case of a small regulatory RNA that binds ≈90 nt downstream from the ribosome binding site and interferes with translation initiation. In contrast, in the well-studied *E.*

coli systems like RyhB/*sodB* (20) or MicA*/ompA* (14, 21), the complementary regions between small RNA and mRNA are located upstream of or overlap the target SD sequence, making an effect on ribosome binding and hence, translation initiation, more plausible. Our results rise the question on the maximal distance between SD sequence and a binding region for a small RNA permitting to affect 30S subunit binding. Furthermore, in many *E. coli* cases the inhibition of translation initiation was accompanied by significantly decreased amounts of the target mRNA(s) (e.g. RyhB/*sodB,* 40, or SgrS*/ptsG,* 41) that was attributed to degradation of the unprotected target RNA by RNase E or of the complex by RNase III (42). Surprisingly, *ahrC* levels were found to be independent of the presence or absence of SR1 (24). To date, no RNase E has been found in *B. subtilis*. Although two novel endoribonucleases with homology to RNase E, RNase J1 and J2, were recently discovered (43), it is unclear, whether they fulfil the role of the main endoribonucleases as it does RNase E in Gram-negative bacteria.

In the few sense/antisense RNA systems, where calculations of the amount of both interacting species were performed (e.g. 44, 45), an at least 10-fold excess of the inhibitory small RNA over its target was determined. Here, the amount of SR1 in *B. subtilis* grown in complex medium was found to increase upon entry into stationary phase from 15-20 to 250 molecules per cell. This is much lower than the 4500 molecules measured for OxyS under oxidative stress conditions (30), but still in the range of RNAIII of plasmid pIP501 (≈1000 molecules). Since we could not detect *ahrC* mRNA in Northern blots under any growth condition, its amount must be significantly lower than 15 molecules/cell ensuring at least a 15-fold excess of SR1.

The analysis of the SR1/*ahrC* mRNA interaction yielded three major issues, which might be important for sRNA/target RNA systems in general: First, whereas the major mechanism of action of trans-encoded sRNAs reported in Gram-negative bacteria is inhibition of translation initiation by direct binding to the RBS or 5' of it, the *B. subtilis* SR1/*ahrC* pair is first case, where translation initiation is prevented by binding of the sRNA ≈90 nt downstream from the RBS. Second, while all sRNA/target RNA pairs studied so far comprise at the most two complementary regions, the SR1/*ahrC* pair is the first case with 7 complementary regions between inhibitor and target RNA, and the major contribution of one region as well as the minor, but measurable contribution of 5 of the other regions has been demonstrated. Third, whereas in *E. coli*, Hfq was required for either sRNA stabilization or promotion of complex formation with the target RNA, at least complex formation in Gram-positive bacteria does not seem to depend on Hfq. The search for and analysis of other SR1 targets will reveal whether this sRNA exerts its function(s) by the same or alternative mechanisms.

References

1. Storz,G., Altuvia,S. and Wassarman,K.M. (2005) An abundance of RNA regulators. *Annu. Rev. Biochem*, **74**, 199-217.
2. Vogel,J. and Papenfort,K. (2006) Small noncoding RNAs and the bacterial outer membrane. *Curr. Opin. Microbiol.*,**9**, 605-611.
3. Silvaggi, J.M., Perkins, J.B. and Losick,R. (2005) Small untranslated RNA antitoxin in *Bacillus subtilis*. *J. Bacteriol.* **187**, 6641-6650.
4. Lee,M., Zhang,S., Saha,S., Santa Anna,S., Jiang,C. and Perkins,J. (2001). RNA expression analysis using an antisense *Bacillus subtilis* genome array. *J. Bacteriol.,* **183**, 7371-7380.
5. Silvaggi,J.M., Perkins,J.B., and Losick,R. (2006) Genes for small, noncoding RNAs under sporulation control in *Bacillus subtilis*. *J. Bacteriol.,* **188**, 532-541.
6. Morfeldt,E., Taylor,D., von Gabain,A. and Arvidson,S. (1995) Activation of alpha-toxin translation in *Staphylococcus aureus* by the trans-encoded antisense RNA, RNAIII. *EMBO J.*, **14**, 4569-4577.
7. Pichon,C. and Felden,B. (2005) Small RNA genes expressed from *Staphyloccoccus aureus* genomic and pathogenicity islands with specific expression among pathogenic strains. *Proc. Natl. Acad. Sci. U. S. A.,* **102**, 14249-14254.
8. Christiansen,J.K., Nielsen,J.S., Ebersbach,T., Valentin-Hansen,P., Søgaard-Andersen,L. and Kallipolitis,B.H. (2006). Identification of small Hfq-binding RNAs in *Listeria monocytogenes*. *RNA,* **12**, 1-14.
9. Mandin,P., Repoila,F., Vergassola,M., Geissmann,T. and Cossart,P. (2007) Identification of new nonconding RNAs in *Listeria monocytogenes* and prediction of mRNA targets. *Nucleic Acids Res.,* **35**, 962-974.
10. Barrick,J.E., Sudarsan,N., Weinberg,Z., Ruzzo,W.L. and Breaker,R.R. (2005) 6S RNA is a widespread regulator of eubacterial RNA polymerase that resembles an open promoter. *RNA,* **11**, 774-784.
11. Trotochaud,A.E. and Wassarman,K.M. (2005) A highly conserved 6S RNA structure is required for regulation of transcription. *Nat. Struct. Mol. Biol.,* **12**, 313-319.
12. Valentin-Hansen,P., Eriksen,M. and Udesen,C. (2004) The bacterial Sm-like protein Hfq: a key player in RNA transactions. *Mol. Microbiol.*, **51**, 1525-1533.
13. Zhang,A., Wassarman,K.M., Ortega,J. Steven,A.C., and Storz,G. (2002) The Sm-like Hfq protein increases OxyS RNA interaction with target mRNAs. *Mol. Cell,* **9**, 11-22.
14. Rasmussen,A.A., Eriksen,M., Gilany,K., Udesen,C., Franch,T., Petersen,C. and Valentin-Hansen,P. (2005) Regulation of *ompA* mRNA stability: the role of a small regulatory RNA in growth phase-dependent control. *Mo.l Microbiol.,* **58**, 1421-1429.
15. Arluison,V., Hohng,S., Roy,R., Pellegrini,O., Regnier P. and Ha,T. (2007) Spectroscopic observation of RNA chaperone activities of Hfq in posttranscriptional regulation by a small non-coding RNA. *Nucleic Acids Res*., **35**, 999-1006.

16. Bohn,C., Rigoulay,C. and Bouloc,P. (2007) No detectable effect of RNA-binding protein Hfq absence in *Staphylococcus aureus*. *BMC Microbiol.,* **7**, 10.

17. Brantl,S. (2007) Regulatory mechanisms employed by cis-encoded antisense RNAs. *Curr. Op. Microbiol*, **10**, 102-109.

18. Schmidt,M., Zheng,P. and Delihas,N.(1995) Secondary structures of *Escherichia coli* antisense MicF RNA, the 5' end of the target *ompF* mRNA, and the RNA/RNA duplex. Biochemistry,**34**, 3621-3631.

19. Møller,T., Franch,T., Udesen,C., Gerdes,K. and Valentin-Hansen,P. (2002). Spot 42 RNA mediates discoordinate expression of the *E. coli* galactose operon. *Genes Dev*., **16**, 1696-1706.

20. Geissmann,T.A. and Touati,D. (2004) Hfq, a new chaperoning role: binding to messenger RNA determines access for small RNA regulator. *EMBO J*., **23**, 396-405.

21. Udekwu,K.I., Darfeuille,F., Vogel,J., Reimegard,J., Holmqvist,E. and Wagner,E.G.H. (2005) Hfq-dependent regulation of OmpA synthesis is mediated by an antisense RNA. *Genes Dev.,* **19**, 2355-2366.

22. Huntzinger,E., Boisset,S., Saveanu,C., Benito,Y., Geissmann,T., Namane,A., *et al*. (2005) *Staphylococcus aureus* RNAIII and the endoribonuclease III coordinately regulate *spa* gene expression. *EMBO J.,* **24,** 824-835.

23. Licht,A., Preis,S. and Brantl,S. (2005) Implication of CcpN in the regulation of a novel untranslated RNA (SR1) in *B. subtilis*. *Mol. Microbiol.,* **58**, 189-206.

24. Heidrich,N., Chinali,A., Gerth,U. and Brantl,S. (2006) The small untranslated RNA SR1 from the *B. subtilis* genome is involved in the regulation of arginine catabolism. *Mol. Microbiol.,* **62**, 520-536.

25. Kawamura,F. and Doi,R.H. (1984) Construction of a *Bacillus subtilis* double mutant deficient in extracellular alkaline and neutral proteases. *J. Bacteriol.,* **160**, 442-444.

26. Heidrich,N. and Brantl,S. (2003) Antisense-RNA mediated transcriptional attenuation: Importance of a U-turn loop structure in the target RNA of plasmid pIP501 for efficient inhibition by the antisense RNA. *J. Mol. Biol.,* **333***,* 917-929.

27. Stoß,O., Mogk,A., and Schumann,W. (1997) Integrative vector for constructing single-copy translational fusions between regulatory regions of *Bacillus subtilis* and the *bgaB* reporter gene encoding a heat-stable β-galactosidase . *FEMS Microbiol. Lett.,* **150**, 49–54.

28. Hartz,D., McPheeters,D.S., Traut,R. and Gold,L. (1988). Extension inhibition analysis of translation initiation complexes. *Methods Enzymol*., **164**, 419-425.

29. Spedding,G. (1990) Isolation and analysis of ribosomes from prokaryotes, eukaryotes, and organelles. In *Ribosomes and Protein Synthesis*: a Practical Approach. Spedding, G. (ed.) New York: IRL Press, Oxford Universtiy Press, 1-29.

30. Altuvia,S., Weinstein-Fischer,D., Zhang,A., Postow,L. and Storz,G. (1997) A small, stable RNA induced by oxidative stress: role as a pleiotropic regulator and antimutator. *Cell*, **90**, 43-53.

31. Benito,Y., Kolb,F.A., Romby,P., Lina,G., Etienne,J. and Vandenesch,F. (2000) Probing the structure of RNAIII, the *Staphylococcus aureus agr* regulatory RNA, and identification of the RNA domain involved in repression of protein A expression. *RNA,* **6**, 668 – 679.

32. Lease,A.L. and Belfort,M. (2000) A trans-acting RNA as a control switch in *Escherichia coli*: DsrA modulates function by forming alternative structures. *Proc. Natl. Acad. Sci. USA,* **97**, 9919-9924.

33. Brantl,S. and Wagner,E.G.H. (1994) Antisense RNA-mediated transcriptional attenuation occurs faster than stable antisense/target RNA pairing: an *in vitro* study of plasmid pIP501. *EMBO J.,* **13**, 3599-3607.

34. Brantl,S, and Wagner,E.G.H. (2000) Antisense-RNA mediated transcriptional attenuation: an *in vitro* study of plasmid pT181. *Mol. Microbiol.*, **35**, 1469-1482.

35. Wagner,E.G.H., Altuvia,S. and Romby,P. (2002) Antisense RNAs in bacteria and their genetic elements. *Adv. Genet.*, **46**, 361-398.

36. Heidrich,N. and Brantl,S. (2007) Antisense RNA-mediated transcriptional attenuation in plasmid pIP501: the simultaneous interaction between two complementary loop pairs is required for efficient inhibition by the antisense RNA. *Microbiol.*, **153**, 420-427.

37. Nakamura, K., Yahagi,S., Yamazaki,T. and Yamane,K. (1999) *Bacillus subtilis* histone-like protein, Hbsu, is an integral component of a SRP-like particle that can bind the Alu domain of small cytoplasmic RNA. *J. Biol. Chem.*, **274**, 13569-13576.

38. Muffler,A., Fischer,D. and Hengge-Aronis,R. (1996) The RNA-binding protein HF-I, known as a host factor for phage Q□ RNA replication, is essential for *rpoS* translation in *Escherichia coli*. *Genes Dev.*, **10**, 1143-1151.

39. Hüttenhofer,A., and Noller,H.F. (1994) Footprinting mRNA-ribosome complexes with chemical probes. *EMBO J.*, **13**, 3892-3901.

40. Massé,E., Escorcia,F.E. and Gottesman,S. (2003) Coupled degradation of a small regulatory RNA and its mRNA targets in *Escherichia coli*. *Genes Dev.*,**17**, 2374-2383.

41. Vanderpool,C.K. and Gottesman,S. (2004) Involvement of a novel transcriptional activator and small RNA in posttranscriptional regulation of the glucose phosphoenolpyruvate phosphotransferase system. *Mol. Microbiol.*, **54**, 1076-1099.

42. Afonyushkin,T., Vecerek,B., Moll,I., Bläsi,U. and Kaberdin,V.R. (2005) Both RNase E and RNAse III control the stability of *sodB* mRNA upon translational inhibition by the small regulatory RNA RyhB. *Nucleic Acids Res.,* **33**, 1678-1689.

43. Even,S., Pellegrini,O., Zig,L., Labas,V., Vinh,J., Brechemmier-Baey,D. and Putzer,H. (2005) Ribonucleases J1 and J2: two novel endoribonucleases in *B. subtilis* with functional homology to *E. coli* RNase E. *Nucleic Acids Res.*, **33**, 22141-2152.

44. Brantl,S. and Wagner,E.G.H. (1996) An unusually long-lived antisense RNA in plasmid copy number control: *in vivo* RNAs encoded by the streptococcal plasmid pIP501. *J. Mol. Biol.*, **255**, 275-288.

45. Brenner,M. and Tomizawa,J.-I. (1991) Quantitation of ColE1-encoded replication elements. *Proc. Natl. Acad. Sci. USA*, **88**, 405-409.

Acknowledgements

The authors thank Eckhard Birch-Hirschfeld, Jena, for synthesis of the oligodeoxyribonucleotides and Poul Valentin-Hansen, Odense, for kindly sending us the *E. coli* strains for overexpression of *B. subtilis* Hfq. We thank Jörg Vogel, Berlin, and Gisela Storz, for critical and helpful suggestions in the course of this work.This work was supported by grant Br1552/6-2 from the Deutsche Forschungsgemeinschaft to S. B.

Figure Legends

Figure 1. Secondary structures of SR1 species of different lengths

A Secondary structure probing of wild-type SR1 (205 nt) and truncated species $SR1_{132}$ and $SR1_{78}$ with RNases.

Purified, 5' end-labelled SR1 was subjected to limited cleavage with the RNases indicated. The digested RNAs were separated on 8 % denaturing gels. Autoradiograms are shown. RNase concentrations used were: T1: 10^{-2} U/µl (1:50), T2: 10^{-1} U/µl(1:500), V1: 10^{-1} U/µl(1:10), C, control without RNase treatment, L, alkaline ladder.

B Proposed secondary structure of SR1.

A structure consistent with the cleavage data in Fig. 1A and additional experiments (data not shown) is depicted. Major and minor cuts are indicated by symbols (see box). The three main stem-loops SL1, SL2 and SL3 are indicated.

Figure 2. Binding assays of wild-type and truncated SR1/*ahrC* RNA pairs

Binding experiments were performed as described in *Experimental Procedures*. Autoradiograms of gel-shift assays are shown. The concentration of unlabelled *ahrC* RNA species or SR1 species is indicated. F, labelled RNA, D duplex between SR1 and *ahrC* RNA.

A. Binding assays with wild-type and truncated SR1 derivatives

SR1 species were 5' end-labelled with [γ ^{32}P]-ATP and used in at least 10-fold lower equimolar amounts compared to the targets. $ahrC_{376}$ comprising the 3' part of *ahrC* mRNA with nt 113 to 483 was used in all cases. Above, the schematic representation of the SR1 species is shown.

B. Binding assays with wild-type and truncated *ahrC* species

ahrC RNA species were 5' end-labelled with [γ ^{32}P]-ATP and used in at least 10-fold lower equimolar amounts compared to $SR1_{186}$.

C. Overview on the *ahrC* mRNA species used in this work

The sequence of the *ahrC* gene is shown. Regions A' to G' complementary to SR1 are indicated by grey boxes, the SD sequence is underlined. Start and stop codon are shown in Italics. Below, a schematic representation of the 5 *ahrC*-mRNA species used in this work is shown. Black rectangle, SD sequence. grey boxes, regions complementary to SR1.

Figure 3. Secondary structure probing of the SR1/*ahrC* complex

A. Alterations in the SR1 secondary structure upon complex formation with *ahrC* mRNA

Purified, 5' end-labelled $SR1_{186}$ (13 nM) was incubated with increasing amounts of unlabelled $ahrC_{376}$ (80 nM, 200 nM, 800 nM), complex allowed to form for 5 min at 37^{o} C and subjected to limited cleavage with the RNases indicated. The digested RNAs were separated on 8 % denaturing gels. Autoradiograms are shown. RNase concentrations used were: T1: 10^{-2} U/µl, T2: 10^{-1} U/µl, V1: 10^{-1} U/µl C, control without RNase treatment, L, alkaline ladder. Left; entire gel. Right, long run of the same samples allowing a better separation of the complementary regions B, C, D, E and F. Nucleotide positions are included. Altered T1, T2 and V cleavages are indicated by the symbols shown in the box.

Right half, below: $SR1_{78}$: For a better resolution of the complex within complementary regions F and G, the secondary structure of the complex between $SR1_{78}$ (6.25 nM) and $ahrC_{376}$ (80, 200, 800, 1600 nM) was mapped, the same concentrations of T1, T2 and V were used and the products separated by a long run on an 8% gel.

B. Alterations in the *ahrC* secondary structure upon complex formation with SR1.

Purified, 5' end-labelled *ahrC* (13 nM) was incubated with increasing amounts of unlabelled SR1 (80 nM, 200 nM, 800 nM), complex formation, cleavage and gel separation were performed as above.

C. Schematic representation of the SR1 secondary structure with indicated structural changes upon binding to *ahrC* RNA. Altered T1, T2 and V cleavages are denoted as shown in the box. Regions complementary to *ahrC* RNA are highlighted by grey boxes.

Figure 4. Binding assays of wild-type and mutated SR1/*ahrC* pairs

Binding experiments were performed as described in *Materials and Methods*. Autoradiograms of gel-shift assays are shown. The concentration of unlabelled $ahrC_{88}$ RNA species is indicated. SR1 derivatives were 5' end-labelled with [γ ^{32}P]-ATP and used in at least 10-fold lower equimolar amounts compared to the targets. F, free SR1, D duplex between SR1 and *ahrC* RNA.

A Analysis of mutations in region G

B Schematic representation of SR1 with the mutations introduced into region G

C Analysis of mutations in regions C, D, E and F.

D Schematic representation of the mutated SR1 species. Grey boxes denote the substituted regions.

Figure 5. Analysis of the role of Hfq

A. Interaction between SR1 and Hfq

Purified *B. subtilis* Hfq was added to final concentrations as indicated to three SR1 species of different lengths comprising the 205 nt, 186 nt or 104 nt of 5' part of wild-type SR1 and binding was assayed as described in *Materials and Methods*

B. Interaction between *ahrC* RNA and Hfq

Purified *B. subtilis* Hfq was added to final concentrations as indicated to 4 *ahrC* species of different length (see Fig. 2C) and binding was assayed as in 5A.

C. Complex formation between SR1 and *ahrC* RNA in the absence and presence of purified *B. subtilis* Hfq.

The interaction between SR1 (final concentration: 1.0 nM) and *ahrC* RNA was assayed in the absence or presence of 10 µM Hfq as described in *Materials and Methods*. The SR1/Hfq complex, the SR1/*ahrC* complex and the ternary SR1/*ahrC*/Hfq complex are indicated.

D. Mapping of the Hfq binding site on *ahrC* mRNA

Purified, 5' end-labelled $ahrC_{483}$ RNA (13 nM) was incubated for 15 min at 37^{o} C with with increasing amounts of Hfq and subsequently subjected to limited cleavage with the RNases T1 and T2 followed by separation on an 8 % denaturing polyacrylamide gel. The autoradiogram is

shown. RNase concentrations used were as in Fig. 1. C, control without RNase treatment, L, alkaline ladder. The Hfq binding site is indicated by a black bar.

Figure 6. Toeprinting analysis

Ternary complex formation upon addition of different amounts of regulatory RNAs to either *ahrC* mRNA or *sodB* mRNA (for details, see *Materials and Methods* and *Results*).

The toeprint signal relative to A of the start codon is marked. Addition of 30S ribosomal subunits and initiator tRNA (lanes 2 and 3) as well as increasing concentrations (50-fold, 100-fold and 200-fold excess) of the regulatory RNAs (lanes 4 to 6 and 7 to 9) are indicated above the gels. In all cases, the DNA sequencing reactions (C T G A) were carried out with the same end-labelled oligonucleotide as in the toeprint analysis assays.

A. Toeprinting analysis with *ahrC* mRNA

An autoradiogram of ternary complex formation on *ahrC* mRNA in the absence or presence of SR1 or heterologus small RNAs (SR2 from *B. subtilis*, RyhB from *E. coli*) is shown. RyhB was added in a 200-fold excess.

B. Toeprinting analysis with *sodB* mRNA

An autoradiogram of ternary complex formation on *sodB* mRNA in the absence or presence of SR1 or the cognate small RNA RyhB and the heterologous RNAIII (200-fold excess) from streptococcal plasmid pIP501 is shown.

C. Calculation of the relative toeprints on *ahrC* mRNA with two SR1 species and heterologous RNA SR2

Figure 7. Intracellular concentration of SR1 under different growth conditions

B. subtilis strain DB104 was grown to OD_{560} = 2 (log phase) or OD_{560} = 4.5 (stationary phase), respectively, 5 ml or 1,5 ml culture, respectively, were withdrawn and used for the preparation of total RNA and subsequent Northern blotting.

Lanes 1 and 2, 6.6 and 33.3 fmol of *in vitro* synthesized, purified SR1, lanes 3 and 4, DB104 (*Δsr1::cat*) with 6.6 and 33.3 fmol of *in vitro* synthesized, purified SR1 mixed at the beginning of the RNA preparation, lanes 5, two and three parallels of RNA isolated from DB104. An autoradiogram of the Northern blot is shown.

Table 1: Plasmids used in this study

Plasmid	Description	Reference
pTYB11-BsHfq	pTYB11 vector with *B. subtilis hfq* gene	P. Valentin-Hansen
pGF-BgaB	integration vector for *amyE* gene, heat-stable β-galactosidase from *B. stearothermophilus* without SD for translational fusions, , Km^R, Ap^R	27
pGGA4	pGF-BgaB with nt 1 to 119 of *ahrC*	this study
pGGA6	pGF-BgaB with nt 1 to 113 *ahrC*	this study
pGGA7	pGF-BgaB with nt 1 to 279 of *ahrC* but lacking nt 102-112	this study
pGGA8	pGF-BgaB with nt 1 to 119 of *ahrC*, but 2 nt exchange	this study

Table 2: β-galactosidase activities

Strain	5' *ahrC* sequence	β-galactosidase activity (Miller units)
DB104::pGGA6	113 nt (no)	251±28
DB104::pGGA4	119 nt (G)	7.6±2
DB104:: pGGA7	280 nt (G, F, E, but Δnt102-112)	3.5±1.4
DB104:: pGGA8	119 nt (G, but 2 nt exchange)	240 ±35
DB104::pGF-BgaB	no	2.9±0.5
DB104::pGGA6 (*Δhfq::cat*)	113 nt (no)	1.3± 0.5

All values represent averages of at least three independent determinations. Plasmid pGF-BgaB is the empty vector. All plasmids contain *ahrC s*equences fused in frame to the promoterless, SD less *gaB* gene encoding the heat-stable β-galactosidase of *B. stearothermophilus* and were inserted into the *amyE* locus of the *B. subtilis* chromosome. β-galactosidase activities were measured at 55° C. In brackets, the presence of complementary regions to SR1 is denoted.

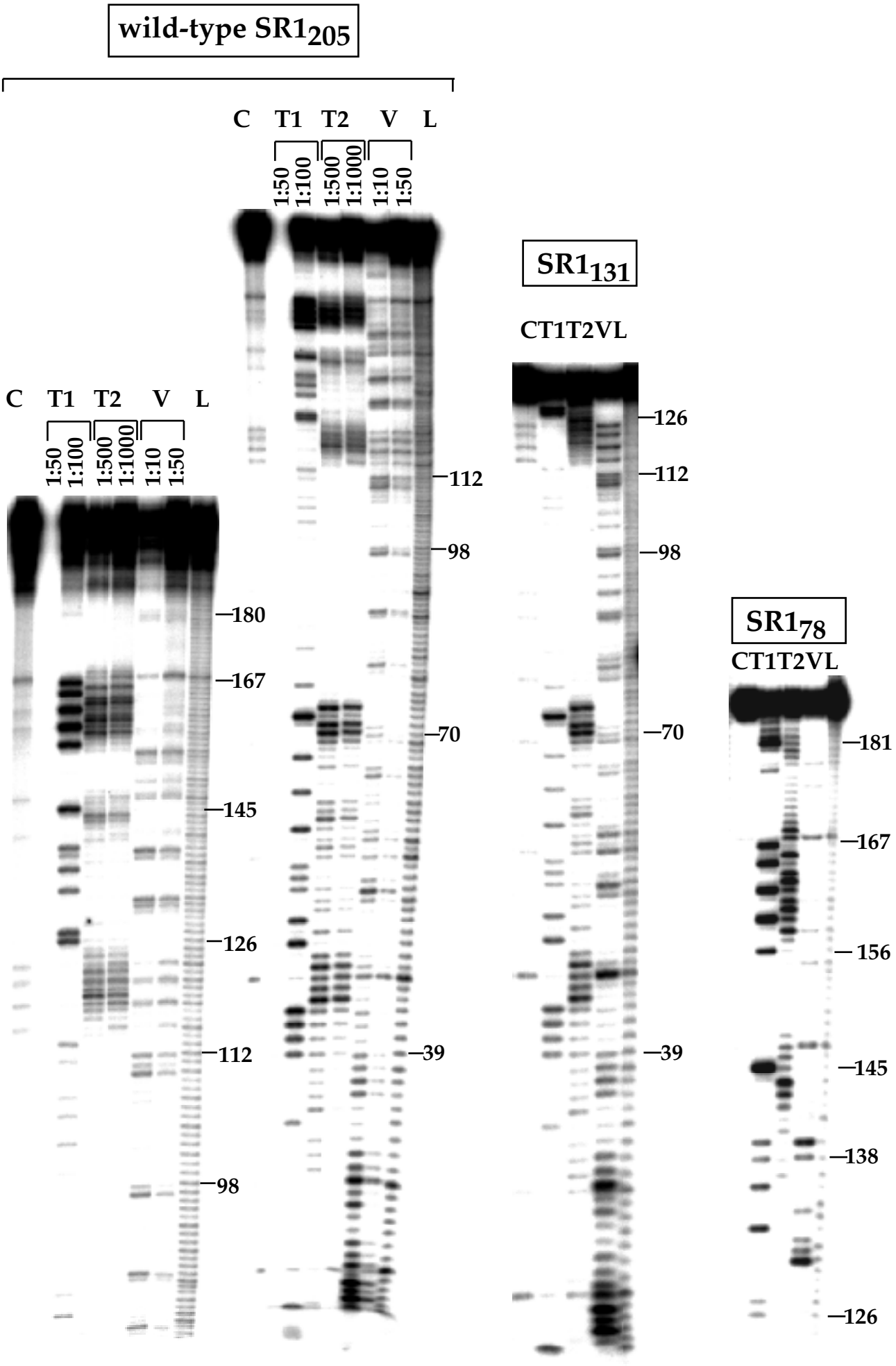

Fig. 1A Heidrich et al.

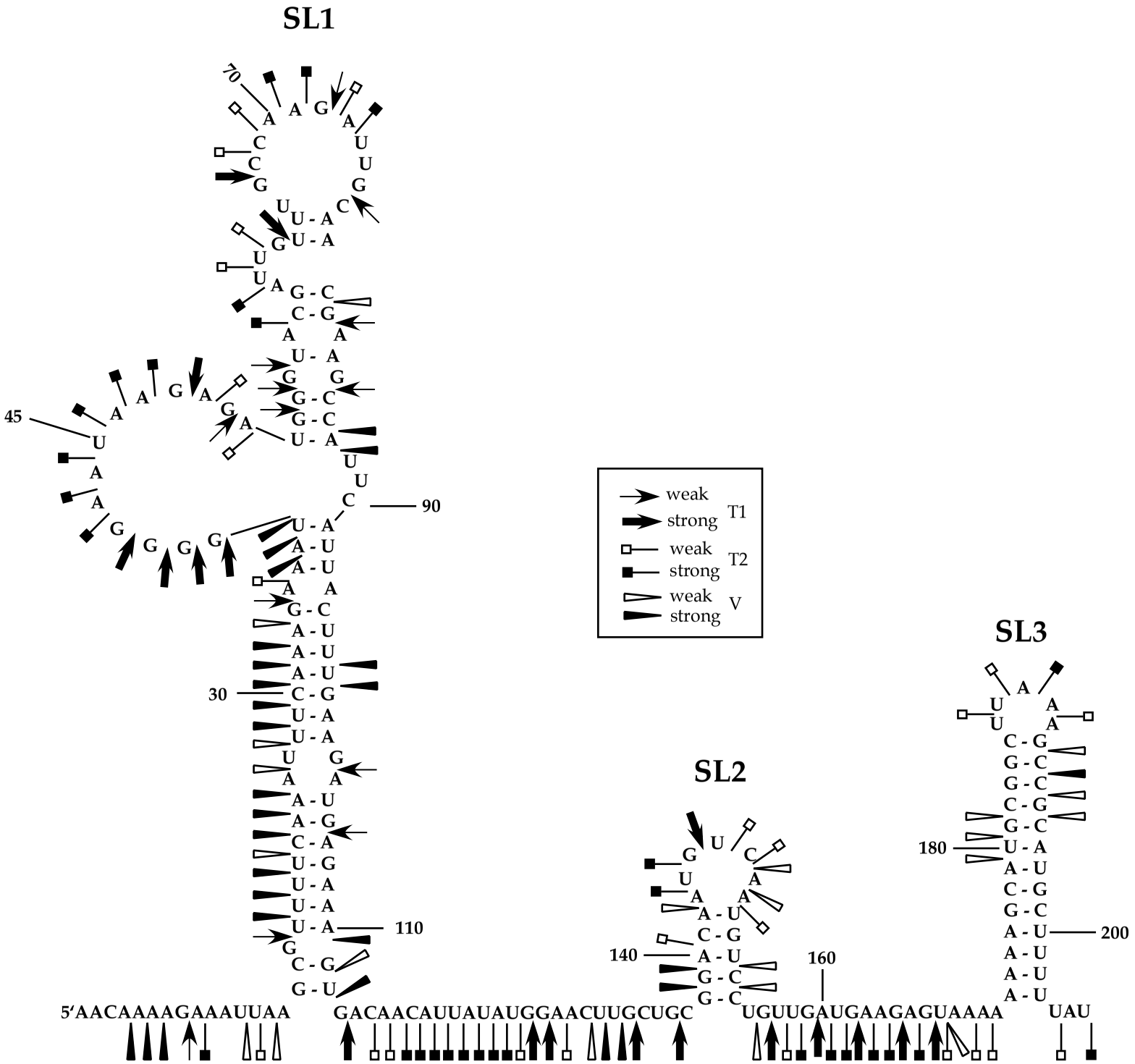

Figure 1 B Heidrich et al.

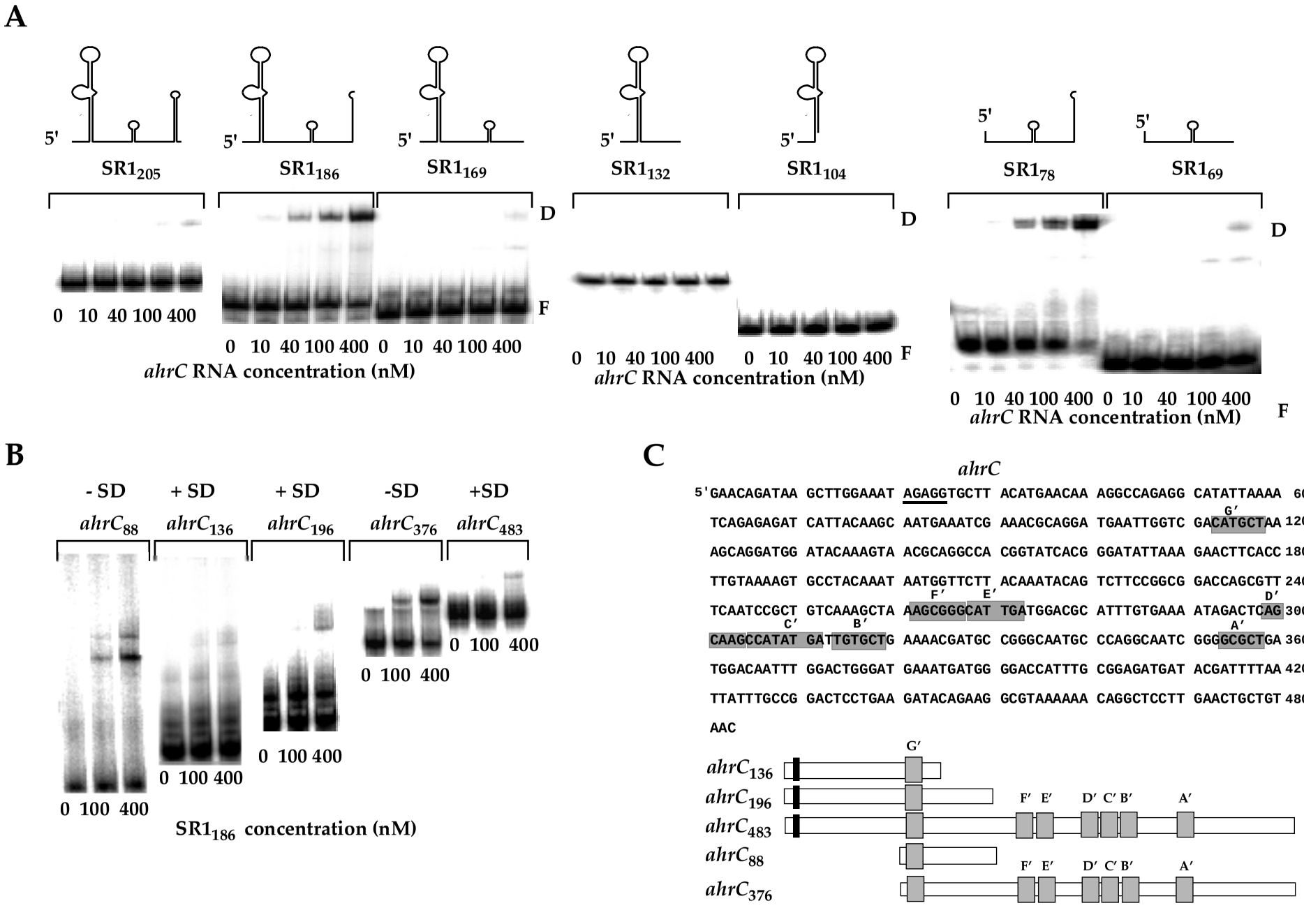

Figure 2 Heidrich et al.

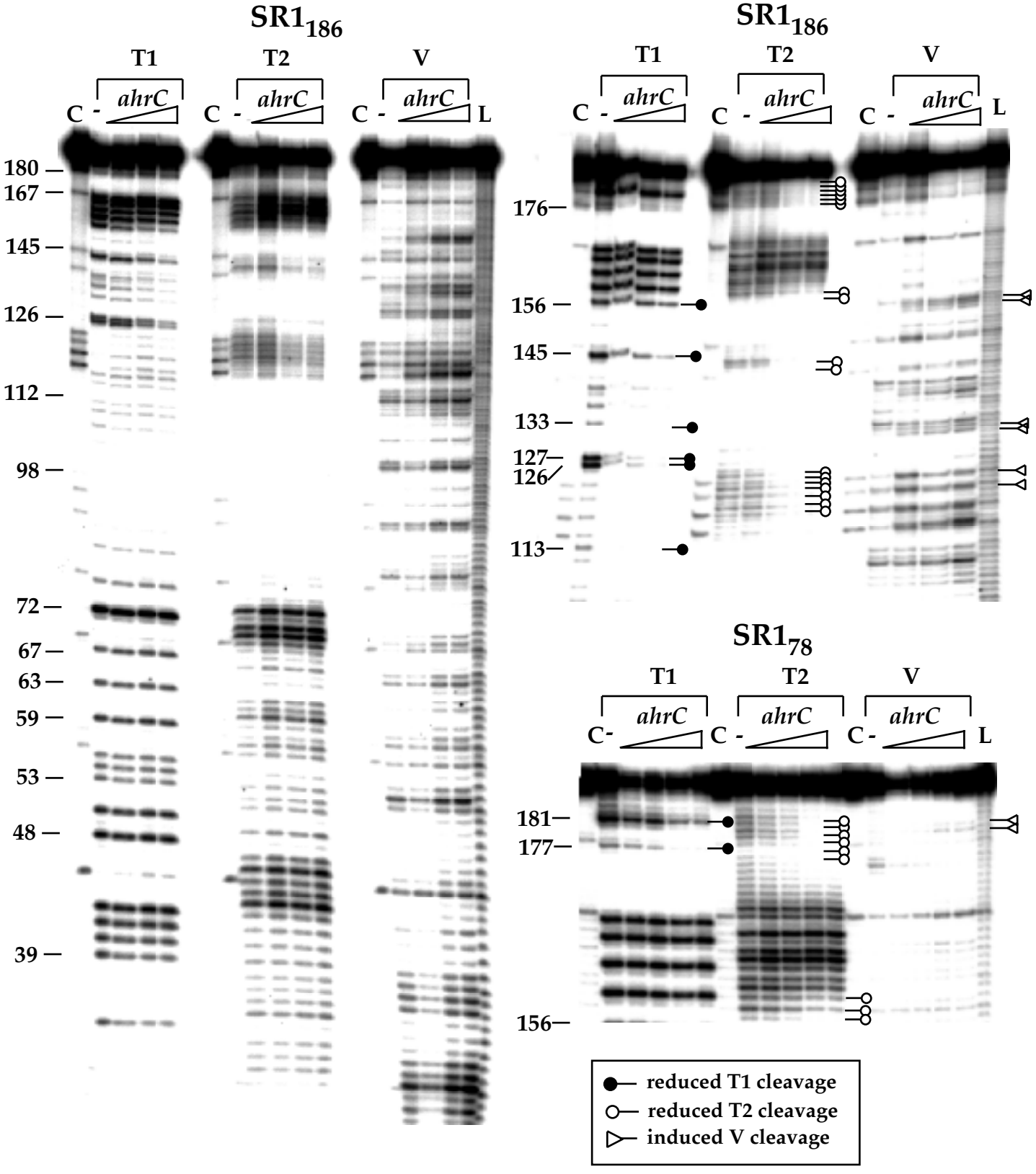

Fig. 3A Heidrich and Brantl

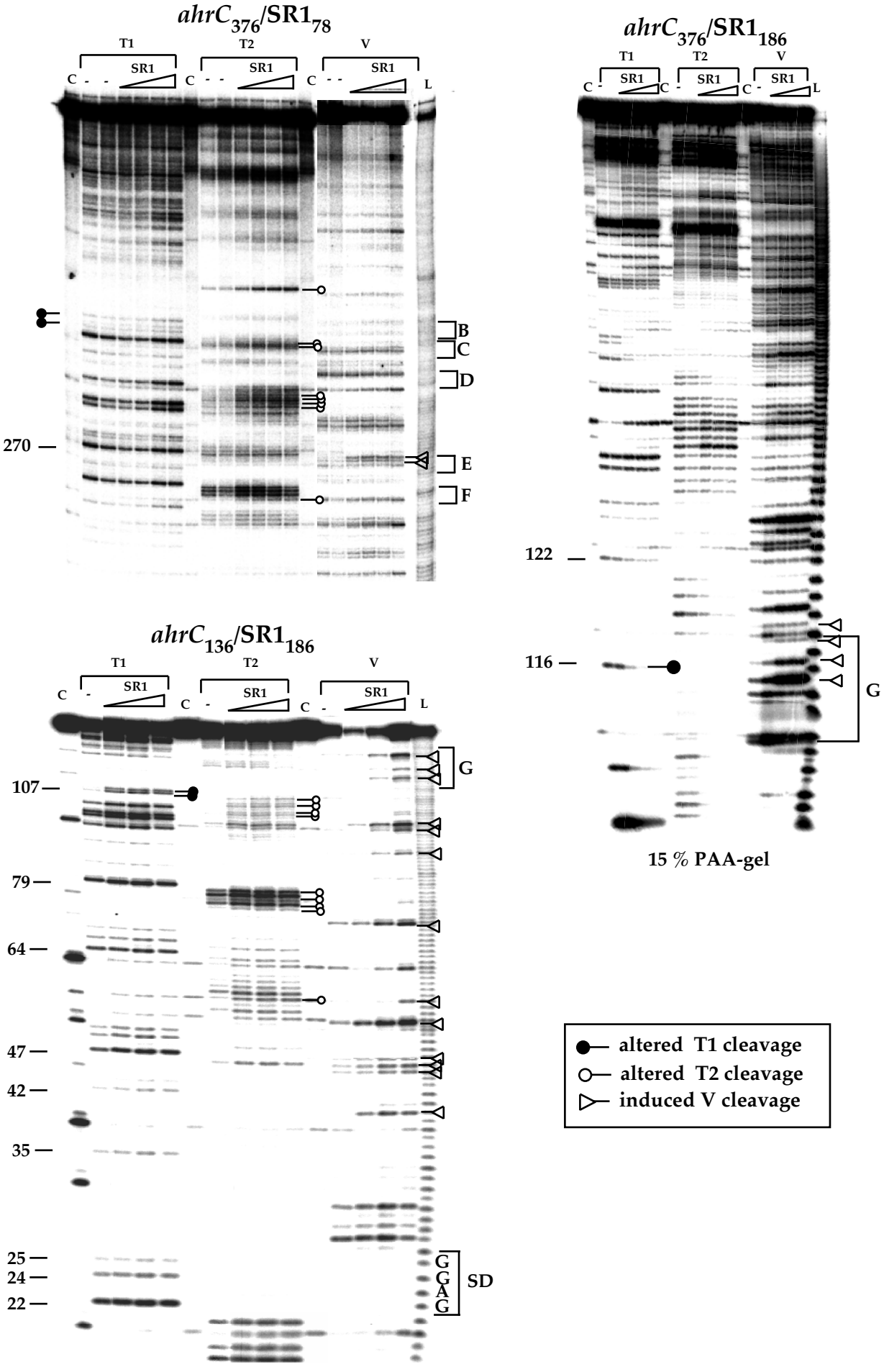

Fig. 3B Heidrich et al.

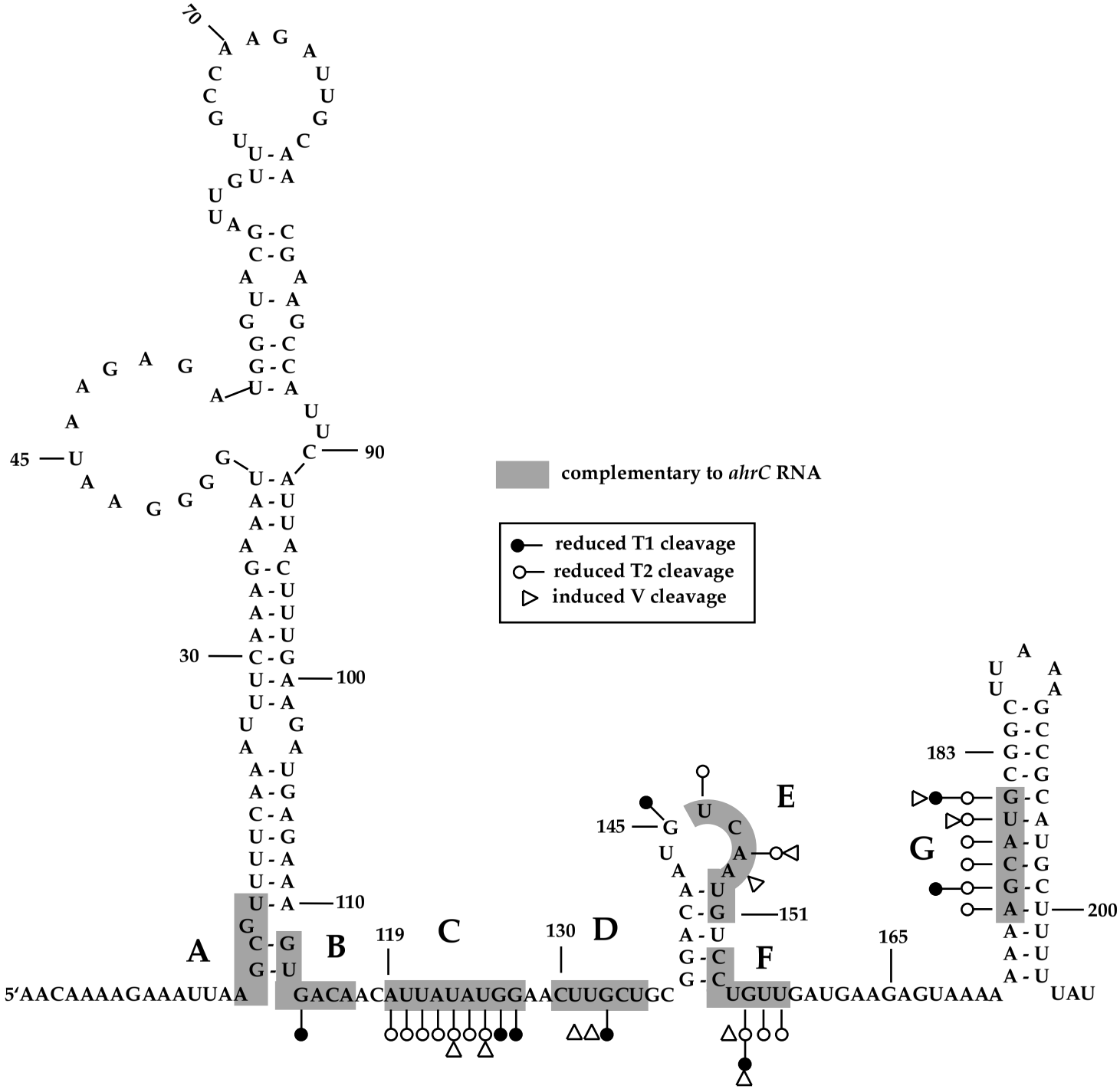

Figure 3C Heidrich et al.

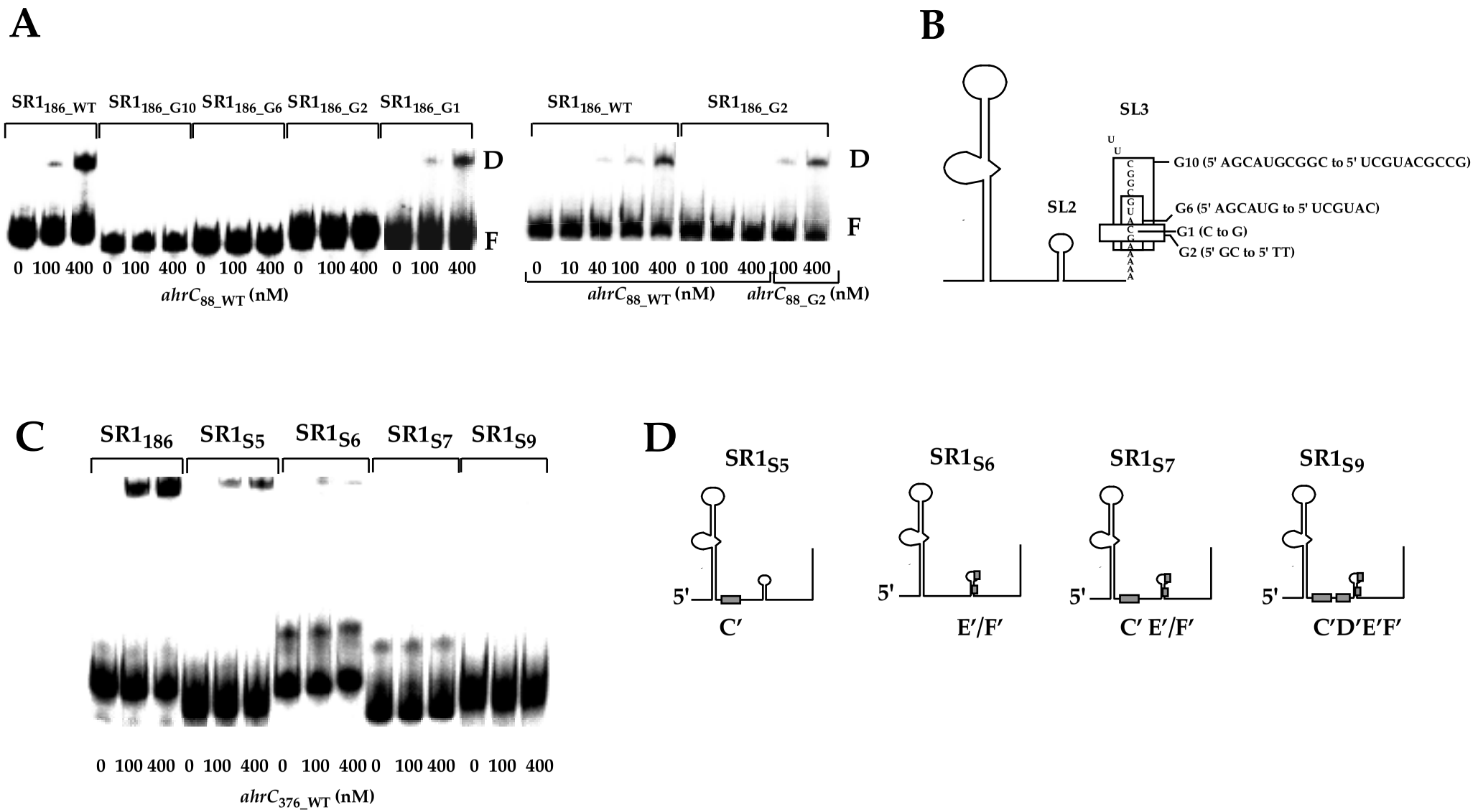

Fig. 4 Heidrich et al.

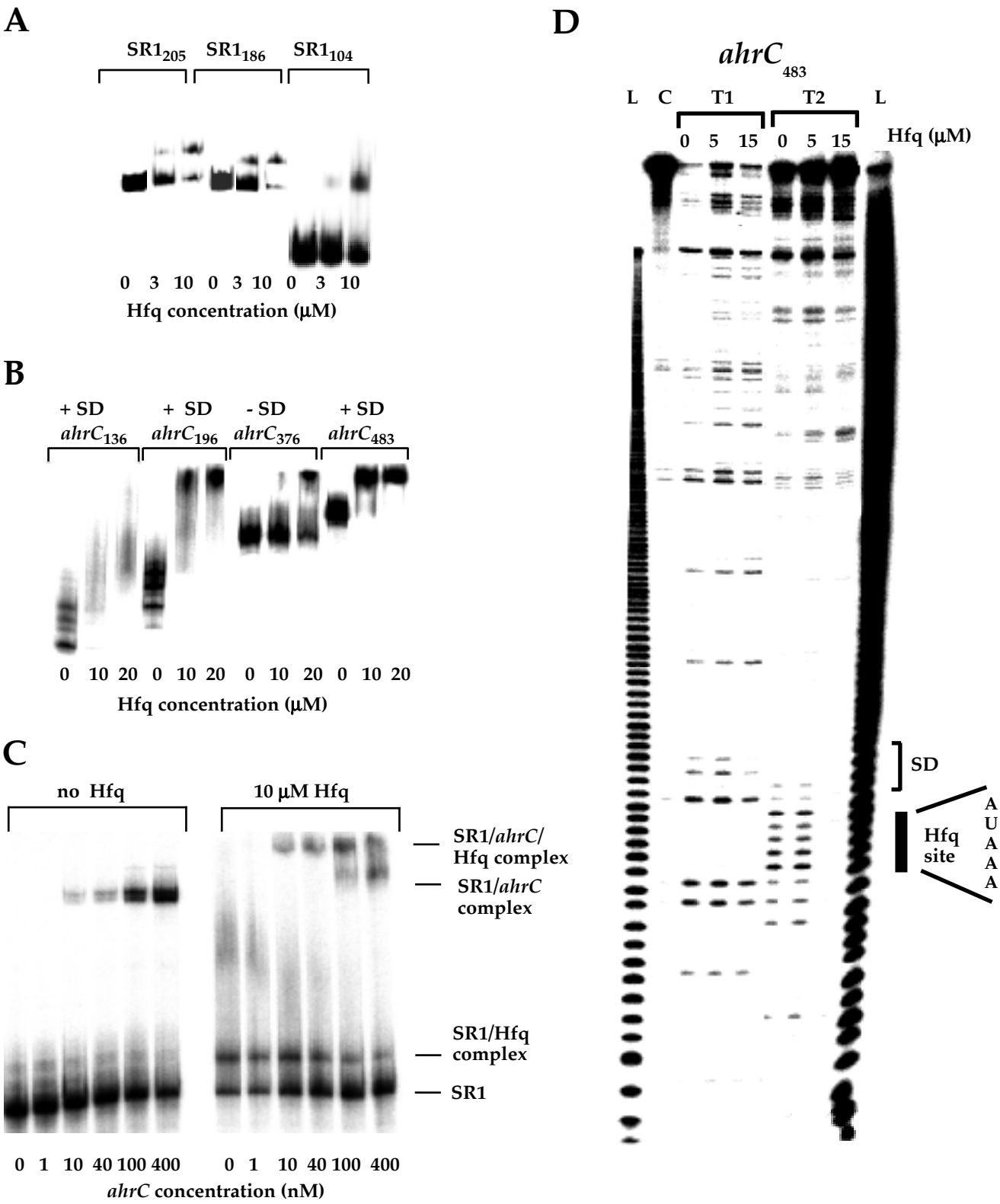

Fig. 5 Heidrich et al.

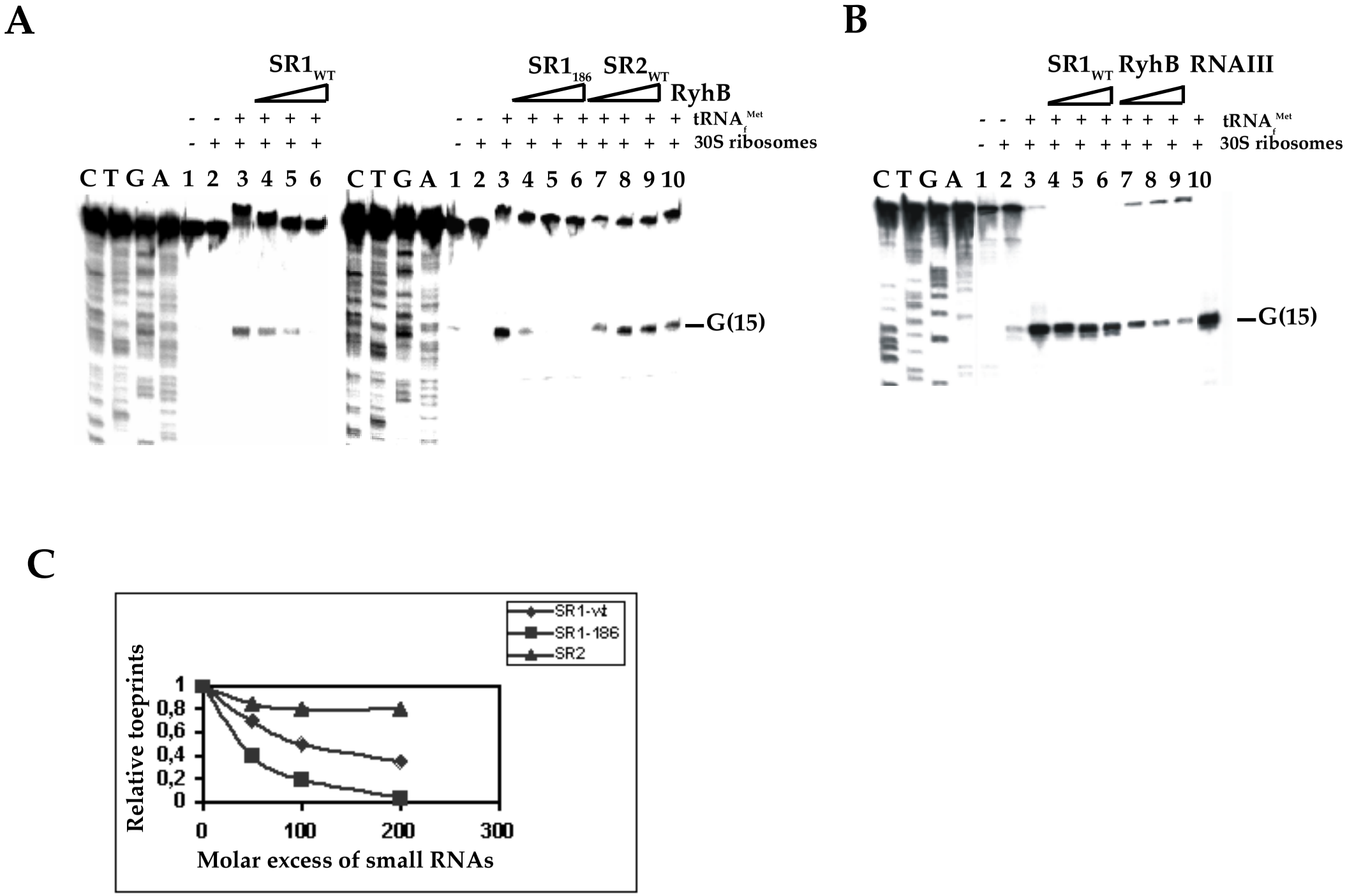

Fig. 6 Heidrich et al.

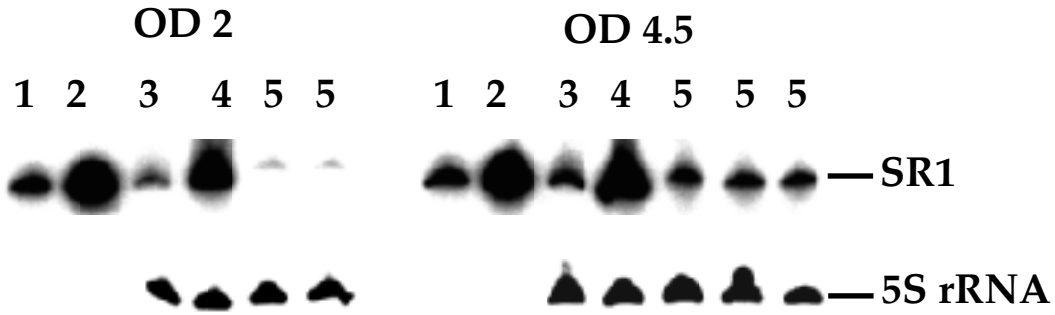

Figure 7 Heidrich et al.

6. FourU – A novel type of RNA thermometer in *Salmonella* and other bacteria

[Manuskript IV]

Torsten Waldminghaus[1], Nadja Heidrich[2], Sabine Brantl[2] and Franz Naberhaus[1]

[1]Institut für Biologie der Mikroorganismen, Ruhr-Universität Bochum, Universitätsstrasse 150, NDEF 06/783, D-44780 Bochum, Germany
[2]AG Bakteriengenetik, Friedrich-Schiller-Universität Jena, Philosophenweg 12, D-07743 Jena, Germany

eingereicht bei *Molecular Microbiology*

Molecular Microbiology manuscript March 2007

FourU – A novel type of RNA thermometer in *Salmonella*

Torsten Waldminghaus[1], Nadja Heidrich[2], Sabine Brantl[2], Franz Narberhaus[1,*]

[1]Lehrstuhl für Biologie der Mikroorganismen, Ruhr-Universität Bochum, 44780 Bochum, Germany, [2]AG Bakteriengenetik, Friedrich-Schiller-Universität Jena, 07743 Jena, Germany

Keywords: heat shock/ riboswitch/ RNA structure/ RNA thermometer/ translational control

Running title: FourU – A novel RNA thermometer

[*]Corresponding author: F. Narberhaus, Lehrstuhl für Biologie der Mikroorganismen, Ruhr-Universität Bochum, Universitätsstrasse 150, NDEF 06/783, 44780 Bochum, Germany. Tel: +41 (0)234 322 3100; Fax: +49 (0)234 321 4620; E-mail: franz.narberhaus@rub.de

Abstract

The translation of many heat shock and virulence genes is controlled by RNA thermometers. Usually, they are located in the 5'-untranslated region (5'-UTR) and block the Shine-Dalgarno (SD) sequence by base pairing. Destabilization of the structure at elevated temperature permits ribosome binding and translation initiation. We have identified a new type of RNA thermometer in the 5'-UTR of the *Salmonella agsA* gene, which codes for a small heat shock protein. Transcription of the *agsA* gene is controlled by the alternative sigma factor σ32. Additional translational control depends on a stretch of four uridines that pair with the SD sequence. Mutations in this region affect translation *in vivo*. Structure probing experiments demonstrate a temperature-controlled opening of the SD region *in vitro*. Toeprinting (primer extension inhibition) shows that ribosome binding is dependent on high temperatures. Together with a postulated RNA thermometer upstream of the *Yersinia pestis* virulence gene *lcrF (virF)*, the 5'-UTR of *Salmonella agsA* might be the founding member of a new class of RNA thermometers that we propose to name 'fourU' thermometers.

Introduction

The induction of heat shock proteins (Hsps) to protect the cell from heat-induced damage is a universal biological process (Gross, 1996; Yura *et al*., 2000). Like all other organisms, *Salmonella* species induce the expression of a large set of chaperones and proteases under heat stress conditions. Substantial cross-talk between the bacterial heat shock response and infection processes has been reported (Gophna and Ron, 2003; Goulhen *et al*., 2003). Several heat shock genes are consistently up-regulated in pathogenic *E. coli* lineages (Takaya *et al*., 2002; Takaya *et al*., 2003; Dowd and Ishizaki, 2006). Moreover, deletion of the ClpXP protease genes in an enterohaemorrhagic *E. coli* strain impaired the secretion of virulence proteins (Tomoyasu *et al*., 2005). Virulence of *Salmonella enterica* serovar Typhimurium requires the DnaK/J chaperone system and the Lon protease (Takaya *et al*., 2002; Takaya *et al*., 2003). Apart from the typical repertoire of molecular chaperones, *Salmonella* encodes a unique heat shock protein, named AgsA (aggregation-suppression protein), which is strongly induced at high temperatures (Tomoyasu *et al*., 2003). AgsA is a distantly related member of the small Hsp family, which comprises molecular chaperones that bind to unfolded proteins in order to maintain them in a folding-competent state (Narberhaus, 2002).

The majority of heat shock genes in *Escherichia coli*, *Salmonella* and related enterobacteria are under control of the alternative sigma factor σ^{32} (Yura *et al*., 2000). Immediately after a temperature upshift, the cellular concentration of the transcription factor increases rapidly and transiently by a complex regulatory circuit involving transcriptional, translational and posttranslational control mechanisms. Other protein-mediated regulatory circuits are based on repressor proteins that inhibit the transcription of heat shock genes at low temperatures (Hurme and Rhen, 1998; Narberhaus, 1999).

Only recently, the fundamental role of RNA in sensing of environmental parameters has been recognized (Winkler and Breaker, 2005; Narberhaus *et al*., 2006). Most RNA sensors are located in the 5'-untranslated region (5'-UTR) of mRNAs, fold into complex structures and control the expression of downstream genes by signal-induced conformational changes. While RNA thermometers sense temperature as a physical stimulus, riboswitches recognize chemical signals. Riboswitches occur in prokaryotes and eukaryotes (Sudarsan *et al*., 2003a). They respond to enzyme cofactors (Winkler *et al*., 2002; Nahvi *et al*., 2004), amino acids (Epshtein *et al*., 2003; Sudarsan *et al*., 2003b), nucleotides (Mandal and Breaker, 2004b), sugars (Winkler *et al*., 2004) or even ions such as Mg^{2+} (Cromie *et al*., 2006). These target molecules are bound by a

so-called aptamer domain with remarkable specificity and affinity. Ligand-induced conformational changes are transduced to the expression platform, which is typically located immediately downstream of the aptamer domain (Winkler, 2005). As a consequence, gene expression is modulated either at the level of translation initiation, transcription termination or RNA processing (Mandal and Breaker, 2004a; Nudler and Mironov, 2004).

RNA thermometers undergo temperature-induced conformational changes. All presently known RNA thermometers control translation initiation. In most cases, entry to the ribosome binding site is blocked by complementary base pairs at low temperatures. At increasing temperatures, melting of the structure permits ribosome access (Narberhaus *et al*., 2006). This simple regulatory principle can be realized by quite different RNA structures. Only a few distinct types of RNA thermometers have been discovered so far.

The first RNA thermometer described regulates development of phage λ by controlling expression of the cIII protein (Altuvia *et al*., 1989). At 37°C, the SD sequence and the AUG start codon are accessible in a single-stranded region flanked by two hairpins. In an alternative structure at 45°C, the AUG start codon and the SD sequence are hidden in a hairpin structure. This RNA thermometer is unique in switching on translation with *decreasing* temperature. Moreover, it is the only known RNA thermometer that does not seem to operate by gradual melting but switches between two mutually exclusive conformations.

The cellular level of the heat-shock sigma factor σ^{32} in *E. coli* is adjusted in part by the most complex RNA thermometer known to date. The RNA structure consists of two segments (region A and B) within the coding region of the *rpoH* mRNA (Morita *et al*., 1999a; Morita *et al*., 1999b). While the SD sequence is accessible irrespective of the temperature, the AUG start codon and region A as part of the ribosome binding site are blocked at low temperatures by base-pairing with region B. Extensive mutational analysis and structure probing experiments demonstrated that the secondary structure is disrupted at heat shock temperatures. Similar structures were predicted in the *rpoH* transcripts of other Gram-negative bacteria (Nakahigashi *et al*., 1995).

The expression of virulence genes can also be controlled by RNA thermometers (Johansson and Cossart, 2003). A temperature-labile stemloop structure blocking the SD sequence was predicted upstream of the *lcrf* gene in *Yersinia pestis* (Hoe and Goguen, 1993). Another RNA thermometer exists in the 5'-UTR of *prfA* in the food-borne pathogen *Listeria monocytogenes* (Johansson *et al*., 2002). The *prfA* gene is transcribed at 30°C. However, within an extended 120-nucleotide hairpin both the SD sequence and the AUG start codon are positioned in internal loop regions allowing only

inefficient translation. Conformational changes in the RNA at body temperature (37°C) increase translation efficiency resulting in production of the virulence regulator.

By far the most common RNA thermometer is the ROSE (Repression Of heat Shock gene Expression) element, which was discovered in the nitrogen-fixing soybean symbiont *Bradyrhizobium japonicum* (Narberhaus *et al*., 1998). Meanwhile, more than 40 ROSE-like RNA thermometers have been predicted in diverse α- and γ-proteobacteria (Waldminghaus *et al*., 2005). They are located in the 5'-UTR of small heat-shock genes and between 70 and 120 nucleotides long. Their computer-predicted secondary structure is composed of three or four stemloops with the SD sequence being masked by imperfect base-pairing in the 3'-proximal hairpin (Balsiger *et al*., 2004; Nocker *et al*., 2001). NMR studies on this functional hairpin revealed a helical structure containing several non-canonical base pairs (Chowdhury *et al*., 2006). Irregular base stacking coupled with a network of weak hydrogen bonds facilitates liberation of the SD sequence in the physiological temperature range.

Here, we present an in-depth characterization of a new type of RNA thermometer that regulates translation of the *Salmonella enterica agsA* gene by four consecutive uracil residues that pair with the SD sequence. Our detailed *in vivo* and *in vitro* experiments demonstrate dynamic temperature-dependent conformational changes in the 5'-UTR of *agsA* that control ribosome access to the SD sequence.

Results

A new RNA thermometer candidate in Salmonella

RNA thermometers are characterized by a short sequence with imperfect complementarity to the SD region. The systematic inspection of a database containing the sequences and predicted secondary structures of 5'-UTRs from annotated protein-coding genes of bacterial genome sequences (Waldminghaus, unpublished) revealed a potential RNA thermometer upstream of the *Salmonella agsA* gene. Unlike the widespread ROSE-like thermometers, the 5'-UTR of *agsA* consists of only two stemloop structures and the anti-SD sequence does not contain the typical U(U/C)GCU motif (Fig. 1). The SD sequence in the second hairpin (hairpin II) pairs with a stretch of four uracil residues. An internal loop (A29/G52), eight AU, four GU and only two GC out of 14 base pairs limit the free energy of this extended hairpin to -9.7 kcal/mol. The interesting novel features of this potential thermoregulator prompted us to investigate its structure and function in more detail.

Temperature-dependent transcriptional regulation of agsA

To assign the 5' end of the *agsA* transcript, primer extension experiments were performed. Total RNA was isolated from cells grown at 30°C and after heat shock at 45°C and reverse transcription was carried out. A strong signal was detected only in the heat-shocked samples (Fig. 2). The deduced -10 and -35 regions correspond well to the consensus sequence (CTTGAA-$N_{(13-18)}$-CNCCATAT) of σ^{32}-type promoters (Wade *et al*., 2006).

To confirm the presence of the putative σ^{32}-dependent promoter, translational fusions of *bgaB* to the *agsA*-promoter region were constructed (Fig. 3A). The *bgaB* gene codes for a heat-stable β-galactosidase from *Bacillus stearothermophilus* (Hirata *et al*., 1984). Promoter activity was measured in an *E. coli* Δ*rpoH* mutant deficient of the heat-shock sigma factor σ^{32} and in the isogenic wildtype (*wt*) MC4100. When cells were grown at 25°C, the β-galactosidase activity was low in both strains (Fig. 3B). After a temperature upshift to 40°C for 30 minutes, expression was induced six-fold in the *wt* strain but not in the Δ*rpoH* mutant. In the *wt*, 30-fold induction was observed 90 minutes after heat shock. Absent induction in the mutant strain demonstrates that the temperature-induced amount of *agsA* mRNA results from transcriptional control by the mapped σ^{32}-type promoter.

The 5'-UTR of agsA confers translational control in vivo

To separate the described transcriptional effects from translational events, translational *agsA-bgaB* fusions were placed downstream of the arabinose-inducible pBAD-promoter (Fig. 4A). Temperature-dependent translational control was monitored upon induction of the promoter with 0.01 % (w/v) of L-arabinose.

Expression of the *agsA-bgaB* fusion in *E. coli* grown at 30°C showed a basal level of 29 MU that increased to 84 MU 30 minutes after a heat shock to 42°C (Fig. 4B). A similar fusion containing only hairpin II (mini-*agsA*) produced overall lower β-galactosidase activities. However, temperature-dependent induction was retained. As a control, we used a fusion to the 5'-UTR of the *E. coli* gyrase gene (*gyrA-bgaB*), which is expected not to be thermally controlled. Starting from 4 MU at 30°C, β-galactosidase activity indeed increased only slightly (about 6 MU) with increasing temperature.

If the 5'-UTR of the *agsA* gene were a functional RNA thermometer, stabilizing and destabilizing point mutations should decrease and increase expression, respectively. Point mutations in the full-length *agsA-bgaB* fusion affecting the stability of hairpin II are outlined in Fig. 1. The stabilizing mutations A29C, U32C and U33C reduced expression approx. 10-fold (from about 30 MU in the *wt* fusion to 3 MU) when cells were grown at 30°C (Fig. 4C). Moreover, induction at 42°C was abolished. In contrast, expression was elevated both at 30 and at 42°C in the presence of the destabilizing mutation CUU30-32AAA.

The G21C exchange introduced a CAU triplett complementary to the AUG start codon, which might result in an extended hairpin II (see Fig. 1) and thus impair ribosome access. Indeed, β-galactosidase activity was reduced at 30 and 42°C as compared to the *wt* fusion (Fig. 4B). Nevertheless, efficient heat-induction (12-fold) was possible.

Taken together, these data demonstrate that the 5'-UTR of *agsA* from *S. enterica* mediates posttranscriptional control to the heat shock gene in a RNA thermometer-like fashion *in vivo*.

Structure probing experiments reveal temperature-mediated conformational changes

The secondary structure of the *agsA* thermometer was probed at different temperatures using RNases T1 (cuts 3' of single-stranded guanines), T2 (cuts 3' of unpaired nucleotides with a slight preference for adenines) and V1 (specific for double-stranded and stacked regions). Separation of the corresponding cleavage products on a denaturing 15% polyacrylamide gel gives an overview of the entire structure (Fig.

5A). For detailed analysis of hairpin II, samples were run on an 8% polyacrylamide gel (Fig. 5B).

The overall cleavage pattern at 30°C is in good agreement with the calculated secondary structure. Both terminal loops around positions 9 and 40 were cut by RNases T1 and T2 but not by RNase V1 (Fig. 5A, B and D). Complete protection of positions 2 to 8 and 11 to 18 against T1 and T2 cleavage and susceptibility of these regions to RNase V1 confirmed the stem region in hairpin I (Fig. 5A and D). This hairpin was not temperature-responsive as it remained resistant against cleavage by RNases T1 and T2 at 45°C (Fig. 5A).

The experimentally defined structure of hairpin II is also consistent with the predicted structure (Fig. 5B and D). However, in contrast to hairpin I it appears to be in a dynamic, temperature-responsive conformation. The tetraloop (nucleotides 39 to 42) is readily accessible to RNase T1 and T2 at low and high temperature. The flanking SD and anti-SD regions are largely resistant to these enzymes at 30°C indicating a double-stranded RNA region that blocks ribosome binding. Residual cleavage by T1 and T2 suggests that a minor population is in an open conformation. The fraction of single-stranded molecules substantially increases at 45°C as illustrated by the accumulation of T1 and T2 derived products in the SD and anti-SD region (Fig. 5B and quantification of four independent experiments in Fig. 5C). Structure probing performed at 50°C showed further opening of stem II while stem I remained stable (data not shown). Our results suggest that hairpin II exists in equilibrium between open and closed structures, which is shifted towards the open conformation after exposure to high temperature.

Stabilizing mutations in hairpin II prevent release of the SD sequence

Point mutations potentially stabilizing hairpin II reduced expression of the reporter gene fusion (see Fig. 4). Structure probing of the U32C and A29C RNAs at 45°C indicates the presence of a thermostable structure in hairpin II (Fig. 6). Neither mutation affected the conformation of hairpin I. Consistent with the data presented in Fig. 5, the SD and anti-SD sequences in hairpin II of the *wt* RNA were accessible to T1 and S1 (cleaving single-stranded nucleotides) enzymes. In contrast, the U32C mutation resulted in a complete protection of G48, G49 and G50 in the SD region (Fig. 6). Moreover, in the A29C RNA all three guanines and G51, which is predicted to pair with C29, were protected against T1 attack. Impaired cleavage of nuclease S1 in the SD sequence supports the T1 results and demonstrates that in both stabilized RNAs the ribosome binding site is kept in a blocked conformation.

The similarity of the V1 cleavage pattern of variant U32C to the *wt* RNA shows that this mutation does not introduce major structural changes. In contrast, V1 cleavage of the

A29C RNA is decreased in the SD segment but increased at nucleotides 26 to 29 suggesting pronounced changes in stem II geometry.

Binding of 30S ribosomes to the 5'-UTR of agsA depends on temperature

To examine the effects of the *agsA*-mRNA structure on formation of the translation initiation complex we performed toeprinting analysis (Hartz *et al.*, 1988). After annealing of the primer, ribosomal subunits and initiator-tRNA were added to *agsA* mRNA (116 nt) and incubated at 30 and 45°C. As shown in Figure 7, primer extension was not inhibited at 30°C. When samples were incubated at 45°C, a toeprint corresponding to position +17 relative to the translation start site was detected indicating formation of an mRNA-ribosome-$tRNA_f^{Met}$ ternary complex. These results demonstrate temperature-controlled binding of the ribosome to the *agsA* translation initiation region in the absence of any other cellular factor.

Discussion

Our knowledge on sensory RNAs, such as riboswitches and RNA thermometers, is just beginning to emerge. The estimation that as many as 2 % of all genes in *Bacillus subtilis* might be controlled by riboswitches (Mandal *et al*., 2003) emphasises that regulatory RNA elements play a fundamental role in the genetic control of metabolic processes in prokaryotes. The recent identification of thiamine pyrophosphate-binding riboswitches in eukaryotes (Sudarsan *et al*., 2003a; Thore *et al*., 2006) suggests that riboswitches derive from an ancient common ancestor of eukaryotes and prokaryotes (Vitreschak *et al*., 2004).

Given the importance of RNA-mediated genetic control, we set out to identify novel RNA thermometers that deviate from the few known examples. Unlike riboswitches, RNA thermometers are not characterized by a highly conserved ligand-binding domain (Narberhaus *et al*., 2006). All known RNA thermometers control translation. In principal, masking of the ribosome binding site can be achieved by diverse RNA sequences and structures. de Smit and van Duin showed that mRNA hairpins incorporating the SD sequence affect translation efficiency only if their free energy is lower than -6 kcal/mol (de Smit and van Duin, 1990, 1994). Thermodynamic considerations argue against a complete unfolding of such a stable stemloop in the physiological temperature range. Known RNA thermometers are complex structures either consisting of one extended stemloop (Johansson *et al*., 2002) or of multiple hairpins (Waldminghaus *et al*., 2005). The intrinsic heat sensitivity is based on internal loops, bulged residues and non-canonical base-pairs (Chowdhury *et al*., 2006).

Here, we describe a comprehensive structure-function analysis of an unusually short RNA thermometer. It consists of only 57 nucleotides, is folded into two hairpins and controls expression of the small heat shock gene *agsA* in *Salmonella enterica* serovar Typhimurium. The sequence of the 5'-UTR bears no similarity to the widespread ROSE element that controls the expression of many small heat shock genes in α- and γ-proteobacteria (Waldminghaus *et al*., 2005). Despite its short sequence and its simple structural design, the *Salmonella agsA* thermometer is fully functional as demonstrated by a complementary set of *in vivo* and *in vitro* experiments. Owing to its simple architecture it might serve as an excellent model for future studies, for example aiming at the structure determination of a full-length RNA thermometer.

In vivo evidence for a functional RNA thermometer was provided by a reporter gene assay, in which the isolated 5'-UTR of *agsA* permitted temperature regulation independent of its natural promoter. Like other RNA thermometers (Johansson *et al*., 2002), the *agsA* leader region alone induced gene expression roughly threefold.

Hence, it is unlikely that the thermometer alone accounts for the massive induction of AgsA protein after temperature upshift and in response to protein aggregation (Tomoyasu *et al*., 2003). Apparently, rapid and efficient induction under stress conditions is achieved by the combination of two separate modules, a σ^{32} promoter and an RNA thermometer. Dual control by a σ^{32} promoter in concert with a ROSE-like RNA thermometer was also shown for the *ibpA* genes of *E. coli* and *Salmonell*a (Waldminghaus *et al*., 2005). The equivalent set-up of the *agsA* promoter suggests that many other σ^{32}-controlled genes might possess a hitherto undiscovered RNA thermometer as additional layer of control. It is a matter of speculation which regulatory mechanism was invented first in evolution. Given the relatively simple mechanistic principle of RNA thermometers one might argue that they evolved earlier than the more complex and multi-factorial transcriptional control by the alternative sigma factor σ^{32}.

Complex control circuits involving several layers of control are common in bacterial stress responses. They allow the integration of multiple signals as was shown for the general stress response in *E. coli* (Hengge-Aronis, 2002). Cross-regulation of the heat shock response by σ^{32} and the repressor protein HrcA occurs in many proteobacteria (Permina and Gelfand, 2003). Using various control elements in a modular composition is predicted to increase the sensitivity and robustness of stress responses (El-Samad *et al*., 2005). Implementing a heat sensing device downstream of a σ^{32} promoter provides at least one additional advantage. Transcriptional control by σ^{32} primarily responds to the accumulation of unfolded proteins in the cell, whereas RNA thermometers are not expected to react to any other signal than temperature. By its modular architecture, the *agsA* promoter has obtained the capacity to integrate at least two separate signals, misfolded proteins and temperature.

The function of *trans*-acting small regulatory RNAs often requires the Hfq protein (Muffler *et al*., 1996; Schumacher *et al*., 2002; Zhang *et al*., 2002). Hfq is a RNA chaperone that assists in RNA-RNA interactions (Valentin-Hansen *et al*., 2004). *In vitro* experiments with the ROSE element suggested that it acts without the aid of Hfq or any other accessory factor (Chowdhury *et al*., 2003; Chowdhury *et al*., 2006). According to our data on the *agsA* thermometer, it seems unlikely that additional cellular factors are required for temperature sensing. First, there was a clear correlation between the computer-calculated free energy and the respective *in vivo* expression of mutated *agsA-bgaB* fusions showing that the intrinsic stability of hairpin II determines the temperature response. Secondly, structure probing experiments revealed that hairpin II of the synthetic 5'-UTR responds to temperature changes in the absence of any additional factors. Hairpin I was not absolutely required for regulation. However, it might play a structural role during co-transcriptional folding of the RNA thermometer *in*

vivo. Finally, toeprinting analyses demonstrated that access of isolated 30S ribosome subunits to naked RNA is temperature-controlled.

Another fascinating aspect of the *agsA* thermometer is its simple structural design. The SD sequence in hairpin II is blocked by a consecutive stretch of four uridine residues. A similar structure composed of four U residues that pair with SD sequence (AGGA) has been predicted but never proven experimentally upstream of the *lcrF* gene in *Yersinia pestis* (Hoe and Goguen, 1993) (Fig. 8). To distinguish this new class of thermosensors from the widespread ROSE-type thermometers, we suggest the designation ‘fourU thermometer’. A search for similar elements in our database revealed at least two promising candidates upstream of heat shock genes, one in the 5’-UTR of the *Brucella melitensis dnaJ* gene and one upstream of the *Staphylococcus aureus groES* gene (Fig. 8). Whether these are functional RNA thermometers remains to be demonstrated.

Experimental procedures

Strains and growth conditions

E. coli cells were grown at 30 or 37°C in Luria-Bertani (LB) medium supplemented with ampicillin (Ap, 200 µg/ml) or kanamycin (Km, 50 µg/ml) if appropriate. Strain KY1612 (Δ*rpoH*) was grown at 25°C in LB. For induction of the pBAD promoter in strains carrying translational *bgaB* fusions, 0.01% (w/v) L-arabinose was added. *Salmonella enterica* serovar Typhimurium M556 was grown in LB medium at 37°C.

Plasmid construction

Recombinant DNA work was performed according to standard protocols (Sambrook *et al*., 1989). PCR-generated fragments were inserted into pUC18 or pK18 digested with *Sma*I to generate plasmids pBO433 and 471 (Table 1). Site-directed mutagenesis to generate pBO653 to 657 was performed according to the instruction manual of the QuikChange mutagenesis kit (Stratagene, La Jolla, USA). Plasmid pBO471 served as template for PCR with mutagenic primers (Table 1). The inserts containing the mutated *agsA* fragment were isolated upon *Nhe*I/*Eco*RI digestion and cloned into the corresponding site upstream of *bgaB* in pBAD-*bgaB*. To construct pBO627 primers miniAgsAfw and miniAgsArv were annealed and cloned into the *Nhe*I/*Eco*RI site of pBAD-*bgaB*. The *agsA* promoter-fusion (pBO626) was constructed by inserting a PCR generated fragment cut with *Eco*RI and *Bam*HI into the corresponding site in pGF-*bgaB* (Stoss *et al*., 1997). The correct nucleotide sequence was confirmed by automated sequencing.

RNA isolation and primer extension

Salmonella cells were grown at 30°C to exponential growth phase before 10 ml where transferred to pre-warmed flasks at 45°C for 5 minutes. Isolation of total RNA using hot phenol was performed as described previously (Waldminghaus *et al*., 2005).
Primer extension was carried out as described previously (Babst *et al*., 1996). Primers STagsAPErv and STagsAPErv2 were used to map the transcription start site of *agsA*.

β-Galactosidase assays

E. coli cells carrying *bgaB* fusions were grown in 25 ml cultures at 25 or 30°C to exponential growth phase before samples of 10 ml where transferred to pre-warmed flasks at 40 or 42°C. After the indicated time periods, β-galactosidase activity was measured according to standard protocols (Miller, 1972) except that enzyme activity was measured at 55°C.

In vitro transcription and structure probing experiments

RNAs were synthesized *in vitro* by runoff transcription with T7 RNA polymerase from PCR-generated DNA templates and 5'-end labelled as described (Brantl and Wagner, 1994). Partial digestions of 5'-end-labelled RNAs with ribonucleases T1, T2, V1 and nuclease S1 were carried out as follows. RNA corresponding to 30,000 cpm was mixed with 1 µl 5x TMN buffer (100 mM tris acetate, pH 7.5 ; 10 mM $MgCl_2$; 500 mM NaCl) and 0.4 µg tRNA, and distilled water was added to a volume of 4 µl. Samples were pre-incubated for 5 minutes at the indicated temperature before 1 µl of different concentrations of nucleases were added. After 5 minutes of cleavage, 5 µl formamide loading dye were added, samples were denatured for 5 minutes at 95°C and aliquots were separated on a denaturing 8 or 15% polyacrylamide gel. Alkaline ladders were generated as described (Brantl and Wagner, 1994). The Aida Image Analyzer v. 4.03 software was used for densitometric quantification. Band intensity for T1 and T2 cleavage were normalized to nucleotides 40 and 39 located in the loop region. Mean values of 4 independent experiments were calculated and the ratio of band intensities at 45°C *versus* 30°C was plotted for each cleaved base position.

Toeprinting analysis

Toeprinting experiments were carried out using 30S ribosomal subunits, target mRNA and $tRNA^{fMet}$ basically according to Hartz *et al.* (1988). The 5'-[^{32}P]-labelled *agsA*-specific oligonucleotide STagsAPErv complementary to nucleotides +58 to +36 of the *agsA* mRNA was used as a primer for cDNA synthesis. An aliquot of 0.04 pmol of *agsA* mRNA annealed to the oligonucleotide was incubated at 30°C and 45°C for 10, 20 and 30 min without or with 0.4 pmol of 30S subunits and 8 pmol of uncharged $tRNA^{fMet}$ (Sigma-Aldrich Co., St. Louis, Missouri) before addition of 1µl M-MuLV-RT (80 units; Fermentas, Burlington, Canada). cDNA synthesis was performed at 37°C. Reactions were stopped after 10 minutes by adding formamide loading dye.

Acknowledgements

We are grateful to Wolf-Diedrich Hardt (Zürich) and Wolfgang Schumann (Bayreuth) for *Salmonella enterica* serovar Typhimurium M556 and vector pGF-bgaB, respectively. We thank Lena Gaubig (Bochum) for construction of the *gyrA-bgaB* fusion and Ursula Aschke-Sonnenborn (Bochum) for excellent technical assistance. Purified samples of 30S ribosomes were kindly provided by Isabella Moll (Vienna). This work was funded by grants from the German Research Foundation (DFG NA240/4 to FN and DFG BR1552/6 to SB).

References

Altuvia, S., Kornitzer, D., Teff, D., and Oppenheim, A.B. (1989) Alternative mRNA structures of the *cIII* gene of bacteriophage lambda determine the rate of its translation initiation. *J Mol Biol* **210**: 265-280.

Babst, M., Hennecke, H., and Fischer, H.M. (1996) Two different mechanisms are involved in the heat-shock regulation of chaperonin gene expression in *Bradyrhizobium japonicum*. *Mol Microbiol* **19**: 827-839.

Balsiger, S., Ragaz, C., Baron, C., and Narberhaus, F. (2004) Replicon-specific regulation of small heat shock genes in *Agrobacterium tumefaciens*. *J Bacteriol* **186**: 6824-6829.

Brantl, S., and Wagner, E.G. (1994) Antisense RNA-mediated transcriptional attenuation occurs faster than stable antisense/target RNA pairing: an in vitro study of plasmid pIP501. *EMBO J* **13**: 3599-3607.

Chowdhury, S., Ragaz, C., Kreuger, E., and Narberhaus, F. (2003) Temperature-controlled structural alterations of an RNA thermometer. *J Biol Chem* **278**: 47915-47921.

Chowdhury, S., Maris, C., Allain, F.H., and Narberhaus, F. (2006) Molecular basis for temperature sensing by an RNA thermometer. *EMBO J* **25**: 2487-2497.

Cromie, M.J., Shi, Y., Latifi, T., and Groisman, E.A. (2006) An RNA sensor for intracellular Mg^{2+}. *Cell* **125**: 71-84.

de Smit, M.H., and van Duin, J. (1990) Secondary structure of the ribosome binding site determines translational efficiency: a quantitative analysis. *Proc Natl Acad Sci U S A* **87**: 7668-7672.

de Smit, M.H., and van Duin, J. (1994) Control of translation by mRNA secondary structure in *Escherichia coli*. A quantitative analysis of literature data. *J Mol Biol* **244**: 144-150.

Dowd, S.E., and Ishizaki, H. (2006) Microarray based comparison of two *Escherichia coli* O157:H7 lineages. *BMC Microbiol* **6**: 30.

El-Samad, H., Kurata, H., Doyle, J.C., Gross, C.A., and Khammash, M. (2005) Surviving heat shock: control strategies for robustness and performance. *Proc Natl Acad Sci U S A* **102**: 2736-2741.

Epshtein, V., Mironov, A.S., and Nudler, E. (2003) The riboswitch-mediated control of sulfur metabolism in bacteria. *Proc Natl Acad Sci U S A* **100**: 5052-5056.

Gophna, U., and Ron, E.Z. (2003) Virulence and the heat shock response. *Int J Med Microbiol* **292**: 453-461.

Goulhen, F., Grenier, D., and Mayrand, D. (2003) Oral microbial heat-shock proteins and their potential contributions to infections. *Crit Rev Oral Biol Med* **14**: 399-412.

Gross, C.A. (1996) Function and regulation of heat shock proteins. In *Escherichia coli and Salmonella: Cellular and Molecular Biology*. Neidhardt, F.C. (ed). Washington, DC: ASM Press, pp. 1382-1399.

Hapfelmeier, S., Stecher, B., Barthel, M., Kremer, M., Muller, A.J., Heikenwalder, M., Stallmach, T., Hensel, M., Pfeffer, K., Akira, S., and Hardt, W.D. (2005) The *Salmonella* pathogenicity island (SPI)-2 and SPI-1 type III secretion systems allow *Salmonella*

serovar Typhimurium to trigger colitis via MyD88-dependent and MyD88-independent mechanisms. *J Immunol* **174**: 1675-1685.

Hartz, D., McPheeters, D.S., Traut, R., and Gold, L. (1988) Extension inhibition analysis of translation initiation complexes. *Methods Enzymol* **164**: 419-425.

Hengge-Aronis, R. (2002) Signal transduction and regulatory mechanisms involved in control of the s^S (RpoS) subunit of RNA polymerase. *Microbiol Mol Biol Rev* **66**: 373-395.

Hirata, H., Negoro, S., and Okada, H. (1984) Molecular basis of isozyme formation of beta-galactosidases in *Bacillus stearothermophilus*: isolation of two beta-galactosidase genes, *bgaA* and *bgaB*. *J Bacteriol* **160**: 9-14.

Hoe, N.P., and Goguen, J.D. (1993) Temperature sensing in *Yersinia pestis*: translation of the LcrF activator protein is thermally regulated. *J Bacteriol* **175**: 7901-7909.

Hurme, R., and Rhen, M. (1998) Temperature sensing in bacterial gene regulation-what it all boils down to. *Mol Microbiol* **30**: 1-6.

Johansson, J., Mandin, P., Renzoni, A., Chiaruttini, C., Springer, M., and Cossart, P. (2002) An RNA thermosensor controls expression of virulence genes in *Listeria monocytogenes*. *Cell* **110**: 551-561.

Johansson, J., and Cossart, P. (2003) RNA-mediated control of virulence gene expression in bacterial pathogens. *Trends Microbiol* **11**: 280-285.

Mandal, M., Boese, B., Barrick, J.E., Winkler, W.C., and Breaker, R.R. (2003) Riboswitches control fundamental biochemical pathways in *Bacillus subtilis* and other bacteria. *Cell* **113**: 577-586.

Mandal, M., and Breaker, R.R. (2004a) Gene regulation by riboswitches. *Nat Rev Mol Cell Biol* **5**: 451-463.

Mandal, M., and Breaker, R.R. (2004b) Adenine riboswitches and gene activation by disruption of a transcription terminator. *Nat Struct Mol Biol* **11**: 29-35.

Miller, J.H. (1972) *Experiments in molecular genetics.* New York: Cold Spring Harbor.

Morita, M., Kanemori, M., Yanagi, H., and Yura, T. (1999a) Heat-induced synthesis of s^{32} in *Escherichia coli*: structural and functional dissection of *rpoH* mRNA secondary structure. *J Bacteriol* **181**: 401-410.

Morita, M.T., Tanaka, Y., Kodama, T.S., Kyogoku, Y., Yanagi, H., and Yura, T. (1999b) Translational induction of heat shock transcription factor s^{32}: evidence for a built-in RNA thermosensor. *Genes Dev* **13**: 655-665.

Muffler, A., Fischer, D., and Hengge-Aronis, R. (1996) The RNA-binding protein HF-I, known as a host factor for phage Qbeta RNA replication, is essential for *rpoS* translation in *Escherichia coli*. *Genes Dev* **10**: 1143-1151.

Nahvi, A., Barrick, J.E., and Breaker, R.R. (2004) Coenzyme B12 riboswitches are widespread genetic control elements in prokaryotes. *Nucleic Acids Res* **32**: 143-150.

Nakahigashi, K., Yanagi, H., and Yura, T. (1995) Isolation and sequence analysis of *rpoH* genes encoding s^{32} homologs from gram negative bacteria: conserved mRNA and protein segments for heat shock regulation. *Nucleic Acids Res* **23**: 4383-4390.

Narberhaus, F., Käser, R., Nocker, A., and Hennecke, H. (1998) A novel DNA element that controls bacterial heat shock gene expression. *Mol Microbiol* **28**: 315-323.

Narberhaus, F. (1999) Negative regulation of bacterial heat shock genes. *Mol Microbiol* **31**: 1-8.

Narberhaus, F. (2002) a-crystallin-type heat shock proteins: socializing minichaperones in the context of a multichaperone network. *Microbiol Mol Biol Rev* **66**: 64-93.

Narberhaus, F., Waldminghaus, T., and Chowdhury, S. (2006) RNA thermometers. *FEMS Microbiol Rev* **30**: 3-16.

Nocker, A., Hausherr, T., Balsiger, S., Krstulovic, N.P., Hennecke, H., and Narberhaus, F. (2001) A mRNA-based thermosensor controls expression of rhizobial heat shock genes. *Nucleic Acids Res* **29**: 4800-4807.

Norrander, J., Kempe, T., and Messing, J. (1983) Construction of improved M13 vectors using oligodeoxynucleotide-directed mutagenesis. *Gene* **26**: 101-106.

Nudler, E., and Mironov, A.S. (2004) The riboswitch control of bacterial metabolism. *Trends Biochem Sci* **29**: 11-17.

Permina, E.A., and Gelfand, M.S. (2003) Heat shock (s^{32} and HrcA/CIRCE) regulons in beta-, gamma- and epsilon-proteobacteria. *J Mol Microbiol Biotechnol* **6**: 174-181.

Peters, J.E., Thate, T.E., and Craig, N.L. (2003) Definition of the *Escherichia coli* MC4100 genome by use of a DNA array. *J Bacteriol* **185**: 2017-2021.

Pridmore, R.D. (1987) New and versatile cloning vectors with kanamycin-resistance marker. *Gene* **56**: 309-312.

Sambrook, J.E., Fritsch, F., and Maniatis, T. (1989) *Molecular cloning: a laboratory manual.* New York: Cold Spring Harbor.

Schumacher, M.A., Pearson, R.F., Moller, T., Valentin-Hansen, P., and Brennan, R.G. (2002) Structures of the pleiotropic translational regulator Hfq and an Hfq-RNA complex: a bacterial Sm-like protein. *EMBO J* **21**: 3546-3556.

Stoss, O., Mogk, A., and Schumann, W. (1997) Integrative vector for constructing single-copy translational fusions between regulatory regions of *Bacillus subtilis* and the *bgaB* reporter gene encoding a heat-stable beta-galactosidase. *FEMS Microbiol Lett* **150**: 49-54.

Sudarsan, N., Barrick, J.E., and Breaker, R.R. (2003a) Metabolite-binding RNA domains are present in the genes of eukaryotes. *RNA* **9**: 644-647.

Sudarsan, N., Wickiser, J.K., Nakamura, S., Ebert, M.S., and Breaker, R.R. (2003b) An mRNA structure in bacteria that controls gene expression by binding lysine. *Genes Dev* **17**: 2688-2697.

Takaya, A., Tomoyasu, T., Tokumitsu, A., Morioka, M., and Yamamoto, T. (2002) The ATP-dependent Lon protease of *Salmonella enterica* serovar Typhimurium regulates invasion and expression of genes carried on *Salmonella* pathogenicity island 1. *J Bacteriol* **184**: 224-232.

Takaya, A., Suzuki, M., Matsui, H., Tomoyasu, T., Sashinami, H., Nakane, A., and Yamamoto, T. (2003) Lon, a stress-induced ATP-dependent protease, is critically important for

systemic *Salmonella enterica* serovar Typhimurium infection of mice. *Infect Immun* **71**: 690-696.

Thore, S., Leibundgut, M., and Ban, N. (2006) Structure of the eukaryotic thiamine pyrophosphate riboswitch with its regulatory ligand. *Science* **312**: 1208-1211.

Tomoyasu, T., Takaya, A., Sasaki, T., Nagase, T., Kikuno, R., Morioka, M., and Yamamoto, T. (2003) A new heat shock gene, AgsA, which encodes a small chaperone involved in suppressing protein aggregation in *Salmonella enterica* serovar Typhimurium. *J Bacteriol* **185**: 6331-6339.

Tomoyasu, T., Takaya, A., Handa, Y., Karata, K., and Yamamoto, T. (2005) ClpXP controls the expression of LEE genes in enterohaemorrhagic *Escherichia coli*. *FEMS Microbiol Lett* **253**: 59-66.

Valentin-Hansen, P., Eriksen, M., and Udesen, C. (2004) The bacterial Sm-like protein Hfq: a key player in RNA transactions. *Mol Microbiol* **51**: 1525-1533.

Vitreschak, A.G., Rodionov, D.A., Mironov, A.A., and Gelfand, M.S. (2004) Riboswitches: the oldest mechanism for the regulation of gene expression? *Trends Genet* **20**: 44-50.

Wade, J.T., Roa, D.C., Grainger, D.C., Hurd, D., Busby, S.J., Struhl, K., and Nudler, E. (2006) Extensive functional overlap between s factors in *Escherichia coli*. *Nat Struct Mol Biol* **13**: 806-814.

Waldminghaus, T., Fippinger, A., Alfsmann, J., and Narberhaus, F. (2005) RNA thermometers are common in a- and g-proteobacteria. *Biol Chem* **386**: 1279-1286.

Winkler, W.C., Cohen-Chalamish, S., and Breaker, R.R. (2002) An mRNA structure that controls gene expression by binding FMN. *Proc Natl Acad Sci U S A* **99**: 15908-15913.

Winkler, W.C., Nahvi, A., Roth, A., Collins, J.A., and Breaker, R.R. (2004) Control of gene expression by a natural metabolite-responsive ribozyme. *Nature* **428**: 281-286.

Winkler, W.C. (2005) Metabolic monitoring by bacterial mRNAs. *Arch Microbiol* **183**: 151-159.

Winkler, W.C., and Breaker, R.R. (2005) Regulation of bacterial gene expression by riboswitches. *Annu Rev Microbiol* **59**: 487-517.

Yura, T., Kanemori, M., and Morita, M. (2000) The heat shock response: regulation and function. In *Bacterial Stress Responses*. Hengge-Aronis, G.S.a.R. (ed). Washington, D.C.: ASM Press, pp. 3-18.

Zhang, A., Wassarman, K.M., Ortega, J., Steven, A.C., and Storz, G. (2002) The Sm-like Hfq protein increases OxyS RNA interaction with target mRNAs. *Mol Cell* **9**: 11-22.

Zhou, Y.N., Kusukawa, N., Erickson, J.W., Gross, C.A., and Yura, T. (1988) Isolation and characterization of *Escherichia coli* mutants that lack the heat shock sigma factor s^{32}. *J Bacteriol* **170**: 3640-3649.

Zuker, M. (2003) Mfold web server for nucleic acid folding and hybridization prediction. *Nucleic Acids Res* **31**: 3406-3415.

Figure legends

Figure 1 Secondary structure prediction of the 5'-UTR of the Salmonella *agsA* gene. The mfold program (version 3.2; (Zuker, 2003) was used to predict the RNA structure. Nucleotides are numbered starting from the mapped transcription start site (+1). The Shine-Dalgarno sequence (SD) and start codon (START) are labelled. Hairpins I and II and the point mutations introduced in this study are indicated.

Figure 2 Mapping of the 5' end of the *agsA* mRNA. Primer extension experiments were carried out with total RNA from *S. enterica* cells grown at 30°C or from cells that were shifted from 30 to 45°C for 8 min. Primer STagsAPErv was used for reverse transcription. A corresponding sequencing reaction (ACGT) with plasmid pBO433 carrying the *agsA* region is shown. The 5' end of the mRNA (+1) is marked by an arrow and the deduced –10 and –35 regions of a σ^{32}-type promoters are underlined in the sequence to the right.

Figure 3 Transcriptional regulation of *agsA* by σ^{32} (RpoH). (A) Schematic representation of the reporter gene fusion on plasmid pBO626. (B) Temperature-dependent expression of the *agsA-bgaB* fusion in *E. coli* MC4100 (*wt)* and the Δ*rpoH* strain KY1612. Cells were grown in LB medium at 25°C and heat-shocked to 40°C for 30, 60 and 90 minutes before β-galactosidase activities were measured. Results shown are the average of three independent measurements with the indicated standard deviations.

Figure 4 Translational control of *agsA* by an RNA thermometer. (A) Schematic representation of the reporter gene fusion used to measure translational control. (B) Expression of *bgaB* fusions to the full length 5'-UTR (*agsA*), only hairpin II (mini-agsA) and the 5'-UTR of *gyrA* from *E. coli*. (C) Expression of *bgaB* fusions to point-mutated variants of the RNA thermometer. Temperature-dependent expression was monitored in *E. coli* DH5α. Cells were grown in LB medium at 30°C and heat-shocked to 42°C for 30 minutes before β-galactosidase activity was measured. Results shown are the average of three independent measurements with the indicated standard deviations.

Figure 5 Temperature-dependent conformations of the RNA thermometer upstream of *agsA*. Enzymatic cleavage of 5'-end-labelled *agsA* RNA was carried out at 30 or 45°C. The RNA fragments were separated on (A) 15% polyacrylamide or (B) 8% polyacrylamide gels. RNase T1 (0.1 and 0.01U), RNase T2 (0.04 and 0.02U) and RNase V1 (0.01 and 0.002 U) were used. Note that V1 creates 3'-hydroxyl ends so that the corresponding bands migrate somewhat slower than products derived from T1, T2 or alkaline hydrolysis. Lane C indicates the incubation control with water instead of RNase. Lane L: alkaline ladder. Selected nucleotides are marked with arrowheads. The SD and anti-SD sequences are labelled. (C) Quantification of temperature-dependent structural differences of the *agsA* thermometer. The results of four independent experiments with RNase T1 and T2 at 30 and 45°C were quantified and

normalized to nucleotides 40 and 39 in loop II. Relative cleavage was calculated by division of the 45°C values by the 30°C values. Grey columns relate to nucleotides in the 5'-part of hairpin II, black columns to the 3'-part and white to the loop of hairpin II. Selected nucleotides are labelled. (D) Secondary structure model of *agsA* RNA and summary of the probing results at 30°C. Cleavage sites by RNases T1, T2 and V1 are shown by arrows as indicated. Dotted arrow lines represent moderate cleavage, full lines strong cleavage. Increased cleavage by T1 and T2 at high temperature occurred at the circled nucleotides (more than 1.8-fold induction from 30 to 45°C).

Figure 6 Comparative RNA structure analysis of the *wt* and stabilized 5'-UTRs of *agsA*. Enzymatic hydrolysis of 5'-end-labelled RNA of the *wt* and U32C and C29A variants was carried out at 45°C and fragments were separated on an 8% polyacrylamide gel. RNase T1 (0.01 U), nuclease S1 (1 U) and RNase V1 (0.02 U) were used. Note that V1 and S1 create 3'-hydroxyl ends so that the corresponding bands migrate somewhat slower than products derived from T1 or alkaline hydrolysis. Lane C: incubation control with water instead of RNase. Lane L: alkaline ladder. Selected nucleotide positions are marked with arrowheads. The Shine-Dalgarno and the anti-Shine-Dalgarno sequences are labelled.

Figure 7 Ribosome binding to the *agsA* 5'-UTR. Formation of a ternary complex on *agsA* mRNA at high temperature was shown by a primer extension inhibition assay (for details, see Materials and Methods, and Results). Addition of 30S ribosomal subunits and initiator tRNA at 30°C (Lanes 1-5) and 45°C (Lanes 6-7) is indicated above the gel. The corresponding DNA sequencing reactions (CTGA) were carried out with the same end-labelled oligonucleotide as in the toeprint experiments. The toeprint signal is located at position + 17 relative to the A of the translation start codon.

Figure 8 Secondary structure models of confirmed and predicted fourU thermometers. The mfold program (version 3.2; (Zuker, 2003) was used to predict the RNA structures of sequences upstream of the AUG start codon of the indicated heat shock or virulence genes. The typical "fourU" sequence in the anti-SD region is marked.

TABLE 1 Strains, plasmids and oligonucleotides used in this study

Strain, plasmid, or oligonucleotide	Relevant characteristic(s) or sequence[a]	Source or reference
Strains		
Escherichia coli DH5α	*supE44 ΔlacU169*(Φ80*lacZ*ΔM15) *hsdR17 recA1 gyrA96*	Gibco-BRL
Escherichia coli MC4100	F- *araD139* Δ(*argF-lac*)*U169 rspL150 relA1 flbB5301 fruA25 deoC1 ptsF25 e14-*	Peters *et al*., 2003
Escherichia coli KY1612	MC4100 Δ*rpoH*30::kan *zhf 50*::Tn10 (λ*imm*21pF13	Zhou *et al*., 1988
Salmonella enterica servovar Typhimurium M556	*sseD::aphT*	Hapfelmeier *et al*., 2005
Plasmids		
pUC18	Cloning vector, Ap^r	Norrander *et al*., 1983
pK18	Cloning vector, Km^r	Pridmore, 1987
pGF-bgaB	Translational *bgaB* fusion vector, Ap^r	Stoss *et al*., 1997
pBAD-bgaB	Translational *bgaB* fusion vector with pBAD-promoter and *araC*, Ap^r	Waldminghaus, unpublished
pBO433	*S. enterica agsA* upstream region in pk18	This study
pBO471	*S. enterica agsA* 5'-UTR in puc18	This study
pBO472	*S. enterica agsA-bgaB* fusion in pBAD-bgaB with full 5'-UTR	This study
pBO626	*S. enterica agsA*-promoter fusion to *bgaB*	This study
pBO627	*S. enterica agsA*-bgaB fusion in pBAD-bgaB with 36 bp upstream of AUG start	This study
pBO653	*S. enterica agsA*-T32C-bgaB fusion in pBAD-bgaB	This study
pBO654	*S. enterica agsA*-A29C-bgaB fusion in pBAD-bgaB	This study
pBO655	*S. enterica agsA*-CTT30-32AAA-bgaB fusion in pBAD-bgaB	This study
pBO656	*S. enterica agsA*-T33C-bgaB fusion in pBAD-bgaB	This study
pBO657	*S. enterica agsA*-G21C-bgaB fusion in pBAD-bgaB	This study
pBO496	*E. coli gyrA-bgaB* fusion in pBAD-bgaB	Gaubig, unpublished
Oligonucleotides		
STagsAPEfw	GAAAAATTGTAAAGATGAAGGGACA (PE of *S. enterica agsA*)	
STagsAPErv	GGTCAGAGAAAAGAGAATCAGCA (PE of *S. enterica agsA*)	
STagsAPErv2	CTGACAAGGTTCTGAGTGCCAT (PE of *S. enterica agsA*)	
STagsAutrfw	GCTAGCGGACAAGCAATGCTTGCCTTG (construction of pBO471)	
STagsAutrrv	CTAGAATTCTGCCATCATTAACCTCCTGAA (construction of pBO471 and pBO626)	
agsABamfw	TGGATCCGGCTTTTATAGACTTGAAAATGT (construction of pBO626)	
minAgsAfw	CTAGCTGTTGAACTTTTGAATAGTGATTCAGGAGGTTAATGATGGCAG (construction of pBO627)	
minAgsArv	AATTCTGCCATCATTAACCTCCTGAATCACTATTCAAAAGTTCAACAG (construction of pBO627)	
agsAG21Cfw	GACAAGCAATGCTTGCCTTCATGTTGAACTTTTG (construction of pBO657)	
agsAG21Crv	CTATTCAAAAGTTCAACATGAAGGCAAGCATTGCTT (construction of pBO657)	
agsAA29Cfw	CTTGCCTTGATGTTGACCTTTTGAATAGTGATTC (construction of pBO654)	
agsAA29Crv	CCTGAATCACTATTCAAAAGGTCAACATCAAGGC (construction of pBO654)	
agsACTT30-32AAAfw	GCTTGCCTTGATGTTGAAAAATTGAATAGTGATTCAGG (construction of pBO655)	
agsACTT30-32AAArv	CCTCCTGAATCACTATTCAATTTTTCAACATCAAGGC (construction of pBO655)	
agsAT32Cfw	GCCTTGATGTTGAACTCTTGAATAGTGATTCAG (construction of pBO653)	
agsAT32Crv	CTCCTGAATCACTATTCAAGAGTTCAACATCAA (construction of pBO653)	
agsAT33Cfw	GCCTTGATGTTGAACTTCTGAATAGTGATTCAG (construction of pBO656)	
agsAT33Crv	CTCCTGAATCACTATTCAGAAGTTCAACATCAA (construction of pBO656)	

[a] Introduced restriction sites are underlined. PE, primer extension.

Figure 1

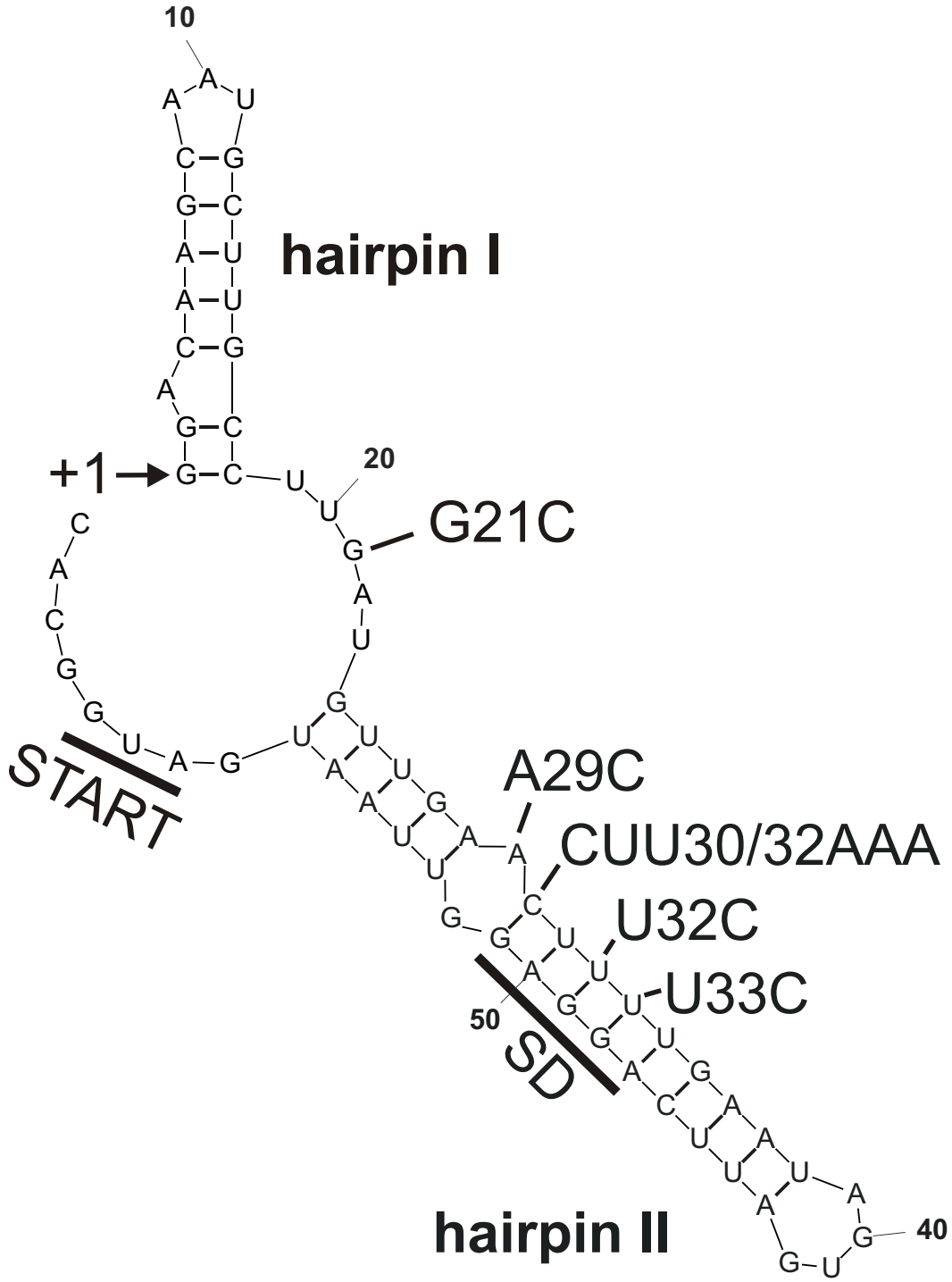
10
hairpin I
+1
20
G21C
START
A29C
CUU30/32AAA
U32C
U33C
50
SD
hairpin II
40

Figure 2

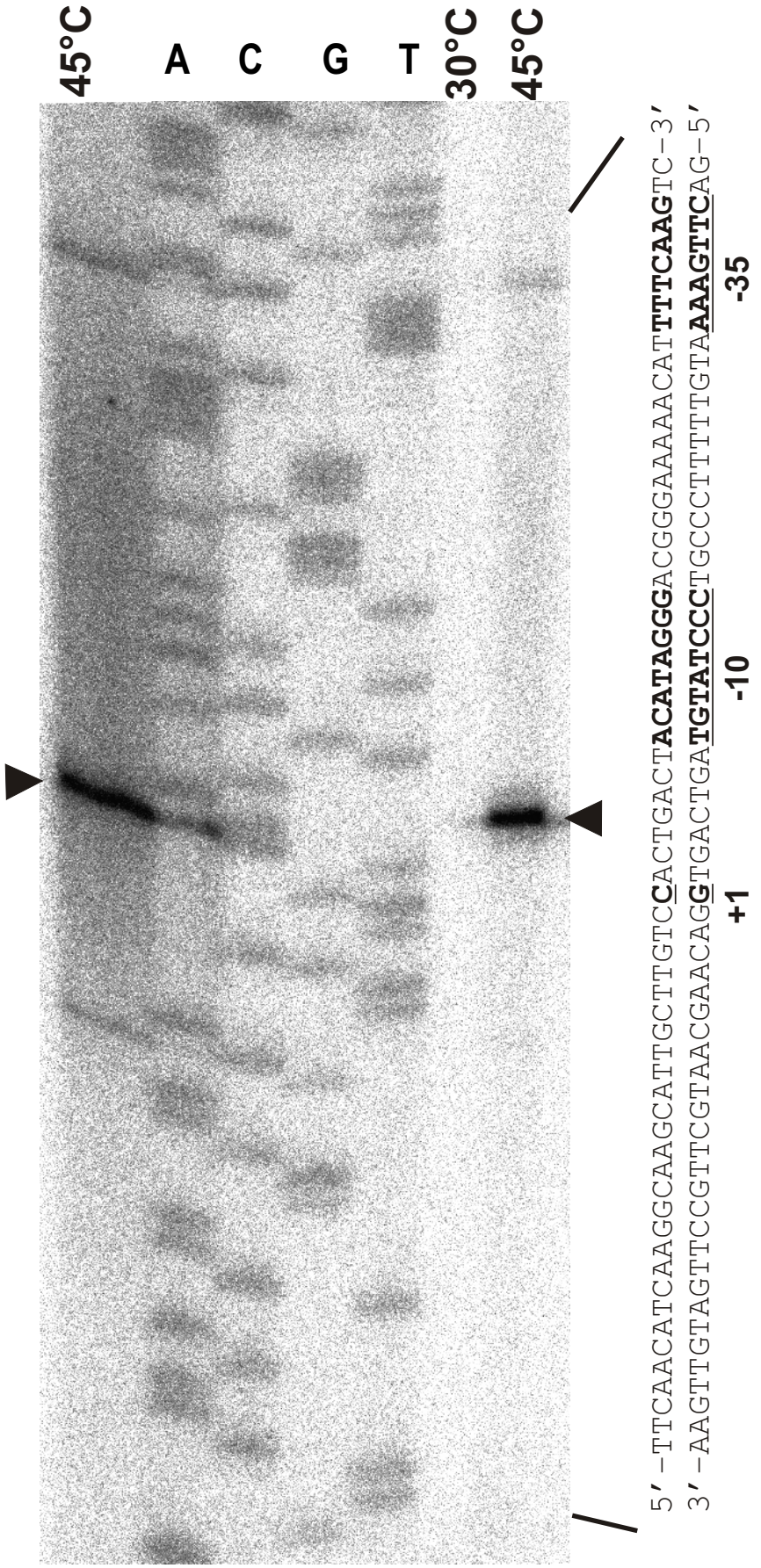
45°C
A
C
G
T
30°C
45°C
5′-TTCAACATCAAGGCAAGCATTGCTTGTCCACTGACTACATAGGGACGGGAAAAACATTTTCAAGTC-3′
3′-AAGTTGTAGTTCCGTTCGTAACGAACAGGTGACTGATGTATCCCTGCCCTTTTTGTAAAAGTTCAG-5′
+1
-10
-35

Figure 3

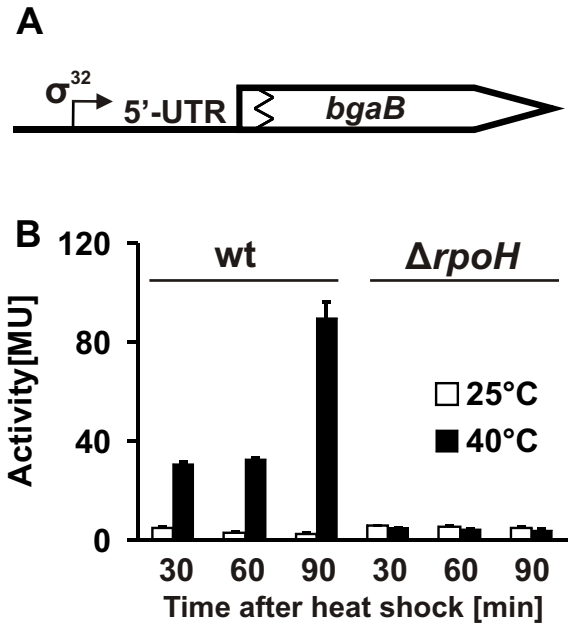
A
σ32
5'-UTR
bgaB
B
120
80
40
0
wt
ΔrpoH
25°C
40°C
Activity[MU]
30
60
90
30
60
90
Time after heat shock [min]

Figure 4

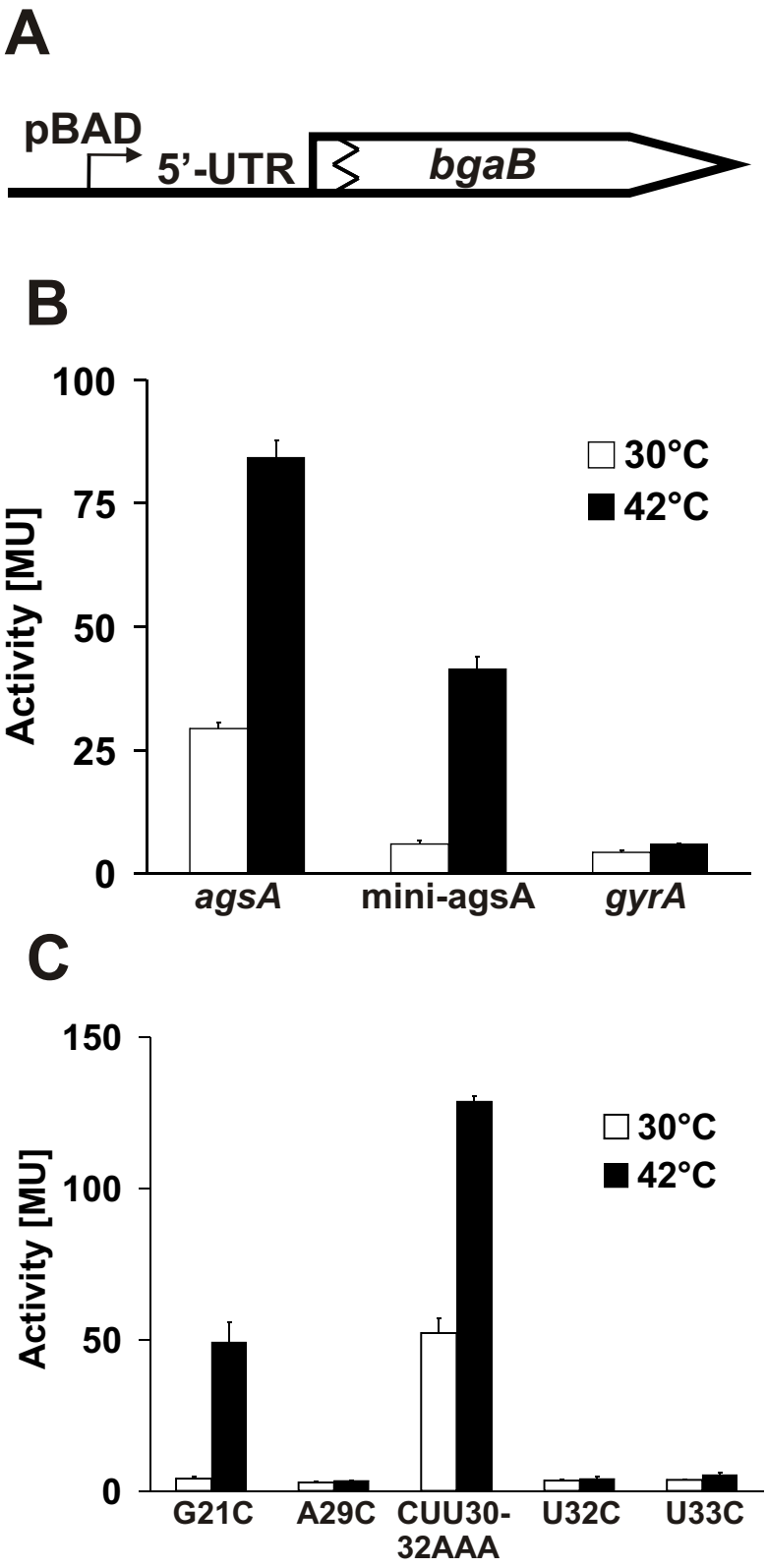
A
pBAD
5'-UTR
bgaB
B
100
75
50
25
0
Activity [MU]
30°C
42°C
agsA
mini-agsA
gyrA
C
150
100
50
0
Activity [MU]
30°C
42°C
G21C
A29C
CUU30-32AAA
U32C
U33C

Figure 5

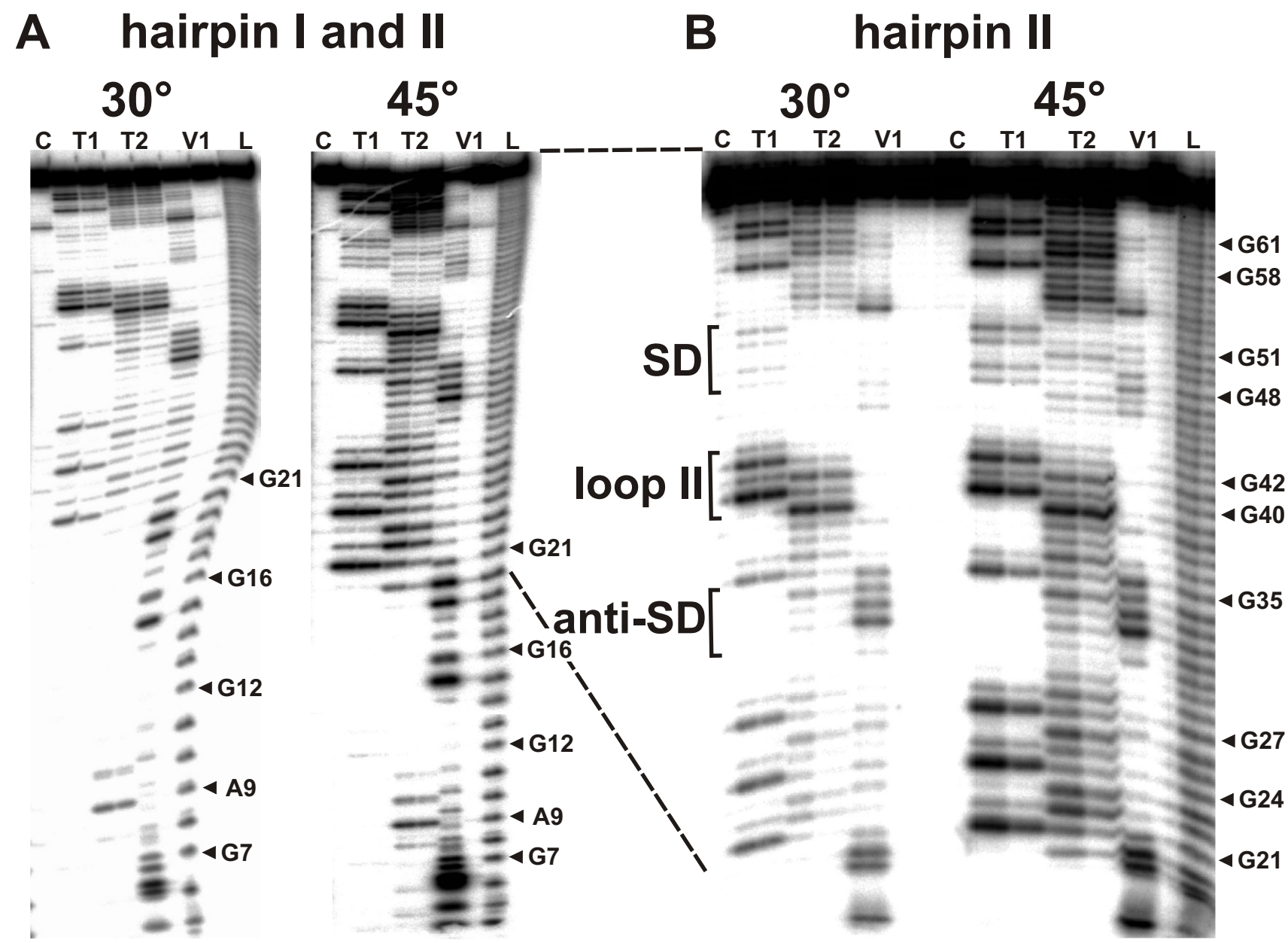
A
hairpin I and II
30°
45°
C T1 T2 V1 L
C T1 T2 V1 L
G21
G16
G12
A9
G7
G21
G16
G12
A9
G7
B
hairpin II
30°
45°
C T1 T2 V1 C T1 T2 V1 L
SD
loop II
anti-SD
G61
G58
G51
G48
G42
G40
G35
G27
G24
G21

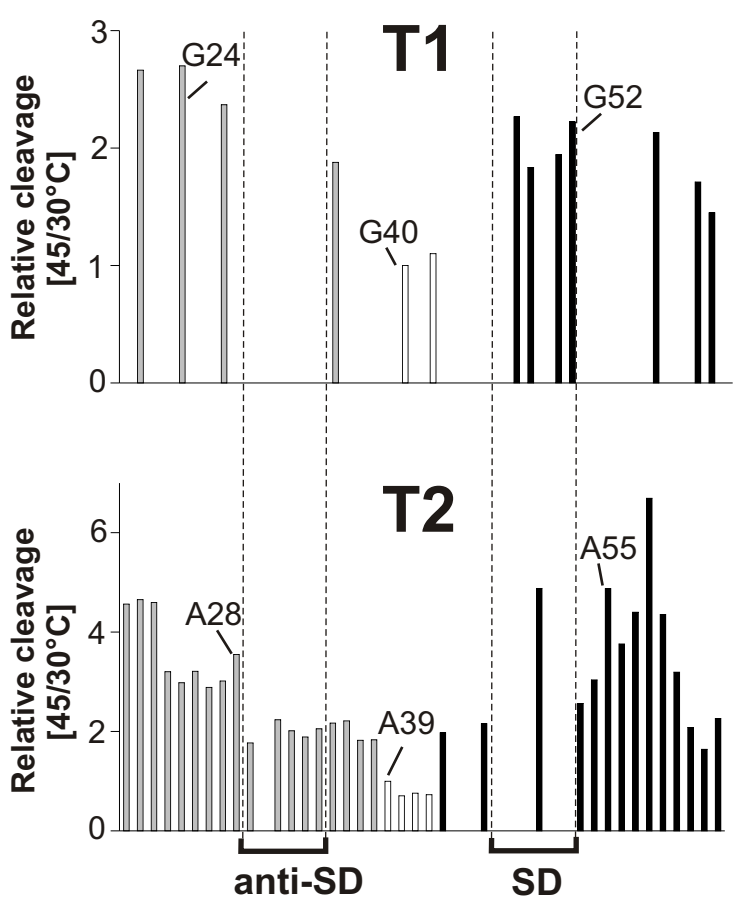
C
T1
Relative cleavage [45/30°C]
G24
G40
G52
T2
A28
A39
A55
anti-SD
SD

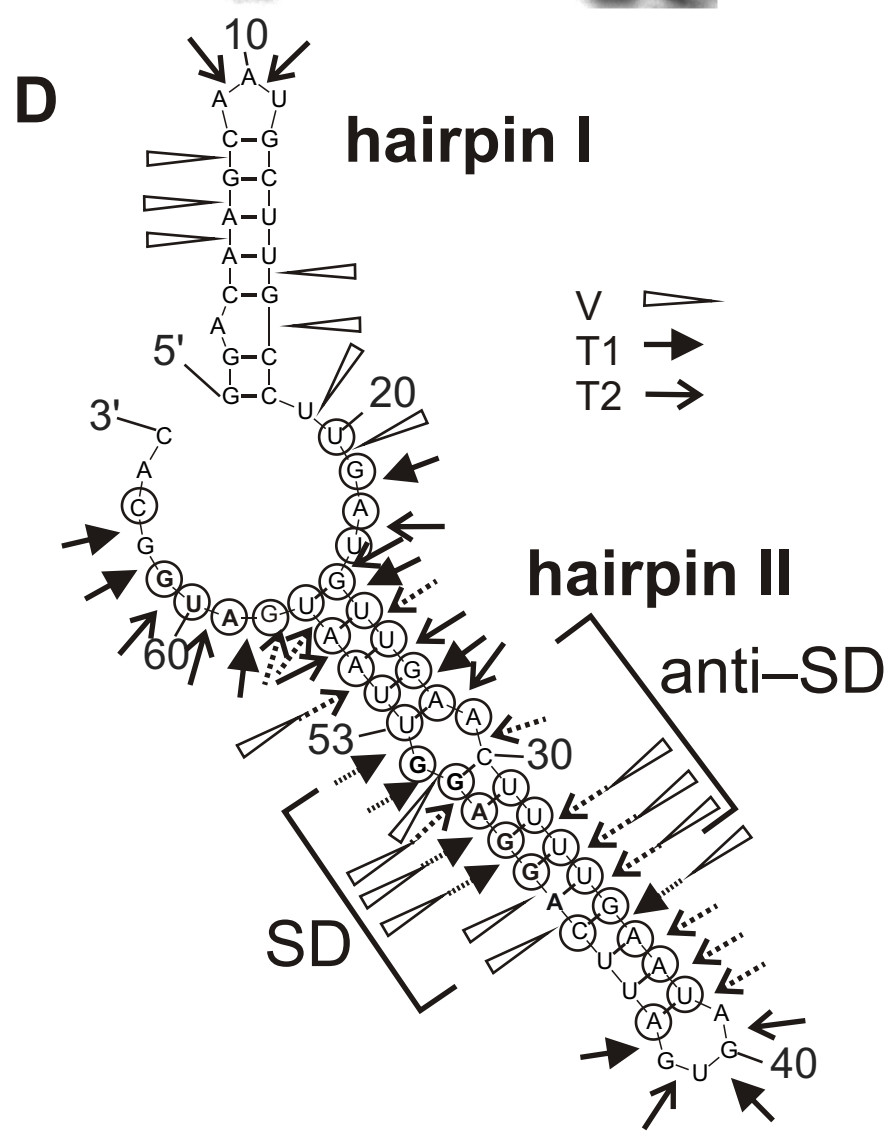
D
hairpin I
hairpin II
5'
3'
10
20
30
40
53
60
V
T1
T2
anti–SD
SD

Figure 6

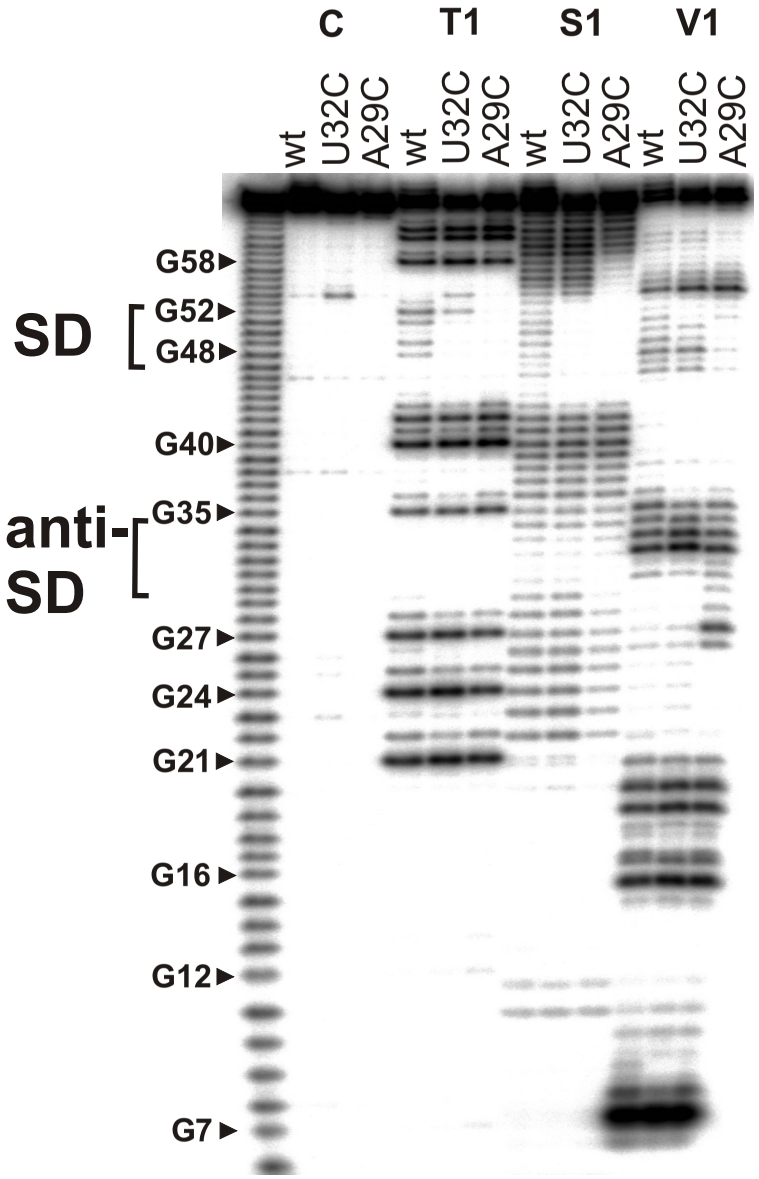
C
T1
S1
V1
wt
U32C
A29C
G58
G52
G48
G40
G35
G27
G24
G21
G16
G12
G7
SD
anti-SD

Figure 7

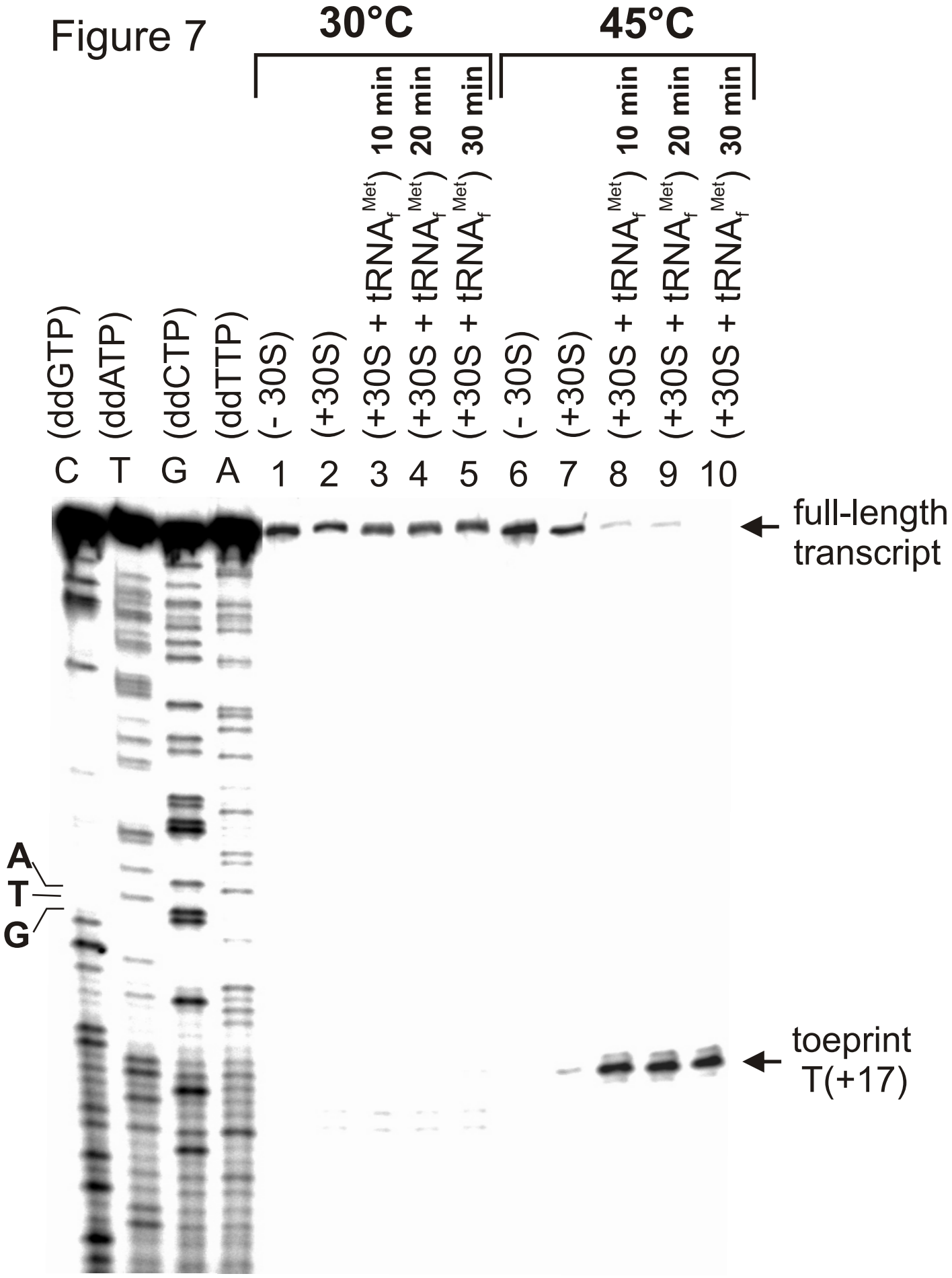
30°C
45°C
10 min
20 min
30 min
(+30S + tRNA$_f^{Met}$)
(- 30S)
(+30S)
(ddGTP)
(ddATP)
(ddCTP)
(ddTTP)
C T G A 1 2 3 4 5 6 7 8 9 10
full-length transcript
toeprint T(+17)
A
T
G

Figure 8

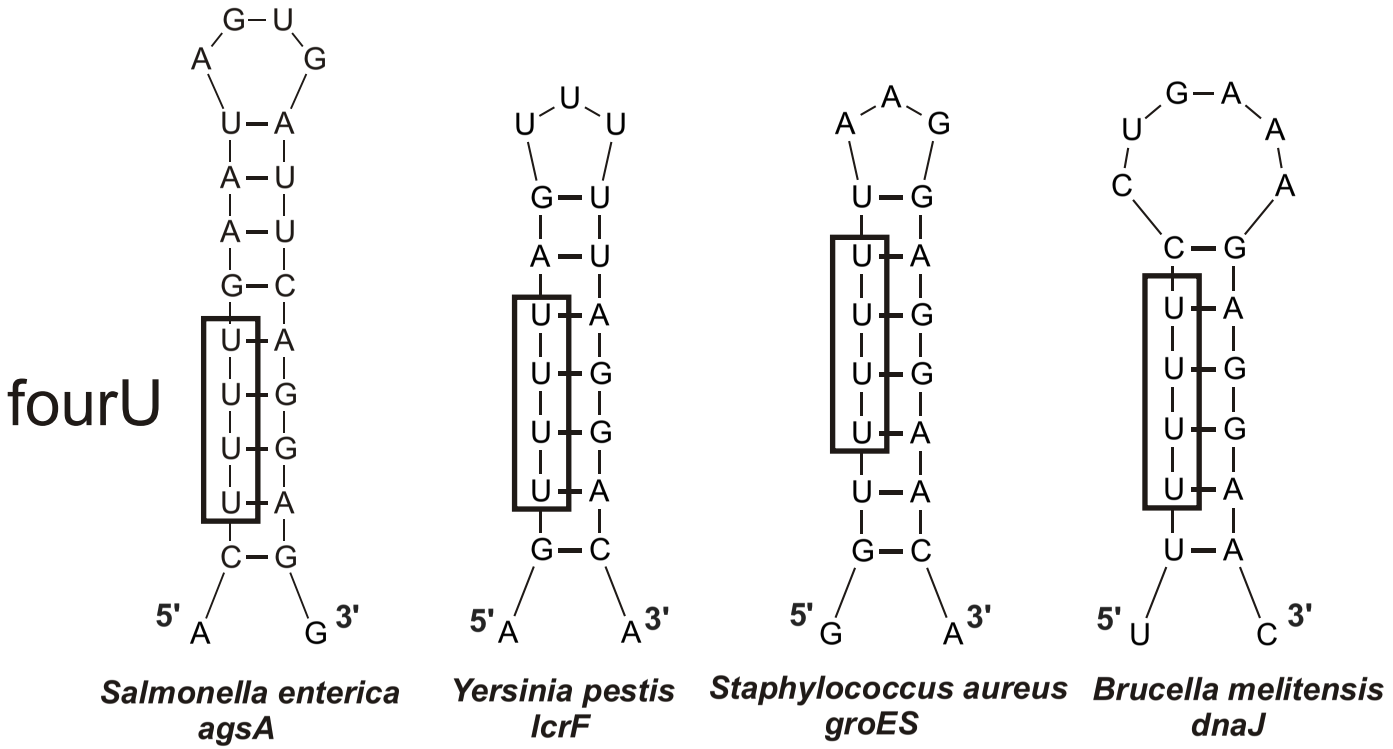
fourU
5' A G 3'
5' A A 3'
5' G A 3'
5' U C 3'
Salmonella enterica agsA
Yersinia pestis lcrF
Staphylococcus aureus groES
Brucella melitensis dnaJ

7. Gesamtdiskussion

7.1. RNAIII: *cis*-kodierte Antisense-RNA vom Streptokokken-plasmid pIP501

Die ersten regulatorischen Antisense-RNAs wurden 1981 bei bakteriellen Plasmiden entdeckt. Es handelt sich dabei um die *cis*-kodierten Antisense-RNAs RNAI (ColE1; Tomizawa *et al.,* 1981) und CopA (R1; Stougaard *et al.,* 1981), die über Interaktion mit ihren jeweiligen Target-RNAs die Plasmidreplikation regulieren. Mittlerweile ist eine Vielzahl *cis*-kodierter Antisense-RNAs in prokaryotischen Begleitelementen bekannt, und ihre biologischen Funktionen und biochemischen Eigenschaften sind zum Teil sehr gut charakterisiert (zusammengefasst in: Wagner *et al.,* 2002; Brantl, 2002, 2007). Dazu gehört auch RNAIII, die 1992 entdeckt wurde und über Transkriptions-attenuierung ihrer Target RNA (RNAII) die Replikation des Streptokokkenplasmides pIP501 reguliert (Brantl und Behnke 1992a; Brantl *et al,* 1993). Ihre Paarungs- und Inhibitionskonstanten sowie ihre intrazelluläre Konzentration und Halbwertszeit wurden bestimmt (Brantl und Wagner, 1994, 1996). Im Gegensatz dazu waren ihre sequenz- und strukturspezifischen Eigenschaften, die für eine effiziente Interaktion mit ihrer Target-RNA von großer Bedeutung sind, noch nicht bekannt. Bislang sind nur in wenigen plasmidkodierten Systemen gramnegativer Bakterien die Anforderungen an eine effiziente Interaktion zwischen Sense- und Antisense-RNA sowie der Bindungsweg beider Spezies untersucht worden. Detaillierte *in vitro*-Analysen zur Struktur des inhibitorischen Komplexes von RNAIII und RNAII des Streptokokkenplasmides pIP501, die im Rahmen dieser Arbeit durchgeführt wurden, liefern damit einen ersten Beitrag zu grampositiven Bakterien (Kapitel 3).

7.1.1. Sequenz- und strukturspezifische Anforderungen an die inhibitorisch wirksame RNAIII des Plasmides pIP501

In vorangehenden Untersuchungen zur inhibitorischen Wirkung von RNAIII wurde bereits herausgefunden, dass RNAIII zwei 5'-terminale kleine Stem-Loops L1 und L2, gefolgt von einer einzelsträngigen Region und zwei 3'-terminale Stem-Loops L3 und L4 aufweist (Brantl und Wagner, 1994) und dass die Stem-Loops L1 und L2 am 5' Ende von RNAIII keine Rolle für die Interaktion mit der Target-RNA (RNAII) spielen (s. Abb. 4), (Brantl *et al.,* 1993).

Um die strukturspezifischen Anforderungen an eine inhibitorisch wirksame RNAIII zu untersuchen, wurde zunächst eine detaillierte Sekundärstruktur von RNAIII mit Hilfe von chemischen Proben im Vergleich zu den bereits verwendeten enzymatischen Reaktionen ermittelt. Die ermittelten Größen der Loops L3 und L4 sowie der Spacer-

Region zwischen den Stem-Loops L3 und L4 und der 5’ gelegenen einzelsträngigen Region von RNAIII stimmen mit den Ergebnissen früherer Arbeiten überein (Manuskript I). Nachdem die Sekundärstruktur von RNAIII mittels chemischer Proben bestätigt werden konnte, wurde eine strukturelle Charakterisierung des Komplexes aus RNAIII und RNAII vorgenommen. Anhand der ermittelten Daten konnte gezeigt werden, dass für die inhibitorische Wirkung von RNAIII keine vollständige Duplex mit RNAII gebraucht wird, sondern ein Bindungsintermediat als vorläufige Struktur (erweiterter 'kissing’-Komplex, partielle Duplex) ausreicht (Manuskrip I). Diese Daten bestätigen die Ergebnisse früherer Versuche, die zeigten, dass im Replikationskontrollsystem von pIP501 die Inhibition 10 x schneller als die Duplexbildung erfolgt (Brantl und Wagner, 1994). Die Beobachtung, dass für die Hemmung der Sense-RNA die Ausbildung einer vollständigen Dulplex zwischen Sense- und Antisense-RNA nicht erforderlich ist, wurde in den vergangenen Jahren z. B. auch für das CopA/CopT-System zur Regulation der Replikation des *E. coli*-Plasmides R1 gemacht. CopA/CopT ist das bisher einzige Sense/Antisense-RNA-System, für das der Bindungsweg von Sense- und Antisense-RNA sowie die Struktur des inhibitorischen Komplexes detailliert aufgeklärt worden sind. Es konnte eindrucksvoll nachgewiesen werden, dass sich ausgehend von einem 'kissing’-Komplex (Persson *et al.,* 1988, 1990a, 1990b) über mehrere weitere Bindungsintermediate eine vollständige Duplex sehr langsam ausbildet, die aber nicht gebraucht wird, da der sogenannte 'hugging’-Komplex, bestehend aus zwei intramolekularen und drei intermolekularen Helices, als Bindungsintermediat für die Inhibition der Sense-RNA vollständig ausreicht (Malmgren *et al*., 1997; Kolb *et al*., 2000a, 2000b). Auch bei anderen Systemen wie dem Hok/Sok-System zur Regulation der Segregationsstabilität von R1 (Gerdes *et al.,* 1997) und dem RNAI/RNAII-System zur Regulation der Replikation des *E. coli*-Plasmides ColE1 (Tomizawa 1990a, 1990b) sind Bindungsintermediate als biologisch aktive Strukturen gefunden wurden.

Die Bildung eines 'kissing’-Komplexes zwischen einzelsträngigen Regionen der Antisense-RNA und ihrer Target-RNA als erstes Bindungsintermediat wird prinzipiell für eine erfolgreiche Interaktion beider RNA-Moleküle vorausgesetzt (Tomizawa, 1984, 1990a, 1990b). In den meisten Fällen erfolgt der initiale Kontakt zwischen einem Loop der Antisense-RNA, dem sogenannten 'recognition'-Loop, und dem entsprechenden Loop der Target-RNA (z. B. CopA/CopT). Allerdings können auch zwei Loops (z. B. bei RNAI/RNAII von Plasmid ColE1, Tomizawa *et al.,* 1990a) oder eine einzelsträngige Region und ein Loop (z.B. bei Hok/Sok von Plasmid R1, Gerdes *et al.,* 1997; RNA-IN/RNA-OUT von Transposon Tn10, Kittle *et al.,* 1989) an der initialen Interaktion zwischen Antisense- und Sense-RNA beteiligt sein. Die Ausbreitung des 'kissing’-

Komplexes in die anschließenden Stem-Regionen führt zur Ausbildung des nächsten Bindungsintermediates, dem ’extended-kissing’-Komplex.

Nachdem festgestellt wurde, dass der inhibitorische Komplex aus RNAII und RNAIII keine vollständige, sondern nur eine partielle Duplex ist, wurde untersucht, ob ein Loop-Loop-Kontakt ('kissing'-Komplex) zwischen RNAIII und RNAII als inhibitorischer Komplex ausreicht oder ob auch die Stems von L3 und L4 von RNAIII mit dem dazwischen liegendem Spacer an der Ausbildung eines inhibitorischen Komplexes ('extended-kissing'-Komplex) beteiligt sind. Dazu sollte der Einfluss von Mutationen im unteren Stem-Bereich von RNAIII-L3 und/oder -L4 und im Spacer zwischen den Stem-Loops L3 und L4 auf die Effizienz der Transkriptionstermination von RNAII getestet werden. Mit Hilfe eines *in vitro*-'single-round’-Transkriptionstests wurden die Inhibitionskonstanten der mutierten RNAIII-Spezies bestimmt und dabei analysiert, wie sich die Effizienz der Transkriptionstermination der einzelnen RNAIII-Spezies verändert. Anhand der *in vitro* bestimmten Inhibitionskonstanten konnte geschlussfolgert werden, dass Mutationen im unteren Bereich der Stem-Loops L3 und/oder L4 von RNAIII, die die Ausdehnung der Interaktion auf die unteren Stem-Bereiche verhindern, einen negativen Einfluss auf die Effizienz der Transkriptions-termination haben. Daraus ließ sich ableiten, dass die Stems von L3 und L4 von RNAIII an der Ausbildung eines inhibitorischen Komplexes mit RNAII beteiligt sind (Manuskript I). Für eine erfolgreiche Interaktion von RNAIII mit ihrer Target-RNA (RNAII) wird deshalb die Ausbildung einer intermolekularen Helix, die sich in die unteren Stem-Bereiche von L3 und L4 von RNAIII ausdehnt, vorausgesetzt. Ähnliche Beobachtungen wurden für das FinP/*traJ*-System zur Regulation der Konjugation des *E. coli*-Plasmides F gemacht. Dort zeigte sich in einem *in vitro*-Duplexbildungs-Assay, dass sich die Interaktion nach anfänglichen Loop-Loop-Kontakten bis in die unteren Stem-Regionen der interagierenden RNAs FinP und *traJ* ausdehnt (Gubbins *et al.,* 2003). Im Gegensatz dazu wurde im CopA/CopT-System von Plasmid R1 nachgewiesen, dass sich die Ausbildung einer intermolekularen Helix zwischen CopA und ihrer Target-RNA (CopT) nur auf den oberen Bereich der Stems beschränkt und die unteren Stem-Bereiche für eine effiziente Interaktion nicht gebraucht werden (Kolb *et al.,* 2000a).

Im Unterschied zu den Auswirkungen der Stem-Mutationen hatten sowohl der nt-Austausch in der Spacer-Region als auch die Deletion, Verlängerung und Verkürzung der Spacer-Region zwischen den Stem-Loops L3 und L4 keinen signifikanten Effekt auf die Inhibitionskonstanten der entsprechenden RNAIII-Mutanten. Damit konnte nachgewiesen werden, dass weder die Sequenz noch die Länge des Spacers einen Einfluss auf die inhibitorische Wirkung von RNAIII haben (Manuskript I). Auf der Basis dieses Ergebnisses war es zulässig, die Frage nach seiner Bedeutung

für eine effiziente Interaktion mit der Target-RNA RNAII zu stellen. Um diese Frage zu beantworten, wurden die Inhibitionskonstanten für die Stem-Loos L3 und L4 einzeln und in Kombination im *in vitro*-'single-round'-Transkriptionstest bestimmt. Die überraschende Beobachtung, dass bei gleichzeitiger Zugabe der einzelnen Stem-Loops L3 und L4 die Effizienz der Inhibition nicht verbessert wurde, zeigte, dass beide Stem-Loops L3 und L4 zusammenhängen müssen, um eine effiziente Transkriptions-attenuierung von RNAII zu ermöglichen. Offensichtlich übernimmt der Spacer zwischen den Stem-Loops L3 und L4 diese verbindende Funktion und bietet damit ein Gerüst, das eine simultane Interaktion der beiden Loops L3 und L4 von RNAIII mit ihren Target-Loops L1 und L2 von RNAII ermöglicht (Manuskript I). Bisher wurde im Fall der RNAII/RNAIII-Interaktion angenommen, dass die Wechselwirkung zwischen RNAIII und RNAII am Loop L3 (dem sogenannten 'recognition'-Loop) von RNAIII initiiert wird und dass der Kontakt zwischen Loop L4 von RNAIII und dem Target-Loop L1 von RNAII von sekundärer Bedeutung ist (Brantl und Wagner, 1996). Untersuchungen zur Rolle eines U-turn-Motivs am 5'-terminalen Target-Loop L1 von RNAII, das dem Loop L4 von RNAIII komplementär ist und mit diesem paart, ergaben jedoch, dass der RNAII-L1/RNAIII-L4-Kontakt ebenfalls von großer Bedeutung für die effiziente Attenuierung von RNAII ist (Heidrich und Brantl, 2003). Die Ergebnisse der hier vorliegenden Arbeit bestätigen diese Daten und zeigen, dass sowohl L3 als auch L4 - ähnlich der RNAI/RNAII-Interaktion beim *E. coli*-Plasmid ColE1 (Tomizawa *et al.,* 1990a) - an der initialen Interaktion mit der Sense-RNA beteiligt sind. Damit wurde nachgewiesen, dass für den initialen Kontakt von RNAIII und RNAII die simultane Interaktion von zwei komplementären Loop-Paaren erforderlich ist (s. Abb. 4), (Manuskript I).

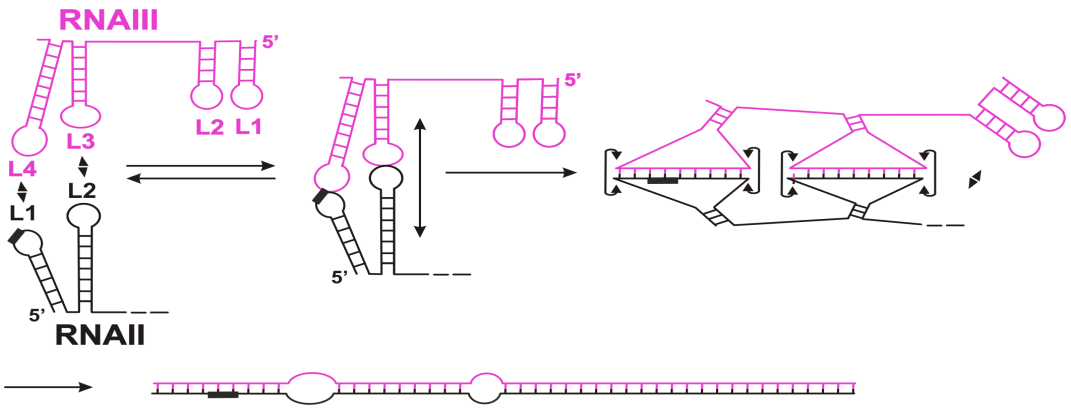

Abb. 4: Vorgeschlagener Paarungsmechanismus von RNAIII und RNAII (Plasmid pIP501). Die Interaktion zwischen den einzelsträngigen Loops von RNAIII (Antisense-RNA, rosa) und RNAII (Sense-RNA, schwarz) führt zur Ausbildung eines 'kissing'-Komplexes. Durch schrittweise Umfaltung kommt es zu Ausbildung einer stabilen partiellen Duplex; schwarzes Rechteck: U-turn-Motiv; (Erläuterungen s. Text) (nach Heidrich und Brantl, 2007)

7.2. SR1: *trans*-kodierte Antisense-RNA aus dem *Bacillus subtilis*-Chromosom

Im Unterschied zu den *cis*-kodierten Antisense-RNAs waren bis 2001 nur ca. 10 *trans*-kodierte Antisense-RNAs aus bakteriellen Genomen bekannt. Während in gramnegativen Bakterien in den letzten 6 Jahren eine große Zahl neuer RNAs (in *E. coli* ca. 70) entdeckt wurde, sind bislang nur wenige *trans*-kodierte regulatorische RNAs aus grampositiven Baktrien bekannt. Mit Hilfe von computergestützten Vorhersagen wurde 2005 eine neue kleine RNA, SR1, in der *phd-speA*-intergenischen Region im Chromosom von *Bacillus subtilis* entdeckt (Licht *et al.,* 2005). SR1 ist nicht essentiell für *B. subtilis* sowie bei Überexpression nicht toxisch und wird unter gluconeogenetischen Bedingungen maximal exprimiert sowie unter glykolytischen Bedingungen reprimiert. Zwei Proteine, CcpN und CcpA, sind an der zuckerabhängigen Transkriptionsregulation des *sr1*-Gens beteiligt. Mit Hilfe von computergestützten Sequenzvergleichen verwandter Organismen konnten homologe RNAs in *Bacillus licheniformis, Bacillus anthracis*, *Bacillus cereus* und *Geobacillus kaustophilus* vorhergesagt werden (Licht *et al.,* 2005). Die biochemische und funktionelle Charakterisierung von SR1 mit dem Hauptschwerpunkt der Analyse der Interaktion mit *ahrC*-mRNA, dem ersten identifizierten Target von SR1, zeigt erstmals im Rahmen dieser Arbeit, dass es sich hierbei um eine regulatorische Antisense-RNA handelt (Kapitel 4 und 5).

7.2.1. Biochemische Eigenschaften von SR1

Um einen Hinweis auf die biochemischen Eigenschaften der chromosomal kodierten RNA SR1 aus *Bacillus subtilis* zu erhalten, mussten zunächst potentielle Targets von SR1 identifiziert werden. Dazu wurden 2D-Gelanalysen von Proteinrohextrakten aus Wildtyp- und SR1-knockout-Stämmen durchgeführt. Es konnten die Gene für RocA, D und F (Enzyme des Arginin-Katabolismus) als mögliche primäre oder sekundäre Targets von SR1 identifiziert werden. Diese Gene sind Bestandteil der *rocABC*- und *rocDEF*- Operons, die einer positiven Kontrolle durch die Transkriptionsaktivatoren AhrC und RocR unterliegen (Calogero *et al.,* 1994; Gardan *et al.,* 1997). Mit Hilfe von Northernblot-Analysen konnte gezeigt werden, dass SR1 die Expression dieser Gene inhibiert. Eine Computer-Analyse der RNA-Sequenzen der identifizierten Targets sowie der *ahrC*-mRNA und *rocR*-mRNA ergab jedoch nur zwischen SR1 und der *ahrC*-mRNA einen Bereich partieller Komplementarität. Mit einem von Zuker und seinen Mitarbeitern 2003 entwickelten Computerprogramm M-fold zur Vorhersage komplementärer Bereiche zwischen zwei RNA-Molekülen wurden sieben aufeinander folgende komplementäre Regionen (A-G) mit einer Größe zwischen 5-8 Nukleotiden in

der 3'-Hälfte von SR1 und im zentralen und 3'-Bereich der *ahrC*-mRNA vorhergesagt. Das legte den Schluss nahe, dass es sich bei der *ahrC*-mRNA um das erste primäre Target von SR1 handelt. Mit Hilfe von Gelshiftassays und Kompetitionsexperimenten konnte eine spezifische Komplexbildung zwischen SR1 und *ahrC*-mRNA nachgewiesen werden. Die ermittelte Dissoziationskonstante für den SR1/*ahrC*-Komplex beträgt 3.21 x 10^{-7} M und liegt damit eine Größenordnung über der mit 2,5 x 10^{-8} M bestimmten Dissoziationskonstante des OxyS/*fhlA*-Komplexes (Argaman und Altuvia, 2000). Die ermittelte Paarungskonstante für den SR1/*ahrC*-Komplex beträgt 1,25 x 10^{3} $M^{-1}s^{-1}$. Für andere Antisense/Sense-RNA-Systeme wurden Paarungskonstanten von ≈ 1-2 x 10^{5} $M^{-1}s^{-1}$ ermittelt (Brantl und Wagner, 1994). Ursache für die Diskrepanz der Konstanten könnte die Tatsache sein, dass ein zusätzlicher Faktor, der die Komplexbildung fördert, benötigt wird. Mit den Komplexbildungsstudien wurde bewiesen, dass es sich bei SR1 tatsächlich um eine *trans*-kodierte Antisense-RNA handelt, die spezifisch an die *ahrC*-mRNA, das erste primäre Target, bindet (Manuskript II).

Eine Abschätzung der intrazellulären SR1-Konzentration in *B. subtilis* zeigte, dass etwa 250 Moleküle pro Zelle (0,35 µM) in der Stationärphase, dem Zeitpunkt ihrer höchsten Expression, vorhanden sind, während in der log-Phase eine 10fach niedrigere Konzentration vorliegt. Damit wurde bestätigt, dass die *in vitro* eingesetzten Mengen an SR1 den Verhältnissen *in vivo* entsprechen (Manuskript III). Entsprechende Bestimmungen der intrazellulären Konzentration einer *trans*-kodierten Antisense-RNA sind bisher nur für OxyS (4500 Moleküle/Zelle) aus *E. coli* bekannt (Altuvia *et al.,* 1997). Für plasmidkodierte Antisense/Sense-RNA-Systeme, wie z. B. für RNAIII (1000 Moleküle/Zelle) und *repR*-mRNA (50 Moleküle/Zelle) von pIP501 wurde analysiert, dass für eine effiziente Interaktion beider RNA-Moleküle ein 10-20 facher Überschuss an Antisense-RNA vorliegen muss (Brantl und Wagner, 1996). Bisherige Grobschätzungen lassen vermuten, dass auch SR1 in einem mindestens 10–20fachen Überschuss gegenüber ihrer Target-mRNA *ahrC* vorliegt. Grund zu dieser Annahme ist die Tatsache, dass es nicht möglich war, die *ahrC*-mRNA in Northern Blots zu detektieren. Das spricht für eine sehr geringe Expression dieses Transkriptionsfaktors. Natürlich vorkommende Antisense-RNAs weisen prominente Sekundär- und Tertiärstrukturen auf, die ihnen eine effiziente Interaktion mit ihren Target-RNA(s) ermöglichen. Für die *in vitro*-Analyse der Interaktion von SR1 mit ihrem ersten bestätigten Target, der *ahrC*-mRNA, war eine Kartierung der Sekundärstruktur von SR1 deshalb unabdingbar. Bisher wurden nur für eine geringe Anzahl *trans*-kodierter Antisense-RNAs die Sekundärstrukturen experimentell bestimmt, und damit wurde bestätigt, dass diese in der Regel 2-3 Stem-Loop-Strukturen besitzen. Dazu gehören

OxyS, (Altuvia *et al.,* 1997), Spot42, (Møller *et al.,* 2002b), RyhB (Geissmann und Touati, 2004), MicA (Udekwu *et al.,* 2005), RNAIII aus *Staphylococcus aureus* (Benito *et al.,* 2000) und DsrA (Lease und Belfort, 2000). Mit Hilfe von RNasen mit unterschiedlichen Spezifitäten für einzel- und doppelsträngige Regionen von SR1 wurde herausgefunden, dass SR1 drei Stem-Loop-Strukturen aufweist: SL1 (nt 1-112), SL2 (nt 138-154) und Terminator-Stem-Loop SL3 (nt 173-205). Diese sind durch zwei einzelsträngige Regionen SSR1 (nt 113-137) und SSR2 (nt 155-172) miteinander verbunden (Manuskript III). Die Lokalisierung der mittels Computerprogramm vorhergesagten 7 komplementären Regionen (A-G) in der experimentell bestimmten SR1-Struktur zeigte, dass diese sowohl in einzelsträngigen als auch in doppelsträngigen Regionen zu finden sind.

7.2.2. *In vitro*-Charakterisierung der Interaktion von SR1 und *ahrC*-mRNA

Alle bisher untersuchten *trans*-kodierten Antisense-RNAs besitzten im Gegensatz zu SR1 nur ein bis zwei komplementäre Regionen mit ihren Target-RNA(s), die für eine erfolgreiche Interaktion und Regulation der Target(s) ausreichend sind. Durch die Analyse der Sekundärstruktur des SR1/*ahrC*-Komplexes unter Verwendung einzel- und doppelstrangspezifischer RNasen sollte deshalb untersucht werden, wie viele Regionen im Fall von SR1 und *ahrC*-mRNA für eine erfolgreiche Interaktion überhaupt gebraucht werden. Aus dem Auftreten von doppelstrangspezifischen RNase-Spaltungen sowie aus der Reduzierung einzelstrangspezifischer RNase-Spaltungen in den sechs von sieben vorhergesagten komplementären Regionen B, C, D, E, F und G, die sich in der 3'-Hälfte von SR1 und im zentralen und 3'-Bereich der *ahrC*-mRNA befinden, konnte geschlussfolgert werden, dass die komplementäre Region A für eine Komplexbildung nicht benötigt wird. Darüber hinaus zeigten einzel- und doppelstrangspezifische RNase-Spaltungen stromabwärts der RBS der gebundenen *ahrC*-mRNA, dass sich durch die SR1-Bindung die Struktur der *ahrC*-mRNA in diesem Bereich ändert und sich intramolekulare Basenpaarungen ausbilden (Manuskript III). Diese Ergebnisse lieferten zudem einen Hinweis auf die Art der Wirkungsweise von SR1 (siehe unten). Entsprechende Komplexkartierungsversuche wurden bislang nur für MicF/*ompF* (Schmidt *et al.,* 1995), Spot42/*galk* (Møller *et al.,* 2002b), RyhB/*sodB* (Geismann und Touati, 2004), MicA/*ompA* (Rasmussen *et al.,* 2005, Udekwu *et al.,* 2005) und RNAIII/*spa* (Huntzinger *et al.,* 2005) vorgenommen.

Basierend auf diesem Ergebnis wurde im Anschluss in Gelshiftassays mit sukzessive verkürzten SR1-Spezies untersucht, welche der sechs komplementären Regionen am initialen Schritt der SR1/*ahrC*-Interaktion beteiligt sind. Es zeigte sich, dass die Bindung von SR1 an *ahrC*-mRNA einerseits in Abwesenheit von Stem-Loop SL1, der

die komplementäre Region A enthält sowie andererseits nur in Anwesenheit der komplementären Region G in der 5'-Hälfte des Terminator-Stems von SL3 erfolgt, und dass die Bindung um ein Vielfaches effizienter ist, wenn die komplementäre Region G einzelsträngig vorliegt. Diese Ergebnisse bestätigten, dass die komplementäre Region A für eine Komplexbildung nicht benötigt wird und zeigten eindeutig, dass die Wechselwirkung zwischen SR1 und *ahrC*-mRNA an der komplementären Region G, die in der 5'-Hälfte des Terminator-Stems von SR1 und 100 bp stromabwärts vom Transkriptionsstart in *ahrC* lokalisiert ist, initiiert wird. Dieser initiale Kontakt erfordert außerdem die Entwindung des doppelsträngigen Terminator-Stems von SR1 (Manuskript III). Anfängliche Kontakte zwischen Antisense- und Target-RNAs erfolgen immer zwischen definierten einzelsträngigen komplementären Regionen, die in der Regel in den einzelsträngigen Loops oder in kurzen linearen Regionen zwischen den Stems zu finden sind. Nur bei wenigen Antisense-RNAs, wie z. B. bei DsrA aus *E. coli* (Lease und Belfort, 2000; Sledjeski *et al.,* 2001) und, wie hier gezeigt, bei SR1, sind die komplementären Regionen, die für einen initialen Kontakt mit der Target-RNA gebraucht werden, nicht in einzelsträngigen Strukturen zu finden. Hier sind zusätzliche Faktoren erforderlich, die durch eine Öffnung doppelsträngiger Sekundärstrukturen eine erfolgreiche Interaktion mit der Target-RNA ermöglichen. Bislang gelang es nicht, den entsprechenden Faktor, der für die Entwindung der komplementären Region G im Terminator-Stem von SL3 erforderlich ist, zu identifizieren. Neben dem RNA-Chaperon Hfq kämen als derartige Faktoren RNasen oder Helikasen in Betracht, jedoch konnte *in vit*ro in Experimenten mit gereinigtem *B. subtilis*-Hfq kein Einfluss von Hfq auf die Komplexbildung zwischen SR1 und *ahrC*-mRNA nachgewiesen werden (siehe unten). Des Weiteren konnte *in vitro* in Northernblot-Analysen von SR1 (Licht *et al.,* 2005) nur eine full-length-Spezies von 205 nt beobachtet werden, so dass die Beteiligung von RNasen an der Öffnung der Terminator-Struktur unwahrscheinlich ist. Interessanterweise wurden in jüngsten Arbeiten aus der AG von Prof. Marahiel zwei *B. subtilis*-Helikasen identifiziert, die doppelsträngige RNA-Strukturen entwinden (Hunger *et al.,* 2006). Entsprechende Versuche mit diesen Helikasen könnten auch für SR1 durchgeführt werden, um eine hypothetische Öffnung dieser Terminator-Stem-Loop-Struktur nachzuweisen.

Die Bedeutung der komplementären Region G im Stem von SL3 für den initialen Kontakt mit *ahrC*-mRNA konnte außerdem durch detaillierte *in vitro*-Mutationsanalysen bestätigt werden. (Manuskript III). Darüber hinaus konnte eine Beteiligung der 5 komplementären Regionen B-F an der SR1/*ahrC*-Interaktion sowohl *in vitro* mittels Mutationsanalysen als auch *in vivo* mit Hilfe von Reportergenfusionen gezeigt werden (Manuskript II und III). Aufgrund dieser Resultate konnte festgestellt werden, dass die

komplementäre Region G maßgeblich an der Interaktion mit der *ahrC*-mRNA beteiligt ist und dass die 5 weiteren komplementären Regionen B-F einen geringen, jedoch messbaren Beitrag zur SR1/*ahrC*-Komplexbildung leisten.

7.2.3. Wirkungsmechanismus von SR1

Als Regulatoren der Genexpression auf post-transkriptionaler Ebene können *trans*-kodierte Antisense-RNAs die Translation und Stabilität ihrer Target-mRNAs sowohl negativ als auch positiv beeinflussen. Die Mehrzahl der bisher untersuchten *trans*-kodierten Antisense-RNAs inhibiert die Translation ihrer Target-mRNA und fördert gleichzeitig den Abbau der Target-mRNA durch Ribonukleasen (zusammengefasst in: Kaberdin und Bläsi, 2006). In allen bekannten Fällen bindet die regulatorische Antisense-RNA dabei direkt an die RBS ihrer Target-mRNA und inhibiert so die Ausbildung des 30S-Initiationskomplexes der für die Translationsinitiation des entsprechenden Targets benötigt wird. Für SR1 konnte mit Hilfe von Northernblot- und 2D-Gelanalysen gezeigt werden, dass sie auch als negativer Regulator wirkt.

Um zu untersuchen, ob die nachgewiesene SR1/*ahrC*-RNA-Interaktion zwischen den komplementären Regionen B-G den Abbau der *ahrC*-mRNA vermittelt, wurde mit Hilfe einer RT-PCR die Menge an *ahrC*-mRNA im Wildtyp- und SR1-knockout-Stamm sowie im Hfq-knockout- und RNase III-defizienten-Stamm bestimmt. Der Nachweis einer unveränderten Menge an *ahrC*-mRNA in allen vier Stämmen zeigte, dass SR1 den Abbau der *ahrC*-mRNA durch RNase III oder eine andere RNase nicht fördert. Dieses Ergebnis legte den Schluss nahe, dass SR1 die Translation ihrer Target-mRNA verhindert. Deshalb wurde der Einfluss von SR1 auf die Proteinmenge an AhrC in einem *in vitro*-Translationsassay untersucht und festgestellt, dass SR1 die Translation der *ahrC*-mRNA inhibiert (Manuskript II). Da SR1 nicht direkt an die RBS der *ahrC*-mRNA bindet und die RBS für eine effiziente SR1/*ahrC*-Komplexbildung nicht benötigt wird, erschien die Inhibierung der Translationsinitiation von AhrC zunächst unwahrscheinlich. Toeprint-Experimente in Anwesenheit von SR1 zeigten jedoch eindeutig, dass SR1 die Ausbildung des 30S-Initiationskomplexes an der *ahrC*-mRNA blockiert. Bezugnehmend auf die Ergebnisse der Komplexstrukturkartierung von SR1 und *ahrC*-mRNA, die gezeigt haben, dass SR1 durch Bindung an die *ahrC*-mRNA eine strukturelle Veränderung stromabwärts der RBS induziert, kann geschlussfolgert werden, dass SR1 dadurch die Translationsinitiation von AhrC verhindert (Manuskript III). Interessanterweise ist SR1 damit die erste identifizierte regulatorische Antisense-RNA, die in der Lage ist, die Translationsinitiation ihrer Target-mRNA ohne direkte Bindung an die RBS zu inhibieren.

7.2.4. Die Rolle von Hfq

Eine Bedeutung von Hfq für den Regulationsprozess *trans*-kodierter Antisense-RNAs wurde zum ersten Mal für OxyS gezeigt (Zhang *et al.,* 1998). Danach konnte für eine Vielzahl *trans*-kodierter Antisense-RNAs aus *E. coli* gezeigt werden, dass sie Hfq für die Stabilität und/oder für die Komplexbildung mit ihren Target-RNAs benötigen (zusammengefasst in: Valentin-Hansen, *et al.,* 2004).

Im Fall von SR1 und ihrer Target-mRNA *ahrC* wurde mit Hilfe von Gelshiftassays gezeigt, dass Hfq *in vitro* sowohl SR1 als auch *ahrC* bei einer Proteinkonzentration von 15 µM sequenzspezifisch bindet, jedoch die Komplexbildung zwischen beiden RNAs nicht begünstigt (Manuskript III). Zudem konnte auch kein Einfluss von Hfq auf die Stabilität von SR1 nachgewiesen werden (Manuskript II). Ähnliche Beobachtungen wurden z. B. auch für die regulatorische RNAs SprA (Pichon and Felden, 2005) und RNAIII (Bohn *et al.,* 2007) aus *Staphylococcus aureus* gemacht. Es ist daher sehr gut vorstellbar, dass alternative RNA-Chaperone in grampositiven Bakterien existieren, die für die Wirkung von regulatorischen Antisense-RNAs benötigt werden.

Durch die Anwendung von Footprinting-Methoden unter Verwendung einzel- und doppelstrangspezifischer RNasen wurden die durch Hfq kontaktierten Regionen an der *ahrC*-mRNA identifiziert. Als Ergebnis wurde sichtbar, dass Hfq an eine einzelsträngige AU-reiche Sequenz stromaufwärts der RBS von *ahrC* bindet. Reportergenfusionen zeigten, dass für die Translation der *ahrC*-mRNA die Bindung von Hfq erforderlich ist (Manuskript III). Ähnliche Beobachtungen, wie die Abhängigkeit der Translation von Hfq und die Bindung von Hfq an eine Sequenz in der Umgebung der RBS wurden auch für die *rpoS*-mRNA aus *E. coli* gemacht, eine mRNA, von der gezeigt werden konnte, dass ihre RBS durch eine doppelsträngige Sekundärstruktur blockiert ist (Muffler *et al.,* 1996; Zhang *et al.,* 1998).

7.3. FourU: neue RNA-Thermometerstruktur im *agsA*-Gen von *Salmonella enterica*

Ebenfalls große Aufmerksamkeit haben die vor kurzem entdeckten sensorischen RNAs erlangt, die als komplexe thermosensitive RNA-Strukturen stromaufwärts von Genen zu finden sind und für viele bakterielle Gene mittels systematischer computergestützter Genomanalysen bereits vorhergesagt wurden (Waldminghaus *et al.,* 2005). Auch im Hitzeschockgen *agsA* von *Salmonella enterica* wurde eine RNA-Thermometerstruktur entdeckt, deren Existenz im Rahmen dieser Arbeit *in vitro* bestätigt werden konnte (Kapitel 6).

7.3.1. Strukturelle und funktionelle Charakterisierung der *agsA*-Thermometerstruktur

Mit Hilfe von computergestützten Vorhersageprogrammen wurde ein RNA-Thermometer in der 5'-UTR des Hitzeschockgens *agsA* von *Salmonella enterica* vorhergesagt, das keinem der bisher identifizierten RNA-Thermometer-Typen entspricht. Es ist mit einer Größe von 57 nt sehr klein, besitzt nur zwei Stem-Loop-Strukturen (Stem-Loop I und II), von denen die letzte (Stem-Loop II) die SD-Sequenz einschließt, und es enthält 4 charakteristische Uridine in der Anti-SD-Sequenz. Durch eine Partialspaltung mit einzel- und doppelstrangspezifischen RNasen bei 30° C und bei 45° C konnte die tatsächliche Sekundärstruktur bei unterschiedlichen Temperaturen identifiziert werden. Dabei bestätigte sich, dass bei einer Temperatur von 30° C die Stem-Loop-Strukturen I und II den mittels Computer vorhergesagten Strukturen entsprechen. Darüber hinaus wurden keine temperaturinduzierten Veränderungen in der Stem-Loop-Struktur I bei einer Temperatur von 45° C beobachtet. Im Gegensatz dazu konnten in der doppelsträngigen Stem-Region von Stem-Loop II, die die eigentliche Thermometer-Region enthält, einzelstrangspezifische RNase-Spaltungen bei 45° C beobachtet werden. Daraus kann geschlussfolgert werden, dass es bei einer Temperatur von 45° C zu einer temperaturinduzierten Konformationsänderung in der Stem-Region von Stem-Loop II kommt, wodurch die SD-Sequenz freigelegt wird (Manuskript IV).

Mit Hilfe von Toeprint-Analysen war nachweisbar, dass die Bindung von Ribosomen an die *agsA*-mRNA tatsächlich nur bei 45° C und ohne einen zusätzlichen Faktor erfolgt. Damit wurde bestätigt, dass es durch einen Temperaturanstieg zum Aufschmelzen der mittels Strukturkartierung bestätigten Sekundärstruktur in der 5'-UTR der *agsA*-mRNA kommt, wodurch die RBS freigelegt und die Translation ermöglicht wird. Proteine oder andere zusätzliche Faktoren sind für diesen Schmelzprozess nicht nötig (Manuskript IV). Ähnliche Beobachtungen wurden auch für Sekundärstrukturen in der 5'-UTR des Hitzeschockgens *rpoH* in *E. coli* (Morita *et al.,* 1999b) und des Virulenzgens *prfA* in *Listeria monocytogenes* (Johansson *et al.,* 2002) gemacht. Im Gegensatz zu den weit verbreiteten ROSE-ähnlichen RNA-Thermometern, die alle ein typisches U(U/C)GCU Motiv wie im ROSE-Element von *Bradyrhizobium japonicum* (Chowdhury *et al.,* 2003, 2006) enthalten, konnte mit dieser Arbeit gezeigt werden, dass 4 charakteristische Uridine in der Anti-SD-Sequenz der Thermometerregion des *agsA*-Gens für den reversiblen Schmelzprozess im Temperaturbereich zwischen 30° C und 45° C verantwortlich sind. Damit wurde das Vorkommen einer neuartigen RNA-Thermometerstruktur in der 5'-UTR der *agsA*-mRNA von *Salmonella enterica* untersucht und *in vitro* nachgewiesen.

8. Zusammenfassung/Summary

Im Rahmen dieser Arbeit wurden eine *cis*-kodierte und eine *trans*-kodierte Antisense-RNA aus *Bacillus subtilis* sowie eine RNA-Thermometerstruktur aus *Salmonella enterica in vitro* strukturell und funktionell untersucht.

Dabei wurden die sequenz- und strukturspezifischen Eigenschaften der inhibitorisch wirksamen *cis*-kodierten Antisense-RNA RNAIII des Streptokokkenplasmides pIP501 identifiziert, die für eine effiziente Interaktion mit der Target-RNA (RNAII) erforderlich sind. Der initiale Kontakt von RNAIII und RNAII erfolgt zwischen einzelsträngigen Loop-Sequenzen in Loop L3 und Loop 4 von RNAIII mit ihrer Target-RNA RNAII und führt zur Ausbildung eines 'kissing'-Komplexes, der sich bis in die unteren Stem-Regionen der interagierenden RNAs ausdehnt. Dieser 'extended-kissing'-Komplex, der mit seinen Dupleces bis in die unteren Stem-Bereiche von L3 und L4 von RNAIII hineinreicht, bildet den inhibitorischen Komplex und gewährleistet eine effiziente Attenuierung der Transkription von RNAII. Die Spacer-Region zwischen den Stem-Loops L3 und L4 von RNAIII ist an der Ausbildung des inhibitorischen Komplexes zwischen RNAIII und RNAII nicht beteiligt. Weder die Sequenz noch die Länge der Spacer-Region haben einen Einfluss auf die inhibitorische Wirkung von RNAIII. Als Verbindungsstück der Stem-Loops L3 und L4 von RNAIII ermöglicht die Spacer-Region eine simultane Interaktion der beiden Loops L3 und L4 von RNAIII mit ihren Target-Loops L2 und L1 von RNAII.
Die in dieser Arbeit durchgeführten *in vitro*-Analysen zur inhibitorischen Wirkung der RNAIII haben gezeigt, dass die Ausbildung einer vollständigen Duplex mit ihrer Target-RNA nicht erforderlich ist. Ein Bindungsintermediat, das lediglich die simultane Beteiligung der Stem-Loops L3 und L4 von RNAIII erfordert, reicht als inhibitorischer Komplex für die Regulation der Replikation des Streptokokkenplasmids pIP501 aus. Damit wurden erstmalig in einem Antisense-RNA-regulierten Kontrollsystem grampositiver Bakterien die minimalen Sequenz- und Struktur-Anforderungen an eine effiziente Interaktion zwischen Antisense- und Sense -RNA untersucht und ermittelt.

Innerhalb dieser Arbeit wurden außerdem die strukturellen und funktionellen Eigenschaften der chromosomal kodierten RNA SR1 aus *Bacillus subtilis in vitro* untersucht. Hierbei konnte das erste primäre Target von SR1, *ahrC*-mRNA, die einen Transkriptionsaktivator der *rocABC*- und *rocDEF*-Operons kodiert, identifiziert werden. Der Nachweis einer spezifischen Komplexbildung zwischen SR1 und *ahrC*-mRNA

zeigte, dass es sich bei SR1 um eine regulatorische *trans*-kodierte Antisense-RNA handelt, die an der Regulation des Arginin-Katabolismus in *B. subtilis* beteiligt ist. SR1 weist eine komplexe Sekundärstruktur mit drei Stem-Loop-Strukturen auf, die durch zwei einzelsträngige Regionen miteinander verbunden werden. Für den SR1/*ahrC*-Komplex konnten eine Dissoziationskonstante von 3.21 x 10^{-7} M und eine Paarungskonstante von 1,25 x 10^{3} $M^{-1}s^{-1}$ ermittelt werden, was dafür spricht, dass ein zusätzlicher Faktor zur Förderung der Komplexbildung benötigt wird.

Unter Verwendung eines computergestützten Vorhersageprogramms wurden für SR1 sieben aufeinander folgende komplementäre Regionen (A-G) mit der *ahrC*-mRNA identifiziert, die in der 3'-Hälfte von SR1 und im zentralen und 3'-Bereich der *ahrC*-mRNA zu finden sind. Für sechs Regionen, und zwar B-G, bestätigte sich experimentell eine Beteiligung an der SR1/*ahrC*-Komplexbildung. Die Interaktion zwischen SR1 und der *ahrC*-mRNA wird an der komplementären Region G initiiert, die in der 5'-Hälfte des Terminator-Stems von SR1 und 100 bp stromabwärts vom Transkriptionsstart in *ahrC* lokalisiert ist. Toeprint- und Sekundärstruktur-Analysen des SR1/*ahrC*-Komplexes zeigten, dass SR1 durch die Bindung an die *ahrC*-mRNA eine strukturelle Veränderung stromabwärts der RBS der *ahrC*-mRNA induziert, wodurch die Ausbildung des 30S-Initiationskomplexes blockiert und damit die Translation von AhrC verhindert wird. Zudem konnte eine spezifische Bindung des RNA-Chaperons Hfq sowohl an SR1 als auch an *ahrC*-mRNA nachgewiesen werden, die zwar keinen Einfluss auf die SR1/*ahrC*-Komplexbildung hatte, jedoch für die Translation der *ahrC*-mRNA erforderlich ist. Eine Abschätzung der intrazellulären Konzentration an SR1 in *B. subtilis* ergab, dass etwa 250 Moleküle pro Zelle (0,35 µM) in der Stationärphase, dem Zeitpunkt ihrer höchsten Expression, vorhanden sind, während in der log-Phase eine 10fach niedrigere Konzentration vorliegt .

Mit der in dieser Arbeit durchgeführten detaillierten Untersuchung ist SR1 neben RNAIII aus *Staphylococcus aureus* die zweite sehr gut charakterisierte *trans*-kodierte regulatorische Antisense-RNA aus grampositiven Bakterien überhaupt: die Mehrheit der bisher im Hinblick auf ihre Targets, Funktionen und Wirkungsweisen untersuchten regulatorischen Antisense-RNAs stammt aus *E. coli*. Darüber hinaus wurde bisher keine weitere *trans*-kodierte Antisense-RNA charakterisiert, die wie SR1 mehr als zwei komplementäre Regionen zu ihrer Target-RNA besitzt und zudem die Ausbildung des 30S-Initiationskomplexes an der RBS ihrer Target-RNA durch strukturelle Veränderung stromabwärts dieser Region inhibiert. Die Mehrzahl der bisher untersuchten regulatorischen Antisense-RNAs inhibiert oder aktiviert die Translationsinitiation ihrer Target-RNA(s) durch direkte Bindung an die RBS.

Ein weiteres Ziel dieser Arbeit war es, eine vorhergesagte RNA-Thermometerstruktur, die stromaufwärts des Hitzeschockgens *agsA* von *Salmonella enterica* lokalisiert ist, biochemisch zu charakterisieren. Dabei konnte eine temperaturabhängige Konformationsänderung der 5'-UTR von *agsA* festgestellt werden, die den Zugang zur RBS kontrolliert. Die Thermometeraktivität dieser Region erfordert vier aufeinander folgende Uracil-Reste, die mit der SD-Sequenz des *agsA*-Gens gepaart sind. Diese destabilisieren die Thermometerstruktur bei einer Temperaturerhöhung und bilden das charakteristische Merkmal einer neuen Klasse von RNA-Thermometern.

Insgesamt konnten mit den in dieser Arbeit vorgestellten Ergebnissen wichtige Erkenntnisse über die biochemischen Eigenschaften einer *cis*-kodierten und einer *trans*-kodierten Antisense-RNA sowie eine RNA-Thermometerstruktur in Prokaryoten, die eine Regulation der Genexpression von prokaryotischen Genen ermöglichen, gewonnen und damit bisherige Forschungsergebnisse erfolgreich ergänzt werden.

Summary

The scope of this investigation was to examine the structural and functional properties of a *cis*-encoded and a *trans*-encoded antisense RNA of *Bacillus subtilis* as well as a RNA thermometer of *Salmonella enterica*.

The specific sequence und structural requirements of the *cis*-encoded inhibitory antisense RNA RNAIII of streptococcal plasmid pIP501 that allow an efficient RNAII/RNAIII interaction were identified. The initial contact between RNAIII and RNAII occurs between single-stranded loop sequences L3 and L4 of RNAIII and its target RNA, RNAII, which forms a 'kissing' complex that progresses into the lower stems of the interacting RNA molecules. This 'extended-kissing' complex, wich extends into the lower parts of the stems L3 and L4 of RNAIII is the inhibitory complex between RNAIII and RNAII that is needed for efficient transcriptional attenuation of RNAII. The spacer region between stem loop L3 and L4 is not involved in the formation of the inhibitory complex. In addition, neither the sequence nor the length of the spacer between L3 and L4 influence the inhibitory function of RNAIII. The spacer region between the stem loops L3 and L4 of RNAIII serves as a connector that enables the simultaneous interaction between the loops L3 and L4 of RNAIII and the target loops L2 and L1 of RNAII.
The *in vitro* analysis of the inhibitory function of RNAIII carried out in the present study revealed that the formation of a fully paired complex between sense and antisense RNA is not needed. A binding intermediate that requires the simultaneous participation of the stem loops L3 and L4 of RNAIII as inhibitory complex is sufficient for the regulation of streptococcal plasmid pIP501 replication. With this study, for the first time the minimal sequence and structural requirements for an efficient interaction between an antisense and a sense RNA of an antisense RNA regulated system from Gram-positive bacteria were determined.

Furthermore, the structural and functional features of the chromosomally encoded RNA SR1 from *Bacillus subtilis* were investigated and the first primary target of SR1, *ahrC*-mRNA encoding the transcripitional activator of the *rocABC* and *rocDEF* operons, was identified. Specific complex formation between SR1 and *ahrC*-mRNA demonstrated that SR1 is a regulatory *trans*-encoded antisense RNA involved in arginine catabolism. SR1 exhibits a complex secondary structure of three main stem loops separated by two single stranded regions. The calculated dissociation rate constant of 3.21 x 10^{-7} M and

association rate constant of 1,25 x 10^3 $M^{-1}s^{-1}$ for the SR1/*ahrC* complex indicated that an additional factor might be required for complex formation.

Using a computational approach, seven consecutive stretches of complementarity (A-G) between SR1 and *ahrC*-mRNA that are located in the 3' half of SR1 and in the central and 3' part of *ahrC*-mRNA were predicted. Six out of these seven complementary regions (B – G) proved to be necessary for the complex formation between SR1 and *ahrC*-mRNA. The initial contact between SR1 and *ahrC*-mRNA requires complementary region G that is located in the 5' half of the terminator stem of SR1 and in a region ≈100 bp downstream from the *ahrC* transcriptional start side. Toeprinting studies and secondary structure probing of the SR1/*ahrC* complex demonstrated that SR1 blocks the binding of the 30S-initiator complex by inducing structural changes downstream from the *ahrC* ribosome binding side and thereby inhibits translation of *ahrC* mRNA. Furthermore, the specific binding of the RNA chaperone Hfq to both, SR1 and *ahrC*-mRNA, is not required to promote SR1/*ahrC* complex formation but to enable the translation of *ahrC*-mRNA. The intracellular concentration of SR1 within one *Bacillus subtilis* cell was estimated to increase from 20 molecules in log phase to ≈ 250 molecules (0,35 µM) in stationary phase when SR1 expression is maximal.

This detailed study makes SR1 – beside RNAIII from *Staphylococcus aureus* – the second best characterized *trans*-encoded antisense RNA in Gram-positive bacteria. The majority of small regulatory antisense RNAs that were analysed in terms of their targets, functions and mechanisms of action were found and investigated in *E. coli.* In addition, no other example of a small regulatory *trans*-encoded antisense RNA has been analysed so far that contains more than two complementary regions with its target RNA and inhibits translation initiation of its target RNA by inducing structural changes downstream from the ribosome binding side, like SR1. The majority of regulatory antisense RNAs that repress or activate translation initiation of their target RNA(s) act by direct binding to the ribosome binding site or upstream of it.

Another aim of the present study was to determine the biochemical properties of a potential RNA thermometer structure upstream of the heat shock gene *agsA* in *Salmonella enterica*. A detailed biochemical characterization revealed dynamic temperature-dependent conformational changes in the 5'-UTR of *agsA,* that control ribosome access to the SD sequence. Thermometer activity within this region requires four consecutive uracil residues that pair with the SD sequence. These uracil residues destabilize the RNA structure at high temperatures and represent the characteristic feature of a novel type of RNA thermometers.

The results of this study allow an important insight into the biochemical characteristics of one *cis*-encoded and one *trans*-encoded antisense RNA as well as one RNA thermometer that regulates the gene expression in prokaryotes, thereby complementing our present knowledge.

9. Literaturverzeichnis

Afonyushkin, T., Vecerek, B., Moll, I., Bläsi, U., and Kaberdin, V.R. (2005). Both RNase E and RNase III control the stability of *sodB* mRNA upon translational inhibition by the small regulatory RNA RyhB. *Nucleic Acids Res.* **33**: 1678-1689.

Altuvia, S., Weinstein-Fischer, D., Zhang, A., Postow, L., and Storz, G. (1997). A small, stable RNA induced by oxidative stress: role as a pleiotropic regulator and antimutator. *Cell.* **90**: 443-53.

Altuvia, S., Zhang, A., Argaman, L., Tiwari, A., and Storz, G. (1998). The *Escherichia coli* OxyS regulatory RNA represses *fhlA* translation by blocking ribosome binding. *EMBO J.* **20**: 6069-6075.

Andersen, J., Forst, S.A., Zhao, K., Inouye, M., and Delihas, N. (1989). The function of micF RNA. micF RNA is a major factor in the thermal regulation of OmpF protein in *Escherichia coli. J Biol Chem.* **264** (30): 17961-70.

Ando, Y., Asari, S., Suzuma, S., Yamane, K., and Nakamura, K. (2002). Expression of a small RNA, BS203 RNA, from the yocI-yocJ intergenic region of *Bacillus subtilis* genome. *FEMS Microbiol Lett*. **207**: 29-33.

Argaman, L., and Altuvia, S. (2000). *FhlA* repression by OxyS RNA: kissing complex formation at two sites results in a stable antisense-target RNA complex. *J Mol Biol.* **300**: 1101-1112.

Argaman, L., Herschberg, R., Vogel, J., Bejerano, G., Wagner, E.G., Margalit, H., and Altuvia, S. (2001) Novel small RNA-encoding genes in the intergenic regions of *Escherichia coli*. *Curr Biol*. **11**: 941-950.

Arini, A., Keller, M.P., and Arber W. (1997). An antisense RNA in IS30 regulates the translational expression of the transposase. *Biol. Chem.* **378:** 1421-1431.

Asano, K., Morikawi, H., and Mizobuchi, K. (1991). An induced mRNA secondary structure enhances *repZ* translation in plasmid CoIIb-P9. *J. Biol. Chem.* **266**: 24549-24556.

Balsiger, S., Ragaz, C., Baron, C., and Narberhaus, F. (2004). Replicon-specific regulation of small heat shock genes in *Agrobacterium tumefaciens*. *J Bacteriol*. **186**: 6824-6829.

Barrick, J.E., Sudarsan, N., Weinberg, Z., Ruzzo, W.L., and Breaker, R.R. (2005). 6S RNA is a widespread regulator of eubacterial RNA polymerase that resembles an open promoter. *RNA.* **11**: 774-784.

Benito, Y., Kolb, F.A., Romby, P., Lina, G., Etienne, J., and Vandenesch, F. (2000). Probing the structure of RNAIII, the Staphylococcus aureus agr regulatory RNA, and identification of the RNA domain involved in repression of protein A expression. *RNA.* **6**: 668-79.

Bohn, C., Rigoulay, C., and Bouloc, P. (2007). No detectable effect of RNA-binding protein Hfq absence in *Staphylococcus aureus. BMC Microbiol*. **7:10**: 1-9.

Brantl, S., and Behnke, D. (1992a). Copy number control of the streptococcal plasmid pIP501 occurs at three levels. *Nucleic Acids Res.* **20**: 395-400.

Brantl, S., and Behnke, D. (1992b). The amount of RepR protein determines the copy number of plasmid pIP501 in *B. subtilis*. *J. Bacteriol.* **174**: 5475-5478.

Brantl, S., Birch-Hirschfeld, E., and Behnke, D. (1993). RepR protein expression on plasmid pIP501 is controlled by an antisense RNA-mediated transcription attenuation mechanism. *J Bacteriol.* **175:** 4052-4061.

Brantl, S., and Wagner, E.G. (1994). Antisense-RNA mediated transcriptional attenuation occurs faster than stable antisense/target RNA pairing: an *in vitro* study of plasmid pIP501. *EMBO J.* **13**: 3599-3607.

Brantl, S., and Wagner, E.G. (1996). An unusually long-lived antisense RNA in plasmid copy number control: *in vivo* RNAs encoded by the streptococcal plasmid pIP501. *J. Mol. Biol.* **255**: 275-288.

Brantl, S. (2002). Antisense-RNA regulation and RNA interference. *Bioch. Biophys. Acta.* **1575**: 15-25.

Brantl, S. (2004). Bacterial gene regulation: from transcription attenuation to riboswitches and ribozymes. *Trends Microbiol.* **12**: 473-5.

Brantl, S. (2007). Regulatory mechanisms employed by cis-encoded antisense RNAs. *Curr Opin Microbiol.* [in press]

Brescia, C.C., Mikulecky, P.J., Feig, A.L., and Sledjeski, D.D. (2003). Identification of the Hfq-binding site on DsrA RNA: Hfq binds without altering DsrA secondary structure. *RNA*. **9**: 33-43

Burrowes, E., Abbas, A., O'Neil, A., Adams, C., and O'Gara, F. (2005). Characterisation of the regulatory RNA RsmB from *Pseudomonas aeruginosa* PAO1. *Res Microbiol*. **156**: 7-16.

Calogero, S., Gardan, R., Glaser, P., Schweizer, J., Rapoport, G., and Débarbouillé, M. (1994). RocR, a novel regulatory protein controlling arginine utilization in *Bacillus subtilis*, belongs to the *NtrC/NifA* family of transcriptional activators. *J Bacteriol.* **176**: 1234-1241.

Chen, S., Lesnik, E.A., Hall, T.A., Sampath, R., Griffey, R.H., Ecker, D.J., and Blyn, L.B. (2002). A bioinformatics based approach to discover small RNA genes in the *Escherichia coli* genome. *Biosystems.* **65**: 157-177.

Chen, S., Zhang, A., Blyn, L.G., and Storz, G. (2004). MicC, a second small-RNA regulator of omp protein expression in *Escherichia coli*. *J Bacteriol*. **186**: 6689-6697.

Chowdhury, S., Ragaz, C., Kreuger, E., and Narberhaus, F. (2003). Temperature-controlled structural alterations of an RNA thermometer. *J Biol Chem*. **278**: 47915-47921.

Chowdhury, S., Maris, C., Allain, F.H., and Narberhaus, F. (2006). Molecular basis for temperature sensing by an RNA thermometer. *EMBO J*. **25**: 2487-2497.

Christiansen, J.K., Nielsen, J.S., Ebersbach, T., Valentin-Hansen, P., Søgaard-Andersen, L., and Kallipolitis, B.H. (2006). Identification of small Hfq-binding RNAs in *Listeria monocytogenes*. *RNA*. **12:** 1-14.

Delihas, N., and Forst, S. (2001). MicF: An antisense RNA gene involved in response of *Escherichia coli* to global stress factors. *J Mol Biol* . **313**: 1-12.

Douchin, V., Bohn, C., and Bouloc, P. (2006). Down-regulation of porins by a small RNA bypasses the essentiality of the regulated intramembrane proteolysis protease RseP in *Escherichia coli. J Biol Chem.* **281**: 122.53-12259.

DuBow, M.S., Ryan, T., Young, R.A., and Blumenthal, T. (1977). Host factor for coliphage Qβ RNA replication: presence in prokaryotes and association with the 30S ribosomal subunit in *Escherichia coli. Mol Gen Genet.* **153**: 39-43.

Dykxhoorn, D.M., and Lieberman, J. (2006). Knocking down Disease with siRNAs. *Cell.* **126**: 231-235.

Eguchi, Y. Ihoth T., and Tomizawa, J. (1991). Complexes formed by complementary RNA stem-loops. Their formations, structures and interaction with ColE1 Rom protein. *J Mol Biol.* **220**: 831-842.

Franch, T., Petersen, M., Wagner, E.G., Jacobsen, J.P., and Gerdes, K. (1999). Antisense RNA Regulation in Prokaryotes: Rapid RNA/RNA Interaction Facilitated by a General U-turn Loop Structure. *J. Mol. Biol.* **294**: 1115-1125.

Franze de Fernandez, M.T., Eoyang, L., and August, J.T. (1968). Factor fraction required for the synthesis of bacteriophage Qβ-RNA. *Nature.* **219**: 588-590.

Frost, L., Lee, S., Yanchar, N., and Paranchych, W. (1989). *FinP* and *finO* mutations in FinP antisense RNA suggest a model for FinOP action in the repression of bacterial conjugation by the Flac plasmid JCFL0. *Mol. Gen. Genet.* **218**: 152-160.

Gardan, R., Rapoport, G., and Débarbouillé, M. (1997). Role of the transcriptional activator RocR in the arginine-degradation pathway of *Bacillus subtilis*. *Mol Microbiol.* **24**: 825-837.

Geissmann,T.A., and Touati, D. (2004). Hfq, a new chaperoning role: binding to messenger RNA determines access for small RNA regulator. *EMBO J*. **23**: 396-405.

Gerdes, K., Gultyaev, A.P., Franch, T., Pedersen, K., and Mikkelsen, N.D. (1997). Antisense RNA-regulated programmed cell death. *Annu. Rev. Genet.* **31:** 1-31.

Grieshaber, N.A., Grieshaber, S.S., Fischer, E.R. and Hackstadt,T. (2006). A small RNA inhibits translation of the histone-like protein Hc1 in *Chlamydia trachomatis. Mol. Microbiol.* **59**: 541-550.

Gualerzi, C.O., Giuliodori, A.M., and Pon, C.L. (2003). Transcriptional and post-transcriptional control of cold-shock genes. *J Mol Biol.* **331**: 527-539.

Gubbins, M.J., Arthur, D.C., Ghetu, A.F., Glover, J.N.M., and Frost, L.S. (2003). Characterizing the structural features of RNA/RNA interactions of the F-plasmid FinOP fertility inhibition system. *J Biol Chem*. **278**: 27663-71.

Guillier, M., and Gottesman, S. (2006). Remodelling of the *Escherichia coli* outer membrane by two small regulatory RNAs. *Mol Microbiol.* **59**: 231-247.

Hjalt, T., and Wagner, E.G. (1992).The effect of loop size in antisense and target RNAs on the efficiency of antisense RNA control. *Nucleic Acids Res*. **20:** 6723-6732.

Hjalt, T., and Wagner, E.G. (1995). Bulged-out nucleotides protect an antisense RNA from RNaseIII cleavage. *Nucleic Acids Res.* **23:** 571-579.

Heidrich, N., and Brantl S. (2003). Antisense-RNA Mediated Transcriptional Attenuation: importance of a U-turn loop structure in the target RNA of plasmid pIP501 for efficient inhibition by the antisense RNA**.** *J.Mol. Biol.* **333:** 917-929.

Heidrich, N., Chinali A., Gerth U., and Brantl S. (2006). The small untranslated RNA SR1 from the *B. subtilis* genome is involved in the regulation of arginine catabolism *Mol. Microbiol.* **62**: 520-36.

Heidrich, N., and Brantl, S. (2007). Antisense RNA-mediated transcriptional attenuation in plasmid pIP501: the simultaneous interaction between two complementary loop pairs is required for efficient inhibition by the antisense RNA. *Microbiology.* **153:** 420-427.

Heidrich, N., Moll, I., and Brantl, S. (2007). *In vitro* analysis of the interaction between the small RNA SR1 and its primary target *ahrC*-RNA. *Nucleic Acids Res. eingereicht.*

Heurlier, K., Williams, F., Heeb, S., Dormond, C., Pessi, G., Singer, D., Camara, M., Williams, P., and Haas, D. (2004). Positive control of swarming, rhamnolipid synthesis, and lipase production by the posttranscriptional RsmA/RsmZ system in *Pseudomonas aeruginosa* PAO1. *J Bacteriol*. **186**: 2936-2945.

Hoe, N.P., and Goguen, J.D. (1993). Temperature sensing in *Yersinia pestis*: translation of the LcrF activator protein is thermally regulated. *J Bacteriol.* **175**: 7901-7909.

Hunger, K., Beckering, C.L., Wiegeshoff, F., Graumann P.L., and Marahiel, M.A. (2006). Cold-induced putative DEAD box RNA helicases CshA and CshB are essential for cold adaptation and interact with cold shock protein B in Bacillus subtilis. *J Bacteriol.* **188**: 240-248.

Huntzinger, E., Boisset, S., Saveanu, C., Benito, Y., Geissmann, T., Namane, A., *et al*. (2005). *Staphylococcus aureus* RNAIII and the endoribonuclease III coordinately regulate *spa* gene expression. *EMBO J.* **24**: 824-835.

Johansson, J., Mandin, P., Renzoni, A., Chiaruttini, C., Springer, M. and Cossart, P. (2002). An RNA thermosensor controls expression of virulence genes in *Listeria monocytogenes*. *Cell*. **110**: 551-561.

Kaberdin, V.R., and Bläsi, U. (2006). Translation initiation and the fate of bacterial mRNAs. *FEMS Microbiol Rev.* **30**: 967-979.

Kawamoto, H., Morita, T., Shimizu, A., Inada, T., and Aiba, H. (2005). Implication of membrane localization of target mRNA in the action of a small RNA: mechanism of post-transcriptional regulation of glucose transporter in *Escherichia coli. Genes Dev.* **19**: 328-338.

Kay, E., Dubuis, C., and Haas, D. (2005). Three small RNAs jointly ensure secondary metabolism and biocontrol in *Pseudomonas fluorescens* CHA0. *Proc Natl Acad Sci USA*. **102**: 17136-17141.

Kittle, J.D., Simons, R.W., Lee, J., and Kleckner, N. (1989). Insertion sequence IS10 antisense pairing initiates by an interaction between the 5'-End of the target RNA and a Loop in the antisense RNA. *J. Mol. Biol.* **210:** 561-572.

Kolb, F.A., Malmgren, C., Westhof, E., Ehresmann, C., Ehresmann, B., Wagner, E.G., and Romby, P. (2000a). An unusual structure formed by antisense-target RNA binding

involves an extended kissing complex with a four-way junction and a side-by-side helical alignment. *RNA*. **6**: 311-324.

Kolb, F.A., Engdahl, H.M., Slagter-Jäger, J.G., Ehresmann, B., Ehresmann, C., Westhof, E., Wagner, E.G., and Romby, P. (2000b). Progression of a loop-loop complex to a four-way junction is crucial for the activity of a regulatory antisense RNA. *EMBO J.* **19**: 5905-5915.

Koraimann, G., Koraimann, C., Koronakis, V., Schlager S., and Högenauer, G. (1991). Repression and derepression of conjugation of plasmid R1 by wild-type and mutated *finP* antisense RNA. *Mol. Microbiol.* **5**: 77-87.

Kreikemeyer, B., Boyle, M.D., Buttaro, B.A., Heinemann, M., and Podbielski, A., (2001). Group A streptococcal growth phase-associated virulence factor regulation by a novel operon (Fas) with homologies to two-component-type regulators requires a small RNA molecule. *Mol Microbiol.* **39**: 392-406.

Krinke, L., and Wulff D.L. (1990): RNase III-dependent hydrolysis of *cII-O* gene mRNA by OOP antisense RNA. *Genes Dev.* **4**: 2223-2233.

Lease, R.A., Cusick, M.E., and Belfort M. (1998). Riboregulation in *Escherichia coli*: DsrA RNA acts by RNA:RNA interactions at multiple loci. *Proc Natl Acad Sci USA*. **95**: 12456-12461.

Lease, R.A., and Belfort, M. (2000). A trans-acting RNA as a control switch in *Escherichia coli*: DsrA modulates function by forming alternative structures. *Proc Natl Acad Sci USA.* **97**: 9919-9924.

Lee, J.M., Zhang, S., Saha, S., Santa Anna, S., Jiang, C., and Perkins, J. (2001). RNA expression analysis using an antisense *Bacillus subtilis* genome array. *J Bacteriol.* **183**: 7371-7380.

Lenz, D.H., Mok, K.C., Lilley, B.N., Kulkarni, R.V., Wingreen, N.S., and Bassler, B.L. (2004). The small RNA chaperone Hfq and multiple small RNAs control quorum sensing in *Vibrio harveyi* and *Vibrio cholerae*. *Cell*. **118**: 69-82.

Lenz, D.H., Miller, M.B., Zhu, J., Kulkarni, R.V., and Bassler, B.L. (2005). CsrA and three redundant small RNAs regulate quorum sensing in *Vibrio cholerae. Mol Microbiol.* **58**: 1186-1202.

Liao, S.M., Wu, T.H., Chiang, C.H., Susskind, M.M., and McClure, W.R. (1987). Control of gene expression in bacteriophage P22 by a small antisense RNA. I. Characterization *in vitro* of the Psar promoter and the sar RNA transcript. *Genes Dev.* **1**: 197-203.

Licht, A., Preis S., and Brantl, S. (2005). Implication of CcpN in the regulation of a novel untranslated RNA (SR1) in *Bacillus subtilis*. *Mol. Microbiol.* **58**: 189-206.

Ma, C., and Simons, R.W. (1990). The IS10 antisense RNA blocks ribosome binding at the transposase translation initiation site. *EMBO J.* **9**: 1267-1274.

Majdalani, N., Cunning, C., Sledjeski, D., Eliott, T., and Gotttesman, S. (1998). DsrA RNA regulates translation of RpoS message by an anti-antisense mechanism, independent of its action as an antisilencer of transcription. *Proc Natl Acad Sci USA*. **95**: 12462-12467.

Majdalani, N., Hernandez, D., and Gottesman, S. (2002). Regulation and mode of action of the second small RNA activator of RpoS translation, RprA. *Mol Microbiol.* **46**: 813-26.

Majdalani, N., Vanderpool, C.K., and Gottesman, S., (2005). Bacterial small RNA regulators. *Crit Rev Biochem Mol Biol.* **40**: 93-113.

Malmgren, C., Wagner, E.G., Ehresmann, C., Ehresmann, B., and Romby, P. (1997). Antisense RNA control of plasmid R1 replication: the dominant product of the antisense RNA-mRNA binding is not a full RNA duplex. *J Biol Chem.* **272**: 12508-12512.

Mandin, P., Repoila, F., Vergassola, M., Geissmann, T. and Cossart, P. (2007). Identification of new nonconding RNAs in *Listeria monocytogenes* and prediction of mRNA targets. *Nucleic Acids Res.* **35**: 962-974.

Mangold, M., Siller, M., Roppenser, B., Vlaminckx, B.J., Penfound, T.A., Klein, R. *et al.* (2004). Synthesis of group A streptococcal virulence factors is controlled by a regulatory RNA molecule. *Mol. Microbiol,* **53**: 1515-1527.

Massé, E., and Gottesman, S. (2002). A small RNA regulates the expression of genes involved in iron metabolism in *Escherichia coli*. *Proc Natl Acad Sci USA*. **99**: 4620-4625.

Massé, E., Escorcia F.E., and Gottesman S. (2003). Coupled degradation of a small regulatory RNA and its mRNA targets in *Escherichia coli. Genes Dev.* **17**: 2374-2383.

Massé, E., Vanderpool, C.K., and Gottesman, S. (2005). Effect of RyhB small RNA on global iron use in *Escherichia coli. J Bacteriol.* **187**: 6962-6971.

Meister, G., and Tuschl, T. (2004). Mechanismus of gene silencing by double-stranded RNA. *Nature.* **431**: 343-349.

Mironov, A.S., Gusarov, I., Rafikov, R., Lopez, L.E., Shatalin, K., Kreneva, R.A., Perumov, D.A., and Nudler, E. (2002). Sensing small molecules by nascent RNA: a mechanism to control transcription in bacteria. *Cell.* **111**: 747-56.

Moll, I., Afonyushkin, T., Vytvytska, O., Kaberdin, V.R., and Blasi, U. (2003). Coincident Hfq binding and RNase E cleavage sites on mRNA and small regulatory RNAs. *RNA.* **9**: 1308-14.

Møller, T., Franch, T., Hojrup, P., Keene, D.R., Bächinger, H.P., Brennan, R.G., and Valentin-Hansen, P. (2002a). Hfq: A bacterial Sm-like protein that mediates RNA-RNA interaction. *Mol Cell.* **9**: 23-30.

Møller, T., Franch, T., Udesen, C., Gerdes, K., and Valentin-Hansen, P. (2002b). Spot 42 RNA mediates discoordinate expression of the *E. coli* galactose operon. *Genes Dev.* **16**: 1696-1706.

Morfeldt, E., Taylor, D., von Gabain, A., and Arvidson, S. (1995). Activation of alpha-toxin translation in *Staphylococcus areus* by the trans-encoded antisense RNA, RNAIII. *EMBO J.* **14**: 4569-4577.

Morita, M., Kanemori, M., Yanagi, H., and Yura, T. (1999a). Heat-induced synthesis of σ^{32} in *Escherichia coli*: structural and functional dissection of *rpoH* mRNA secondary structure. *J Bacteriol*. **181**: 401-410.

Morita, M.T., Tanaka, Y., Kodama, T.S., Kyogoku, Y., Yanagi, H., and Yura, T. (1999b). Translational induction of heat shock transcription factor σ^{32}: evidence for a built-in RNA thermosensor. *Genes Dev*. **13**: 655-665.

Muffler, A., Fischer, D., and Hengge-Aronis, R. (1996). The RNA-binding protein HF-I, known as a host factor for phage Qb RNA replication, is essential for *rpoS* translation in *Escherichia coli*. *Genes Dev*. **10**: 1143-1151.

Muffler, A., Traulsen, D.D., Fischer, D., Lange, R., and Hengge-Aronis, R. (1997). The RNA-binding protein HF-I plays a global regulatory role which is largely, but not exclusively, due to its role in expression of the sigmaS subunit of RNA polymerase in *Escherichia coli. J Bacteriol.* **179**: 297-300.

Nakamura, K., Yahagi, S., Yamazaki, T., and Yamane, K. (1999). *Bacillus subtilis* histone-like protein, Hbsu, is an integral component of a SRP-like particle that can bind the Alu domain of small cytoplasmic RNA. *J. Biol. Chem*. **274**: 13569-13576.

Narberhaus, F., Käser, R., Nocker, A., and Hennecke, H. (1998). A novel DNA element that controls bacterial heat shock gene expression. *Mol Microbiol*. **28**: 315-323.

Narberhaus, F., Waldminghaus, T., and Chowdhury, S. (2006). RNA thermometers. *FEMS Microbiol Rev*. **30**: 3-16.

Nocker, A., Krstulovic, N.P., Perret, X., and Naberhaus, F. (2001). ROSE elements occur in disparate rhizobia and are functionally interchangeable between species. *Arch Microbiol.* **176**: 44-51.

Novick, R.P., Iordanescu, S., Projan, S.J., Kornblum, J., and Edelman, I. (1989). pT181 plasmid replication is regulated by a countertranscript-driven transcriptional attenuator. *Cell*. **59**: 395-404.

Ohtani, K., Bhowmik, S.K., Hayashi, H., and Shimizu, T., (2002). Identification of a novel locus that regulates expression of toxin genes in *Clostridium perfringens*. *FEMS Microbiol Lett.* **209**: 113-118.

Opdyke, K., and Storz, G. (2004): GadY, a small-RNA regulator of acid response genes in *Escherichia coli. J Bacteriol.* **186**: 6698-6705.

Papenfort, K., Pfeiffer, V., Mika F., Lucchini, S., Hinton, J.C.D. and Vogel, J. (2006). σ^{E}-dependent small RNAs of *Salmonella* respond to membrane stress by accelerating global *omp* mRNA decay. *Mol Microbiol*. **62**: 1674-1688.

Persson, C., Wagner, E.G., and Nordström, K. (1988). Contol of replication of plasmid R1: kinetics of *in vitro* interaction between the antisense RNA, CopA, and its target, CopT. *EMBO J*. **7**: 3279-3288.

Persson, C., Wagner, E.G., and Nordström, K. (1990a). Contol of replication of plasmid R1: structures and sequences of the antisense RNA, CopA, required for its binding to the target RNA, CopT. *EMBO J*. **9**: 3767-3775.

Persson, C., Wagner, E.G., and Nordström, K. (1990b). Control of replication of plasmid R1: formation of an initial transient complex is rate-limiting for antisense RNA--target RNA pairing. *EMBO J.* **9**: 3777-3785.

Pichon, C., and Felden, B. (2005). Small RNA genes expressed from *Staphyloccoccus aureus* genomic and pathogenicity islands with specific expression among pathogenic strains. *Proc Natl Acad Sci USA.* **102**: 14249-14254.

Rasmussen, A.A., Eriksen, M., Gilany, K., Udesen, C., Franch, T., Petersen, C., and Valentin-Hansen, P. (2005). Regulation of *ompA* mRNA stability: the role of a small regulatory RNA in growth phase-dependent control. *Mol Microbiol.* **58**: 1421-1429.

Repoila, F., Majdalani, N., and Gottesman S. (2003). Small non-coding RNAs, co-ordinators of adaptation processes in *Escherichia coli*: the RpoS paradigm. *Mol Microbiol.* **48**: 855-861.

Rivas, E., Klein, R.J., Jones, T.A., and Eddy, S.R. (2001). Computational identification of noncoding RNAs in *E. coli* by comparative genomics. *Curr Biol.* **11**: 1369-1373.

Romby, P., Vandenesch, F., and Wagner, E.G. (2006). The role of RNAs in the regulation of virulence-gene expression. *Curr Opin Microbiol.* **9**: 229-36.

Romeo, T. (1998). Global regulation by the small RNA-binding protein CsrA and the non-coding RNA molecule CsrB. *Mol Microbiol.* **29**: 1321-1330.

Sauter, C., Basquin, J., and Suck, D. (2003). Sm-like proteins in Eubacteria: the crystal structure of the Hfq protein from *Escherichia coli. Nucleic Acids Res.* **31**: 4091-4098.

Schmidt, M., Zheng, P., and Delihas, N.(1995). Secondary structures of *Escherichia coli* antisense MicF RNA, the 5' end of the target *ompF* mRNA, and the RNA/RNA duplex. *Biochemistry.* **34**: 3621-3631.

Schuhmacher, M.A., Pearson, R.F., Møller, T., Valentin-Hansen, P., and Brennan, R.G. (2002). Structures of the pleiotropic translational regulator Hfq and an Hfq-RNA complex: a bacterial Sm-like protein. *EMBO J.* **21**: 3546-3556.

Senear, A.W., and Steitz, J.A. (1976). Site-specific interaction of Qβ host factor and ribosomal protein S1 with Qβ and R17 bacteriophage RNAs. *J Biol Chem.* **251**: 1902-1912.

Shimizu, T., Yaguchi, H., Ohtani, K., Banu, S., and Hayashi, H. (2002). Clostridial VirR/VirS regulon involves a regulatory RNA molecule for expression of toxins. *Mol. Microbiol.* **43:** 257-265.

Silvaggi, J.M., Perkins, J.B., and Losick R. (2005). Small untranslated RNA antitoxin in *Bacillus subtilis*. *J Bacteriol* **187**: 6641-6650.

Sledjeski, D.D., and Gottesman S. (1995). A small RNA acts as an antisilencer of the H-NS-silenced *rcsA* gene of *Escherichia coli. Proc Natl Acad Sci USA.* **92**: 2003-2007.

Sledjeski, D.D., Gupta, A., and Gottesman, S. (1996). The small RNA, DsrA, is essential for the low temperature expression of RpoS during exponential growth in *Escherichia coli. EMBO J.* **15**: 3993-4000.

Sledjeski, D.D., Whitman, C., and Zhang, A. (2001). Hfq is necessary for regulation by the untranslated RNA DsrA. *J Bacteriol.* **183**: 1997-2005.

Silvaggi, J.M., Perkins, J.B., and Losick, R. (2006). Genes for small, noncoding RNAs under sporulation control in *Bacillus subtilis*. *J. Bacteriol.* **188**: 532-541.

Storz, G., Altuvia, S., and Wassarman, K.M. (2005). An abundance of RNA regulators. *Annu Rev Biochem.* **74:** 199-217.

Stougaard, P., Molin, S., and Nordström, K. (1981). RNAs involved in copy-number control and incompatibility of plasmid R1. *Proc Natl Acad Sci USA.* **78**: 6008-6012

Suzuma, S., Asari, S., Bunai, K., Yoshino, K., Ando, Y., Kakeshita, H., *et al.* (2002) Identification and characterization of novel small RNAs in the *aspS-yrvM* intergenic region of the *Bacillus subtilis* genome. *Microbiol*. **148**: 2591-2598.

The RNA World (Cold Spring Harbor Monograph), (2006). Gesteland, R.F., Cech, T.R., and Atkins J.F., Cold Spring Harbor Laboratory Press, U.S. pp. 575, 584.

Thieringer, H.A., Jones, P.G., and Inouye, M. (1998). Cold shock and adaptation. *Bioessays.* **20**: 49-57.

Tomizawa, J., Itoh, T., Selzer, G., and Som, T. (1981). Inhibition of ColE1 RNA primer formation by a plasmid-specified small RNA. *Proc Natl Acad Sci USA.* **78**: 1421-1425.

Tomizawa, J. (1984). Control of ColE1 plasmid replication: the process of binding of RNAI to the primer transcript. *Cell.* **38**: 861-870.

Tomizawa, J. (1990a). Control of ColE1 plasmid replication-intermediates in the binding of RNAI and RNAII. *J. Mol. Biol.* **212**: 638-69.

Tomizawa, J. (1990b). Control of ColE1 plasmid replication. Interaction of Rom protein with an unstable complex formed by RNAI and RNAII. *J. Mol. Biol.* **212**: 695-708.

Trotochaud, A.E., and Wassarman,K.M. (2004). 6S RNA function enhances long-term cell survival. *J Bacteriol.* **186**: 4978-4985.

Trotochaud, A.E., and Wassarman,K.M. (2005). A highly conserved 6S RNA structure is required for regulation of transcription. *Nat. Struct. Mol. Biol.* **12**: 313-319.

Tsui, H.C., Leung, H.C., and Winkler, M.E. (1994). Characterization of broadly pleiotropic phenotypes caused by an hfq insertion mutation in *Escherichia coli* K-12. *Mol Microbiol.* **13**: 35-49.

Udekwu, K.I., Darfeuille, F., Vogel, J., Reimegard, J., Holmqvist, E., and Wagner, E.G. (2005). Hfq-dependent regulation of OmpA synthesis is mediated by an antisense RNA. *Genes Dev.* **19:** 2355-2366.

Valentin-Hansen, P., Eriksen, M., and Udesen, C. (2004). The bacterial Sm-like protein Hfq: a key player in RNA transactions. *Mol Microbiol*. **51**: 1525-1533.

Valverde, C., Lindell, M., Wagner, E.G., and Haas, D. (2004). A repeated GGA motif is critical for the activity and stability of the riboregulator RsmY of *Pseudomonas fluorescens. J Biol Chem.* **279**: 25066-25074.

Vanderpool, C.K., and Gottesman, S. (2004). Involvement of a novel transcriptional activator and small RNA in post-transcriptional regulation of the glucose phosphoenolpyruvate phosphotransferase system. *Mol Microbiol.* **54**: 1076-1089.

Vogel, J., Argaman, L., Wagner, E.G., and Altuvia, S. (2004). The small RNA IstR inhibits synthesis of an SOS-induced toxic peptide. *Curr Biol.* **14**: 2271-2276.

Vytvytska, O., Moll, I., Kaberdin, V.R., von Gabain, A., and Blasi, U. (2000). Hfq (HF1) stimulates *ompA* mRNA decay by interfering with ribosome binding. *Genes Dev.* **14**: 1109-1118.

Wagner, E.G., and Simons, R.W. (1994). Antisense RNA control in bacteria, phages, and plasmids. *Annu. Rev. Microbiol.* **48**: 713-742.

Wagner, E.G., and Brantl, S. (1998). Kissing and RNA stability in antisense control of plamid replication. *Trends Biochem. Sci.* **23**: 451-454.

Wagner, E.G., Altuvia, S., and Romby P. (2002). Antisense RNAs in bacteria and their genetic elements. *Adv Genet.* **46**: 361-398.

Waldminghaus, T., Fippinger, A., Alfsmann, J., and Narberhaus, F. (2005). RNA thermometers are common in α- and γ-proteobacteria. *Biol Chem*. **386**: 1279-1286.

Waldminghaus, T., Heidrich, N., Brantl, S., and Naberhaus, F. (2007). FourU – A novel type of RNA thermometer in *Salmonella* and other bacteria. *Mol. Microbiol.. eingereicht.*

Wassarman, K.M., Zhang, A., and Storz, G. (1999). Small RNAs in *Escherichia coli*. *Trends Microbiol.* **7**: 37-45.

Wassarman, K.M., and Storz, G. (2000). 6S RNA regulates *E. coli* RNA polymerase activity. *Cell.* **101**: 613-23.

Wassarman, K.M., Repoila, F., Rosenow, C., Storz, G., and Gottesman, S. (2001). Identification of novel small RNAs using comparative genomics and microarrays. *Genes Dev.* **15**: 1637-1651.

Weilbacher, T., Suzuki, K., Dubey, A.K., Wang, X., Gudapaty, S., Morozov, I., Baker, C.S., Georgellis, D., Babitzke, P., and Romeo, T. (2003). A novel sRNA component of the carbon storage regulatory system of *Escherichia coli. Mol Microbiol.* **48**: 657-70.

Wilderman, P.J., Sowa, N.A., FitzGerald, D.J., FitzGerald, P.C., Gottesman, S., Ochsner, U.A., and Vasil, M.L. (2004). Identification of tandem duplicate regulatory small RNAs in *Pseudomonas aeruginosa* involved in iron homeostasis. *Proc Natl Acad Sci USA.* **101**: 9792-9797.

Wilson, I.W., Praszkier, J., and Pittard, A.J. (1993). Mutations affecting pseudoknot control of the replication of B group plasmids. *J. Bacteriol.* **175:** 6476-6483.

Winkler, W.C. and Breaker, R.R. (2005). Regulation of bacterial gene expression by riboswitches. *Annu Rev Microbiol*. **59**: 487-517.

Yura, T., Kanemori, M. and Morita, M. (2000). The heat shock response: regulation and function. In Hengge-Aronis, G.S.a.R. (ed.), *Bacterial Stress Responses*. ASM Press, Washington, D.C., pp. 3-18.

Zhang, A., Altuvia, S., Tiwari, A., Argaman, L., Hengge-Aronis, R., and Storz, G. (1998). The *oxyS* regulatory RNA represses *rpoS* translation by binding Hfq (HF-1) protein. *EMBO J.* **17**: 6061-6068.

Zhang, A., Wassarman, K.M., Ortega, J., Steven, A.C., and Storz, G. (2002). The Sm-like Hfq protein increases OxyS RNA interaction with target mRNAs. *Mol. Cel.* **9**: 11-22.

Zuker, M. (2003). Mfold web server for nucleic acid folding and hybridization prediction. *Nucleic Acids Res*. **31**: 3406-3415.

Danksagung

Zuerst und ganz besonders möchte ich Frau HD Dr. Sabine Brantl danken. Für die Überlassung dieses interessanten und hochspannenden Themas und für ihre sehr gute Betreuung. Ihre vielen guten Ratschläge und ihre hochmotivierende und konstruktive Begleitung waren mir eine große Hilfe und eine stetige Quelle der Inspiration. Damit hat sie meine Forschung auf vielen Ebenen bereichert und ist mir so zu einem großen fachlichen Vorbild geworden.
Herzlicher Dank!

Auch Prof. Franz Naberhaus von der Ruhr-Universität Bochum gilt mein Dank für die Möglichkeit der Forschung an RNA-Thermometern in Prokaryoten, die zu einem wichtigen Teilgebiet für diese Arbeit geworden sind. In diesem Zusammenhang war mir insbesondere sein Mitarbeiter Torsten Waldminghaus ein sehr guter Diskussionspartner.

An dieser Stelle möchte ich auch Dr. Isabella Moll danken für die Möglichkeit, mehrere Wochen am Max F. Perutz Institut in Wien in der Arbeitsgruppe von Prof. Udo Bläsi geforscht haben zu können. Insbesondere ihre Hilfestellungen zu den Toeprint-Experimenten, ihre konstruktiven Fragen und ihr Interesse waren mir eine große Hilfe.

Mein Dank gilt weiterhin Dr. Eckhard Birch-Hirschfeld, der sämtliche in dieser Arbeit verwendeten synthetischen Oligonukleotide in hervorragender Qualität und mit hohem Einsatz für mich hergestellt hat.

Für die Durchführung der 2D-Gelanalysen im Labor von Dr. Ulf Gerth an der Ernst-Moritz-Arndt-Universität möchte ich herzlich danken.

Außerdem gilt mein Dank Alberto Chinali, Andreas Licht und Christina Stacke für konstruktive Gespräche innerhalb unserer Arbeitsgruppe Bakteriengenetik.

Nicht zuletzt danke ich meinen Freunden, die willkommene Pausen in meinen Forschungsalltag gebracht haben und zu jeder Zeit eine offene Tür und ein offenes Ohr für mich hatten.

Wichtigster Begleiter auf dem Weg zu dieser Arbeit war jedoch Mark Möbius, der durch seine positive und motivierende Art in den Höhen und Tiefen des Forschens eine unschätzbare Hilfe war.

Abschließend und ganz besonders möchte ich meinen Eltern danken, die mich zu jeder Zeit geduldig unterstützt haben und mir auf jede erdenkliche Art den Boden unter den Füßen gesichert haben. Ihnen ist diese Arbeit gewidmet.

Selbstständigkeitserklärung

Ich erkläre, dass ich die vorliegende Arbeit selbständig und nur unter Verwendung der angegebenen Hilfsmittel und Literatur angefertigt habe.

Jena, 20.04.2007

Erklärung zur Bewerbung

Ich erkläre, dass ich mich mit der vorliegenden Arbeit an keiner anderen Hochschule um den akademischen Grad Dr. rer. nat. beworben habe und dass ich weder früher noch gegenwärtig die Eröffnung eines Verfahrens zum Erwerb des o. g. akademischen Grades an einer anderen Hochschule beantragt habe.

Jena, 20.04.2007

Curriculum Vitae

Nadja Heidrich

Persönliche Daten

Anschrift	Weimarer Str.36 99428 Weimar Germany
Telefon	+49. (0)178. 3436380
eMail	nadja.heidrich@uni-jena.de
Staatsangehörigkeit	Bundesrepublik Deutschland
Geburtsdatum	19. April 1978
Geburtsort	Leipzig

Ausbildung

seit 05| 2003	Promotionsstudium an der Friedrich-Schiller-Universität Jena, AG Bakteriengenetik
2002 - 2003	Diplomarbeit in der AG Bakteriengenetik, FSU Jena, „Bedeutung einer U-turn-Loop-Struktur in der Sense-RNA von Plasmid pIP501 für die effiziente Regulation der Replikation“ Abschlussnote: 1,0
1999 - 2003	Friedrich- Schiller-Universität Jena Hauptstudium der Biologie
1996 - 1999	Martin-Luther-Universität Halle Grundstudium der Biologie
1991 - 1996	Hoffmann-von-Fallersleben-Gymnasium, Weimar Abiturnote: 1.8

Arbeitserfahrung

seit 05| 2003	Wissenschaftliche Mitarbeiterin an der Hochschuldozentur Bakteriengenetik, FSU Jena

Praktika und Auslandsaufenthalt

12| 2006	Forschungsaufenthalt am Max F. Perutz Institut in Wien in der Arbeitsgruppe von Prof. Udo Bläsi (4 Wochen)
08| 2003	Teilnahme am Kurs “Non-Coding RNAs –Structure and Function” in Sandhamn, Schweden (1 Woche)
07| 1999 - 09| 1999	MAX-PLANCK-INSTITUT FÜR CHEMISCHE ÖKOLOGIE, Jena: molekularbiologische Untersuchungen an *Nicotiana sylvestris*

Publikationen

Heidrich, N., Moll, I., and Brantl, S. (2007). *In vitro* analysis of the interaction between the small RNA SR1 and its primary target *ahrC*-RNA. *Nucleic Acids Res*. *eingereicht.*

Waldminghaus, T., Heidrich, N., Brantl, S., and Naberhaus, F. (2007). FourU – A novel type of RNA thermometer in *Salmonella* and other bacteria, *Mol. Microbiol*. *eingereicht.*

Heidrich, N., and Brantl, S. (2007). Antisense-RNA mediated transcriptional attenuation in plasmid pIP501: the simultaneous interaction between two complementary loop pairs is required for efficient inhibition by the antisense RNA. *Microbiol.* 153: 420-427.

Heidrich, N., Chinali, A., Gerth, U., and Brantl, S. (2006). The small untranslated RNA SR1 from the *B. subtilis* genome is involved in the regulation of arginine catabolism. *Mol. Microbiol.* 62: 520-36.

Heidrich, N., and Brantl, S. (2003). Antisense-RNA mediated transcriptional attenuation: importance of a U-turn loop structure in the target RNA of plasmid pIP501 for efficient inhibition by the antisense RNA**.** *J.Mol. Biol.* 333: 917-929.

Voelckel, C., Krügel, T., Gase, K., Heidrich, N., van Dam, N.M., Winz, R., and Baldwin, I.T. (2001). Anti-sense expression of putrescine N-methyltransferase confirms defensive role of nicotine in *Nicotiana sylvestris* against *Manduca Sexta. Chemoecology* 11:121–126.

Kongressbeiträge

Heidrich, N.: The regulatory RNA SR1 from *B. subtilis* inhibits translation of AhrC by a novel mechanism. Vortrag. RNA Biochemistry Meeting, Kassel 2006

Heidrich, N., and Brantl, S.: *In vitro* study of the interaction between the novel untranslated RNA SR1 and its target, *ahrC* mRNA. Poster. Cold Spring Harbor 71ST Symposium: Regulatory RNAs. Cold Spring Harbor (CSHL), USA 2006

Heidrich, N., and Brantl, S.: *In vitro* study of the interaction between the novel untranslated RNA SR1 and its target, *ahrC* mRNA. Poster. VAAM Kongress, Jena 2006

Heidrich, N., and Brantl, S.: The simultaneous interaction between two complementary loop pairs is required for efficient inhibition by the antisense RNA. Poster. Plasmid-Meeting, Korfu, Griechenland 2004

Heidrich, N., and Brantl, S.: Importance of a U-turn loop structure in the target RNA of plasmid pIP501 for efficient inhibition by the antisense RNA. Poster. “Non-Coding RNAs - Structure and Function”, Sandhamn, Schweden 2003

Heidrich, N., and Brantl, S.: Importance of a U-turn loop structure in the target RNA of plasmid pIP501 for efficient inhibition by the antisense RNA. Poster. 8th Annual Meeting of the RNA Society, Vienna, Östereich 2003

Thesen zur Dissertation

1. Im Rahmen dieser Arbeit wurden eine *cis*-kodierte und eine *trans*-kodierte Antisense-RNA aus *Bacillus subtilis* sowie eine RNA-Thermometerstruktur aus *Salmonella enterica* detailliert strukturell und funktionell *in vitro* untersucht.

2. Die *cis*-kodierte Antisense-RNA RNAIII (136 nt) reguliert über Transkriptions-attenuierung der essentiellen *repR*-mRNA (RNAII) die Replikation des Streptokokkenplasmides pIP501. Eine Strukturkartierung des Komplexes aus RNAIII und RNAII zeigte sowohl einzelsträngige als auch doppelsträngige Regionen. Das bedeutet, dass die Ausbildung einer vollständigen Duplex mit der RNAII für die inhibitorische Wirkung von RNAIII nicht gebraucht wird.

3. Mutationen im unteren Bereich der Stem-Loops L3 und/oder L4 von RNAIII haben einen negativen Einfluss auf die Effizienz der Transkriptionstermination von RNAII. Demzufolge sind die Stems von L3 und L4 von RNAIII für eine effiziente Attenuierung der Transkription von RNAII erforderlich.

4. Mutationen in der Spacer-Region zwischen den Stem-Loops L3 und L4 haben keinen signifikanten Effekt auf die Inhibitionskonstanten der entsprechenden RNAIII-Mutanten. Die Spacer-Region ist demnach an der Ausbildung eines inhibitorischen Komplexes aus RNAII und RNAIII nicht beteiligt.

5. Die Spacer-Region verbindet die Stem-Loops L3 und L4 von RNAIII und ermöglicht damit eine simultane Interaktion der beiden Loops L3 und L4 von RNAIII mit den komplementären Target-Loops L2 und L1 von RNAII.

6. Im Gegensatz zu anderen Antisense-RNA-regulierten Kontrollsystemen grampositiver Bakterien ist für den initialen Kontakt von RNAIII und RNAII die simultane Interaktion von zwei komplementären Loop-Paaren erforderlich.

7. Die chromosomal kodierte RNA SR1 aus *Bacillus subtilis* ist eine 205 nt lange *trans*-kodierte Antisense-RNA, die durch direkte Basenpaarung regulierend auf ihr Target, *ahrC*-mRNA, einwirken kann. Sie besitzt sieben komplementäre Regionen (A-G) zur *ahrC*-mRNA, die in der 3'-Hälfte von SR1 und im zentralen und 3'-Bereich der *ahrC*-mRNA zu finden sind. SR1 weist eine komplexe

Sekundärstruktur mit drei Stem-Loop-Strukturen und zwei einzelsträngigen Regionen auf.

8. Die Dissoziationskonstante des SR1/*ahrC*-Komplexes beträgt ca. 3.21 x 10^{-7} M. Für die Paarungskonstante des SR1/*ahrC*-Komplexes wurde ein Wert von etwa 1,25 x 10^{3} $M^{-1}s^{-1}$ errechnet. Die ermittelten Werte beider Konstanten unterscheiden sich um eine Größenordnung von den Werten anderer Antisense/Target-RNA-Komplexe. Möglicherweise wird ein zusätzlicher Faktor zur Förderung der SR1/*ahrC*-Komplexbildung benötigt.

9. Die Wechselwirkung zwischen SR1 und *ahrC*-mRNA wird an der komplementären Region G in der 5'-Hälfte des Terminator-Stems von SR1 initiiert. Dieser initiale Kontakt erfordert die Öffnung des doppelsträngigen Terminator-Stems von SR1 durch zusätzliche Faktoren.

10. Neben der Region G werden 5 weitere komplementäre Regionen (B-F) für die Interaktion von SR1 und *ahrC*-mRNA benötigt. Diese Regionen leisten einen geringen, jedoch messbaren Beitrag zur SR1/*ahrC*-Komplexbildung.

11. Die SR1-vermittelte Inhibierung der *ahrC*-mRNA erfolgt nicht über den Abbau der *ahrC*-mRNA durch RNase III oder eine andere RNase.

12. SR1 induziert durch Bindung an die *ahrC*-mRNA strukturelle Veränderungen stromabwärts der Ribosomenbindungsstelle von *ahrC*-mRNA, wodurch die Ausbildung des 30S-Initiationskomplexes blockiert und damit die Translationsinitiation von AhrC verhindert wird. Das bedeutet, dass SR1 auf post-transkriptionaler Ebene die Translation des Transkriptionsaktivators AhrC in *Bacillus subtilis* inhibiert.

13. Das RNA-Chaperon Hfq bindet spezifisch sowohl an SR1 als auch an die *ahrC*-mRNA. Die Bindung von Hfq fördert nicht die Komplexbildung von SR1 mit *ahrC*-mRNA, wie es für viele Antisense/Target-RNA-Interaktionen in *E. coli* gezeigt werden konnte.

14. Hfq bindet an eine AU-reiche Sequenz in der *ahrC*-mRNA, die stromaufwärts der Ribosomenbindungsstelle lokalisiert ist. Die Bindung von Hfq ist für die Translation der *ahrC*-mRNA erforderlich.

15. Eine Bestimmung der intrazellulären Konzentration von SR1 in *B. subtilis* ergab, dass etwa 250 Moleküle pro Zelle (0,35 µM) in der Stationärphase, dem Zeitpunkt ihrer höchsten Expression, vorhanden sind, während in der log-Phase eine 10fach niedrigere Konzentration vorliegt. Damit liegt SR1 in einem 10-20fachem Überschuss gegenüber ihrer Target-RNA vor.

16. Nach RNAIII aus *Staphylococcus aureus*, die schon seit mehreren Jahren intensiv untersucht wird, ist SR1 die zweite sehr gut charakterisierte *trans*-kodierte Antisense-RNA aus grampositiven Bakterien.

17. Die potentielle RNA-Thermometerstruktur, die stromaufwärts des Hitzeschockgens *agsA* von *Salmonella enterica* lokalisiert ist, besitzt zwei Stem-Loop-Strukturen I und II. Die Stem-Loop-Struktur II enthält 4 aufeinander folgende Uracil-Reste, die mit der SD-Sequenz des *agsA*-Gens gepaart sind.

18. Ein Temperaturanstieg von 30° C auf 45° C führt zu einer Konformationsänderung der Stem-Loop-Struktur II. Dabei wird die SD-Sequenz freigelegt.

19. Toeprint-Analysen bei 30° C und bei 45° C weisen nach, dass nur bei erhöhten Temperaturen die Bindung von Ribosomen an die *agsA*-mRNA erfolgen kann.

20. Die Translationskontrolle des *agsA*-Transkriptes in *Salmonella enterica* erfolgt über eine experimentell bestätigte RNA-Thermometer-Struktur, die keinem der bisher identifizierten RNA-Thermometertypen entspricht.